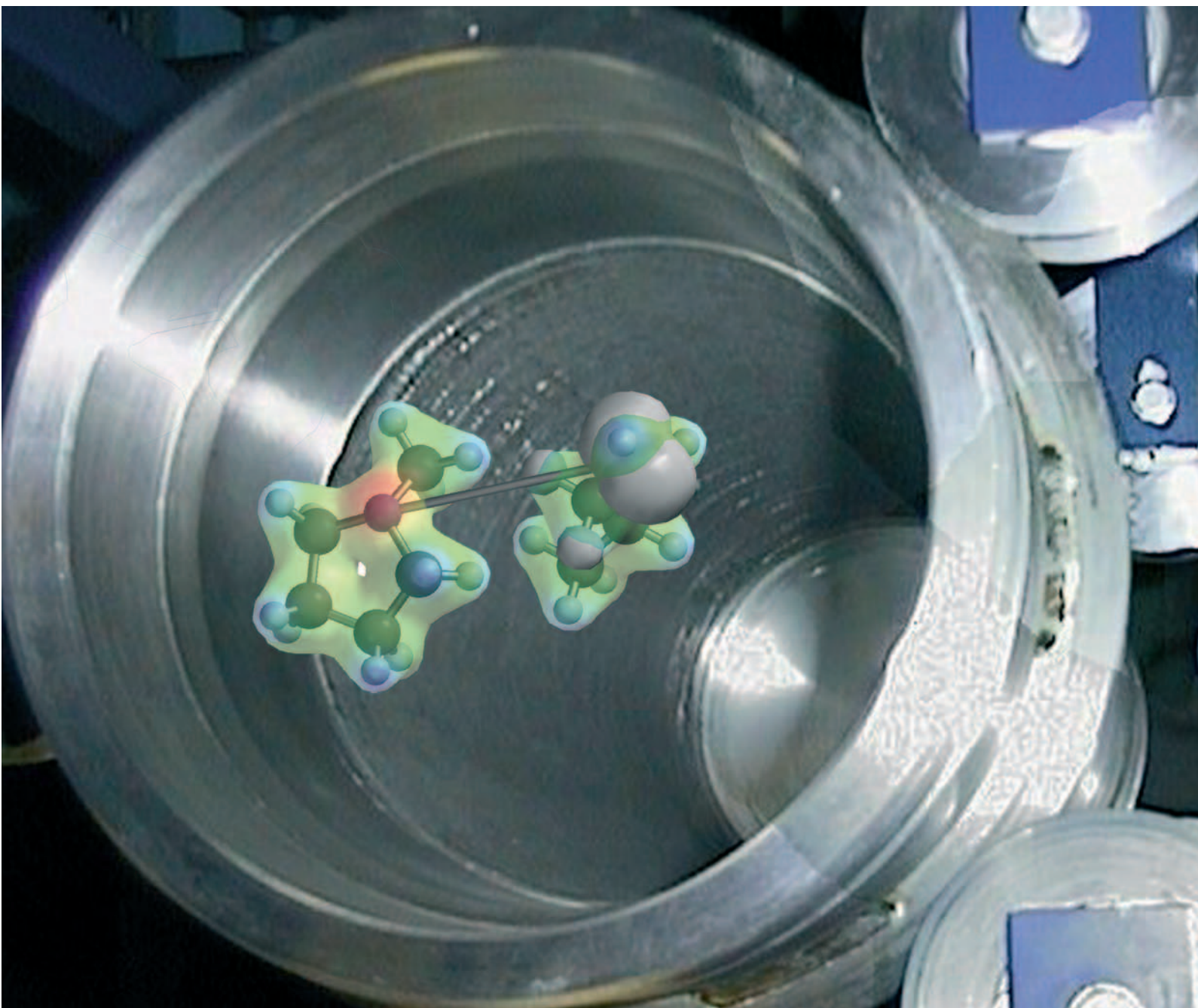


# Green Chemistry

Cutting-edge research for a greener sustainable future

[www.rsc.org/greenchem](http://www.rsc.org/greenchem)

Volume 8 | Number 3 | March 2006 | Pages 225–312



ISSN 1463-9262

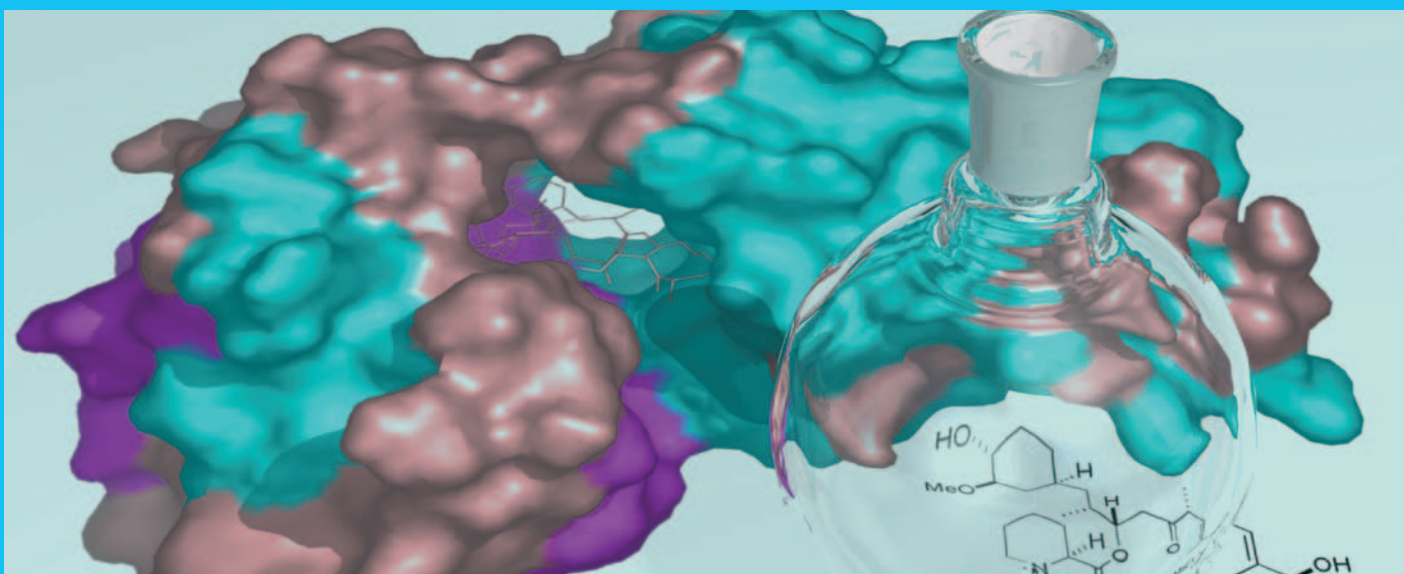
RSC Publishing

**Special issue**

Papers from the 1st International Congress on Ionic Liquids (COIL)



1463-9262 (2006) 8:3;1-B



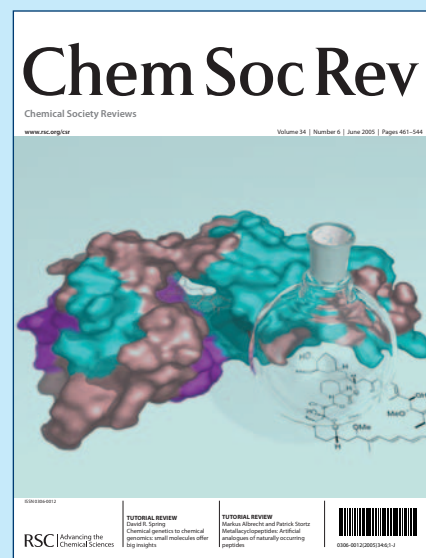
# Chem Soc Rev

## Chemical Society Reviews

An international, multidisciplinary journal publishing accessible, succinct and reader-friendly articles on topics of current interest in the chemical sciences.

Keeping you at the forefront of chemical science

- Impact factor: 10.836
- Now 12 issues a year
- High visibility - cited in MEDLINE



# Green Chemistry

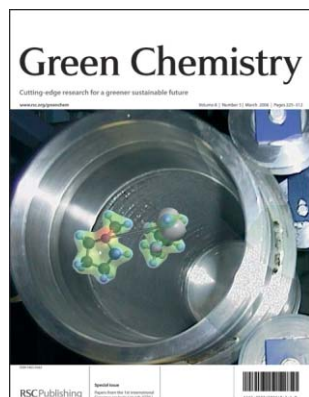
Cutting-edge research for a greener sustainable future

[www.rsc.org/greenchem](http://www.rsc.org/greenchem)

RSC Publishing is a not-for-profit publisher and a division of the Royal Society of Chemistry. Any surplus made is used to support charitable activities aimed at advancing the chemical sciences. Full details are available from [www.rsc.org](http://www.rsc.org)

## IN THIS ISSUE

ISSN 1463-9262 CODEN GRCHFJ 8(3) 225-312 (2006)



### Cover

Pure products can be removed from ionic liquids either by extraction with carbon dioxide as co-solvent, or by precipitation using carbon dioxide as anti-solvent. Image reproduced by permission of Maaïke Kroon from *Green Chem.*, 2006, 8(3), 246.

## CHEMICAL TECHNOLOGY

T9

Chemical Technology highlights the latest applications and technological aspects of research across the chemical sciences.

## Chemical Technology

March 2006/Volume 3/Issue 3

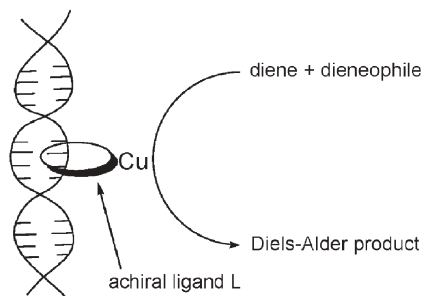
[www.rsc.org/chemicaltechnology](http://www.rsc.org/chemicaltechnology)

## HIGHLIGHT

235

### Highlights

Markus Hölscher reviews some of the recent literature in green chemistry.



## EDITORIAL STAFF

**Editor**

Sarah Ruthven

**News writer**

Markus Hölscher

**Publishing assistant**

Emma Hacking

**Team leader, serials production**

Stephen Wilkes

**Administration coordinator**

Sonya Spring

**Editorial secretaries**

Lynne Braybrook, Jill Segev, Julie Thompson

**Publisher**

Adrian Kybett

Green Chemistry (print: ISSN 1463-9262; electronic: ISSN 1463-9270) is published 12 times a year by the Royal Society of Chemistry, Thomas Graham House, Science Park, Milton Road, Cambridge, UK CB4 0WF.

All orders, with cheques made payable to the Royal Society of Chemistry, should be sent to RSC Distribution Services, c/o Portland Customer Services, Commerce Way, Colchester, Essex, UK CO2 8HP. Tel +44 (0) 1206 226050; E-mail sales@rscdistribution.org

2006 Annual (print + electronic) subscription price: £859; US\$1571. 2006 Annual (electronic) subscription price: £773; US\$1414. Customers in Canada will be subject to a surcharge to cover GST. Customers in the EU subscribing to the electronic version only will be charged VAT.

If you take an institutional subscription to any RSC journal you are entitled to free, site-wide web access to that journal. You can arrange access via Internet Protocol (IP) address at [www.rsc.org/ip](http://www.rsc.org/ip). Customers should make payments by cheque in sterling payable on a UK clearing bank or in US dollars payable on a US clearing bank. Periodicals postage paid at Rahway, NJ, USA and at additional mailing offices. Airfreight and mailing in the USA by Mercury Airfreight International Ltd., 365 Blair Road, Avenel, NJ 07001, USA.

US Postmaster: send address changes to Green Chemistry, c/o Mercury Airfreight International Ltd., 365 Blair Road, Avenel, NJ 07001. All despatches outside the UK by Consolidated Airfreight.

PRINTED IN THE UK

**Advertisement sales:** Tel +44 (0) 1223 432246; Fax +44 (0) 1223 426017; E-mail [advertising@rsc.org](mailto:advertising@rsc.org)

# Green Chemistry

Cutting-edge research for a greener sustainable future

[www.rsc.org/greenchem](http://www.rsc.org/greenchem)

Green Chemistry focuses on cutting-edge research that attempts to reduce the environmental impact of the chemical enterprise by developing a technology base that is inherently non-toxic to living things and the environment.

## EDITORIAL BOARD

**Chair**

Professor Colin Raston,  
Department of Chemistry  
University of Western Australia  
Perth, Australia  
E-mail [clration@chem.uwa.edu.au](mailto:clration@chem.uwa.edu.au)

Dr Janet Scott, Centre for Green  
Chemistry, Monash University,  
Australia

Professor Buxing Han, Chinese  
Academy of Sciences  
E-mail [hanbx@iccas.ac.cn](mailto:hanbx@iccas.ac.cn)

Dr A Michael Warhurst,  
University of Massachusetts,  
USA  
E-mail [michael-warhurst@uml.edu](mailto:michael-warhurst@uml.edu)

**Associate editors**

Professor C. J. Li, McGill  
University, Canada  
E-mail [cj.li@mcgill.ca](mailto:cj.li@mcgill.ca)

Professor Kyoko Nozaki  
Kyoto University, Japan  
E-mail [nozaki@chembio.tu-tokyo.ac.jp](mailto:nozaki@chembio.tu-tokyo.ac.jp)

Professor Tom Welton,  
Imperial College, UK  
E-mail [t.welton@ic.ac.uk](mailto:t.welton@ic.ac.uk)

Professor Roshan Jachuck,  
Clarkson University, USA  
E-mail [rjachuck@clarkson.edu](mailto:rjachuck@clarkson.edu)

Dr Paul Anastas, Green Chemistry  
Institute, USA  
E-mail [p\\_anastas@acs.org](mailto:p_anastas@acs.org)

**Scientific editor**

Professor Walter Leitner,  
RWTH-Aachen, Germany  
E-mail [leitner@itmc.rwth-aachen.de](mailto:leitner@itmc.rwth-aachen.de)

**Members**

Professor Joan Brennecke,  
University of Notre Dame, USA  
Professor Steve Howdle, University  
of Nottingham, UK

## INTERNATIONAL ADVISORY EDITORIAL BOARD

James Clark, York, UK  
Avelino Corma, Universidad  
Politécnica de Valencia, Spain  
Mark Harmer, DuPont Central  
R&D, USA  
Herbert Hugel, Lanxess Fine  
Chemicals, Germany  
Makato Misono, Kogakuin  
University, Japan  
Robin D. Rogers, Centre for Green  
Manufacturing, USA

Kenneth Seddon, Queen's  
University, Belfast, UK  
Roger Sheldon, Delft University of  
Technology, The Netherlands  
Gary Sheldrake, Queen's  
University, Belfast, UK  
Pietro Tundo, Università ca  
Foscari di Venezia, Italy  
Tracy Williamson, Environmental  
Protection Agency, USA

## INFORMATION FOR AUTHORS

Full details of how to submit material for publication in Green Chemistry are given in the Instructions for Authors (available from <http://www.rsc.org/authors>). Submissions should be sent via ReSource: <http://www.rsc.org/resource>.

Authors may reproduce/republish portions of their published contribution without seeking permission from the RSC, provided that any such republication is accompanied by an acknowledgement in the form: (Original citation) – Reproduced by permission of the Royal Society of Chemistry.

© The Royal Society of Chemistry 2006. Apart from fair dealing for the purposes of research or private study for non-commercial purposes, or criticism or review, as permitted under the Copyright, Designs and Patents Act 1988 and the Copyright and Related Rights Regulations 2003, this publication may only be reproduced, stored or transmitted, in any form or by any means, with the prior permission in writing of the Publishers or in the case of reprographic reproduction in accordance with the terms of

licences issued by the Copyright Licensing Agency in the UK. US copyright law is applicable to users in the USA.

The Royal Society of Chemistry takes reasonable care in the preparation of this publication but does not accept liability for the consequences of any errors or omissions.

⊗ The paper used in this publication meets the requirements of ANSI/NISO Z39.48-1992 (Permanence of Paper).

Royal Society of Chemistry: Registered Charity No. 207890

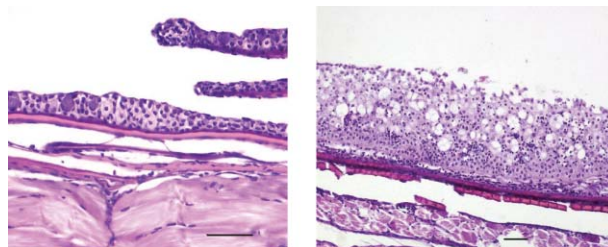
## COMMUNICATION

238

**Acute toxicity of ionic liquids to the zebrafish (*Danio rerio*)**

Carlo Pretti, Cinzia Chiappe, Daniela Pieraccini, Michela Gregori, Francesca Abramo, Gianfranca Monni and Luigi Intorre

The acute toxicity towards zebrafish of several ionic liquids with different anions and cations has been assessed. The results reveal that ionic liquids may cause a completely different effect according to their chemical structure.



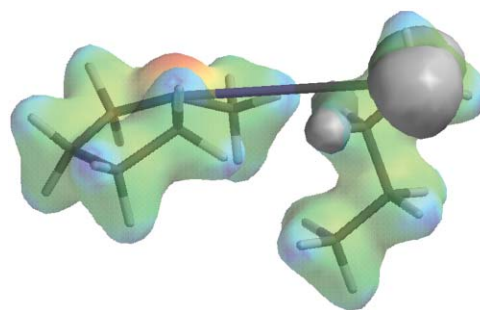
## PAPERS

241

**Decomposition of ionic liquids in electrochemical processing**

Maaik C. Kroon, Wim Buijs, Cor J. Peters and Geert-Jan Witkamp\*

Using quantum chemical calculations it is predicted that the ionic liquid [bmpyrrol<sup>+</sup>][NTf<sub>2</sub><sup>-</sup>] will electrochemically decompose at the cathodic limit into methylpyrrolidine and a butyl radical; this was also validated by experiments.

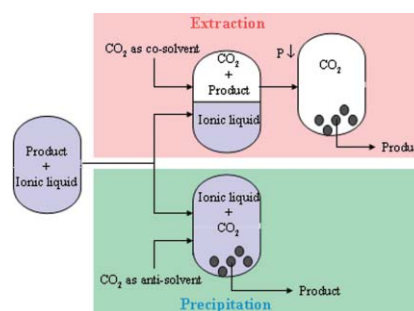


246

**Recovery of pure products from ionic liquids using supercritical carbon dioxide as a co-solvent in extractions or as an anti-solvent in precipitations**

Maaik C. Kroon, Jaap van Spronsen, Cor J. Peters, Roger A. Sheldon and Geert-Jan Witkamp\*

Pure products can be recovered either by extraction with carbon dioxide as a co-solvent, or by precipitation using carbon dioxide as an anti-solvent.

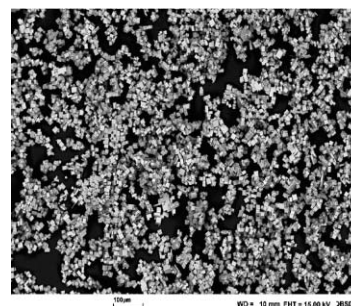


250

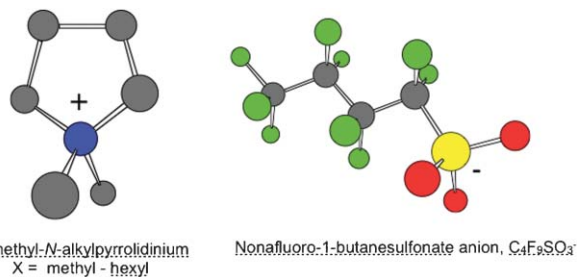
**Aliquat 336<sup>®</sup>—a versatile and affordable cation source for an entirely new family of hydrophobic ionic liquids**

Jyri-Pekka Mikkola, Pasi Virtanen and Rainer Sjöholm

A novel family of ionic liquids based on the tricaprilmethylammonium cation ([C<sub>25</sub>H<sub>54</sub>N]<sup>+</sup>) combined with a number of anions that are easily and elegantly prepared by means of simple replacement of the chloride ([Cl<sup>-</sup>]) anion in Aliquat 336<sup>®</sup> is introduced.



256

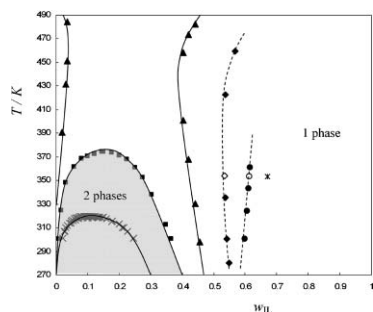


### *N*-methyl-*N*-alkylpyrrolidinium nonafluoro-1-butane-sulfonate salts: Ionic liquid properties and plastic crystal behaviour

Stewart A. Forsyth, Kevin J. Fraser, Patrick C. Howlett, Douglas R. MacFarlane\* and Maria Forsyth

The thermophysical characteristics of a series of *N*-methyl-*N*-alkylpyrrolidinium nonafluoro-1-butanesulfonate salts have been investigated with respect to potential use as ionic liquids and solid electrolytes.

262

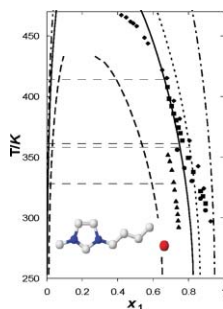


### Changing from an unusual high-temperature demixing to a UCST-type in mixtures of 1-alkyl-3-methylimidazolium bis{(trifluoromethyl)sulfonyl}amide and arenes

Joanna Łachwa, Jerzy Szydłowski, Anna Makowska, Kenneth R. Seddon, José M. S. S. Esperança, Henrique J.R. Guedes and Luís Paulo N. Rebelo\*

Due to specific interactions, it was found, for the first time, that the system [C<sub>*n*</sub>mim][NTf<sub>2</sub>] + aromatic compounds evolves from an unusual high-temperature phase splitting to a low-temperature UCST-type of phase diagram as the alkyl chain length, *n*, increases.

268

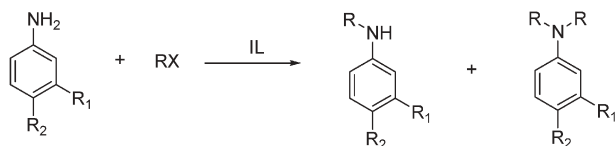


### Liquid-liquid equilibria in the binary systems (1,3-dimethylimidazolium, or 1-butyl-3-methylimidazolium methylsulfate + hydrocarbons)

Urszula Domańska,\* Aneta Pobudkowska and Frank Eckert

The mutual solubility of [mmim][CH<sub>3</sub>SO<sub>4</sub>] and [bmim][CH<sub>3</sub>SO<sub>4</sub>] with hydrocarbons have been measured for technological use. The COSMO-RS model was used for the prediction of experimental data. This method has shown the correct trends for both the variation of UCST and the alkyl chain length.

277



### Selective *N*-alkylation of anilines in ionic liquids

Cinzia Chiappe,\* Paolo Piccioli and Daniela Pieraccini

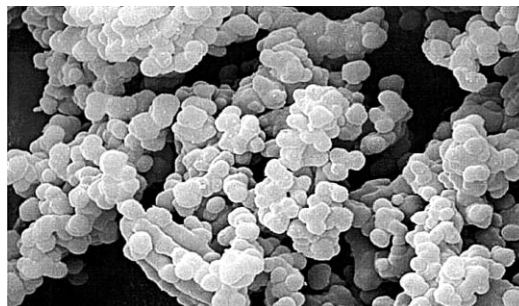
The dependence of selectivity of *N*-alkylation process of anilines on substituents on aromatic ring and alkylating agent has been investigated in several ILs.

282

### Structure and activity of *Candida antarctica* lipase B in ionic liquids

Fred van Rantwijk, Francesco Secundo and Roger A. Sheldon\*

*Candida antarctica* lipase B maintained transesterification activity upon dissolution in the ionic liquid [Et<sub>3</sub>MeN][MeSO<sub>4</sub>], but not in other ionic liquids that dissolved CaLB, such as [BMIm][dca]. Cross-linked enzyme aggregates of CaLB, in contrast, remained active in this latter ionic liquid.

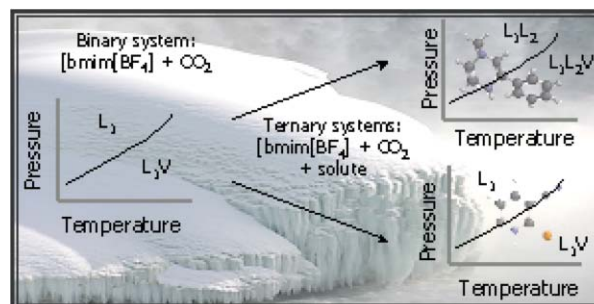


287

### Solubility of carbon dioxide in systems with [bmim][BF<sub>4</sub>] and some selected organic compounds of interest for the pharmaceutical industry

Eliane Kühne, Cor J. Peters,\* Jaap van Spronsen and Geert-Jan Witkamp

The effects of the addition of certain compounds used in the pharmaceutical industry to the system [bmim][BF<sub>4</sub>] + CO<sub>2</sub> were studied. It is shown that a solute could dramatically change the original binary phase behaviour.



292

### A new method for dialkyl peroxides synthesis in ionic liquids as solvents

Stefan Baj,\* Anna Chrobok and Sebastian Derfla

A new method for synthesis of unsymmetrical dialkyl peroxides from alkyl hydroperoxides and alkyl bromides in the presence of 30% NaOH water solution using ionic liquids is presented.



where: R<sup>1</sup> are H, cumyl or *tert*-butyl

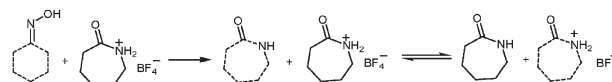
R<sup>2</sup>X are alkyl bromides (C<sub>2</sub>-C<sub>7</sub>) or alkyl methanesulfonates

296

### Clean Beckmann rearrangement of cyclohexanone oxime in caprolactam-based Brønsted acidic ionic liquids

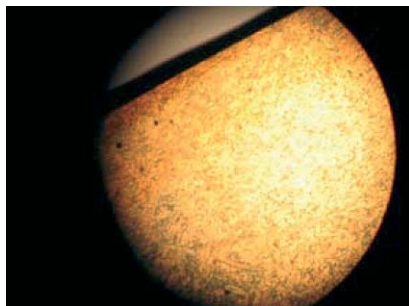
Shu Guo, Zhengyin Du, Shiguo Zhang, Dongmei Li, Zuopeng Li and Youquan Deng\*

The Beckmann rearrangement of cyclohexanone oxime to afford caprolactam in a novel caprolactam-based Brønsted acidic ionic liquid as catalyst and reaction medium proceeded with high conversion and selectivity at 100 °C.



## PAPERS

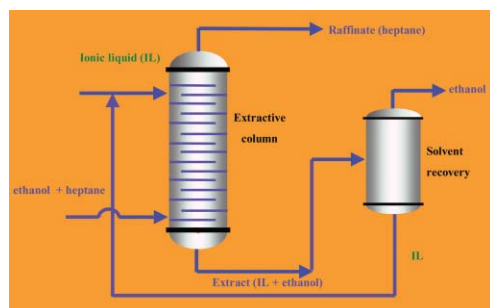
301

**Acylation and carbanilation of cellulose in ionic liquids**

Susann Barthel and Thomas Heinze\*

Ionic liquids (IL) were applied in cellulose chemistry. Cellulose with a degree of polymerisation up to 1200 can be dissolved without any degradation and chemically modified to various esters.

307

**HMImPF<sub>6</sub> ionic liquid that separates the azeotropic mixture ethanol + heptane**

A. B. Pereiro, E. Tojo, A. Rodríguez,\* J. Canosa and J. Tojo

Separation of azeotropic mixtures is difficult and expensive using conventional processes. Our research has identified HMImPF<sub>6</sub> as a good candidate for separating the mixture by means of an environmentally friendly extractive process.

## AUTHOR INDEX

Abramo, Francesca, 238  
Baj, Stefan, 292  
Barthel, Susann, 301  
Buijs, Wim, 241  
Canosa, J., 307  
Chiappe, Cinzia, 238, 277  
Chrobok, Anna, 292  
Deng, Youquan, 296  
Derfla, Sebastian, 292  
Domańska, Urszula, 268  
Du, Zhengyin, 296  
Eckert, Frank, 268  
Esperança, José M. S. S., 262

Forsyth, Maria, 256  
Forsyth, Stewart A., 256  
Fraser, Kevin J., 256  
Gregori, Michela, 238  
Guedes, Henrique J.R., 262  
Guo, Shu, 296  
Heinze, Thomas, 301  
Howlett, Patrick C., 256  
Intorre, Luigi, 238  
Kroon, Maaik C., 241, 246  
Kühne, Eliane, 287  
Lachwa, Joanna, 262  
Li, Dongmei, 296

Li, Zuopeng, 296  
MacFarlane, Douglas R., 256  
Makowska, Anna, 262  
Mikkola, Jyri-Pekka, 250  
Monni, Gianfranca, 238  
Pereiro, A. B., 307  
Peters, Cor J., 241, 246, 287  
Piccioli, Paolo, 277  
Pieraccini, Daniela, 238, 277  
Pobudkowska, Aneta, 268  
Pretti, Carlo, 238  
Rebelo, Luis Paulo N., 262  
Rodríguez, A., 307

Secundo, Francesco, 282  
Seddon, Kenneth R., 262  
Sheldon, Roger A., 246, 282  
Sjöholm, Rainer, 250  
Szydłowski, Jerzy, 262  
Tojo, E., 307  
Tojo, J., 307  
van Rantwijk, Fred, 282  
van Spronsen, Jaap, 246, 287  
Virtanen, Pasi, 250  
Witkamp, Geert-Jan, 241, 246, 287  
Zhang, Shiguo, 296

## FREE E-MAIL ALERTS AND RSS FEEDS

Contents lists in advance of publication are available on the web *via* [www.rsc.org/greenchem](http://www.rsc.org/greenchem) - or take advantage of our free e-mail alerting service ([www.rsc.org/ej\\_alert](http://www.rsc.org/ej_alert)) to receive notification each time a new list becomes available.

**RSS** Try our RSS feeds for up-to-the-minute news of the latest research. By setting up RSS feeds, preferably using feed reader software, you can be alerted to the latest Advance Articles published on the RSC web site. Visit [www.rsc.org/publishing/technology/rss.asp](http://www.rsc.org/publishing/technology/rss.asp) for details.

## ADVANCE ARTICLES AND ELECTRONIC JOURNAL

Free site-wide access to Advance Articles and the electronic form of this journal is provided with a full-rate institutional subscription. See [www.rsc.org/ejs](http://www.rsc.org/ejs) for more information.

\* Indicates the author for correspondence: see article for details.

Electronic supplementary information (ESI) is available *via* the online article (see <http://www.rsc.org/esi> for general information about ESI).



# Elegant Solutions

## Ten Beautiful Experiments in Chemistry

### Where does the true beauty reside in experimental chemistry?

In the clarity of the experiment's conception? .... the design of the instruments? .... the nature of the knowledge gained .... or of the product made?

'Philip Ball is one of the most prolific and imaginative of contemporary science writers.'

*Chemistry in Britain*

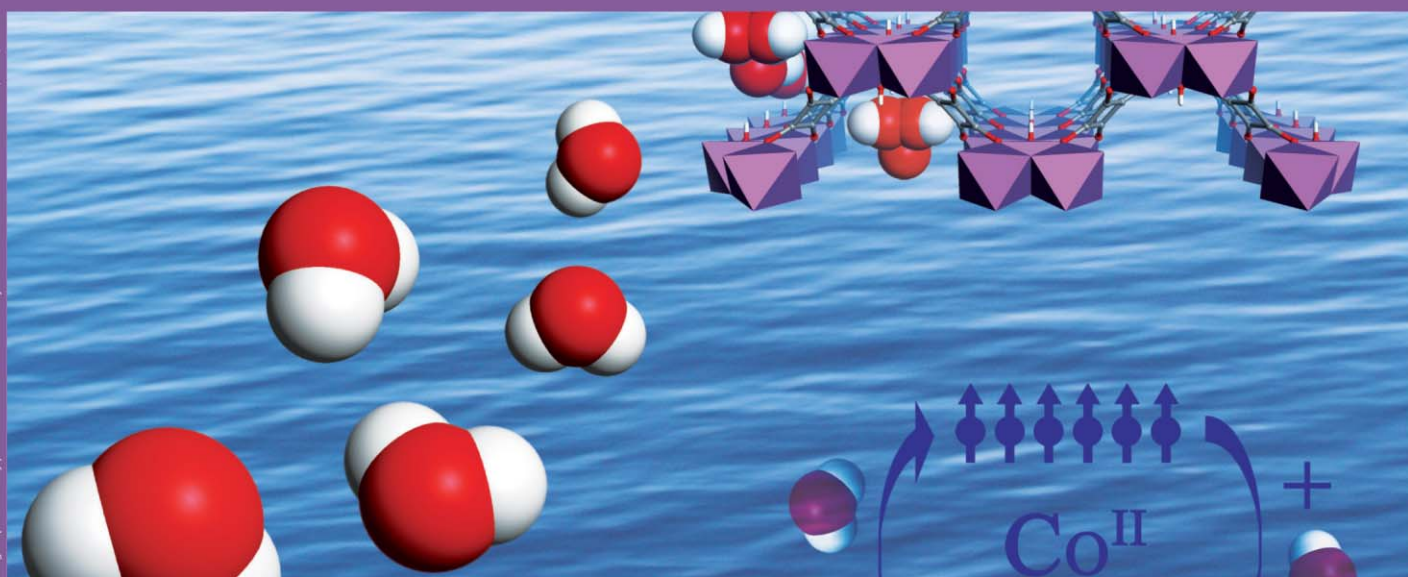
Winner of the Aventis Prize for Science Books 2005,

**Philip Ball,**  
offers ten suggestions in his latest book

Hardcover | 0 85404 674 7 | 208 pages | 2005 | £19.95 | RSC member price £12.75

RSC Publishing

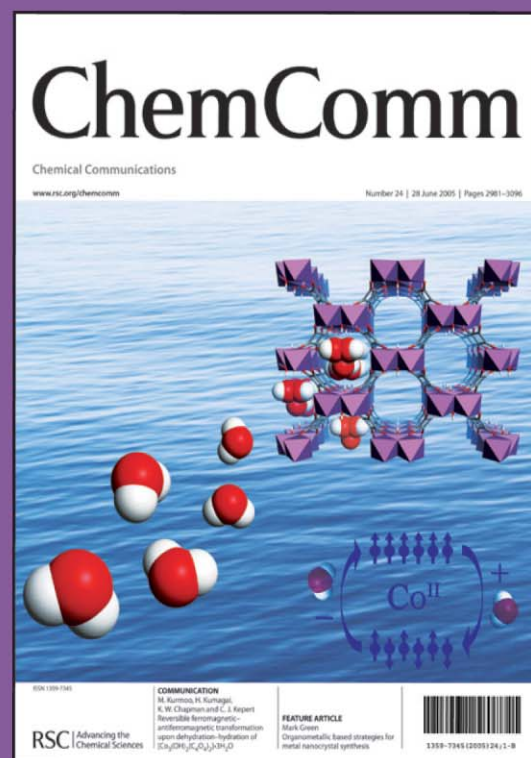
[www.rsc.org/elegantsolutions](http://www.rsc.org/elegantsolutions)



# ChemComm

The leading international journal for the publication of communications on important new developments in the chemical sciences.

- Weekly publication
- Impact factor: 3.997
- Rapid publication – typically 60 days
- 3 page communications – providing authors with the flexibility to develop their results and discussion
- 40 years publishing excellent research
- High visibility – indexed in MEDLINE
- Host of the RSC's new journal, *Molecular BioSystems*



RSC Publishing

[www.rsc.org/chemcomm](http://www.rsc.org/chemcomm)

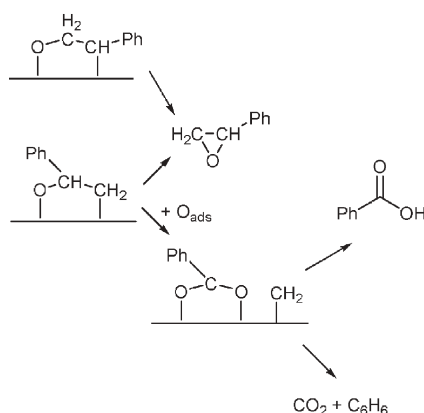
# Highlights

DOI: 10.1039/b601093h

Markus Hölscher reviews some of the recent literature in green chemistry

## Selectivity limitations in partial oxidations of styrene

The oxidation of olefins to the corresponding epoxides is a very useful reaction which is widely exploited industrially for the oxidation of ethylene. The direct epoxidation of other olefins is highly desirable, however, selectivity issues contribute to problems associated with the heterogeneously catalyzed transformation of substituted ethylene derivatives such as styrene. Data that add to the understanding of the reaction mechanism are considered valuable in determining the problematic side reactions in these reactions more precisely with the long term aim of developing better catalysts with higher selectivities. Klust and Madix from Stanford University used temperature-programmed reaction spectroscopy (TPRS) and X-ray photoelectron spectroscopy (XPS) to investigate the reaction of styrene with coadsorbed oxygen on the Ag(111) surface.<sup>1</sup> The authors found CO<sub>2</sub>, H<sub>2</sub>O, styrene, styrene oxide, benzene and benzoic acid to be generated during the reaction, which desorb at different temperatures. From the results of XPS analyses of the product mixture and by comparison with literature data the formation of an oxametallacycle was postulated, which is formed as a result of the



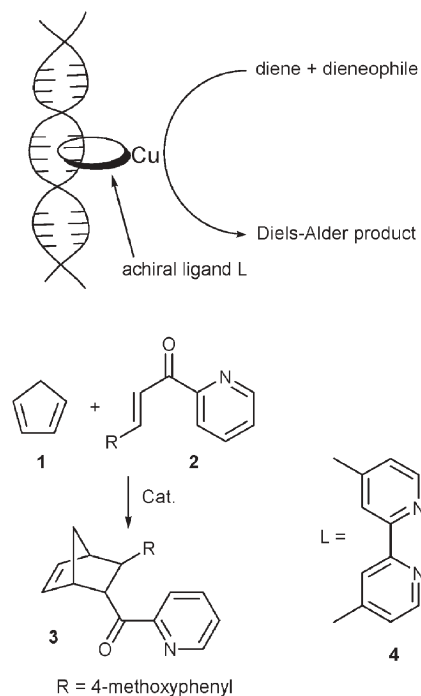
reaction of styrene with adsorbed O at either the terminal C atom of the alkyl chain or at the internal C atom.

Both intermediates can react to the desired styrene oxide. However, the internal, electron deficient C atom is very susceptible to nucleophilic attack by oxygen, leading to the formation of benzoate, which in turn reacts to benzoic acid or benzene/CO<sub>2</sub>. As the decomposition temperature of benzoate is relatively high compared to the temperature at which styrene oxide is generated, the relatively slow steady-state oxidation of styrene over Ag might be a result of this circumstance.

## Highly enantioselective Diels–Alder reactions by DNA induced chirality transfer

As DNA has a chiral helix structure it is an interesting molecule for the construction of asymmetric catalysts. Roelfes *et al.* recently succeeded in putting into practice the concept of bringing a catalytically active metal centre into close proximity of the DNA helix generating active catalysts for asymmetric Diels–Alder reactions.<sup>2</sup> The idea is based on the assumption that intercalation of achiral Cu complexes, which are comprised of achiral polyaromatic bidentate ligands and a Cu<sup>2+</sup> centre, with the double helix structure of DNA forms non-covalently bonded chiral Cu complexes stable enough for catalytic reactions. Chirality transfer is expected to occur by the influence of the chiral DNA molecule.

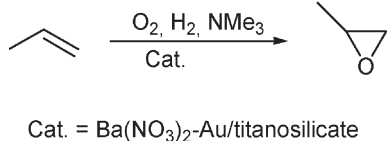
In a set of Diels–Alder experiments between cyclopentadiene (**1**) and a variety of dienophiles remarkably high enantioselectivities were obtained with dienophile **2** showing the best results generating product **3** with an *endo* : *exo* ratio of 99 : 1 while the ee value was >99%. Although other ligands also yielded high enantioselectivities ligand **4** proved to be the best choice for a variety of dienophiles.



## Efficient propylene epoxidation over supported gold catalysts using trimethylamine as promoter

Propylene oxide (PO) is a widely used bulk chemical which serves as starting material for the production of polyether polyols and propylene glycol. Currently the industrial syntheses relies on the chlorohydrin process and the Halcon process (organic hydroperoxide process), which both generate a large amount of by-products. Direct epoxidation using propylene, O<sub>2</sub> and H<sub>2</sub> in combination with an appropriate heterogeneous catalyst would be a more sustainable alternative if the industrially necessary level of efficiency could be met. During the past years gold catalysts have been under investigation for this reaction with remarkable success. However, industrial application has not yet been possible mainly due to the deactivation of the catalyst caused by oligomerized

and oxidized PO by-products. Haruta *et al.* from Tokyo Metropolitan University recently showed that trimethylamine (TMA) can act as promoter—presumably by blocking vacant  $Ti^{4+}$  centres of the support, which are believed to be responsible for the production of the by-products, which after formation deactivate the gold nanoparticles.<sup>3</sup>

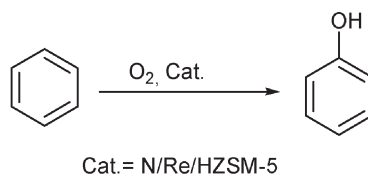


The comparison with the industrial ethylene oxide production showed the PO syntheses using trace amounts (10 to 20 ppm) of TMA in the feed mixture to result in a catalyst efficiency which is close to the industrial process. Under ambient pressure the PO production rate amounts to  $0.064\text{--}0.080\text{ g h}^{-1}(\text{g cat}^{-1})$ . According to the mechanism postulate  $H_2$  and  $O_2$  react to produce  $H_2O_2$  at the Au surfaces. Once produced the  $H_2O_2$  is converted to Ti-hydroperoxo species at tetrahedrally coordinated Ti sites. Subsequently these hydroperoxo species react with propylene adsorbed at the  $SiO_2$  surface generating PO. Spectroscopic analyses suggest the TMA to be adsorbed at the Au particles, depressing direct  $H_2O$  formation and thus increasing the  $H_2$  efficiency for this process. Furthermore PO and TMA are believed to compete in adsorption at  $Ti^{4+}$  sites, *i.e.* pre-adsorption of TMA at these sites diminishes the adsorption of PO and thus reduces the formation of by-products, which are the main source for catalyst deactivation.

### Phenol synthesis by oxidation of benzene with molecular oxygen

Currently phenol is produced industrially by the cumene process, which converts benzene into phenol, acetone and  $\alpha$ -methylstyrene with a phenol yield as low as 5% based on the benzene used initially. A more efficient phenol synthesis could theoretically be achieved

by oxidizing benzene with oxygen. However, the activation of molecular oxygen in a way that selectively produces only phenol is not an easy task. Iwasawa *et al.* from the University of Tokyo recently undertook studies of this kind employing zeolite catalyst which contained Re-clusters.<sup>4</sup>



The authors found that Re/H-ZSM5 catalysts were able to generate phenol from benzene and molecular oxygen with a selectivity of as high as 94% in the presence of  $NH_3$ . Interestingly only CVD prepared Re/H-ZSM5 catalysts performed acceptably well, while catalysts prepared by impregnation proved to be far less effective. Also the presence of  $NH_3$  was absolutely mandatory, with catalysts being completely inactive in the absence of ammonia, while additives like  $H_2O$  and  $N_2O$  had no positive effects on the catalytic performance either. Detailed activity studies showed the  $SiO_2/Al_2O_3$  ratio of the zeolite to have a large influence on the catalytic performance with a value of 19 to be best in this study. Other zeolite structures such as H-Mordenite, H-Beta and H-USY performed less well. Detailed EXAFS analyses revealed the existence of  $Re_{10}$ -clusters, which by careful interpretation of the analytic data were suggested to be edge-sharing Re-octahedra, which can only exist under the catalytic conditions as long as one interstitial N-atom per octahedron is present, that stem from the  $NH_3$  pre-treatment of the catalyst. These postulations were corroborated successfully by DFT calculations on different cluster models. The catalytic reaction itself proceeds without the presence of ammonia, but then the clusters are turned into inactive Re species during the reaction, indicating the clusters to be unstable in the absence of  $NH_3$ . In the absence of  $O_2$  no catalysis was observed indicating that the oxygen contained in the  $Re_{10}$  cluster framework

is not the oxygen source in the catalytic reaction.

### Voluntary program for the reduction of hydrofluorocarbons in the production of refrigerators and freezers

Hydrofluorocarbons (HFCs) are the replacement of chlorofluorocarbons, formerly used in the manufacturing of cooling equipment, as they were shown to deplete the stratospheric ozone. HFCs don't harm the ozone, however they are greenhouse gases—up to 1300 times more potent than carbon dioxide. HFCs are used in refrigerators and freezers as the “working fluid” and as a “blowing agent” for the insulation foam. To reduce the amount of greenhouse gas emitted to the atmosphere the US environmental protection agency (EPA) and the association of home appliance manufacturers (AHAM) have launched a voluntary program to reduce the emission of HFCs by recommending specific strategies for all stages of production, delivering and storing of refrigerants and blowing agents. This initiative might be very helpful even if only low reductions were achieved as more than 12 million refrigerators and freezers are produced in the United States annually (60 million worldwide).

### EPA energy star label for battery chargers

The US environmental protection agency (EPA) certifies energy efficient products within the Energy Star programme. The latest product family added to the programme are battery chargers for cordless tools which are used for recharging a variety of products including personal care products like electric toothbrushes and electric shavers, garden tools such as weed and hedge trimmers and many more products used in today's households. As more and more devices are becoming cordless energy efficient battery chargers can save a lot of energy as many of them draw as much as 5 to 20 times more energy than is actually stored in the battery. Accordingly the Energy Star guidelines favor chargers with “non-active” modes such as

standby modes (charger is plugged in, but no product is connected) and battery maintenance mode (charger is connected to a fully charged product). In the US the Energy Star labeled products have already helped in saving a lot of energy,

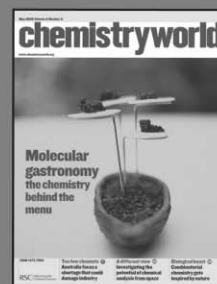
which is estimated to be in the \$10 billion range.

### References

- 1 A. Klust and R. J. Madix, *J. Am. Chem. Soc.*, 2006, DOI: 10.1021/ja054845s.
- 2 G. Roelfes, A. J. Boersma and B. L. Feringa, *Chem. Commun.*, 2006, DOI: 10.1039/b516552k.
- 3 B. Chowdhury, J. J. Bravo-Suarez, M. Date, S. Tsuboty and M. Haruta, *Angew. Chem.*, 2006, **118**, 426.
- 4 R. Bal, M. Tada, T. Sasaki and Y. Iwasawa, *Angew. Chem.*, 2006, **118**, 462.

# chemistryworld

A "must-read" guide to current chemical science!



**Chemistry World** provides an international perspective on the chemical and related sciences by publishing scientific articles of general interest. It keeps readers up-to-date on economic, political and social factors and their effect on the scientific community.

16050521

RSC Publishing

[www.chemistryworld.org](http://www.chemistryworld.org)

# Acute toxicity of ionic liquids to the zebrafish (*Danio rerio*)†

Carlo Pretti,<sup>a</sup> Cinzia Chiappe,<sup>b</sup> Daniela Pieraccini,<sup>b</sup> Michela Gregori,<sup>a</sup> Francesca Abramo,<sup>a</sup> Gianfranca Monni<sup>a</sup> and Luigi Intorre<sup>c</sup>

Received 15th August 2005, Accepted 14th September 2005

First published as an Advance Article on the web 26th September 2005

DOI: 10.1039/b511554j

Acute toxicity and histological damage derived from exposure of *Danio rerio* (zebrafish) to several ionic liquids have been evaluated.

Interest in ionic liquids (ILs) for their potential in different chemical processes is increasing as they are claimed to be environmentally safe and they are very good non-volatile solvents for a wide range of applications.<sup>1</sup> Although the information about physical, thermodynamic, kinetic or engineering data has been extended continuously, only little data with regard to the toxicity and ecotoxicity of ILs have been available until now.<sup>2–4</sup> The “green character” of ILs has usually been justified with their negligible vapour pressure, but even if ILs do not evaporate and do not contribute to air pollution most of them are water soluble and might enter the environment by this path (e.g. accidental spills, effluents).<sup>5</sup> To the best of our knowledge no data are available in the international literature on the acute toxicity of ILs on fish. The aim of the present work was therefore to evaluate the acute toxicity of 15 widely used ILs (bearing different anions and cations, Fig. 1) to fish (zebrafish, *Danio rerio*). Fish were also subjected to histopathological examination.

Acute toxicity of ILs for zebrafish was assessed measuring their lethal effect after 96 h exposure. The main test was preceded by a limit test performed at the concentration of 100 mg L<sup>-1</sup> in order to demonstrate that the LC<sub>50</sub> was greater than this concentration. If mortality occurred in the limit test, the full LC<sub>50</sub> study was then carried out. All tests were performed according to the International Standard Organization procedure 7346.<sup>6</sup> Procedures for the care and management of animals were performed in accordance with the provisions of the EC Council Directive 86/609 EEC, recognised and adopted by the Italian Government (DL 27.01.1992, n° 116). The water temperature was 23 ± 1 °C and fish were kept under normal laboratory illumination with a daily photoperiod of 12 h. No food was provided during the test. On the day of experiment, 10 fish were placed in 5 L-glass aquaria containing test or control solution and aerate to restore the concentration of dissolved oxygen to at least 90% of its air saturation value. ILs were directly dissolved in rearing water. Each

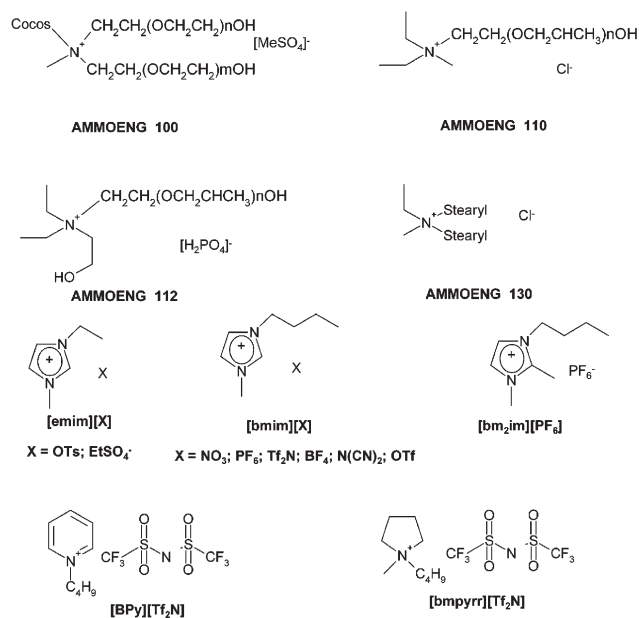


Fig. 1 Ionic liquids tested.

IL was tested at five concentrations (1.25, 2.5, 5.0, 10.0 and 20.0 mg L<sup>-1</sup>). The number of dead was recorded after 1, 12, 24, 48, 72 and 96 h. Acute toxicity was expressed as the median lethal concentration (LC<sub>50</sub>) that is the concentration in water which kills 50% of the test batch of fish within a continuous period of exposure of 96 h. LC comprised in the range of LC1 to LC99 were also determined. The LC values and their 95% confidence limits were determined by probit analysis<sup>7</sup> using a computer software (USEPA Probit Analysis Program used for calculating EC values, version 1.5).

Histopathological examination was performed on control and on all dead fish. Fish were fixed in a 10% buffered formalin solution. The entire fish body was longitudinally sectioned, and placed directly into pre-labelled histological cassettes. Fixed samples were routinely processed and included in paraffin-blocks. Five μm thick whole body sagittal sections were cut and stained with Hematoxylin-Eosin for histological evaluation.

Results of the limit test are shown in Table 1. Thirteen out of 15 of the tested ILs had 96 h LC<sub>50</sub> values greater than 100 mg L<sup>-1</sup>. By contrast mortality was observed for AMMOENG 100<sup>™</sup> and AMMOENG 130<sup>™</sup> which were then subjected to the full LC<sub>50</sub> study. Calculated LCs for AMMOENG 100<sup>™</sup> and AMMOENG 130<sup>™</sup> are shown in Table 2. LCs were similar for both ILs and were in the range of 1.9–13.9 mg L<sup>-1</sup> for AMMOENG 130 and of 2.2–15.4 mg L<sup>-1</sup> for AMMOENG 100<sup>™</sup>. LC<sub>50</sub> were 5.2 mg L<sup>-1</sup>

<sup>a</sup>Dipartimento di Patologia Animale, Profilassi ed Igiene degli Alimenti, Università di Pisa, Viale delle Piagge 2, Pisa, Italy.

E-mail: cpretti@vet.unipi.it; Fax: +39 0502216941; Tel: +39 0502216947

<sup>b</sup>Dipartimento di Chimica Bioorganica e Biofarmacia, Università di Pisa, Via Bonanno 33, Pisa, Italy. E-mail: cinziac@farm.unipi.it; Fax: +39 0502219660; Tel: +39 0502219700

<sup>c</sup>Dipartimento di Clinica Veterinaria, Università di Pisa, Viale delle Piagge 2, Pisa, Italy. E-mail: intorre@vet.unipi.it; Fax: +39 0502216813; Tel: +39 0502216810

† This work was presented at the 1st International Conference on Ionic Liquids (COIL), held in Salzburg, Austria, 19–22 June, 2005.

**Table 1** Limit test ( $100 \text{ mg L}^{-1}$ ) on 15 ionic liquids

Ionic liquids	LC <sub>50</sub> 96 h zebrafish
[bmim][PF <sub>6</sub> ]	>100 mg L <sup>-1</sup>
[bmim][Tf <sub>2</sub> N]	>100 mg L <sup>-1</sup>
[bmim][BF <sub>4</sub> ]	>100 mg L <sup>-1</sup>
[bmim][N(CN) <sub>2</sub> ]	>100 mg L <sup>-1</sup>
ECOENG 212	>100 mg L <sup>-1</sup>
<b>AMMOENG 100</b>	<100 mg L <sup>-1</sup>
[bpyrr][Tf <sub>2</sub> N]	>100 mg L <sup>-1</sup>
[emim][OTs]	>100 mg L <sup>-1</sup>
<b>AMMOENG 130</b>	<100 mg L <sup>-1</sup>
AMMOENG 110	>100 mg L <sup>-1</sup>
AMMOENG 112	>100 mg L <sup>-1</sup>
[bmim][OTf]	>100 mg L <sup>-1</sup>
[BPy][Tf <sub>2</sub> N]	>100 mg L <sup>-1</sup>
[bm <sub>2</sub> im][PF <sub>6</sub> ]	>100 mg L <sup>-1</sup>
[bmim][NO <sub>3</sub> ]	>100 mg L <sup>-1</sup>

**Table 2** 96 h LCs ( $\text{mg L}^{-1}$ , confidence limits 95%)

—	AMMOENG 100™	AMMOENG 130™
LC <sub>1</sub>	2.2 (0.6; 3.3)	1.9 (0.5; 2.9)
LC <sub>5</sub>	2.9 (1.1; 4.1)	2.5 (1.0; 3.5)
LC <sub>10</sub>	3.4 (1.6; 4.6)	3.0 (1.4; 4.0)
LC <sub>15</sub>	3.8 (1.9; 4.9)	3.3 (1.7; 4.3)
LC <sub>50</sub>	5.9 (4.3; 8.0)	5.2 (3.8; 7.0)
LC <sub>85</sub>	9.0 (6.9; 17.9)	8.0 (6.1; 15.6)
LC <sub>90</sub>	10.0 (7.5; 22.3)	8.9 (6.7; 19.4)
LC <sub>95</sub>	11.6 (8.4; 31.1)	10.4 (7.5; 26.9)
LC <sub>99</sub>	15.5 (10.3; 58.6)	13.9 (9.2; 50.5)

and  $5.9 \text{ mg L}^{-1}$  for AMMOENG 130™ and AMMOENG 100™, respectively. These values were remarkably lower than the fish 96 h LC<sub>50</sub> data reported for other solvents such as methanol ( $12\,700\text{--}29\,400 \text{ mg L}^{-1}$ ), dichloromethane ( $>100 \text{ mg L}^{-1}$ ), acetonitrile ( $>100 \text{ mg L}^{-1}$ ), aniline (up to  $100 \text{ mg L}^{-1}$ ), and triethylamine ( $44 \text{ mg L}^{-1}$ ) indicating a high lethality potential of the tested ILs in fish (source: individual Material Safety Data Sheets).

No behavioural changes were observed in control fish. On the contrary, treated fish exposed to both ILs at concentrations of  $10 \text{ mg L}^{-1}$  or more showed, compared to controls, reduction in general activity, loss of equilibrium, erratic swimming and staying motionless at mid-water level for prolonged periods.

The gills and the skin of control zebrafish appeared normal and well formed (Fig. 2 and 3).

After exposure to AMMOENG 100™ or AMMOENG 130™, the gross structure of gill primary filaments appeared normal, while secondary gill lamellae showed marked disorganization (Fig. 4).

The main abnormalities observed were represented by desquamation of the epithelium, hypertrophy (hyperplasia) and lifting up of epithelial layer from the pillar cells. Additionally to these changes, intraepithelial oedema and cytoplasmic vacuolation within epithelial cells were observed (Fig. 4). In all treated fish the epidermal covering of the skin showed a variable degree of hyperplasia (mild to marked) in the dorsal, ventral and cephalic area (Fig. 5). In the hyperplastic areas most of the epidermal cells contained distinct intracytoplasmic vacuolation; the fusion of affected adjacent cells gave rise to small skin vesicles (Fig. 5). Wide erosions were focally present in the superficial layer (Fig. 5), while secondary gill lamellae showed marked disorganization (Fig. 4).



**Fig. 2** Control fish. Histological section of gills. Primary lamellae (pl) and parallel structure of the secondary lamellae (sl) are observed. The secondary lamellae are covered by epithelial cells (H&E where H = haematoxylin and E = eosin, bar =  $50 \mu\text{m}$ ).

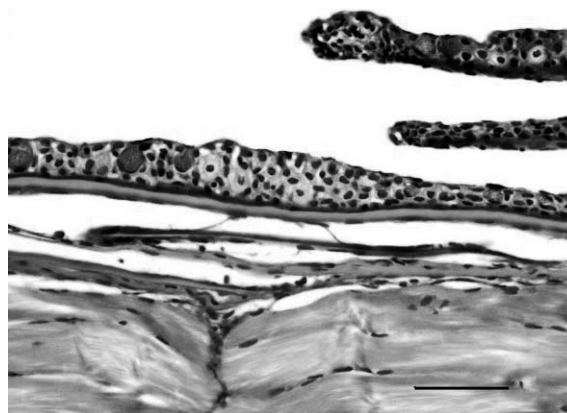


**Fig. 3** Control fish. Histological sections of the skin. The skin epidermis is composed of 3-4 epithelial layers; goblet cells are also present (H&E, bar =  $50 \mu\text{m}$ ).

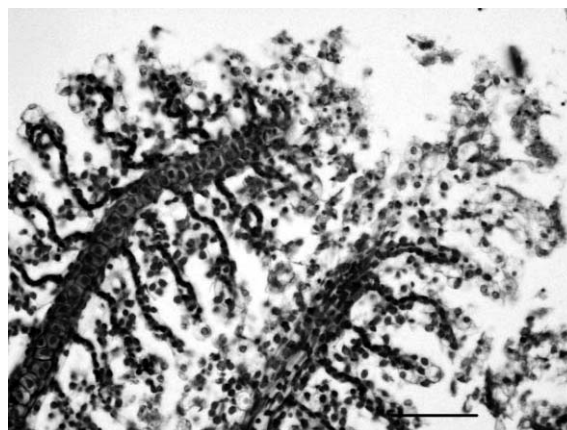


**Fig. 4** Treated fish. Enlargement and disorganization of secondary lamellae with disepithelialization. Lifted epithelial cells show intracytoplasmic vacuolation (H&E, bar =  $50 \mu\text{m}$ ).

The histological alterations induced by AMMOENG 100™ and AMMOENG 130™ correlate with the well known surfactant action of these ammonium salts on biological membranes which

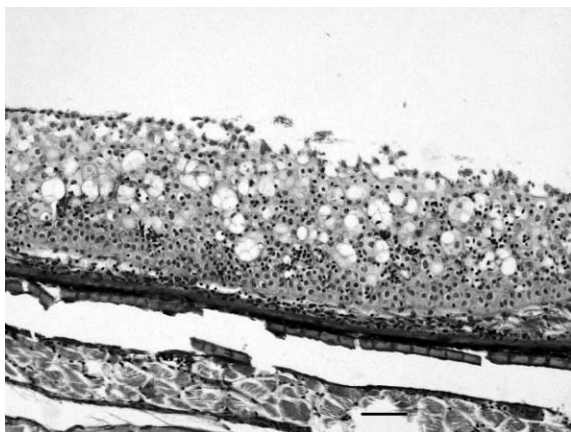


**Fig. 5** Treated fish. Marked hyperplasia of the skin, intracytoplasmic vacuolization within the epithelial cells and erosions of the superficial layer (H&E, bar = 50  $\mu\text{m}$ ).

increases membrane permeability altering the physical properties of the lipid bilayer and also enhancing its permeability for external ions. In particular, increased  $\text{Ca}^{2+}$  influx from the external medium into the cytoplasm which results in detachment of the membranes has been observed following exposure of cells to lipophilic chemicals.<sup>8</sup> It may be speculated that the cellular damage induced by AMMOENG 100<sup>TM</sup> and AMMOENG 130<sup>TM</sup> in terms of vacuolations might have impaired the gill and the skin functions, reducing the respiratory surface area and interrupting the integrity of the external barrier, respectively. In particular, modifications in the relatively thin lamellar epithelium of the gills may have affected the fish gas-exchange capability.<sup>9</sup>

The acute toxicity towards zebrafish of several ionic liquids with different anions and cations has been assessed. The results presented in this paper clearly reveal that ionic liquids may cause a completely different effect on fish according to their chemical structure. As imidazolium, pyridinium and pyrrolidinium showed a  $\text{LC}_{50} > 100 \text{ mg L}^{-1}$ , they can be regarded as non-highly lethal towards zebrafish. On the other hand, the ammonium salts

AMMOENG 100<sup>TM</sup> and AMMOENG 130<sup>TM</sup> showed  $\text{LC}_{50}$  values remarkably lower than that reported for organic solvents and tertiary amines. Histological evaluation of dead zebrafish showed skin alteration represented by epithelial hyperplasia with single keratinocyte vesiculation and wide erosions together with disepithelialization of gill lamellae. Considering that both the anion and the cation have been changed in these two latter compounds, in principle it is not possible to identify which part of the salt is responsible of the detrimental effect on aquatic environment. By the way, the known toxic effect exerted by cationic surfactants<sup>8</sup> suggests that modifications of the cationic counterpart are responsible for the toxic behaviour of these new solvents. This observation is in agreement with recent published papers dealing with ionic liquids biodegradability<sup>10</sup> and their effect on other aquatic trophic levels.<sup>3,4</sup>

## References

- (a) K. Seddon, *Green Chem.*, 2002, **4**, G35; (b) R. D. Rogers and K. R. Seddon, *Ionic Liquids: Industrial Applications to Green Chemistry*, ACS Symposium Series 818, American Chemical Society, Washington, DC, 2002.
- R. J. Bernot, M. A. Brueske, M. A. Evans-White and G. A. Lamberti, *Environ. Toxicol. Chem.*, 2005, **24**, 87.
- A. Latala, P. Stepnowski, M. Nedzi and W. Mrocz, *Aquat. Toxicol.*, 2005, **73**, 91.
- R. J. Bernot, E. E. Kennedy and G. A. Lamberti, *Environ. Toxicol. Chem.*, 2005, **24**, 1759.
- Z. B. Alfassi, R. E. Huie, B. L. Milman and P. Neta, *Anal. Bioanal. Chem.*, 2003, **377**, 159.
- ISO, International Organization for Standardization, Geneva, Switzerland, 1996b, ISO/DIS 7346-1.
- D. J. Finney, *Probit Analysis*, Cambridge University Press, Cambridge, 3rd edn, 1971.
- (a) J. Cross, *Introduction to cationic surfactants: Analytical and Biological Evaluation*, Marcel Dekker, Inc., New York, 3rd edn, 1994; (b) J. Gartzke, K. Lange, U. Brandt and J. Bergmann, *Sci. Total Environ.*, 1997, **199**, 213.
- H. M. Lease, Ph Master's Thesis, University of Wyoming, Laramie, WY, 2001.
- (a) M. T. Garcia, N. Gathergood and P. J. Scammells, *Green Chem.*, 2005, **7**, 9; (b) N. Gathergood, M. T. Garcia and P. J. Scammells, *Green Chem.*, 2004, **6**, 166; (c) N. Gathergood and P. J. Scammells, *Aust. J. Chem.*, 2002, **55**, 557.



# Decomposition of ionic liquids in electrochemical processing†

Maaïke C. Kroon,<sup>ab</sup> Wim Buijs,<sup>c</sup> Cor J. Peters<sup>a</sup> and Geert-Jan Witkamp<sup>\*b</sup>

Received 9th September 2005, Accepted 31st October 2005

First published as an Advance Article on the web 17th November 2005

DOI: 10.1039/b512724f

The stability of ionic liquids with respect to high voltage differences is important for their use in electrochemical applications. Ionic liquids decompose when voltage differences larger than their electrochemical window (4–6 V) are applied. However, little is known about the decomposition mechanism and products. In this work the electrochemical breakdown of the ionic liquids 1,1-butylmethylpyrrolidinium bis(trifluoromethylsulfonyl)imide and 1-butyl-3-methylimidazolium tetrafluoroborate on the cathode is predicted using quantum chemical calculations and validated by experiments. The quantum chemical calculations showed to be an excellent method to predict the electrochemical decomposition reactions and products.

## Introduction

In the last two decades ionic liquids have received much interest for use as water-free electrolytes. Ionic liquids are molten salts with melting points close to room temperature.<sup>1–3</sup> The use of ionic liquids as electrolytes in electrochemical processing is promising, because it can solve some problems of traditional liquid electrolytes. Ionic liquids show large electrochemical stabilities<sup>4–6</sup> and high ionic conductivities.<sup>6,7</sup> Moreover, they are non-volatile and non-flammable and possess lower toxicity compared to conventional mixed electrolyte systems.<sup>8</sup> In principle, ionic liquids can be tailored for a specific application by the right choice of cation and anion.<sup>1,2</sup> Applications include the use of ionic liquids as electrolytes in fuel cells,<sup>9</sup> solar cells,<sup>10</sup> electrochemical capacitors<sup>11–13</sup> and battery systems.<sup>14</sup> A high electrochemical stability of ionic liquids is indispensable to reach a high energy and power density of these electrochemical devices.

The electrochemical stability of an ionic liquid is manifested by the width of the electrochemical window. This is the range of voltages over which the ionic liquid is electrochemically inert.<sup>1</sup> Many research groups have measured the electrochemical window of a wide variety of ionic liquids.<sup>4–6,8,15–18</sup> They found that phosphonium-, ammonium-, pyrrolidinium- and piperidinium-based ionic liquids with triflate or triflyl anions have the largest electrochemical windows.<sup>5,6,14,15,18</sup> Moreover, it was found that impurities like residual halides and water have a profound impact on the electrochemical stability of the ionic liquid.<sup>1,19</sup> However, a detailed study on

the electrochemical reactions at the cathode and anode limits of different ionic liquids does not exist. However, it is believed that at these limits, the cathodic reaction is the reduction of the cation,<sup>7,17,20</sup> and the anodic reaction is oxidation of the anion.<sup>4,7,21</sup> Further studies are necessary to characterize the reactions at both the cathodic and anodic limits of ionic liquids when voltages larger than their electrochemical window are applied.

Quantum chemical calculations have been used to predict the electrochemical stability of ionic liquids.<sup>21,22</sup> In our previous study we showed that the potential of the cathode limit (reductive stability) can be correlated to the lowest unoccupied molecular orbital (LUMO) energy level of the cation.<sup>22</sup> Also, Koch *et al.*<sup>21</sup> have correlated the electrochemical oxidation potentials of several anions with their respective highest occupied molecular orbital (HOMO) energies. Other data obtained by quantum chemical calculations on ionic liquids include structural information<sup>23–26</sup> and vibrational spectra.<sup>24–27</sup> Quantum chemical calculations can also be used to predict reaction paths for all sorts of reacting systems.<sup>28</sup> For example, they are able to predict the type of electrochemical decomposition reactions and products that occur when voltages higher than the electrochemical window are applied over the ionic liquid, but their use for this purpose has never been described.

In this work the electrochemical breakdown phenomena in the ionic liquids 1,1-butylmethylpyrrolidinium bis(trifluoromethylsulfonyl)imide ([bmpyrrol<sup>+</sup>][NTf<sub>2</sub><sup>-</sup>]) and 1-butyl-3-methylimidazolium tetrafluoroborate ([bmim<sup>+</sup>][BF<sub>4</sub><sup>-</sup>]) on the cathode side under high voltages are predicted using quantum chemical calculations and verified by experiments. It may be complicated to prove that the predicted decomposition products are formed, because it is difficult to separate the decomposition products from the ionic liquid. A reason for this is that these molecules resemble each other. Moreover, ionic liquids do not have a measurable vapor pressure. As a result analytical methods such as GC and HPLC are difficult to perform. Therefore, a good design of the experiments on the basis of the expected decomposition products is important for the validation of the quantum chemical results.

<sup>a</sup>Physical Chemistry and Molecular Thermodynamics, Department of Chemical Technology, Faculty of Applied Sciences, Delft University of Technology, Julianalaan 136, 2628 BL Delft, The Netherlands

<sup>b</sup>Laboratory for Process Equipment, Department of Process & Energy, Faculty of Mechanical, Maritime and Materials Engineering, Delft University of Technology, Leeghwaterstraat 44, 2628 CA Delft, The Netherlands. E-mail: G.J.Witkamp@3me.tudelft.nl; Fax: +31-15-2786975; Tel: +31-15-2783602

<sup>c</sup>Biocatalysis and Organic Chemistry, Department of Chemical Technology, Faculty of Applied Sciences, Delft University of Technology, Julianalaan 136, 2628 BL Delft, The Netherlands

† This work was presented at the 1st International Conference on Ionic Liquids (COIL), held in Salzburg, Austria, 19–22 June, 2005.

## Experimental

### Computational methods

All quantum chemical calculations were carried out using the Spartan '04 molecular modeling suite of programs.<sup>29</sup> All structures were fully optimized on the semi-empirical level (PM3).<sup>28</sup>

### Materials

The ionic liquid [bmpyrrol<sup>+</sup>][NTf<sub>2</sub><sup>-</sup>] was prepared with a purity of >99.0% as previously described.<sup>30</sup> The purity was measured using <sup>1</sup>H NMR (300.2 MHz., DMSO, TMS): δ 0.92 (t, 3H), 1.33 (m, 2H), 1.69 (m, 2H), 2.11 (s, 4H), 2.98 (s, 3H), 3.29 (m, 2H), 3.44 (m, 4H). The ionic liquid [bmim<sup>+</sup>][BF<sub>4</sub><sup>-</sup>] was prepared according to the method of Huddleston *et al.*<sup>31</sup> with a purity of >99.0%. The purity was measured using boron analysis (ICP-AES) and NMR analysis. <sup>1</sup>H NMR (300.2 MHz., CDCl<sub>3</sub>, TMS): δ 0.93 (t, 3H), 1.34 (m, 2H), 1.86 (m, 2H), 3.95 (s, 3H), 4.20 (t, 2H), 7.47 (s, 2H), 8.71 (s, 1H). Prior to use both ionic liquids were dried under vacuum conditions in the presence of calcium chloride at room temperature for several days. The water content of the dried ionic liquids was measured using Karl Fischer moisture analysis and was <10 ppm.

### Electrochemical decomposition

An electrochemical cell with two glassy carbon electrodes (inter-electrode distance = 2.5 cm, electrode area = 1.3 cm<sup>2</sup>) was filled with ionic liquid. Voltage differences larger than the electrochemical window (8 V) were applied over the ionic liquid at room temperature during 3 h. Thereafter, the power source was shut down and the electrochemically decomposed ionic liquid was analyzed. The decomposition products from electrochemically decomposed [bmpyrrol<sup>+</sup>][NTf<sub>2</sub><sup>-</sup>] were extracted with toluene. Thereafter the toluene phase was analyzed using gas chromatography and mass spectroscopy (GC-MS), type VG70-250SE, operated in the electron impact ionization mode at 70 eV. From the decomposed [bmim<sup>+</sup>][BF<sub>4</sub><sup>-</sup>] the <sup>1</sup>H and <sup>13</sup>C (Attached Proton Test) nuclear magnetic resonance (NMR) spectra were measured (Varian Unity Inova 300 s) and compared to the NMR spectra of the pure [bmim<sup>+</sup>][BF<sub>4</sub><sup>-</sup>] in order to see the changes in ionic liquid structure.

## Results and discussion

In this work the electrochemical reactions that occur at the cathodic limit of the ionic liquids [bmpyrrol<sup>+</sup>][NTf<sub>2</sub><sup>-</sup>] and [bmim<sup>+</sup>][BF<sub>4</sub><sup>-</sup>] are studied. On the cathodic limit the ionic liquid is reduced, which means that an electron is added to the ionic liquid molecule. For most ionic liquids, it is easier to reduce the cation than the anion (exceptions are the acidic chloroaluminate ionic liquids, where the reduction of the heptachloroaluminate (Al<sub>2</sub>Cl<sub>7</sub><sup>-</sup>) anion is the limiting cathode process).<sup>1,7,17,20,22</sup> The reduction of the cation, in principle, leads to the formation of the analogous radical. Therefore, in order to predict the electrochemical reactions that take place at the cathodic limit, these radicals should be modeled.

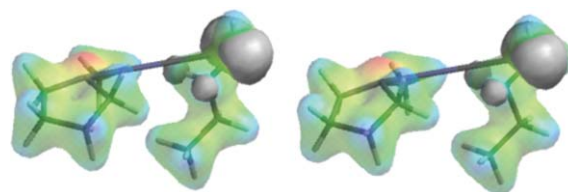


**Fig. 1** Stereo-graphic of the decomposition of the 1,1-butylmethylpyrrolidinium radical into methylpyrrolidine and a butyl radical (surface = electron density of 0.08 e au<sup>-3</sup>; property = electrostatic potential). The electron density is high at the red positions (large negative values of the potential) and low at the blue positions (large positive values of the potential). The grey positions indicate a high spin density.

Generally, radicals can undergo different types of reactions. First of all, it is possible that the radical itself is not stable and will decompose into a neutral fragment and a smaller more stable radical. Secondly, two radicals can react with each other under the formation of one neutral molecule (radical–radical coupling) or two neutral molecules (disproportionation). Finally, radicals can react with alkenes, where the radical combines with one of the electrons of the π-bond under the formation of a larger radical (radical addition reaction).

When an electron is added to the [bmpyrrol<sup>+</sup>] cation, the resulting radical is not stable and will decompose into a neutral molecule and a smaller radical, according to quantum chemical calculations (PM3). Three possible decomposition reactions are predicted. The most likely solution (lowest energy level of the formed radical,  $E = -61$  kJ mol<sup>-1</sup> in vacuum) is that the 1,1-butylmethylpyrrolidinium radical will decompose into methylpyrrolidine and a butyl radical (Fig. 1 and 2). Another solution, but less likely than the first one ( $E = -43$  kJ mol<sup>-1</sup>), is that the radical will decompose into a dibutylmethylamine radical by ring opening, where the unpaired electron is located on one of the butyl groups (Fig. 3 and 4). The last solution with the lowest probability ( $E = -21$  kJ mol<sup>-1</sup>) is that the radical decomposes into butylpyrrolidine and a methyl radical (Fig. 5 and 6).

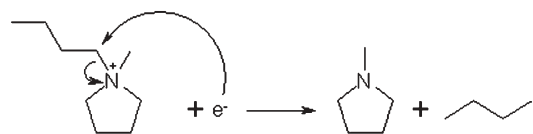


**Fig. 2** Formation of methylpyrrolidine and the butyl radical.

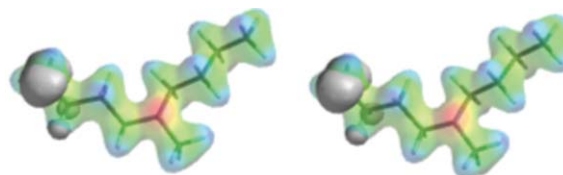


**Fig. 3** Stereo-graphic of the decomposition of the 1,1-butylmethylpyrrolidinium radical into a dibutylmethylamine radical (surface = electron density of 0.08 e au<sup>-3</sup>; property = electrostatic potential). The electron density is high at the red positions (large negative values of the potential) and low at the blue positions (large positive values of the potential). The grey positions indicate a high spin density.

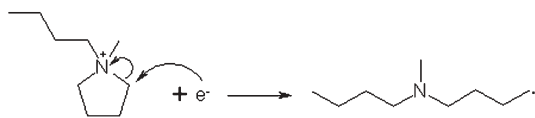


Fig. 4 Formation of the dibutylmethylamine radical.

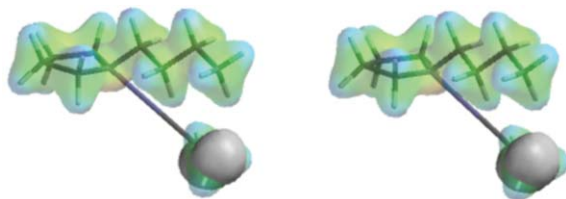


Fig. 5 Stereo-graphic of the decomposition of the 1,1-butylmethylpyrrolidinium radical into butylpyrrolidine and a methyl radical (surface = electron density of  $0.08 \text{ e au}^{-3}$ ; property = electrostatic potential). The electron density is lowest at the blue positions (largest positive values of the potential). The grey positions indicate a high spin density.

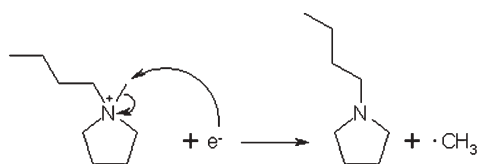


Fig. 6 Formation of butylpyrrolidine and the methyl radical.

However, when an electron is added to the [bmim<sup>+</sup>] cation, the resulting radical is stable and the radical will not decompose ( $E = 75 \text{ kJ mol}^{-1}$ ). According to quantum chemical semi-empirical calculations, the unpaired electron is located mainly on the C2 carbon (Fig. 7). In contrast to the [bmim<sup>+</sup>] cation, the 1-butyl-3-methylimidazolium radical has no resonance possibilities and is thus less aromatic (Fig. 8). The 1-butyl-3-methylimidazolium radical can undergo several reactions. The most probable solution is that two radicals react with each other under the formation of a dimer (radical–radical coupling). Fig. 9 and 10 show the lowest energy conformation ( $E = 33 \text{ kJ mol}^{-1}$ ) of the dimer. Another solution ( $E = 41 \text{ kJ mol}^{-1}$ ) is that the radical picks up a hydrogen atom from another radical present in the system (disproportionation). This transfer of a hydrogen atom from

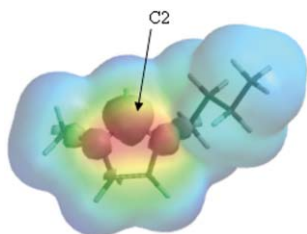


Fig. 7 Structure and electrostatic potential (surface = electron density of  $0.002 \text{ e au}^{-3}$ ; property = electrostatic potential) of the 1-butyl-3-methylimidazolium radical (at the semi-empirical PM3 level). The electron density is high at the red positions (large negative values of the potential) and low at the blue positions (large positive values of the potential). The grey lobes (on the C2 atom and adjacent positions) indicate a high spin density.

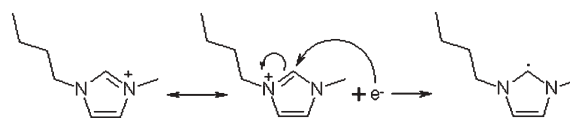


Fig. 8 Formation of the 1-butyl-3-methylimidazolium radical.

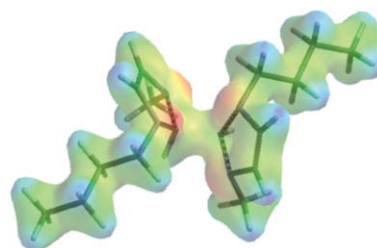


Fig. 9 1-Butyl-3-methylimidazolium radical coupling (surface = electron density of  $0.08 \text{ e au}^{-3}$ ; property = electrostatic potential). The electron density is high at the red positions (large negative values of the potential) and low at the blue positions (large positive values of the potential).

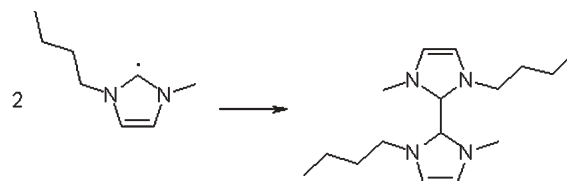


Fig. 10 Coupling reaction of two 1-butyl-3-methylimidazolium radicals.

one radical to another results in the formation of an alkane and an alkene (Fig. 11 and 12). The last solution (but not likely due to the very high energy,  $E = 235 \text{ kJ mol}^{-1}$ ) is that the radical reacts with the double bond from another radical under the formation of a cage-like structure (Fig. 13 and 14).

The predicted results for the electrochemical decomposition of both ionic liquids were verified with experiments. Since the predicted electrochemical decomposition products of [bmprrol<sup>+</sup>][NTf<sub>2</sub><sup>-</sup>] are small and soluble in toluene, but

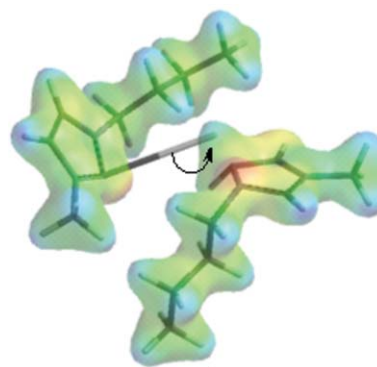
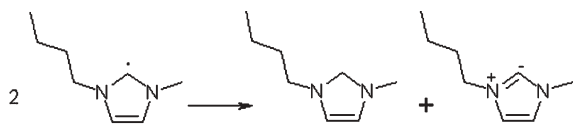
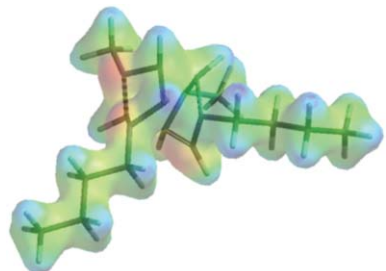


Fig. 11 Reaction of two 1-butyl-3-methylimidazolium radicals, resulting in hydrogen transfer/disproportionation (surface = electron density of  $0.08 \text{ e au}^{-3}$ ; property = electrostatic potential). The electron density is high at the red positions (large negative values of the potential) and low at the blue positions (large positive values of the potential).



**Fig. 12** Disproportionation reaction of two 1-butyl-3-methylimidazolium radicals.



**Fig. 13** Reaction of 1-butyl-3-methylimidazolium radical with the double bond of another radical, leading to cage-formation (surface = electron density of  $0.08 \text{ e au}^{-3}$ ; property = electrostatic potential). The electron density is high at the red positions (large negative values of the potential) and low at the blue positions (large positive values of the potential).

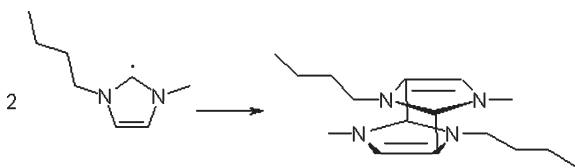


**Fig. 14** Cage-formation reaction of two 1-butyl-3-methylimidazolium radicals.

the ionic liquid itself is not, it was decided to extract the decomposition products with toluene. Thereafter, the toluene phase was analyzed with GC-MS, where the different decomposition products were separated and identified. The detected decomposition products are listed in Table 1.

From Table 1 it can be concluded that all three predicted decomposition reactions occur. The presence of methylpyrrolidine, octanes, octenes and 2-butanol in the toluene phase prove that the 1,1-butylmethylpyrrolidinium radical has decomposed into methylpyrrolidine and a butyl radical. The octanes are formed by a reaction of two butyl radicals with each other (radical–radical coupling). Because a secondary radical is more stable than a primary radical, the unpaired electron in the butyl radical will be located on the 2-position. Therefore, from all possible octane isomers it is most probable

**Table 1** Detected decomposition products of  $[\text{bmpyrrol}^+][\text{NTf}_2^-]$  using GC-MS

Compound	Peaks
1-Methylpyrrolidine ( $\text{C}_5\text{H}_{11}\text{N}$ )	$m/z = 85(\text{M}), 57$
Octanes ( $\text{C}_8\text{H}_{18}$ )	$m/z = 114(\text{M}), 85, 71, 57$
Octenes ( $\text{C}_8\text{H}_{16}$ )	$m/z = 112(\text{M}), 97, 69, 55$
2-Butanol ( $\text{C}_4\text{H}_{10}\text{O}$ )	$m/z = 74(\text{M}), 59, 45$
Dibutylmethylamine ( $\text{C}_9\text{H}_{21}\text{N}$ )	$m/z = 143(\text{M}), 128, 99, 85, 71, 57$
1-Butylpyrrolidine ( $\text{C}_8\text{H}_{17}\text{N}$ )	$m/z = 127(\text{M}), 84, 55$

that 3,4-dimethylhexane is the main product. The peaks in the mass spectrum indeed correspond with library search results for 3,4-dimethylhexane with a NIST library matching factor of 96.5%. The identified 2-butanol also indicates that 2-butyl radicals are formed during the electrochemical decomposition of  $[\text{bmpyrrol}^+][\text{NTf}_2^-]$ , because 2-butanol is produced by reaction of the 2-butyl radical with chloride, followed by reaction of 2-butyl chloride with water (chloride and water are both impurities present in the ionic liquid in ppm-range). The octenes are formed by reaction of a butyl radical with a butene molecule, which in turn is produced together with butane in a disproportionation reaction of two butyl radicals. No butane was detected in the decomposition product mixture due to its low boiling point. The second decomposition reaction, where the 1,1-butylmethylpyrrolidinium radical decomposes by a ring opening reaction, is proven by the presence of dibutylmethylamine in the decomposition product mixture. Even the decomposition reaction with the lowest probability according to quantum chemical calculations has proceeded; butylpyrrolidine was also detected in the toluene phase. So all the expected decomposition reaction products were found and all the found chemicals were predicted. Therefore, it is believed that all decomposition products can be dissolved and extracted in toluene. Finally, as a blank the pure ionic liquid  $[\text{bmpyrrol}^+][\text{NTf}_2^-]$  was extracted with toluene. None of the decomposition compounds could be detected.

Also, the electrochemical decomposition products of  $[\text{bmim}^+][\text{BF}_4^-]$  predicted by quantum chemical calculations were verified in experiments. Since the predicted decomposition products are large dimers that are very similar to the monomer, it is difficult to separate them using chromatography. Therefore, it was decided to measure an NMR spectrum of the electrochemically decomposed  $[\text{bmim}^+][\text{BF}_4^-]$  and to compare this with the NMR spectrum of pure  $[\text{bmim}^+][\text{BF}_4^-]$  in order to see the changes in ionic liquid structure.

In Table 2 the  $^1\text{H}$  NMR spectra of electrochemically decomposed and pure  $[\text{bmim}^+][\text{BF}_4^-]$  are compared. From Table 2 it can be concluded that the position of only one peak (the hydrogen attached to the C2 carbon) has changed from  $\delta = 8.71$  to lower chemical shifts ( $\delta = 5.72$ ). This means that the hydrogen in the decomposition products is no longer connected to an aromatic carbon, which is consistent with the predicted radical structure. The  $^{13}\text{C}$  APT NMR spectrum of electrochemically decomposed and pure  $[\text{bmim}^+][\text{BF}_4^-]$  are compared in Table 3. The  $^{13}\text{C}$  APT NMR spectra are similar, except for the last peak, which is positive (and small) in the

**Table 2** Comparison of  $^1\text{H}$  NMR spectra of pure  $[\text{bmim}^+][\text{BF}_4^-]$  and electrochemically decomposed  $[\text{bmim}^+][\text{BF}_4^-]$  (300.2 MHz,  $\text{CDCl}_3$ , TMS)

$\delta$ ( $^1\text{H}$ NMR) pure $[\text{bmim}^+][\text{BF}_4^-]$		$\delta$ ( $^1\text{H}$ NMR) electrochemically decomposed $[\text{bmim}^+][\text{BF}_4^-]$	
0.93	(t, 3H)	0.91	(t, 3H)
1.34	(m, 2H)	1.30	(m, 2H)
1.86	(m, 2H)	1.81	(m, 2H)
3.95	(s, 3H)	3.89	(s, 3H)
4.20	(t, 2H)	4.20	(t, 2H)
7.47	(s, 2H)	5.72	(s, 1H)
8.71	(s, 1H)	7.67	(d, 1 H)
		7.74	(d, 1H)

**Table 3** Comparison of  $^{13}\text{C}$  APT NMR spectra of pure  $[\text{bmim}^+][\text{BF}_4^-]$  and electrochemically decomposed  $[\text{bmim}^+][\text{BF}_4^-]$  (300.2 MHz,  $\text{CDCl}_3$ , TMS)

$\delta$ ( $^{13}\text{C}$ NMR) pure $[\text{bmim}^+][\text{BF}_4^-]$		$\delta$ ( $^{13}\text{C}$ NMR) electrochemically decomposed $[\text{bmim}^+][\text{BF}_4^-]$	
13.34	( $\text{CH}_3$ )	13.18	( $\text{CH}_3$ )
19.33	( $\text{CH}_2$ )	18.84	( $\text{CH}_2$ )
31.93	( $\text{CH}_2$ )	31.43	( $\text{CH}_2$ )
36.12	( $\text{CH}_3$ )	35.68	( $\text{CH}_3$ )
49.69	( $\text{CH}_2$ )	48.68	( $\text{CH}_2$ )
122.57	(CH)	122.27	(CH)
123.87	(CH)	123.58	(CH)
136.07	(CH)	136.53	(C or $\text{CH}_2$ )

electrochemically decomposed  $[\text{bmim}^+][\text{BF}_4^-]$ , indicating a C or  $\text{CH}_2$  carbon, and negative (and large) in the pure  $[\text{bmim}^+][\text{BF}_4^-]$ , indication a CH carbon. Therefore, when  $[\text{bmim}^+][\text{BF}_4^-]$  is electrochemically decomposed, the disproportionation reaction is the most probable decomposition reaction. Dimer formation is also possible, because the peaks from corresponding carbons in both monomers are located exactly at the same position (the corresponding carbons are identical) and no additional peaks are noticed in the  $^{13}\text{C}$  spectrum. Cage formation has not taken place, since that would change the chemical nature of the compound and shifts in the peak positions are not detected. This also followed from the quantum chemical calculations that predicted a very high energy barrier for the cage formation.

The quantum chemical calculations at the semi-empirical level (PM3) are able to predict the electrochemical decomposition reactions and products of these two ionic liquids well. In this case there is no need for a more rigorous quantum chemical method.

## Conclusions

Quantum chemical calculations are an excellent tool to predict the possible electrochemical breakdown products of ionic liquids. Semi-empirical PM3 calculations are sufficient. The electrochemical decomposition of the ionic liquids  $[\text{bmpyrrol}^+][\text{NTf}_2^-]$  and  $[\text{bmim}^+][\text{BF}_4^-]$  on the cathode limit were successfully predicted and verified by experiments.  $[\text{Bmpyrrol}^+][\text{NTf}_2^-]$  decomposes into methylpyrrolidine, octanes, octenes, 2-butanol, dibutylmethylamine and butylpyrrolidine. In the electrochemical breakdown of  $[\text{bmim}^+][\text{BF}_4^-]$ , 1-butyl-3-methylimidazolium radicals are formed, that react with each other in a radical-radical coupling reaction and in a disproportionation reaction. All the expected decomposition reaction products were found and all the found chemicals were predicted.

## Acknowledgements

The authors would like to thank J. van Spronsen, A. van Estrik and A. H. Knol-Kalkman for their help.

## References

- 1 *Ionic Liquids in Synthesis*, ed. P. Wasserscheid and T. Welton, Wiley-VCH Verlag, Weinheim, 2003.
- 2 M. J. Earle and K. R. Seddon, *Pure Appl. Chem.*, 2000, **72**, 1391–1398.
- 3 J. G. Huddleston, A. E. Visser, W. M. Reichert, H. D. Willauer, G. A. Broker and R. D. Rogers, *Green Chem.*, 2001, **3**, 156–164.
- 4 P. A. Z. Suarez, V. M. Selbach, J. E. L. Dullius, S. Einloft, C. M. S. Piatnicki, D. S. Azambuja, R. F. de Souza and J. Dupont, *Electrochim. Acta*, 1997, **42**, 2533–2535.
- 5 J. Sun, M. Forsyth and D. R. MacFarlane, *J. Phys. Chem. B*, 1998, **102**, 8858–8864.
- 6 K. Matsumoto, R. Hagiwara and Y. Ito, *Electrochem. Solid State Lett.*, 2004, **7**, E41–E44.
- 7 P. Bonhôte, A. P. Dias, N. Papageorgiou, K. Kalyanasundaram and M. Grätzel, *Inorg. Chem.*, 1996, **35**, 1168–1178.
- 8 R. Hagiwara and Y. Ito, *J. Fluorine Chem.*, 2000, **105**, 221–227.
- 9 R. Hagiwara, T. Nohira, K. Matsumoto and Y. Tamba, *Electrochem. Solid State Lett.*, 2005, **8**, A231–A233.
- 10 N. Papageorgiou, Y. Athanassov, M. Armand, P. Bonhôte, H. Pettersson, A. Azam and M. Grätzel, *J. Electrochem. Soc.*, 1996, **143**, 3099–3108.
- 11 A. B. McEwen, H. L. Ngo, K. LeCompte and J. L. Goldman, *J. Electrochem. Soc.*, 1999, **146**, 1687–1695.
- 12 M. Ue, M. Takeda, A. Toriumi, A. Kominato, R. Hagiwara and Y. Ito, *J. Electrochem. Soc.*, 2003, **150**, A499–A502.
- 13 T. Sato, G. Masuda and K. Takagi, *Electrochim. Acta*, 2004, **49**, 3603–3611.
- 14 H. Sakaebe and H. Matsumoto, *Electrochem. Commun.*, 2003, **5**, 594–598.
- 15 S. Forsyth, J. Golding, D. R. MacFarlane and M. Forsyth, *Electrochim. Acta*, 2001, **46**, 1753–1757.
- 16 R. Hagiwara, T. Hirashige, T. Tsuda and Y. Ito, *J. Electrochem. Soc.*, 2002, **149**, D1–D6.
- 17 J. Fuller, R. T. Carlin and R. A. Osteryoung, *J. Electrochem. Soc.*, 1997, **144**, 3881–3886.
- 18 D. R. MacFarlane, P. Meakin, J. Sun, N. Amini and M. Forsyth, *J. Phys. Chem. B*, 1999, **103**, 4164–4170.
- 19 U. Schröder, J. D. Wadhawan, R. G. Compton, F. Marken, P. A. Z. Suarez, C. S. Consorti, R. F. de Souza and J. Dupont, *New J. Chem.*, 2000, **24**, 1009–1015.
- 20 C. Nanjundiah, S. F. McDevitt and V. R. Koch, *J. Electrochem. Soc.*, 1997, **144**, 3392–3397.
- 21 V. R. Koch, L. A. Dominey, C. Nanjundiah and M. J. Ondrechen, *J. Electrochem. Soc.*, 1996, **143**, 798–803.
- 22 M. C. Kroon, W. Buijs, C. J. Peters and G. J. Witkamp, *J. Electrochem. Soc.*, submitted.
- 23 Z. Meng, A. Dölle and W. R. Carper, *J. Mol. Struct. (THEOCHEM)*, 2002, **585**, 119–128.
- 24 J. H. Antony, D. Mertens, T. Breitenstein, A. Dölle, P. Wasserscheid and W. R. Carper, *Pure Appl. Chem.*, 2004, **76**, 255–261.
- 25 G. J. Mains, E. A. Nantsis and W. R. Carper, *J. Phys. Chem. A*, 2001, **105**, 4371–4378.
- 26 S. A. Katsyuba, P. J. Dyson, E. E. Vandyukova, A. V. Chernova and A. Vidis, *Helv. Chim. Acta*, 2004, **87**, 2556–2565.
- 27 Y. U. Paulechka, G. J. Kabo, A. V. Blokhin and O. A. Vydrov, *J. Chem. Eng. Data*, 2003, **48**, 457–462.
- 28 W. J. Hehre, *A Guide to Molecular Mechanics and Quantum Chemical Calculations*, Wavefunction, Inc., Irvine, 2003.
- 29 Wavefunction, Inc., 18401 Von Karman Avenue, Suite 370, Irvine, CA 92612, USA.
- 30 N. L. Lancaster, P. A. Salter, T. Welton and G. B. Young, *J. Org. Chem.*, 2002, **67**, 8855–8861.
- 31 J. G. Huddleston, H. D. Willauer, R. P. Swatloski, A. E. Visser and R. D. Rogers, *Chem. Commun.*, 1998, 1765–1766.

# Recovery of pure products from ionic liquids using supercritical carbon dioxide as a co-solvent in extractions or as an anti-solvent in precipitations†

Maaïke C. Kroon,<sup>ab</sup> Jaap van Spronsen,<sup>b</sup> Cor J. Peters,<sup>a</sup> Roger A. Sheldon<sup>c</sup> and Geert-Jan Witkamp<sup>\*b</sup>

Received 31st August 2005, Accepted 6th December 2005

First published as an Advance Article on the web 14th December 2005

DOI: 10.1039/b512303h

In this paper two advanced methods for separation and purification of products from ionic liquids by using supercritical carbon dioxide as a co-solvent in extractions or as an anti-solvent in precipitations are demonstrated. As an example, the recovery of the product *N*-acetyl-(*S*)-phenylalanine methyl ester (APAM) from the ionic liquid 1-butyl-3-methylimidazolium tetrafluoroborate ([bmim][BF<sub>4</sub>]) was studied experimentally. APAM is the product of the asymmetric hydrogenation of methyl-(*Z*)- $\alpha$ -acetamidocinnamate (MAAC). For extraction of the product, the solubility of APAM in CO<sub>2</sub> should be sufficiently high. This solubility is 1.78 g kg<sup>-1</sup> at 12.0 MPa and 323 K, whereas [bmim][BF<sub>4</sub>] has a negligible solubility in scCO<sub>2</sub>. The extracted product was found to contain no detectable amount of ionic liquid. The solubility of the reactant MAAC in scCO<sub>2</sub> is five times lower than the solubility of APAM, which means that a selectivity towards extraction of APAM exists. The product APAM was also precipitated out of the ionic liquid phase using scCO<sub>2</sub> as an anti-solvent, enabled by the lower solubility of APAM in ionic liquid/scCO<sub>2</sub> mixtures compared to the solubility in the pure ionic liquid at atmospheric conditions (650 g l<sup>-1</sup>). For example, the solubility of APAM in ionic liquid + scCO<sub>2</sub> (1:1.34 g g<sup>-1</sup>) at 313 K and 18.0 MPa is 162 g l<sup>-1</sup>. After precipitation the formed crystals can be washed using CO<sub>2</sub> to obtain pure product.

## Introduction

Ionic liquids have been described as novel, environmentally benign solvents that can replace traditional volatile organic solvents as reaction or separation media.<sup>1–3</sup> Ionic liquids have negligible vapour pressure. Therefore, they are non-volatile and non-flammable. Ionic liquids can be recycled and reused, without leading to solvent emissions into the atmosphere.

When ionic liquids are used as reaction media, the recovery of products from ionic liquids can be difficult. Only when the product is immiscible with the ionic liquid, and the catalyst highly prefers the ionic liquid phase, can the product then be easily separated by means of decantation.<sup>2</sup> However, if the product and ionic liquid show partial mutual solubility, the separation is much more complicated. Distillation or evaporation is a reasonable option for solute recovery, due to the lack of any measurable ionic liquid vapour pressure,<sup>3</sup> but distillation is only suited for the recovery of volatile and thermally stable products. Another option to recover products from

ionic liquids is extraction.<sup>4</sup> However, the possibility of cross-contamination between the phases presents a problem. Also, the partitioning of the solute between the phases limits the extent of solute extraction. Finally, an additional product recovery from the co-solvent can lead to further problems.

A solution to these problems is the use of supercritical carbon dioxide as a co-solvent for product extractions or as an anti-solvent for product precipitations from ionic liquids. Brennecke and co-workers<sup>5,6</sup> showed that it was possible to extract a solute from an ionic liquid using supercritical carbon dioxide without any contamination by the ionic liquid. The reason is that carbon dioxide is not able to dissolve any ionic liquid. Other groups have shown that the extraction of solutes from ionic liquids using supercritical CO<sub>2</sub> can be combined with reaction operations.<sup>7–9</sup> However, precipitation of products from ionic liquids using supercritical carbon dioxide as an anti-solvent has never been reported in literature yet. It was believed that precipitation of products from ionic liquids using supercritical carbon dioxide is impossible, because the ionic liquids do not expand significantly when carbon dioxide is dissolved.<sup>6</sup> Therefore, the influence of dissolving carbon dioxide on the solubility of the product was considered to be low. In this study we show that it is possible to recover products from ionic liquids using carbon dioxide as an anti-solvent in precipitations.

In this work the recovery of the product *N*-acetyl-(*S*)-phenylalanine methyl ester (APAM) from the ionic liquid 1-butyl-3-methylimidazolium tetrafluoroborate ([bmim][BF<sub>4</sub>]) using supercritical carbon dioxide (scCO<sub>2</sub>) as a co-solvent in extractions and as an anti-solvent in precipitations is investigated. APAM is the product of the asymmetric hydrogenation

<sup>a</sup>Physical Chemistry and Molecular Thermodynamics, Department of Chemical Technology, Faculty of Applied Sciences, Delft University of Technology, Julianalaan 136, 2628 BL Delft, The Netherlands

<sup>b</sup>Laboratory for Process Equipment, Department of Process & Energy, Faculty of Mechanical, Maritime and Materials Engineering, Delft University of Technology, Leeghwaterstraat 44, 2628 CA Delft, The Netherlands. E-mail: G.J.Witkamp@3me.tudelft.nl; Fax: +31-15-2786975; Tel: +31-15-2783602

<sup>c</sup>Biocatalysis and Organic Chemistry, Department of Chemical Technology, Faculty of Applied Sciences, Delft University of Technology, Julianalaan 136, 2628 BL Delft, The Netherlands

† This work was presented at the 1st International Conference on Ionic Liquids (COIL), held in Salzburg, Austria, 19–22 June, 2005.

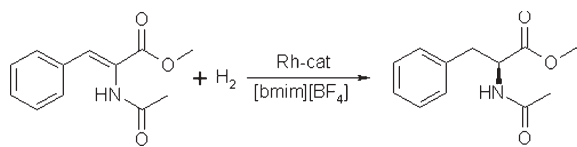


Fig. 1 Asymmetric hydrogenation of MAAC, yielding APAM.

of methyl-(*Z*)- $\alpha$ -acetamidocinnamate (MAAC), see Fig. 1. According to Berger *et al.*<sup>10</sup> this reaction can be carried out in the ionic liquid [bmim][BF<sub>4</sub>] with conversion and enantioselectivity comparable to conventional solvents.<sup>11</sup> However, Berger *et al.* did not investigate the separation of APAM from [bmim][BF<sub>4</sub>]. In this study we tried to find the best solution and conditions for the separation process.

## Experimental

### Materials

APAM was prepared with a purity of over 99.0% by a reaction of the corresponding acid with thionyl chloride, followed by esterification with methanol. *N*-acetyl-(*L*)-phenylalanine (98.0 g, 0.473 mole) was dissolved in methanol (430 ml) and this solution was cooled to 0 °C. Thereafter a small excess of thionyl chloride (65.6 g, 0.551 mole) was slowly added. The mixture was stirred for an additional four hours after which all volatiles were removed by evaporation. The residue was taken up in 100 ml water, which was extracted with 3 × 50 ml dichloromethane. The organic layer was dried with sodium sulfate and evaporated to dryness. A yield as high as 99.5% was reached (104.1 g APAM, 0.471 mole). The purity was analysed using <sup>1</sup>H NMR (300.2 MHz, CDCl<sub>3</sub>, TMS):  $\delta$  1.93 (s, 3H), 3.06 (m, 2H), 3.67 (s, 3H), 4.84 (q, 1H), 6.66 (d, 1H), 7.18 (m, 5H). MAAC was prepared according to the method of Gladiali and Pinna<sup>12</sup> with a purity of over 99.0%. The purity was measured using <sup>1</sup>H NMR (300.2 MHz, CDCl<sub>3</sub>, TMS):  $\delta$  1.61 (s, 1H), 2.14 (s, 3H), 3.85 (s, 3H), 7.38 (m, 6H). The CO<sub>2</sub> used for the measurements was supplied by Air Products and had a purity of 99.95%. The ionic liquid [bmim][BF<sub>4</sub>] was prepared with a purity of over 99.0% as previously described.<sup>4</sup> The purity was measured using a boron analysis (ICP-AES) and a NMR analysis. <sup>1</sup>H NMR (300.2 MHz, CDCl<sub>3</sub>, TMS):  $\delta$  0.93 (t, 3H), 1.34 (m, 2H), 1.86 (m, 2H), 3.95 (s, 3H), 4.20 (t, 2H), 7.47 (s, 2H), 8.71 (s, 1H). Prior to use, the [bmim][BF<sub>4</sub>] was dried under vacuum conditions at room temperature for several days. The water content of the dried ionic liquid was measured using Karl-Fischer moisture analysis and was less than 0.03 mass%. Within the temperature range of the experiments, the ionic liquid did not show any decomposition or reaction with carbon dioxide.

### Extraction experiments

The solubility of APAM (or MAAC) in scCO<sub>2</sub> at different conditions was measured in the following way: at the bottom of an autoclave a well-defined amount of solid APAM (resp. MAAC) was placed. CO<sub>2</sub> at the desired temperature was pumped into the autoclave until the desired pressure was reached. With a flow meter the amount of entering CO<sub>2</sub> was measured. The autoclave with APAM and CO<sub>2</sub> was closed and

kept at fixed temperature by a heat jacket. The CO<sub>2</sub> was stirred in order to enhance mass transport of APAM from the solid phase into the CO<sub>2</sub> phase. After waiting until equilibrium was reached (30 minutes), the pressure was released and the autoclave was opened. The amount of APAM that was still left in the autoclave was measured. The dissolved amount was calculated from the difference between the initial and final amount of solid APAM in the autoclave.

In the extraction process step a solution of APAM in ionic liquid with known concentration was put into the autoclave (10.0 g APAM in 163.5 ml [bmim][BF<sub>4</sub>] = 61.2 g l<sup>-1</sup>). CO<sub>2</sub> was continuously pumped through the autoclave during 30 minutes, while keeping the vessel at a temperature of 323 K and a pressure of 12.0 MPa. The amount of CO<sub>2</sub> that was pumped through the autoclave was measured using a flow meter (5.595 kg CO<sub>2</sub> in 30 minutes). After leaving the autoclave, the CO<sub>2</sub> entered an expansion vessel in which the pressure was relieved and the product precipitated due to the negligible solubility at ambient pressure. After extraction during 30 minutes, the pump was turned off and the pressure in the autoclave was relieved. The concentration of APAM in ionic liquid after extraction was measured using high performance liquid chromatography (HPLC) from Waters, type Waters 510 HPLC pump & Waters Symmetry C<sub>18</sub>-column. The purity of the precipitated APAM was determined using inductively coupled plasma atomic emission spectroscopy (ICP-AES) from Spectro, type Spectroflame.

### Precipitation experiments

The solubility of APAM in ionic liquid at atmospheric conditions was measured by dissolving APAM into the ionic liquid under continuous stirring until saturation was reached. The solubility data of APAM in mixtures of [bmim][BF<sub>4</sub>] + CO<sub>2</sub> were determined by adding supercritical CO<sub>2</sub> to a mixture of [bmim][BF<sub>4</sub>] and APAM in an autoclave, waiting until the precipitation stops and measuring the amount of APAM that is still dissolved in the [bmim][BF<sub>4</sub>] + CO<sub>2</sub> mixture after precipitation: a solution of [bmim][BF<sub>4</sub>] with APAM with known concentration (76.3 g APAM in 171.4 ml [bmim][BF<sub>4</sub>] = 445 g l<sup>-1</sup>) was put into an autoclave vessel with a filter on the bottom. CO<sub>2</sub>, after heating to the desired temperature (313 K), was pumped into the autoclave until the desired pressure was reached (18.0 MPa). With a flow meter the amount of entered CO<sub>2</sub> was measured (278 g). The autoclave was closed and kept at fixed temperature by a heating jacket. The mixture in the autoclave was stirred for 30 minutes. Thereafter, the valve at the bottom of the autoclave was opened and at the same time, more CO<sub>2</sub> was pressed into the autoclave to keep the pressure at constant level. In this way the liquid phase was pushed through the filter at the bottom of the autoclave and recovered, but the formed precipitate could not pass through the filter. At the moment that no liquid left the autoclave anymore, the CO<sub>2</sub> pump was turned off and the pressure in the autoclave was relieved. The concentration of APAM in the filtrate was measured with HPLC to determine the solubility of APAM in a mixture of [bmim][BF<sub>4</sub>] + CO<sub>2</sub>. The crystal form of the precipitated APAM was analysed using scanning electron microscopy (SEM) from Jeol, type JSM-5400.

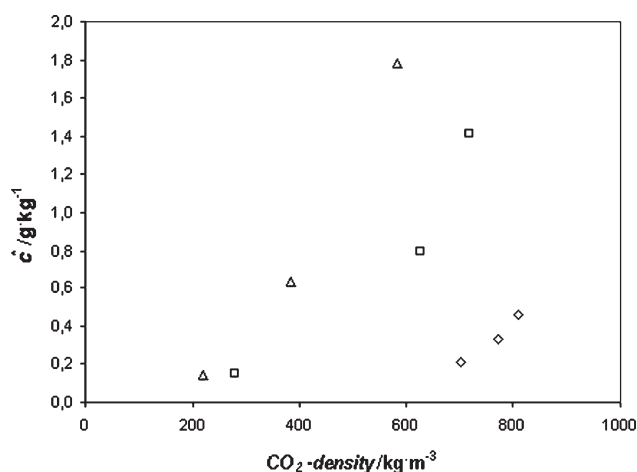
**Table 1** Solubility of APAM in CO<sub>2</sub> at different conditions

T/K	p/MPa	$\rho_{\text{CO}_2}/\text{kg m}^{-3}$	$c^*/\text{g kg}^{-1}$
303	8.0	701.72	0.207
303	10.0	771.50	0.329
303	12.0	808.93	0.457
313	8.0	277.90	0.150
313	10.0	628.61	0.798
313	12.0	717.76	1.412
323	8.0	219.18	0.142
323	10.0	384.33	0.628
323	12.0	584.71	1.781

The autoclave used allows extractions and precipitations using CO<sub>2</sub> within a pressure range from (0.1 to 20) MPa and temperatures from (255 to 470) K, depending on the heat-transferring fluid in the heat jacket. The uncertainty in temperature is  $\pm 0.1$  K, which is due to temperature fluctuations of the water bath. The uncertainty of the pressure in the autoclave is  $\pm 0.01$  MPa. The uncertainty of the solubility measurements in the extraction experiments is  $\pm 1.0\%$ . The concentrations of APAM in ionic liquid before and after separation were measured using HPLC and have an uncertainty of  $\pm 0.5\%$ . The overall uncertainty in the whole precipitation experiment is therefore  $\pm 1.0\%$ .

## Results and discussion

When the solubility of APAM in supercritical CO<sub>2</sub> is high enough, APAM can be extracted from [bmim][BF<sub>4</sub>] by CO<sub>2</sub>. The solubility of APAM in CO<sub>2</sub> as function of CO<sub>2</sub> density was measured by determining the difference in weight of APAM before and after exposure to a well-defined amount of CO<sub>2</sub> at certain conditions. In Table 1 the solubility of APAM in CO<sub>2</sub> at different temperatures and pressures is shown. In Fig. 2 the solubility of APAM in CO<sub>2</sub> is plotted against the CO<sub>2</sub>-density. Fig. 2 shows that it is possible to extract APAM from the ionic liquid phase using CO<sub>2</sub>, because APAM is soluble in CO<sub>2</sub> (typically in the order of a few grams per kg CO<sub>2</sub>). Moreover, the solubility of APAM in CO<sub>2</sub> increases when higher temperatures are used at fixed CO<sub>2</sub>-density and when the density is increased (by increasing the pressure) at

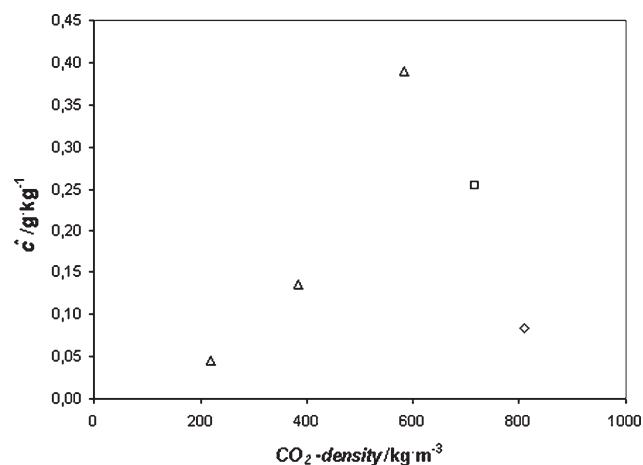
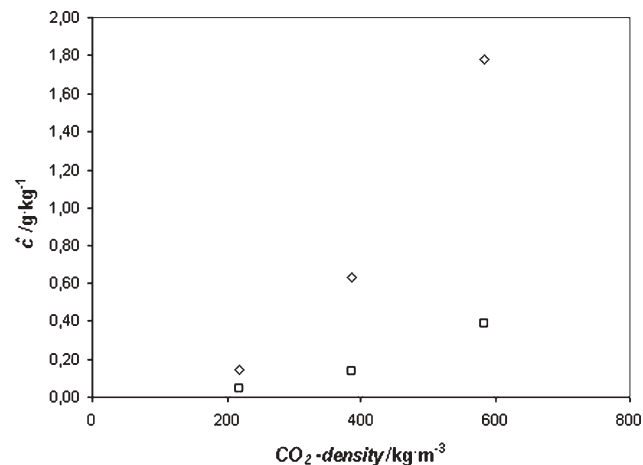
**Fig. 2** Solubility of APAM in CO<sub>2</sub>:  $\diamond$ , 303 K;  $\square$ , 313 K;  $\triangle$ , 323 K.**Table 2** Solubility of MAAC in CO<sub>2</sub> at different conditions

T/K	p/MPa	$\rho_{\text{CO}_2}/\text{kg m}^{-3}$	$c^*/\text{g kg}^{-1}$
303	12.0	808.93	0.084
313	12.0	717.76	0.254
323	8.0	219.18	0.045
323	10.0	384.33	0.135
323	12.0	584.71	0.390

fixed temperature. This is a common trend for the solubility of solutes in supercritical CO<sub>2</sub>.

Also, the solubility of the reactant MAAC in CO<sub>2</sub> was measured. In Table 2 the solubility of MAAC in CO<sub>2</sub> at different temperatures and pressures is shown. In Fig. 3 the solubility of MAAC in CO<sub>2</sub> is plotted against the CO<sub>2</sub>-density. The solubility of APAM in CO<sub>2</sub> is compared to the solubility of MAAC in CO<sub>2</sub>. At the same conditions the solubility of MAAC in CO<sub>2</sub> is five times lower than the solubility of APAM in CO<sub>2</sub> (see Fig. 4). Therefore, a selectivity towards extraction of the product exists when reaction and extraction are simultaneously carried out.

Thereafter, the real extraction process was carried out. APAM was extracted from the ionic liquid [bmim][BF<sub>4</sub>] using

**Fig. 3** Solubility of MAAC in CO<sub>2</sub>:  $\diamond$ , 303 K;  $\square$ , 313 K;  $\triangle$ , 323 K.**Fig. 4** Comparison of solubility of APAM and MAAC in carbon dioxide at 323 K:  $\diamond$ , APAM;  $\square$ , MAAC.



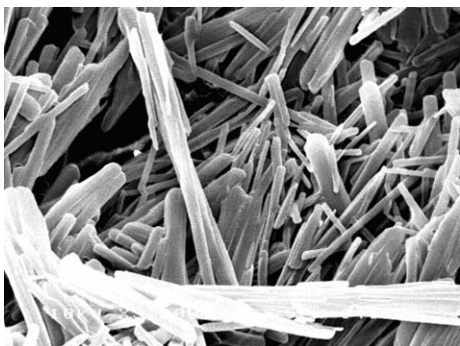


Fig. 5 SEM image of APAM (5000 $\times$  magnified, 10 kV).

supercritical CO<sub>2</sub> at 12.0 MPa and 323 K. A solution of 10.0 g APAM in 163.5 ml [bmim][BF<sub>4</sub>] (61.2 g l<sup>-1</sup>) was extracted with 5.595 kg CO<sub>2</sub> for 30 minutes (flow rate = 0.187 kg CO<sub>2</sub> min<sup>-1</sup>). After extraction, the concentration of APAM in [bmim][BF<sub>4</sub>] was only 10.1 g l<sup>-1</sup> (=1.7 g per 163.5 ml [bmim][BF<sub>4</sub>]). The amount of dissolved APAM in CO<sub>2</sub> is thus 10.0 - 1.7 = 8.3 g in 5.595 kg CO<sub>2</sub> (1.48 g kg<sup>-1</sup>, recovery = 83%), which is lower than the solubility in CO<sub>2</sub> (1.78 g kg<sup>-1</sup>). This can be due to mass transfer limitations during the real extraction process. The presence of boron in APAM, which indicates the presence of ionic liquid in the product, was determined using ICP-AES. The precipitated APAM contains no detectable [bmim][BF<sub>4</sub>], indicating that the solubility of ionic liquid in CO<sub>2</sub> is lower than 10<sup>-5</sup> mole fraction. Therefore, pure product can be recovered without any ionic liquid contamination.

We also investigated the precipitation of APAM out of [bmim][BF<sub>4</sub>] using CO<sub>2</sub> as an anti-solvent. The product APAM can only be precipitated out of the ionic liquid phase when the solubility of APAM in pure ionic liquid is higher than the solubility in an ionic liquid + CO<sub>2</sub> mixture. In that case supersaturation can be created by adding CO<sub>2</sub>. The solubility of APAM in [bmim][BF<sub>4</sub>] is 650 g l<sup>-1</sup> at ambient conditions, whereas the solubility of APAM in ionic liquid + carbon dioxide (1:1.34 kg kg<sup>-1</sup>) at 313 K and 18.0 MPa is 162 g l<sup>-1</sup>. Therefore, in principle it is possible to precipitate 650 - 162 = 488 g out of 1 litre ionic liquid (single step recovery = 75%). We precipitated APAM out of a solution with an initial APAM concentration in [bmim][BF<sub>4</sub>] of 445 g l<sup>-1</sup> (76.3 g APAM per 171.4 ml (=207.4 g) ionic liquid) using 278 g CO<sub>2</sub>. The amount of remaining APAM in ionic liquid is 162 g l<sup>-1</sup> (=27.8 g in 171.4 ml). The amount of precipitated APAM is 76.3 - 27.8 = 48.5 g (recovery = 64%). After precipitation the formed crystals can be washed using CO<sub>2</sub> to obtain pure product. The product APAM was obtained as crystals in the form of small needles (see Fig. 5). From the fact that it is possible to precipitate products out of ionic liquids it can be concluded that it is not the expansion of the fluid that determines whether a product can be precipitated or not. Rather, the interaction between the molecules determines solubility behaviour.

The solubility of the starting material MAAC under precipitation conditions was not investigated. Since the

separation step is carried out after the reaction step, and in the reaction step 100% conversion can be reached,<sup>10</sup> it is assumed that the desired product APAM will not be contaminated with the starting material MAAC.

Both methods to separate the product APAM from the ionic liquid [bmim][BF<sub>4</sub>] worked well. In a real process, the recovery can reach 100% with a proper process lay-out. However, we only optimised pressure and temperature for high product recovery. The experiments were not optimised for CO<sub>2</sub> flow rate and duration of the experiments. Therefore, in our experiments we do not reach 100% recovery. Although the separation methods were only tested on the recovery of APAM from [bmim][BF<sub>4</sub>], the authors believe that both methods are generally applicable for the recovery of other solutes from ionic liquids, because for each solute an optimised ionic liquid can be designed.

## Conclusions

The recovery of the product APAM out of the ionic liquid [bmim][BF<sub>4</sub>] using supercritical CO<sub>2</sub> was studied experimentally. On the one hand, CO<sub>2</sub> can be used to extract APAM from the ionic liquid phase without any measurable ionic liquid contamination. On the other hand, CO<sub>2</sub> can be used as an anti-solvent to precipitate APAM out of the ionic liquid phase and to wash the solid product. Both methods are a solution to the problem of recovering soluble and thermally labile products from ionic liquids and can be used to recover other products from ionic liquids in a simple and straightforward way, without any contamination by the ionic liquid.

## Acknowledgements

The authors would like to acknowledge G. W. Hofland, L. J. Florusse, C. Simons and A. van Estrik for their help.

## References

- 1 R. A. Sheldon, *Chem. Commun.*, 2001, **23**, 2399–2407.
- 2 M. J. Earle and K. R. Seddon, *Pure Appl. Chem.*, 2000, **72**, 1391–1398.
- 3 D. Zhao, M. Wu, Y. Kou and E. Min, *Catal. Today*, 2002, **74**, 157–189.
- 4 J. G. Huddleston, H. D. Willauer, R. P. Swatloski, A. E. Visser and R. D. Rogers, *Chem. Commun.*, 1998, **16**, 1765–1766.
- 5 L. A. Blanchard, D. Hancu, E. J. Beckman and J. F. Brennecke, *Nature*, 1999, **399**, 28–29.
- 6 L. A. Blanchard and J. F. Brennecke, *Ind. Eng. Chem. Res.*, 2001, **40**, 287–292.
- 7 R. A. Brown, P. Pollet, E. McKoon, C. A. Eckert, C. L. Liotta and P. G. Jessop, *J. Am. Chem. Soc.*, 2001, **123**, 1254–1255.
- 8 F. Liu, M. B. Abrams, R. T. Baker and W. Tumas, *Chem. Commun.*, 2001, **5**, 433–434.
- 9 M. F. Sellin, P. B. Webb and D. J. Cole-Hamilton, *Chem. Commun.*, 2001, **8**, 781–782.
- 10 A. Berger, R. F. de Souza, M. R. Delgado and J. Dupont, *Tetrahedron: Asymmetry*, 2001, **12**, 1825–1828.
- 11 M. J. Burk, J. E. Feaster, W. A. Nugent and R. L. Harlow, *J. Am. Chem. Soc.*, 1993, **115**, 10125–10138.
- 12 S. Gladiali and L. Pinna, *Tetrahedron: Asymmetry*, 1991, **2**, 623–632.

# Aliquat 336<sup>®</sup>—a versatile and affordable cation source for an entirely new family of hydrophobic ionic liquids†‡

Jyri-Pekka Mikkola,<sup>a</sup> Pasi Virtanen<sup>a</sup> and Rainer Sjöholm<sup>b</sup>

Received 9th September 2005, Accepted 27th January 2006

First published as an Advance Article on the web 15th February 2006

DOI: 10.1039/b512819f

A novel family of ionic liquids based on the tricaprylmethylammonium§ cation [C<sub>25</sub>H<sub>54</sub>N<sup>+</sup>] combined with a number of anions that are easily and elegantly prepared by means of simple replacement of the chloride, [Cl<sup>-</sup>], anion in Aliquat 336<sup>®</sup>—an ionic liquid itself—is introduced. Ionic liquids for engineering purposes should be affordable, easy to handle (*i.e.* air and moisture stable) and preferably simple to prepare by a non-expert in synthetic chemistry. Consequently, this paper introduces a viable option as a family of engineering-purpose ionic liquids derived from Aliquat 336<sup>®</sup>. Moreover, the prepared materials can be utilized, *e.g.* in heterogenized form as a catalyst incorporating catalytically active metal species (Pd) for the hydrogenation of an  $\alpha,\beta$ -unsaturated aldehyde, citral.

## Introduction

A number of relatively recent papers, *e.g.*, ref. 1–5, introduce a multitude of simple and efficient preparation methods for ‘room temperature ionic liquids’ (RTILs). These methodologies do not require very special equipment or appliances of a state-of-the-art chemistry laboratory. Several more complex preparation recipes reported in the literature require working practices and equipment typically available only at laboratories dealing primarily with synthesis chemistry (*i.e.* organic chemistry *etc.*). Therefore, the threshold for a chemical engineer, who often is not very familiar with the details of organic synthesis, to prepare RTILs is considerable. Moreover, the relatively high cost and, even today, relatively cumbersome commercial availability of larger amounts of RTILs inhibits applied engineering research. Ionic liquids are merely ‘liquid solids’ that are considered to have green characteristics, *i.e.* chemical and thermal stability, very low vapour pressure, often non-flammable, non-coordinating yet highly solvating as well as viable, recyclable, substitutes for volatile organic solvents. It is estimated that approximately 10<sup>18</sup> combinations<sup>6</sup> potentially exist and, indeed, an ever growing number of cation–anion combinations, zwitterions and deep eutectics have been introduced.

Aliquat 336<sup>®</sup>, which is commonly employed as a surfactant and phase-transfer catalyst, is in fact an ionic liquid. This RTIL could, naturally, be directly utilized as solvent *etc.* in many applications. However, in the case of, for instance,

transition metal catalysis, the use of Aliquat 336<sup>®</sup> as such could be limited due to the strong coordination effect of the chloride anion in many reactions. Thus, in this paper a number of straight-forward, easy-to-carry out recipes following the guidelines of published methods (such as precipitation, evaporation and microwave-assisted synthesis) for modification of an existing RTIL, into an avenue of numerous novel, low-cost RTILs is described. Surprisingly, many attempts have resulted in novel RTILs with melting points either close to room temperature or even far below the freezing point of water. Application investigation as well as characterization of these novel RTILs was conducted and further work is in progress.

## Experimental

Aliquat 336<sup>®</sup> or tricaprylmethylammonium chloride (A336), is a common phase transfer catalyst and an ionic liquid itself. The cation in A336 is displayed in Fig. 1, whereas a few prepared A336-based ionic liquids are depicted in Fig. 2. As can be seen, tricaprylmethylammonium bicarbonate, [A336][HCO<sub>3</sub>], the first one from the left, is a very viscous oil (almost solid) at room temperature, whereas most of the liquids prepared remained liquids—some even with relatively low viscosities, at ambient temperature.

By elimination of the added co-solvent, the amount of organic solvent waste is reduced. Moreover, the purity of the resulting ionic liquid can potentially be improved due to the elimination of the trace organic solvent residue. After the completed precipitation–filtration sequence, the resulting ionic

<sup>a</sup>Industrial Chemistry Laboratory, Biskopsgatan 8, 20500, Finland

<sup>b</sup>Organic Chemistry Laboratory, Process Chemistry Centre, Åbo Akademi University, Biskopsgatan 8, 20500, Finland.

E-mail: jpmikkol@abo.fi

† This work was presented at the 1st International Conference on Ionic Liquids (COIL), held in Salzburg, Austria, 19–22 June, 2005.

‡ Electronic supplementary information (ESI) available: Preparation (Part A) and characterization (Part B) of A336 ionic liquids. See DOI: 10.1039/b512819f

§ Note: Aliquat 336<sup>®</sup> is actually a 2 : 1 mixture of methyl trioctyl- and methyl tridecylammonium chloride.

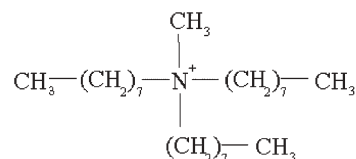


Fig. 1 Tricaprylmethylammonium cation.



**Fig. 2** Sample Aliquat 336<sup>®</sup>-based ILs. From left to right: [A336][HCO<sub>3</sub>], [A336][H<sub>2</sub>PO<sub>4</sub>], [A336][Cl] (neat Aliquat 336<sup>®</sup>), [A336][HSO<sub>4</sub>], [A336][NO<sub>3</sub>] and [A336][OCN] (from NaOCN).

liquid can naturally be diluted with appropriate organic solvent and/or washed with water, followed by another filtration and consequent evaporation of the co-solvent and moisture in vacuum. Therefore, a number of anions were initially incorporated by direct dissolution of the replacement anion salt and further work-up for improved purity was conducted. All ionic liquids were prepared in a normal atmosphere, since an as simple as possible preparation procedure was desired. Although the humidity in air potentially causes more impure ionic liquids, it seems that the subsequent vacuum treatment and filtration provided ionic liquids with acceptable technical quality. The preparation details of the A336-based ionic liquids are collected in Part A of the ESI.† It is important to observe that the molar weight of Aliquat 336<sup>®</sup> (Cognis) as reported in various sources is claimed to be 404 g mol<sup>-1</sup>. However, Aliquat 336<sup>®</sup> is actually a 2 : 1 mixture of methyl trioctyl- and methyl tridecylammonium chloride. Instead, a molar weight of 432 g mol<sup>-1</sup> was used in this work.<sup>7</sup>

The synthesized ionic liquids were dried in high vacuum, at elevated temperatures and characterized: density measurements (Anton Paar DMA512P densitometer), thermogravimetric analysis (TGA), differential scanning calorimetry (DSC, melting and freezing point determinations) as well as Fourier-transfer infrared spectroscopy (FTIR) were carried out. <sup>1</sup>H and <sup>13</sup>C NMR spectra of the ionic liquids were recorded in DMSO-d<sub>6</sub>. The chlorine content of the ionic liquids was determined by AgNO<sub>3</sub> method. The salt precipitates formed in synthesis were studied by means of scanning electron microscopy (SEM-EDX) to verify the formation of the desired salt precipitate. Viscosity measurements were carried out for a few samples with a Bohlin VOR rheometer.

In order to study the performance of one of the newly formed ionic liquids, Aliquat hexafluorophosphate ionic liquid was utilized in a heterogenized form, together with a dissolved transition metal complex, palladium acetylacetonate (Pd(acac)<sub>2</sub>), on an active carbon cloth (Kynol<sup>®</sup>), in a three-phase hydrogenation of an  $\alpha,\beta$ -unsaturated aldehyde, citral. The primary hydrogenation product was either citronellal or dihydrocitronellal, depending on the experimental conditions.<sup>8</sup> The simplified citral hydrogenation scheme is introduced in Fig. 3. The novel IL [A336][PF<sub>6</sub>] was synthesized and dissolved in dry acetone (Acros Organics, 50 ppm H<sub>2</sub>O). The transition metal salt (palladium acetylacetonate, Aldrich 99%) was also dissolved in dry acetone, the acetone mixtures were combined and, thereafter, a pre-dried (105 °C, 1 h) structural solid, high surface area Kynol<sup>®</sup> active carbon cloth/mat was wetted ('incipient wetness') with the solution. Upon this, the capillary forces instantaneously sucked the liquid into the support, resulting in a seemingly 'dry' texture. The active carbon cloth has excellent mechanical strength (tensile strength 6 kg per 50 mm) and high surface area (ca. 1500 m<sup>2</sup> g<sup>-1</sup>; manufacturer

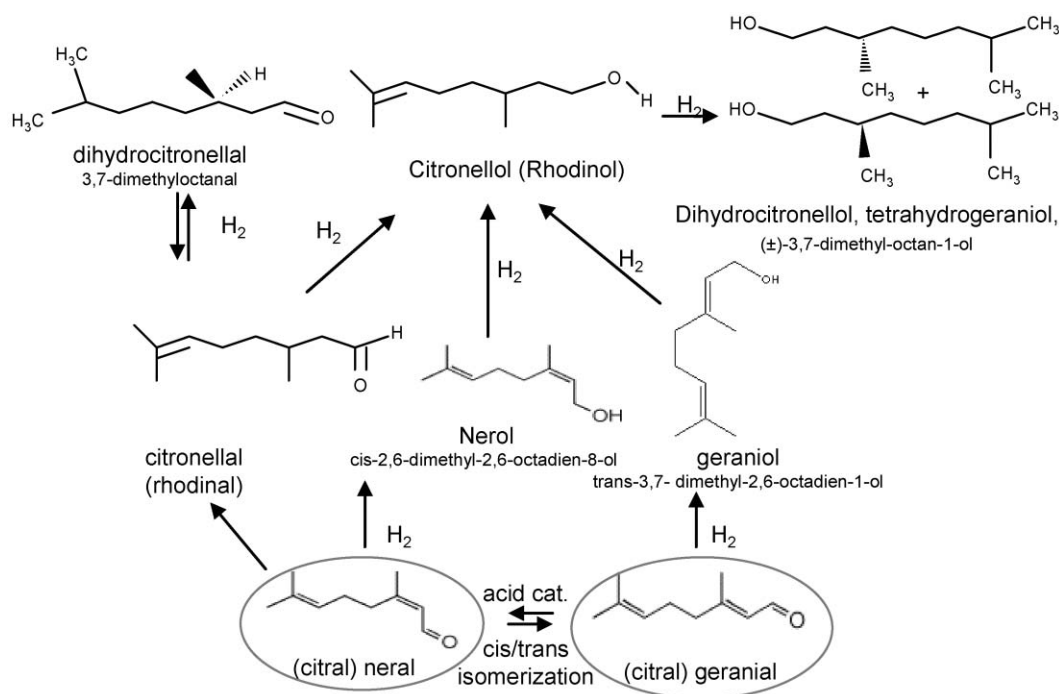


**Fig. 3** Simplified citral hydrogenation scheme.

**Table 1** Characterisation data for the ionic liquids

Compound	Cl <sup>-</sup> cont. (wt%)	H <sub>2</sub> O cont. (wt%)	Decomp. T/°C	mp/°C	ρ/g cm <sup>-3</sup> (50 °C)	η/cP (50 °C)
[A336 <sup>+</sup> ][NO <sub>3</sub> <sup>-</sup> ]	<3	3.1 <sup>b</sup>	202	6–20	0.90	630
[A336 <sup>+</sup> ][cro <sup>-</sup> ]	<6	3.6 <sup>b</sup>	183	16–20	0.87	—
[A336 <sup>+</sup> ][BF <sub>4</sub> <sup>-</sup> ]	0	4.9 <sup>b</sup>	294	60	0.87	—
[A336 <sup>+</sup> ][BH <sub>4</sub> <sup>-</sup> ]	<6	4.2 <sup>b</sup>	144	-8	0.87	650
[A336 <sup>+</sup> ][SO <sub>2</sub> <sup>-</sup> ]	<6	3.2 <sup>b</sup>	157	-9(-5)	0.87	—
[A336 <sup>+</sup> ][CH <sub>3</sub> COO <sup>-</sup> ]	<6	0.9 <sup>a</sup>	175	-22(-23)	0.87	—
[A336 <sup>+</sup> ][H <sub>2</sub> PO <sub>4</sub> <sup>-</sup> ]	Reacts	0.5 <sup>a</sup>	176	-22(-24)	0.87	—
[A336 <sup>+</sup> ][HSO <sub>4</sub> <sup>-</sup> ]	<3	0.2 <sup>a</sup>	196	-19(-25)	0.91	—
[A336 <sup>+</sup> ][PF <sub>6</sub> <sup>-</sup> ]	<3	0.5 <sup>a</sup>	274	51–66	—	—
[A336 <sup>+</sup> ][HCOO <sup>-</sup> ]	<6	0.4 <sup>a</sup>	174	1–7	0.88	—
[A336 <sup>+</sup> ][HCO <sub>3</sub> <sup>-</sup> ]	<6	0.1 <sup>a</sup>	176	-6(-7)	—	—
[A336 <sup>+</sup> ][(CF <sub>3</sub> SO <sub>2</sub> ) <sub>2</sub> N <sup>-</sup> ]	0	6.1 <sup>b</sup>	367	-39	1.06	—

<sup>a</sup> Water content was determined straight after drying of the sample. <sup>b</sup> Water content was determined from the sample, which had gained moisture from the air.

information). In the next step acetone was evaporated from the ACC cloth in an oven at 105 °C (15 min) or exposed to high vacuum in a rotary evaporator and cut into pieces that fitted into our tailor-made laboratory autoclave internals. The catalyst was exposed for a flow of hydrogen (Aga Oy, 99.999%) for 1 h at 100 °C, thereby facilitating reduction (Pd<sup>0</sup>) or complex formation and stabilization of Pd. The reduction treatment is reported to induce the formation of Pd-nanoparticles<sup>9</sup> or, in the case of a complex formation, molecular size catalytic species. The immobilization relies on the simple fact that the bulk solvent, n-hexane, and the ionic liquids are not co-miscible. The leaching of ionic liquids into the bulk solvent (n-hexane) was studied by means of high precision liquid chromatography (HPLC). Detection of ionic liquids in citral hydrogenation samples by HPLC was made by reversed-phase HPLC with UV detection.

X-ray photoelectron spectroscopy (XPS) was used to study the reduction state of the Pd-species residing in the ionic liquid on the ACC support. To the best of our knowledge, XPS has not been reported previously for studying the reduction state of metal species in (supported) ionic liquids.<sup>8</sup> A Perkin-Elmer 5400 ESCA was used for the XPS analysis. The ionic liquid catalyst was analysed *ex-situ* as a residue on Kynol<sup>®</sup> support material after an out-gassing of several hours in vacuum.

## Results

### Preparation of Aliquat 336-based ionic liquids

Many of the tried combinations led to formation of new, hydrophobic ionic liquids. Generally, the synthesis was carried out by the metathesis procedure as follows: 0.0094 mol of Aliquat 336<sup>®</sup> (or tricaprilmethylammonium chloride), a common phase transfer catalyst and an ionic liquid itself (Aldrich), as well as 0.01 mol of a sodium, potassium or ammonium salt of the replacement anion were dissolved in a suitable solvent, mixed together and the formed precipitate separated with a Millipore Millex 0.45 μm filter, followed by a thermal treatment under high vacuum (rotary evaporator). The details can be found in Part A of the ESI.‡

Although several of the new compounds were rather viscous, the viscosity rapidly dropped at elevated temperatures. By means of varying the anions of Aliquat 336<sup>®</sup>, the lowest

melting point obtained was 234 K (-39 °C) and the highest decomposition temperature 640 K (367 °C), for the compound [A336<sup>+</sup>][(CF<sub>3</sub>SO<sub>2</sub>)<sub>2</sub>N<sup>-</sup>], whereas the melting point and decomposition temperatures of neat Aliquat 336<sup>®</sup> are 253 K (-20 °C) and 493 K (220 °C), respectively. A summary of the properties of ionic liquids is presented in Table 1. Generally, the newly formed ionic liquids that were tested for mutual solubility were soluble in acetone, ethyl alcohol, 2-propanol, acetonitrile, toluene and ethyl acetate. However, the solubility in hexane was limited or the compound was insoluble (like [A336][BF<sub>4</sub>]). Mutual solubility data can be found in Table 2. The densities varied from 0.87–1.06 g cm<sup>-3</sup> (50 °C) (Aliquat 336<sup>®</sup> has a density of 0.88 g cm<sup>-3</sup>). The FTIR spectra were recorded and new peaks from the corresponding anion were observed. The <sup>1</sup>H (600 MHz) and <sup>13</sup>C (150 MHz) NMR spectra of the ionic liquids were recorded in DMSO-d<sub>6</sub>. The NMR spectra of [A336<sup>+</sup>][PF<sub>6</sub><sup>-</sup>] are shown in Fig. 4, with signal assignments based on H–H and C–H shift correlation data. The chemical shifts of the signals of the cation were almost identical in all spectra and the chemical shift differences between samples were *ca.* 0.02 ppm in the case of <sup>1</sup>H NMR and 0.2 in the case of <sup>13</sup>C NMR. The shifts are given in Tables S1 and S2; Part B, Section VI of the ESI.‡ Most of the ionic liquids were found out to contain 3–6 wt% chlorine, except [A336<sup>+</sup>][BF<sub>4</sub><sup>-</sup>] and [A336<sup>+</sup>][(CF<sub>3</sub>SO<sub>2</sub>)<sub>2</sub>N<sup>-</sup>] which didn't contain any chlorine. Chlorine content of [A336<sup>+</sup>][H<sub>2</sub>PO<sub>4</sub><sup>-</sup>] couldn't be determined by this method because it reacted with AgNO<sub>3</sub>. Detailed characterization data on the synthesized ionic liquids can be found in Part B of the ESI.‡ Although most of the samples prepared contained significant amounts of chlorine, this can be attributed to the fact that they were prepared in normal, moist air. Upon use of an inert atmosphere, the chlorine residues can certainly be minimized. Alternatively, purification *e.g.* by means of an anion exchange process is possible, provided that an anion exchange resin can be loaded with the desired anion.

### Sample application of prepared ionic liquids: Hydrogenation of citral

The catalyst containing an immobilized [A336][PF<sub>6</sub>] ionic liquid–Pd acetylacetonate that was utilized in the hydrogenation of citral was found to be very durable towards deactivation and the selectivity profiles could be nicely controlled by

**Table 2** Mutual solubilities of the ionic liquids with different organic solvents<sup>a</sup>

Compound	Ethanol	Acetone	2-Propanol	Ethyl acetate	Acetonitrile	Hexane	Toluene
[A336 <sup>+</sup> ][NO <sub>3</sub> <sup>-</sup> ]	p	y	y	y	y	n	y
[A336 <sup>+</sup> ][cro <sup>-</sup> ]	y	y	y	y	y	p	y
[A336 <sup>+</sup> ][BF <sub>4</sub> <sup>-</sup> ]	y	y	p	y	y	n	y
[A336 <sup>+</sup> ][BH <sub>4</sub> <sup>-</sup> ]	y	y	y	y	y	p	y
[A336 <sup>+</sup> ][SO <sub>2</sub> <sup>-</sup> ]	y	y	y	y	p	p	y
[A336 <sup>+</sup> ][CH <sub>3</sub> COO <sup>-</sup> ]	y	y	y	y	y	p	y
[A336 <sup>+</sup> ][H <sub>2</sub> PO <sub>4</sub> <sup>-</sup> ]	y	y	y	y	p	y	y
[A336 <sup>+</sup> ][HSO <sub>4</sub> <sup>-</sup> ]	y	y	y	y	p	n	y
[A336 <sup>+</sup> ][PF <sub>6</sub> <sup>-</sup> ]	y	y	p	y	p	n	y
[A336 <sup>+</sup> ][HCOO <sup>-</sup> ]	y	y	y	y	y	p	y
[A336 <sup>+</sup> ][HCO <sub>3</sub> <sup>-</sup> ]	y	y	y	y	p	y	y
[A336 <sup>+</sup> ][(CF <sub>3</sub> SO <sub>2</sub> ) <sub>2</sub> N <sup>-</sup> ]	y	y	y	y	p	n	y

<sup>a</sup> y denotes totally soluble, p partly soluble and n insoluble.

means of different experimental conditions. Concentration evolution for a sample hydrogenation experiment is introduced in Fig. 5. The performance of the catalyst was good although no specially dried solvents (*n*-hexane) or reactants were used. However, one should take note of the reported fact that, in particular, moisture can cause the PF<sub>6</sub><sup>-</sup> anion to deteriorate, followed by formation of toxic HF. Therefore, this ionic liquid should be merely considered as an example in comparison to commonly applied 1-butyl-3-methyl hexafluorophosphate ([bmim][PF<sub>6</sub>]) ionic liquid. Further studies on various supported ionic liquid systems are in progress.

## Discussion

The constantly growing number of cations, coupled to a multitude of anions is not a surprise: once that a suitable cation is discovered—often initially prepared to incorporate a halide, such as chloride or bromide, the halide can elegantly be exchanged into another one *e.g.* by means of metathesis. Upon this the ionic liquid and the new counter-anion (as *e.g.* sodium, ammonium or lithium salt) are dissolved in a suitable co-solvent (*e.g.* dry acetone, acetonitrile, ethyl acetate or ethyl alcohol) in which the formed simple inorganic salt, such as

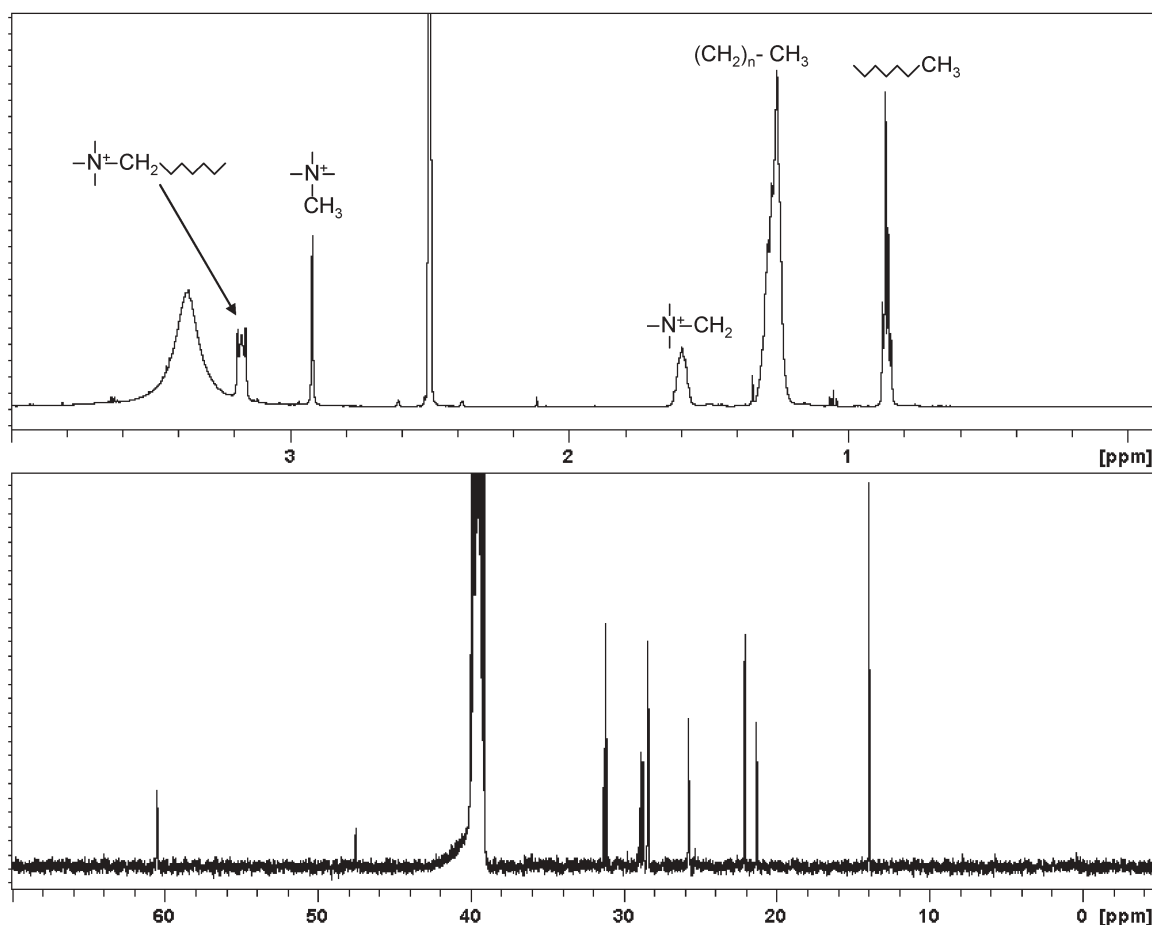


**Fig. 4** <sup>1</sup>H (upper, 600 MHz) and <sup>13</sup>C NMR (lower, 150 MHz) spectra of [A336<sup>+</sup>][PF<sub>6</sub><sup>-</sup>] in DMSO-*d*<sub>6</sub>.

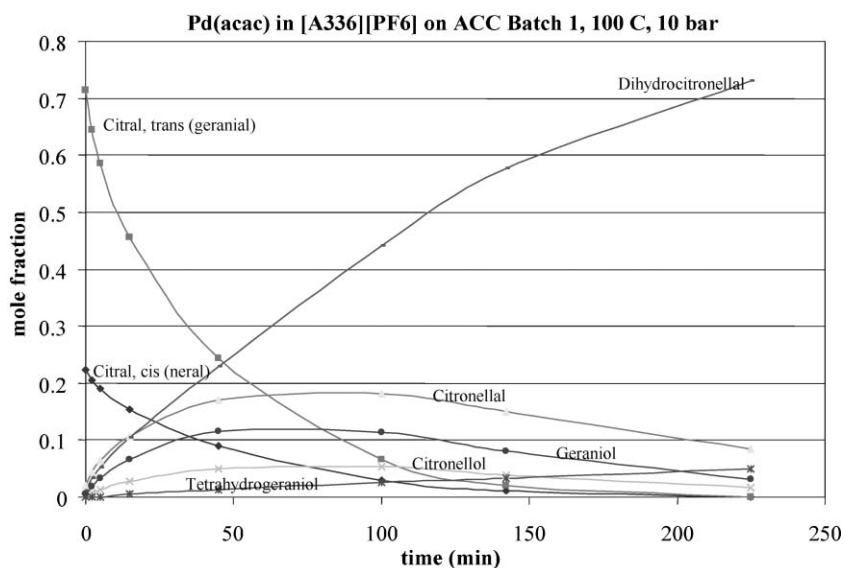


Fig. 5 Sample hydrogenation experiment of citral with an immobilized [A336][PF<sub>6</sub>]-Pd acetylacetonate system.

NaCl, KCl or NH<sub>4</sub>Cl, is not soluble but will form a precipitate that can be filtered out of the newly formed cation–anion pair. In addition to that, another environmentally more benign method was applied in several cases: direct dissolution of the new anion salt into the original ionic liquid and consequent filtration of the formed precipitate. At least in the case of the Aliquat 336<sup>®</sup> (A336)-derived ionic liquids (A336 has a convenient chloride anion) the procedure worked nicely, *e.g.* due to the relative good dissolution capability of A336 of many salts as well as its relatively low viscosity. However, the existence of chlorine anion in A336 as such imposes potential problems in applications involving *e.g.* transition metal catalysis, since trace amounts of chloride ions are difficult to remove and can retard or even poison the reaction involving transition metal species. Moreover, the physico–chemical properties of ILs are influenced by the purity of them. Therefore, some recently published methods<sup>9</sup> for synthesis of ionic liquids that do not involve the chloride anion at any stage are very welcome. Nevertheless, there are plenty of examples of ionic liquids prepared with chlorine containing precursors, which can be purified and applied in catalytic processes. Thus, it is clear that the properties of Aliquat 336<sup>®</sup>-based ionic liquids can be significantly influenced by means of simple exchange of the counter-ion. Detailed preparation procedures of the synthesized ionic liquids can be found in Part A of the ESI.†

Unexpectedly, an interesting result was obtained when looking at the crystals precipitated upon formation of [A336][OCN]: regular and smooth crystal-cubes with remarkably narrow size distribution at around 20 μm, resembling ‘Lego<sup>®</sup>’ blocks were observed (Fig. 6). We believe this to be indirect evidence about the structured character of the ionic liquid formed. At the moment it is not clear why the salt precipitated was organized in such a manner. Furthermore, whether this can be observed from metathesis salts over some other ionic liquids remains a mystery at the moment. However, the authors encourage the scientific community to investigate this further.

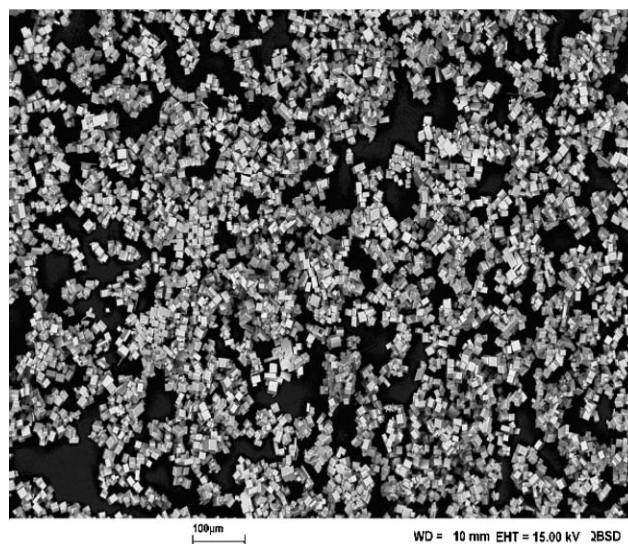


Fig. 6 SEM image showing the remarkably organized, regular crystal-cubes of KCl from the metathesis for [A336][OCN].

## Acknowledgements

The authors are grateful to Clifford Ekholm (SEM) and colleagues from Åbo Akademi University for their assistance. Financial support from the Academy of Finland is gratefully acknowledged (Decision nos. 209391 and 211463). This work is part of the activities at the Åbo Akademi Process Chemistry Centre (PCC) within the Finnish Centre of Excellence Programme (2000–2005 and 2006–2011) of the Academy of Finland.

## References

- P. J. Dyson, *Transition Metal Chem.*, 2002, **27**, 353–358.
- H. Zhao, S. V. Malhotra and R. G. Luo, *Phys. Chem. Liq.*, 2003, **41**, 487–492.

- 3 V. Singh, S. Kaur, V. Sapehiyia, J. Singh and G. L. Kad, *Catal. Commun.*, 2005, **6**, 57–60.
- 4 M. Deetlefs and K. R. Seddon, *Green Chem.*, 2003, **5**, 181–186.
- 5 B. M. Khadilkar and G. L. Rebeiro, *Org. Proc. Res. Dev.*, 2002, **6**, 826–828.
- 6 J. D. Holbrey and K. R. Seddon, *Clean Prod. Proc.*, 1999, **1**, 223–236.
- 7 28.12.2005; <http://www.phasetransfer.com/05tipJan.htm>, courtesy of Mr Mark Halpern, PCT Organics Inc., New Jersey, USA.
- 8 J.-P. Mikkola, P. Virtanen, H. Karhu, T. Salmi and D. Yu. Murzin, *Green Chem.*, 2006, **8**, 197–205.
- 9 J. D. Holbrey, W. M. Reichert, R. P. Swatloski, G. A. Broker, W. R. Pitner, K. R. Seddon and R. D. Rogers, *Green Chem.*, 2002, **4**, 407–413.

# Chemical Biology

An exciting news supplement providing a snapshot of the latest developments in chemical biology



Free online and in print issues of selected RSC journals!\*

**Research Highlights** – newsworthy articles and significant scientific advances

**Essential Elements** – latest developments from RSC publications

**Free links** to the full research paper from every online article during month of publication

\*A separately issued print subscription is also available

30110653

RSCPublishing

[www.rsc.org/chemicalbiology](http://www.rsc.org/chemicalbiology)

# *N*-methyl-*N*-alkylpyrrolidinium nonafluoro-1-butanesulfonate salts: Ionic liquid properties and plastic crystal behaviour†

Stewart A. Forsyth,‡<sup>a</sup> Kevin J. Fraser,<sup>a</sup> Patrick C. Howlett,<sup>a</sup> Douglas R. MacFarlane\*<sup>a</sup> and Maria Forsyth<sup>b</sup>

Received 12th September 2005, Accepted 19th December 2005

First published as an Advance Article on the web 23rd January 2006

DOI: 10.1039/b512902h

A series of *N*-methyl-*N*-alkylpyrrolidinium nonafluoro-1-butanesulfonate salts were synthesised and characterised. The thermophysical characteristics of this family of salts have been investigated with respect to potential use as ionic liquids and solid electrolytes. *N*-Methyl-*N*-butylpyrrolidinium nonafluoro-1-butanesulfonate (p<sub>1,4</sub>NfO) has the lowest melting point of the family, at 94 °C. Electrochemical analysis of p<sub>1,4</sub> NfO in the liquid state shows an electrochemical window of ~6 V. All compounds exhibit one or more solid–solid transitions at sub-ambient temperatures, indicating the existence of plastic crystal phases.

## Introduction

The search for new materials with combinations of advantageous properties with respect to electrolyte applications coincides with a large expansion in the range and diversity of molten salts (or ionic liquids if their melting point is below 100 °C) that have recently been identified.<sup>1–14</sup> Properties such as negligible vapour pressure, thermal stability, electrochemical stability and, importantly, ionic conductivity are recognised as critical characteristics if these materials are to not only match current electrolytes, but to surpass them. Ionic materials having several solid phases, some of which exhibit distinctly higher conductivity than the low temperature phase, often also display plastic material properties as described by Timmermans.<sup>15</sup> The ionic conductivity of such solid electrolytes is thought to be intimately linked with the nature and degree of molecular rotational motions within the crystal lattice.<sup>13</sup> These temperature dependent crystal lattice alterations and phase changes can be observed using differential scanning calorimetry.

The pyrrolidinium cation (1) has gained attention as an ionic liquid and plastic crystal former with anions such as tetrafluoroborate,<sup>16</sup> hexafluorophosphate<sup>17</sup> and bis(trifluoromethanesulfonyl)amide.<sup>18</sup> These low melting salts exhibit high

ionic conductivity in both solid and liquid phases and have received attention for use as electrolytes in a range of applications including lithium batteries.<sup>19</sup> In the battery application the pyrrolidinium cation coupled with the fluorinated anion in particular provide stable cycling of Li metal in the ionic liquid, an observation which may enable a safe lithium metal battery technology. Some of the plastic phases are also able to act as hosts for dopant ions such as Li<sup>+</sup>,<sup>20</sup> where the Li<sup>+</sup> ion in this case can show fast-ion conduction properties. It has, therefore, become of interest to identify these useful electrochemical and transport properties in a range of related compounds.

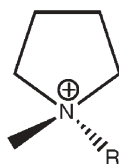
The nonafluoro-1-butanesulfonate anion (nonaflate, 2) belongs to an expanding group of fluorinated anions including tetrafluoroborate, hexafluorophosphate and bis(trifluoromethane)sulfonimide. The nonaflate anion is far more stable than the very common tetrafluoroborate and hexafluorophosphate anions. For example, hexafluorophosphate salts have been shown to be susceptible to hydrolysis even under relatively mild conditions. Warming an aqueous solution of a PF<sub>6</sub> salt results in considerable formation of HF over several hours.<sup>21</sup> Nonaflate salts of organic cations were first prepared as a by-product from the reaction between nonafluoro-1-butanesulfonyl fluoride, 4-(dimethylmethoxysilyl)-butylamine and an amine such as; pyridine, triethylamine, 1-methylimidazole, 1-methylmorpholine and 1-methylpyrrolidine.<sup>22</sup> A number of imidazolium nonaflate salts have previously been prepared, by the metathesis of 1-alkyl-3-methylimidazolium bromide and the readily available potassium salt of nonafluorobutanesulfonic acid.<sup>23</sup> Wasserscheid and Hilgers have also described the synthesis of perfluoroalkylsulfonate salts with many different cations.<sup>24</sup>

<sup>a</sup>School of Chemistry, Monash University, Wellington Road, Clayton, VIC 3800, Australia. E-mail: douglas.macfarlane@sci.monash.edu.au; Fax: +61 3 9905 4597; Tel: +61 3 9905 4540

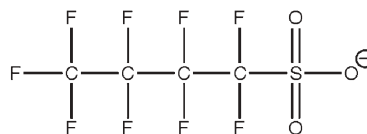
<sup>b</sup>Department of Materials Engineering, Australian Centre of Excellence in Electromaterials Science (ACES), Monash University, Wellington Road, Clayton, VIC 3800, Australia

† This work was presented at the 1st International Conference on Ionic Liquids (COIL), held in Salzburg, Austria, 19–22 June, 2005.

‡ Current address: Queens University, Belfast, Northern Ireland, UK.



*N*-methyl-*N*-alkylpyrrolidinium cation (1)



Nonafluoro-1-butanesulfonate anion (nonaflate, 2)



**Table 1** Thermal properties of pyrrolidinium nonaflate salts

Compound	Abbrev.	$T_g$ /°C	$T_{s-s}$ /°C	$T_x$ /°C	$T_{s-s}$ /°C	$T_{s-s}$ /°C	$T_m$ /°C	$\Delta S_f/J K^{-1} mol^{-1}$ ( $\pm 10\%$ )	$T_{dec}$ /°C
<i>N,N</i> -Dimethylpyrrolidinium nonaflate	p <sub>1,1</sub> NfO	—	—	—	−1	24	198	26	360
<i>N</i> -Ethyl- <i>N</i> -methylpyrrolidinium nonaflate	p <sub>1,2</sub> NfO	—	—	—	−59	−51	176	25	350
<i>N</i> -Propyl- <i>N</i> -methylpyrrolidinium nonaflate	p <sub>1,3</sub> NfO	—	−64	−22	−5	3 <sup>a</sup>	109	24	350
<i>N</i> -Butyl- <i>N</i> -methylpyrrolidinium nonaflate	p <sub>1,4</sub> NfO	−79	—	−4	5	—	94	32	350
<i>N</i> -Pentyl- <i>N</i> -methylpyrrolidinium nonaflate	p <sub>1,5</sub> NfO	—	—	—	—	−47	116–118	34	350
<i>N</i> -Hexyl- <i>N</i> -methylpyrrolidinium nonaflate	p <sub>1,6</sub> NfO	—	—	—	−60	97	120	29	350
1-Ethyl-3-methylimidazolium nonaflate	emiNfO	—	—	—	—	—	28 <sup>b</sup>	—	—
1-Butyl-3-methylimidazolium nonaflate	bmiNfO	—	—	—	—	—	20 <sup>b</sup>	—	—

<sup>a</sup> Peak has shoulder. <sup>b</sup> See Bonhote *et al.*<sup>23</sup> <sup>c</sup> Notes: all transitions quoted for peak temperatures. <sup>d</sup>  $T_g$  = Glass transition (onset),  $T_x$  = Temperature of crystallization (peak),  $T_{ss}$  = Solid–solid transition (peak),  $T_{dec}$  = Decomposition temperature.

Alkali-metal nonaflate salts have been used in a wide variety of applications including; oil and water-proofing of textiles,<sup>25</sup> fireproofing agents<sup>26</sup> and organic electrolytes for batteries.<sup>27</sup> More recently, nonaflate ionic liquids have been used as solvent replacements for 1,3-dipolar cycloaddition reactions<sup>28</sup> where significant rate enhancements and improved yields were observed.

This paper describes the synthesis and characterisation of a novel series of *N*-methyl-*N*-alkylpyrrolidinium nonaflates (p<sub>1,*x*</sub>NfO). Thermophysical and electrochemical analyses were used to evaluate the compounds for potential use in a variety of electrolyte applications. For simplicity, the nomenclature of the prepared compounds has been abbreviated (see Table 1). The cation nomenclature is abbreviated to p<sub>1,*x*</sub> where p indicates the pyrrolidinium cation, the subscript 1 indicates the *N*-methyl substituent and the *x* indicates the carbon number of the *N*-alkyl substituent. The anion is abbreviated to NfO as used in previous publications.<sup>23</sup> For example the *N*-methyl-*N*-butylpyrrolidinium nonaflate is denoted p<sub>1,4</sub>NfO.

## Results and discussion:

### Thermal analysis—melting point

Fig. 1 displays melting point data as a function of alkyl chain length for the current series of nonaflates and also a number of other pyrrolidinium salts (PF<sub>6</sub>,<sup>17</sup> BF<sub>4</sub><sup>16</sup> and Ntf<sub>2</sub><sup>18</sup>). The melting points of the nonaflate salts decrease with increasing

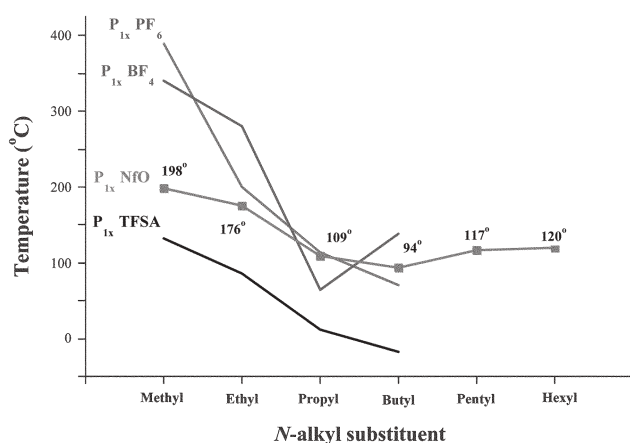


**Fig. 1** Melting point trend as a function of alkyl chain length for *N*-methyl-*N*-alkylpyrrolidinium salts.

alkyl chain length up to p<sub>1,4</sub> NfO. This trend is also apparent for the other salts displayed, with the exception of a ‘dip’ in the tetrafluoroborate series.

For the nonaflate series, the *N*-methyl derivative (p<sub>1,1</sub>NfO) and *N*-ethyl derivative (p<sub>1,2</sub>NfO) melt at 198 °C and 176 °C respectively. The downward trend continues with a substantial drop in melting point for the *N*-propyl (p<sub>1,3</sub>NfO) and *N*-butyl (p<sub>1,4</sub>NfO) derivatives, which melt at 109 °C and 94 °C respectively. This relatively large drop in melting point (67 °C) between p<sub>1,2</sub>NfO and p<sub>1,3</sub>NfO is not unique to pyrrolidinium nonaflate salts. Significant melting point depressions between the *N*-ethyl and *N*-propyl derivatives are also found in pyrrolidinium hexafluorophosphates, p<sub>1,2</sub>PF<sub>6</sub> (mp 200 °C) and p<sub>1,3</sub>PF<sub>6</sub> (mp 113 °C), pyrrolidinium tetrafluoroborates, p<sub>1,2</sub>BF<sub>4</sub> (mp 280 °C) and p<sub>1,3</sub>BF<sub>4</sub> (mp 64 °C) and pyrrolidinium bis(trifluoromethane)sulfonamides, p<sub>1,2</sub> TFSA (mp 86 °C) and p<sub>1,3</sub> TFSA (mp 12 °C). The melting points of the p<sub>1,*x*</sub>NfO series therefore are only low enough to produce a sub 100 °C melting point in one case. The temperature range around 100 °C is of significant interest in some electrochemical applications. Nonetheless, mixing of cations, and in particular addition of a lithium salt to produce a typical lithium battery electrolyte will further lower the melting points.

### Thermal analysis—phase behavior

Differential scanning calorimetry (DSC) traces from −120 °C to 60 °C and 60 °C to the melting point have been compiled in Fig. 2. All of the thermal data are summarised in Table 1. Employing phase nomenclature, as used previously,<sup>16</sup> multiple solid phases are numbered sequentially from the highest temperature crystalline phase to the lowest temperature phase.

The nonaflate salts were heated to 20 °C above the melting point then quenched and held at −100 °C before heating began. In Fig. 2 all the pyrrolidinium nonaflate salts exhibit multiple transitions below 60 °C and only a melting transition above 60 °C. All the salts in the series are in Phase 1 up to at least 90 °C, which may be important for solid electrolyte applications at moderate temperatures. Both the *N*-methyl and *N*-ethyl derivatives have two solid–solid transitions quite close together. The *N*-methyl derivative has two broad transitions between −1 °C and 24 °C, while *N*-ethyl has two quite sharp transitions at −59 °C and −51 °C. The *N*-propyl and *N*-butyl derivatives also have at least two solid–solid transitions but also display exothermic crystallisation at −22 °C and −4 °C respectively. The *N*-butyl, pentyl and hexyl (not shown)

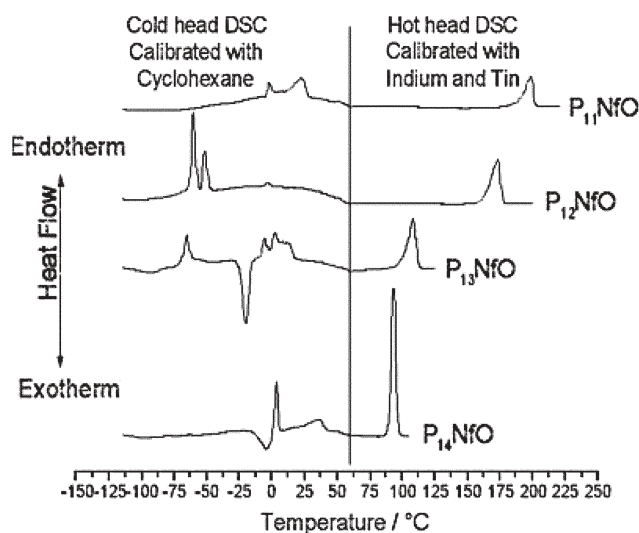


Fig. 2 Differential scanning calorimetry for  $p_{1,x}$ NfO series of salts.

have quite sharp melting points compared to the other salts in the series.

The multiple phases seen in this series of salts are likely to arise from rotational motions of one or both of the ions. As observed in other compounds exhibiting this behavior, the increasing complexity of the rotator motions involved (*e.g.* uniaxial *vs.* isotropic), with respect to either or both the ions present, generates a number of distinct rotator phases.<sup>13,18</sup> Each phase has entropy closer to the liquid state as the complexity approaches that of isotropic motion of both ions. This behavior makes these compounds very interesting from the point of view of ion conductors, in particular doped ion conductors.

The melting transitions for the series of nonaflates have entropy of fusion ( $\Delta S_f$ ) values between 24 and 34  $\text{J K}^{-1} \text{mol}^{-1}$ . The  $\Delta S_f$  values are calculated by integration of the melting endotherm ( $\Delta H_f$ ) and the relationship  $\Delta S_f = \Delta H_f/T_m$ . Timmermans<sup>15</sup> observed that materials which have entropies of fusion less than 20  $\text{J K}^{-1} \text{mol}^{-1}$  often have sub-melting phases with special properties; these phases are also known as plastic crystal phases.<sup>14</sup> The entropies of fusion for the nonaflate series are somewhat higher than the record low entropies for pyrrolidinium tetrafluoroborate salts (5–18  $\text{J K}^{-1} \text{mol}^{-1}$ ),<sup>16</sup> but are close to that of other pyrrolidinium salts; hexafluorophosphate<sup>17</sup> (13–17  $\text{J K}^{-1} \text{mol}^{-1}$ ) and bis(trifluoromethane)sulfonamide<sup>18</sup> (38–43  $\text{J K}^{-1} \text{mol}^{-1}$ ). These values are sufficiently low to suggest that the nonaflates fit the plastic crystal definition as outlined by Timmermans.<sup>15</sup>

Clearly a significant part of the total entropy is consumed by sub-melting transitions resulting in a low energy melt. It would be interesting to compare the thermal properties of the new nonaflate salts and the closely related triflate equivalents. Unfortunately this was not possible because the broad pyrrolidinium triflate series have not been studied or published in the journal literature (some patents do claim the synthesis of these compounds).<sup>29</sup> This void in the literature represents a possible avenue for future research, and related compounds yet to be fully investigated include  $\text{CF}_3\text{SO}_3^-$  and  $\text{F}_3\text{C}(\text{CF}_2)_n\text{SO}_3^-$ , with only  $n = 3$  having been studied thus far.

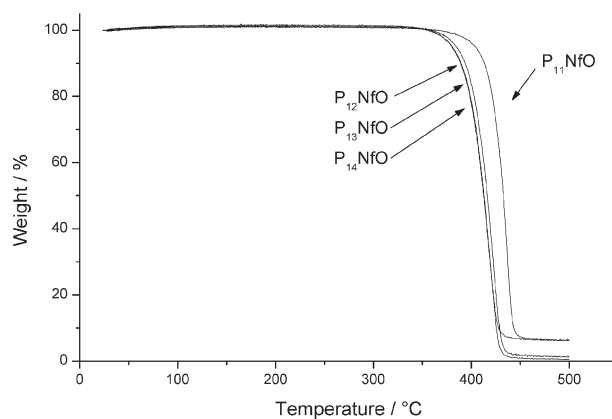


Fig. 3 Thermogravimetric analysis of  $p_{1,x}$ NfO salts.  $p_{15}$ ,  $p_{16}$  NfO not shown for clarity.

### Thermogravimetric analysis

Fig. 3 shows thermogravimetric traces for the pyrrolidinium nonaflates. The thermal decomposition temperatures for all of the series are recorded in Table 1.

The decomposition temperature,  $T_{\text{dec}}$ , is defined as the temperature at which irreversible mass loss begins. The nonflate series are thermally stable, showing virtually no weight loss between 30 °C and 350 °C.

This thermal stability is at least as good as 1,3-dialkylimidazolium triflates<sup>23,30</sup> and superior ( $\sim 50$  °C higher) than other pyrrolidinium alkylsulfonate ionic liquids, *i.e.* mesylates and tosylates.<sup>31</sup> The greater thermal stability of perfluoroalkylsulfonates compared to non-fluorinated alkylsulfonates is an advantage for higher temperature applications, or at least brief excursions to high operating temperatures.

### Cyclic voltammetry

Cyclic voltammograms are shown in Fig. 4A, B and C for  $p_{1,4}$ NfO cycled on a Pt working electrode at 150 °C. Fig. 4A shows that the sample is completely stable between  $-2.0$  V and  $+2.3$  V *vs.*  $\text{Ag}/\text{Ag}^+$ . The lack of any oxidative or reductive processes in this potential range indicates not only electrochemical stability of the solvent but also an absence of impurities that would normally be reactive in this range.

Fig. 4B shows an extended cyclic voltammogram, which indicates an electrochemical window approaching 6.0 V. Oxidation processes at  $\sim +2.75$  V are followed by a corresponding reduction event at around  $-1.59$  V in the reverse scan. Reduction processes at around  $-3.0$  V are followed by a corresponding oxidation process around  $+1.0$  V. The large potential differences between these melt breakdown processes and their corresponding reverse reactions indicate the strongly irreversible nature of the reactions involved.

Fig. 4C shows the result of extending the potential range to  $+5.0$  V. The oxidation process resolves into a well-defined peak indicating a diffusion or kinetic limit to the process. Given the appearance of a corresponding reduction peak (commencing at  $\sim 1.0$  V) and the fact that the reaction involves solvent molecules it is likely that the limit is imposed by reaction kinetics, possibly due to the formation of a solid passivating film. The peak from the corresponding reduction process

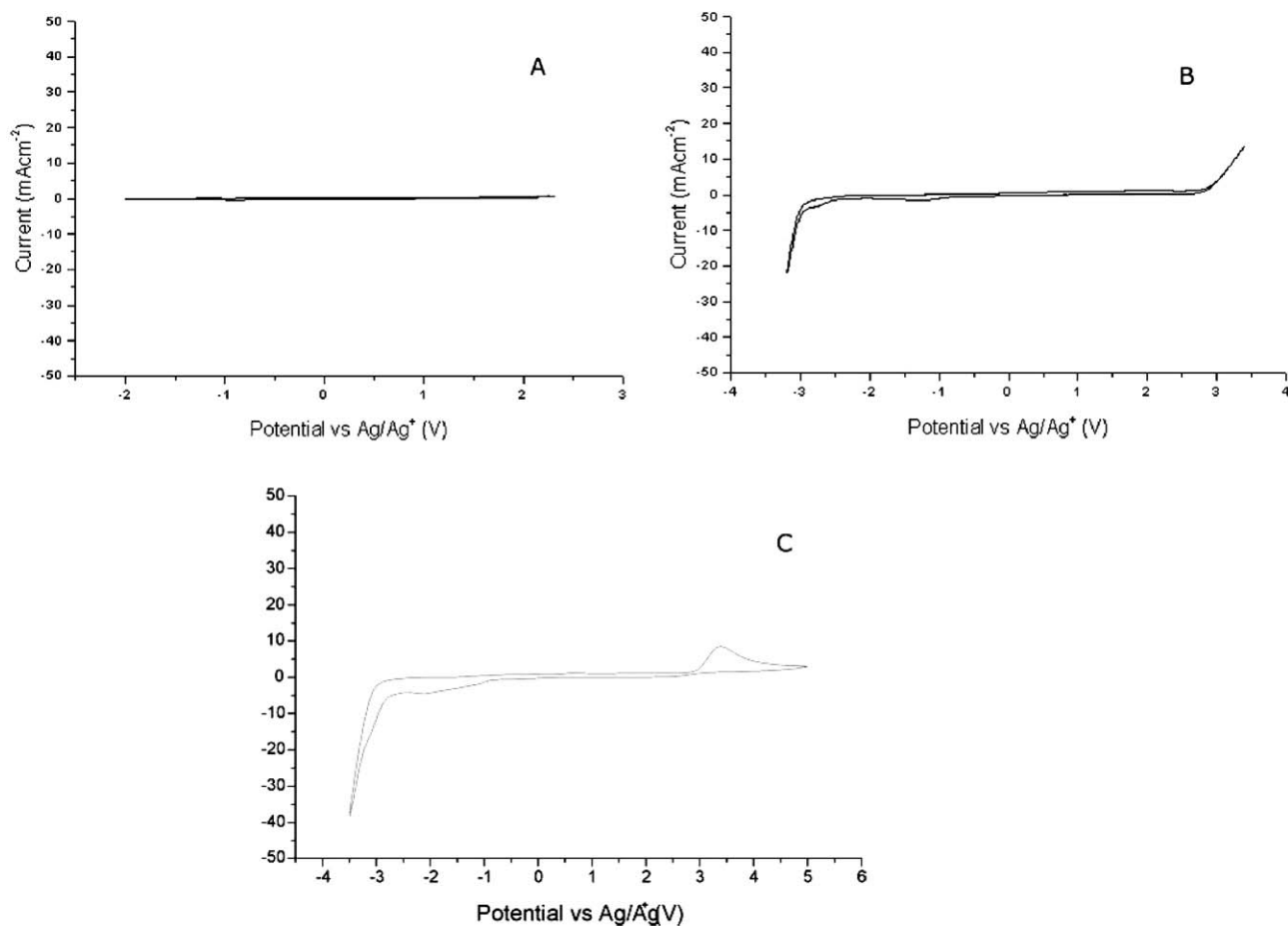


**Fig. 4** (A) Electrochemical stability between  $-2$  and  $2.3$  V vs.  $\text{Ag}/\text{Ag}^+$  for  $\text{p}_{1,4}\text{NfO}$ . (B) Electrochemical window for  $\text{p}_{1,4}\text{NfO}$  approaching  $6$  V vs.  $\text{Ag}/\text{Ag}^+$ . (C) Extended potential range results in electrochemical oxidation.

increases proportionately. Also of note is the similarity in appearance of the cyclic voltammograms for  $\text{p}_{1,4}\text{NfO}$  and that of  $\text{p}_{1,4}\text{TFSA}$ .<sup>18</sup> The oxidation/reduction processes occur at almost identical potentials and behave in the same manner indicating similar reaction mechanisms are occurring in both materials.

### Conductivity

Fig. 5 shows the conductivity behavior of  $\text{p}_{1,4}\text{NfO}$  versus temperature. The phase I conductivity is quite low and relatively constant, over the temperature range  $25$  °C to  $80$  °C, having a conductivity of around  $10^{-8}$   $\text{S cm}^{-1}$  at  $25$  °C. Approaching the melt, conductivity increases to  $5 \times 10^{-3}$   $\text{S cm}^{-1}$  in the liquid state. The DSC traces (Fig. 2) indicate the presence of plastic crystal phase I over a wide temperature range for these materials, particularly in the case of  $\text{p}_{1,2}\text{NfO}$  ( $>200$  °C), although that of  $\text{p}_{1,4}\text{NfO}$  ( $\sim 100$  °C) is still appreciable. The presence of sufficient rotational disorder in these substances at room temperature to exhibit appreciable conductivity in the solid state makes them interesting candidates for lithium doping. Increases in conductivity of up to four orders of magnitude have been reported in  $\text{p}_{1,1}\text{TFSA}$  and  $\text{p}_{1,2}\text{TFSA}$  by doping with Li-TFSA; these materials are thought to conduct by a fast ion conduction mechanism.<sup>20</sup> However, the highest

conductivity was exhibited by a 30 mol%  $\text{p}_{1,2}\text{TFSA}$  Li-TFSA binary system which melted at  $30$  °C. It was proposed that for the higher melting  $\text{p}_{1,x}\text{NfO}$  series, a high melting solid displaying fast ion conduction might be obtained. This is being further investigated.

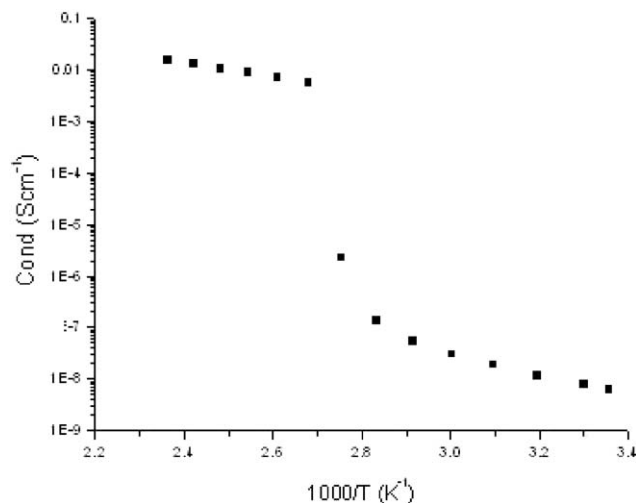


**Fig. 5** Conductivity of  $\text{p}_{1,4}\text{NfO}$ .

## Conclusions

The synthesis and characterisation of a series of *N*-methyl-*N*-alkyl-pyrrolidinium nonaflate salts has been described. The thermal and electrochemical properties have been assessed with regard to potential use in electrolyte applications. The combination of two plastic crystal forming ions has produced a series of salts with multiple solid phases below the melting point. All of the salts are in plastic phase I at ambient temperature, which may be important for their potential use in electrochemical devices. The nonaflate salts display remarkable thermal and electrochemical stability, with thermal decomposition temperatures approaching 350 °C and an electrochemical window of approximately 6 V (*vs.* Ag/Ag<sup>+</sup>). Ionic liquid applications for these pyrrolidinium nonaflate salts are possible at temperatures around 100 °C.

## Experimental

### Synthesis

*N*-Methylpyrrolidine, iodomethane, bromoethane, bromopropane, bromobutane, bromopentane and bromohexane were obtained from Aldrich (all > 99%) and used as received. Potassium nonaflate (Fluka > 97%) was recrystallised from water before use. The six nonaflate salts were prepared by a two-step process (see Scheme 1, in which the alkylmethylpyrrolidinium halide was initially prepared from literature methods<sup>18,32</sup> and then metathesised with potassium nonaflate in water.<sup>23</sup>

***N,N*-Dimethylpyrrolidinium nonafluorobutanesulfonate (p<sub>1,1</sub>NfO).** Potassium nonafluorobutanesulfonate (KNfO, 7.5 g, 22.2 mmol) was dissolved in 50 mL of water at 70 °C. An aqueous solution of *N,N*-dimethylpyrrolidinium iodide (p<sub>1,1</sub>I, 5 g, 22.0 mmol) was added and the mixture stirred at 70 °C for 2–3 hours. The solution was cooled and then extracted with dichloromethane. The organic layer was washed three times with water and then evaporated to dryness using a rotary evaporator. The white solid product was dried under high vacuum for 24 h and stored in a vacuum desiccator (4.0 g, 45%). The relatively low yield is attributed to the partition co-efficient of p<sub>1,1</sub>NfO in DCM/water. The halide content of the pure product was below the limit of detection (no precipitate when added to a silver nitrate solution), further DCM extractions from the aqueous layer resulted in product that was contaminated with halide. IR  $\nu_{\max}/\text{cm}^{-1}$ : 3576, 1353, 1259, 1133, 1058, 1059, 1005, 977, 934, 871, 804, 751, 736, 898, 737, 657. <sup>1</sup>H nmr  $\delta_{\text{H}}$  (300 MHz; CDCl<sub>3</sub>) 2.25–2.35 (4H, m, CH<sub>2</sub>), 3.26 (6H, s, N-CH<sub>3</sub>), 3.60–3.68 (4H, m, N-CH<sub>2</sub>). ES-MS: ES<sup>+</sup> *m/z* 100 p<sub>1,1</sub><sup>+</sup>. ES<sup>-</sup> *m/z* 299 NfO<sup>-</sup>.

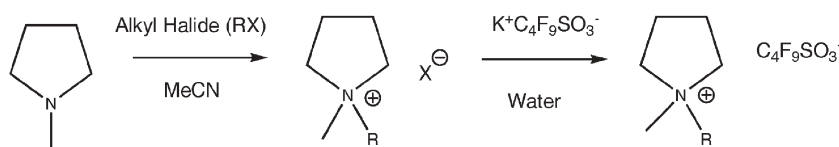
***N*-Methyl-*N*-ethylpyrrolidinium nonafluorobutanesulfonate (p<sub>1,2</sub>NfO).** Same procedure as for p<sub>1,1</sub>NfO. KNfO (7.6 g, 22.6 mmol) and p<sub>1,2</sub>Br (4 g, 20.6 mmol) afforded the title compound as a white solid (7.2 g, 85%). IR  $\nu_{\max}/\text{cm}^{-1}$ : 3418, 1353, 1258, 1133, 1058, 1057, 1005, 975, 908, 871, 803, 750, 736, 656. <sup>1</sup>H nmr  $\delta_{\text{H}}$  (300 MHz; CDCl<sub>3</sub>) 1.38–1.48 (3H, t, CH<sub>3</sub>), 2.21–2.32 (4H, m, CH<sub>2</sub>), 3.10 (3H, s, N-CH<sub>3</sub>), 3.50–3.60 (2H, m, N-CH<sub>2</sub>), 3.58–3.68 (4H, m, N-CH<sub>2</sub>). ES-MS: ES<sup>+</sup> *m/z* 114 p<sub>1,2</sub><sup>+</sup>. ES<sup>-</sup> *m/z* 299 NfO<sup>-</sup>.

***N*-Methyl-*N*-propylpyrrolidinium nonafluorobutanesulfonate (p<sub>1,3</sub>NfO).** Same procedure as for p<sub>1,1</sub>NfO. KNfO (11.6 g, 34.3 mmol) and p<sub>1,3</sub>Br (4 g, 19.2 mmol) afforded the title compound as a white solid (7.7 g, 94%). IR  $\nu_{\max}/\text{cm}^{-1}$ : 3564, 1352, 1260, 1135, 1058, 1059, 1006, 972, 907, 870, 802, 750, 698, 656. <sup>1</sup>H nmr  $\delta_{\text{H}}$  (300 MHz; CDCl<sub>3</sub>) 0.95–0.99 (3H, t, CH<sub>3</sub>), 1.83–1.97 (2H, m, CH<sub>2</sub>), 2.25–2.34 (4H, m, CH<sub>2</sub>), 3.22 (3H, s, N-CH<sub>3</sub>), 3.45–3.50 (2H, m, N-CH<sub>2</sub>), 3.66–3.71 (4H, m, N-CH<sub>2</sub>). ES-MS: ES<sup>+</sup> *m/z* 128 p<sub>1,3</sub><sup>+</sup>. ES<sup>-</sup> *m/z* 299 NfO<sup>-</sup>.

***N*-Methyl-*N*-butylpyrrolidinium nonafluorobutanesulfonate (p<sub>1,4</sub>NfO).** Same procedure as for p<sub>1,1</sub>NfO. KNfO (6.70 g, 19.8 mmol) and p<sub>1,4</sub>Br (4 g, 18.0 mmol) afforded the title compound as a white solid (7.3 g, 92%). IR  $\nu_{\max}/\text{cm}^{-1}$ : 3518, 1353, 1258, 1233, 1058, 1057, 1005, 975, 908, 871, 803, 750, 736, 656. <sup>1</sup>H nmr  $\delta_{\text{H}}$  (300 MHz; CDCl<sub>3</sub>) 0.92–0.97 (3H, t, CH<sub>3</sub>), 1.34–1.46 (2H, m, CH<sub>2</sub>), 1.81–1.92 (2H, m, CH<sub>2</sub>), 2.25–2.31 (4H, m, CH<sub>2</sub>), 3.22 (3H, s, N-CH<sub>3</sub>), 3.49–3.55 (2H, m, N-CH<sub>2</sub>), 3.66–3.72 (4H, m, N-CH<sub>2</sub>). ES-MS: ES<sup>+</sup> *m/z* 142 p<sub>1,4</sub><sup>+</sup>. ES<sup>-</sup> *m/z* 299 NfO<sup>-</sup>.

***N*-Methyl-*N*-pentylpyrrolidinium nonafluorobutanesulfonate (p<sub>1,5</sub>NfO).** Same procedure as for p<sub>1,1</sub>NfO. KNfO (6.70 g, 19.8 mmol) and p<sub>1,5</sub>Br (4.23 g, 18.0 mmol) afforded the title compound as a white solid (7.54 g, 92%). IR  $\nu_{\max}/\text{cm}^{-1}$ : 3575, 1462, 1377, 1133, 1058, 1050, 1007, 934, 908, 870, 803, 751, 736, 656. <sup>1</sup>H nmr  $\delta_{\text{H}}$  (300 MHz; CDCl<sub>3</sub>) 0.92–0.97 (3H, t, CH<sub>3</sub>), 1.34–1.46 (4H, m, CH<sub>2</sub>), 1.81–1.92 (2H, m, CH<sub>2</sub>), 2.25–2.31 (4H, m, CH<sub>2</sub>), 3.22 (3H, s, N-CH<sub>3</sub>), 3.49–3.55 (2H, m, N-CH<sub>2</sub>), 3.66–3.72 (4H, m, N-CH<sub>2</sub>). ES-MS: ES<sup>+</sup> *m/z* 156 p<sub>1,5</sub><sup>+</sup>. ES<sup>-</sup> *m/z* 299 NfO<sup>-</sup>.

***N*-Methyl-*N*-hexylpyrrolidinium nonafluorobutanesulfonate (p<sub>1,6</sub>NfO).** Same procedure as for p<sub>1,1</sub>NfO. KNfO (6.70 g, 19.8 mmol) and p<sub>1,6</sub>Br (4.48 g, 18.0 mmol) afforded the title compound as a white solid (7.85 g, 93%). IR  $\nu_{\max}/\text{cm}^{-1}$ : 3589, 1463, 1377, 1193, 1057, 1020, 1005, 975, 908, 871, 803, 750, 736, 656. <sup>1</sup>H nmr  $\delta_{\text{H}}$  (300 MHz; CDCl<sub>3</sub>) 0.92–0.97 (3H, t, CH<sub>3</sub>), 1.34–1.46 (4H, m, CH<sub>2</sub>), 1.81–1.92 (4H, m, CH<sub>2</sub>), 2.25–2.31 (4H, m, CH<sub>2</sub>), 3.22 (3H, s, N-CH<sub>3</sub>), 3.49–3.55 (2H, m,



**Scheme 1** Two-step process involves alkylation of *N*-methylpyrrolidine followed by metathesis with potassium nonaflate.

N-CH<sub>2</sub>), 3.66–3.72 (4H, m, N-CH<sub>2</sub>). ES-MS: ES<sup>+</sup> *m/z* 170 p<sub>1,6</sub><sup>+</sup>. ES<sup>-</sup> *m/z* 299 NfO<sup>-</sup>.

### Analysis

Infrared spectra were obtained in the range of 4000–650 cm<sup>-1</sup> on a Perkin-Elmer 1600 series FTIR spectrometer using KBr discs. <sup>1</sup>H NMR spectra were recorded on a Bruker DPX 300 spectrometer for solutions in CDCl<sub>3</sub>. Positive and Negative ion electrospray mass spectra (ESMS) were recorded with a Micromass Platform electrospray mass spectrometer for samples dissolved in methanol. Thermal analysis and temperature dependent phase behavior was studied in the range -100 °C to 300 °C by differential scanning calorimetry under N<sub>2</sub> at a rate of 10 °C min<sup>-1</sup> (Perkin Elmer DSC7). Thermal scans below room temperature were calibrated with the cyclohexane solid–solid transition and melting point at -87.0 °C and 6.5 °C respectively.

Thermal scans above room temperature were calibrated with the indium melting point at 156.6 °C. Transition temperatures were recorded at the peak maximum of the thermal transition. Thermogravimetric analysis was conducted using a STA1500 (Rheometric Scientific) in a flowing dry nitrogen atmosphere (50 ml min<sup>-1</sup>) between 30 °C and 500 °C with a heating rate of 10 °C per minute. The instrument was calibrated using four melting points (indium, tin, lead and zinc) and aluminium pans were used in all experiments. Electrochemistry was carried out in an argon drybox using a Maclab potentiostat, and Maclab software. Electrodes consisted of a platinum working electrode (polished, 0.05 μm Al<sub>2</sub>O<sub>3</sub>), a platinum coiled wire counter electrode and a silver wire pseudo reference electrode. All cyclic voltammograms were obtained at scanning rates of 200 mV s<sup>-1</sup> starting from 0 V and going to higher V first. The platinum working electrode surface area was determined by applying the Randles–Sevcik equation to the peak currents determined for a 5 mM ferrocene/acetonitrile solution ( $D = 2.3 \times 10^{-5}$  cm<sup>2</sup> s<sup>-1</sup>) at scanning rates of 50, 100, 200 mV s<sup>-1</sup>. Conductivity measurements were performed using a locally designed dip cell probe consisting of two platinum wires sheathed in glass. The sample was loaded (in the glovebox) in the molten state and allowed to cool to room temperature for a period of several hours, an o-ring seal between the sample vial and the probe wall allowed removal of the cell from the glovebox for measurement. The cell constant was determined with a solution of 0.01 M KCl at 25 °C. Conductivities were obtained by measurement of the complex impedance spectra between 10 MHz and 10 KHz on a Solartron SI 1296 Dielectric interface. The temperature was controlled at 10 °C intervals ( $\pm 1$  °C) using a Eurotherm 2204e temperature controller interfaced to the Solartron and a cartridge heater set in a brass block with a cavity for the cell. A T-type thermocouple was set in the block adjacent to the cell. The conductance was determined from the first real axis touch-down point in the Nyquist plot of the impedance data.

### References

- 1 C. A. Angell, W. Xu, J.-P. Belieres and M. Yoshizawa, *World Pat.*, WO2004114445, 2004.
- 2 E. Frackowiak, G. Lota and J. Pernak, *Appl. Phys. Lett.*, 2005, **161**64104/1–164104/3.
- 3 E. Marwanta, T. Mizumo, N. Nakamura and H. Ohno, *Polymer*, 2005, **11**, 3795–3800.
- 4 *Ionic Liquids in Synthesis*, ed. P. Wasserscheid and T. Welton, 2003, p. 364.
- 5 *Ionic Liquids: Industrial Applications to Green Chemistry*, ed. Robin D. Rogers and Kenneth R. Seddon, 2003, vol. **125**, p.7480.
- 6 W. Lu, I. D. Norris and B. R. Mattes, *Aust. J. Chem.*, 2005, **4**, 263–269.
- 7 J. Pernak, F. Stefaniak and J. Weglewski, *Eur. J. Org. Chem.*, 2005, **4**, 650–652.
- 8 K. Kim, C. M. Lang and P. A. Kohl, *J. Electrochem. Soc.*, 2005, **2**, E56–E60.
- 9 H. Matsui, K. Okada, N. Tanabe, R. Kawano and M. Watanabe, *Trans. Mater. Res. Soc. Jpn.*, 2004, **3**, 1017–1020.
- 10 D. Bansal, F. Cassel, F. Croce, M. Hendrickson, E. Plichta and M. Salomon, *J. Phys. Chem. B*, 2005, **10**, 4492–4496.
- 11 J. S. Lee, J. Y. Bae, H. Lee, N. D. Quan, H. S. Kim and H. Kim, *J. Ind. Eng. Chem. (Seoul, Republic of Korea)*, 2004, **7**, 1086–1089.
- 12 C. A. Angell, *Molten Salts: From Fundamentals to Applications*, *NATO Science Series, II: Mathematics, Physics and Chemistry*, 2002, pp. 305–320.
- 13 D. R. MacFarlane, P. Meakin, N. Amini and M. Forsyth, *J. Phys.: Condens. Matter*, 2001, **36**, 8257–8267.
- 14 D. R. MacFarlane and M. Forsyth, *Adv. Mater. (Weinheim, Ger.)*, 2001, **12–13**, 957–966.
- 15 J. Timmermans, *Phys. Chem. Solids*, 1961, **18**, 1–8.
- 16 S. Forsyth, J. Golding, D. R. MacFarlane and M. Forsyth, *Electrochim. Acta*, 2001, **10–11**, 1753–1757.
- 17 J. Golding, N. Hamid, D. R. MacFarlane, M. Forsyth, C. Forsyth, C. Collins and J. Huang, *Chem. Mater.*, 2001, **2**, 558–564.
- 18 D. R. MacFarlane, P. Meakin, J. Sun, N. Amini and M. Forsyth, *J. Phys. Chem. B*, 1999, **20**, 4164–4170.
- 19 N. Papageorgiou, Y. Athanassov, M. Armand, P. Bonhote, H. Pettersson, A. Azam and M. Graetzel, *J. Electrochem. Soc.*, 1996, **10**, 3099–3108.
- 20 D. R. MacFarlane, J. Huang and M. Forsyth, *Nature (London)*, 1999, **6763**, 792–794.
- 21 J. G. Huddleston, A. E. Visser, W. M. Reichert, H. D. Willauer, G. A. Broker and R. D. Rogers, *Green Chem.*, 2001, **4**, 156–164.
- 22 V. Beyl, H. Niederpruem and P. Voss, *Justus Liebigs Ann. Chem.*, 1970, 58–66.
- 23 P. Bonhote, A.-P. Dias, N. Papageorgiou, K. Kalyanasundaram and M. Graetzel, *Inorg. Chem.*, 1996, **5**, 1168–78.
- 24 P. Wasserscheid and C. Hilgers, *Eur. Pat.*, EP1182196, 2002.
- 25 M. Wechsberg and H. Niederpruem, *Ger. Pat.*, DE2319078, 1974.
- 26 G. Fennhoff, W. Schneider, K. Berg, V. Winkhaus and K. Horn, *Ger. Pat.*, DE4408215, 1995.
- 27 F. Kita and A. Kawakami, *Jpn. Pat.*, JP3238757, 1991.
- 28 J. F. Dubreuil and J. P. Bazureau, *Tetrahedron Lett.*, 2000, **38**, 7351–7355.
- 29 N. Ignatyev, M. Schmidt, U. Heider, P. Sartori and A. Kucheryna, *EP*, 2002098844, 2002.
- 30 H. L. Ngo, K. LeCompte, L. Hargens and A. B. McEwen, *Thermochim. Acta*, 2000, 97–102.
- 31 J. Golding, S. Forsyth, D. R. MacFarlane, M. Forsyth and G. B. Deacon, *Green Chem.*, 2002, **3**, 223–229.
- 32 J. Sun, D. R. MacFarlane and M. Forsyth, *Ionics*, 1997, **5&6**, 356–362.

# Changing from an unusual high-temperature demixing to a UCST-type in mixtures of 1-alkyl-3-methylimidazolium bis{(trifluoromethyl)sulfonyl}amide and arenes†‡

Joanna Łachwa,<sup>a</sup> Jerzy Szydłowski,<sup>b</sup> Anna Makowska,<sup>b</sup> Kenneth R. Seddon,<sup>c</sup> José M. S. S. Esperança,<sup>a</sup> Henrique J.R. Guedes<sup>a</sup> and Luís Paulo N. Rebelo<sup>\*a</sup>

Received 19th September 2005, Accepted 22nd December 2005

First published as an Advance Article on the web 23rd January 2006

DOI: 10.1039/b513308d

Upper critical solution temperature (UCST) combined with a high-temperature demixing type of phase diagrams are reported for binary liquid mixtures containing the ionic liquids, 1-alkyl-3-methylimidazolium bis{(trifluoromethyl)sulfonyl}amide ([C<sub>n</sub>mim][NTf<sub>2</sub>], where *n* = 2, 4, 6, 8, 10) and benzene, toluene, or  $\alpha$ -methylstyrene (PhC(Me)=CH<sub>2</sub>), at atmospheric and moderately high pressure. The phase diagrams were determined either using a dynamic method with visual detection of phase transitions or a laser light scattering technique. In our investigations, as the imidazolium alkyl chain length of the ionic liquid increases, the mixtures containing an arene evolve from a rarely found high-temperature demixing behaviour, to “hour-glass”, to the common phase splitting as temperature diminishes (UCST, whenever a critical point was found). For the three systems containing specifically [C<sub>10</sub>mim][NTf<sub>2</sub>] with benzene, toluene, or  $\alpha$ -methylstyrene, data were also collected up to 5 MPa using a high-pressure laser light scattering apparatus. For all phase diagrams, the critical compositions correspond to low concentrations of the ionic liquid. This fact underlies the possibility that ionic liquids, even in relatively dilute solutions, tend to form multiple-ion aggregates. This was corroborated by electro-spray mass spectrometry.

## Introduction

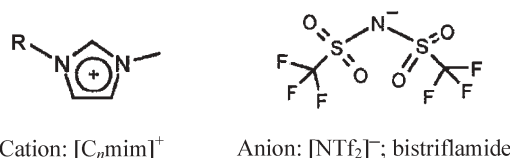
Stable low-temperature molten salts exert negligible vapour pressure at or about room temperature.<sup>1,2</sup> Hence, they are perceived as environmentally benign to the atmosphere, having thus become extremely attractive as alternative solvents. However, many interesting features of their peculiar, surprising behaviour in solution<sup>3–9</sup> are still to be discovered.

Ionic liquids based on the 1-alkyl-3-methylimidazolium cation, [C<sub>n</sub>mim]<sup>+</sup>, are among the most popular and commonly studied. As for the anions, [NTf<sub>2</sub>]<sup>−</sup> is much superior compared to the more commonly investigated hexafluorophosphate and tetrafluoroborate, being hydrolytically stable and less viscous.<sup>10,11</sup>

In a very recent, previous work,<sup>3</sup> we found the first evidence for the existence of closed-loop type liquid phase diagrams in ionic liquid solutions as well as critical demixing phenomena upon temperature increase—lower critical solution temperature (LCST). We concluded that, depending on the working temperature range considered, two distinct mechanisms for

phase splitting upon temperature rise exist. Additionally, it was anticipated that benzene and benzene derivatives would interact with [C<sub>n</sub>mim][NTf<sub>2</sub>] in such a fashion that there would also be chances of finding unusual high-temperature demixing.

Therefore, in this work, liquid–liquid equilibria of binary mixtures containing the ionic liquids, 1-alkyl-3-methylimidazolium bis{(trifluoromethyl)sulfonyl}amide ([C<sub>n</sub>mim][NTf<sub>2</sub>], where *n* = 2, 4, 6, 8, 10) and benzene, toluene, or  $\alpha$ -methylstyrene have been investigated. The structural formulas of the cations and the anions of the ionic liquids are:



Some equilibrium studies in the ionic liquid/arene systems can be found in the literature.<sup>12,13</sup> Generally, they demonstrate partial miscibility but no liquid–liquid critical phenomena; in some cases, clathrate formation has been found.<sup>9</sup> So far, liquid–liquid critical behaviour has seemed to be exclusive to ionic liquids in either water or alcohols,<sup>5,14</sup> or in chloroalkanes:<sup>3</sup> in this work, it was also found in arenes.

## 2. Experimental

### 2.1. Materials

1-alkyl-3-methylimidazolium bis{(trifluoromethyl)sulfonyl}amides ([C<sub>n</sub>mim][NTf<sub>2</sub>], where *n* = 2, 4, 6, 8, 10) were

<sup>a</sup>Instituto de Tecnologia Química e Biológica, ITQB 2, Universidade Nova de Lisboa, Apartado 127, 2780-901 Oeiras, Portugal.

E-mail: luis.rebelo@itqb.unl.pt

<sup>b</sup>Department of Chemistry, Warsaw University, Zwirki i Wigury 101, 02-093 Warsaw, Poland

<sup>c</sup>The QUILL Centre, The Queen's University of Belfast, Stranmillis Road, Belfast, UK BT9 5AG

† This work was presented at the 1st International Conference on Ionic Liquids (COIL), held in Salzburg, Austria, 19–22 June, 2005.

‡ Electronic supplementary information (ESI) available: Experimental data (Tables S1–S4). See DOI: 10.1039/b513308d

synthesised at QUILL (The Queen's University Ionic Liquid Laboratories, Belfast) according to methods found elsewhere,<sup>10</sup> where they underwent first-stage purification. These ionic liquids were washed several times with water to decrease the chloride content. It was confirmed that no precipitation (of AgCl) occurred by adding AgNO<sub>3</sub> to the wash water. NMR analyses showed no major impurities in the untreated, original samples, except for the presence of water. All samples were further thoroughly degassed, dried, and freed from any small traces of volatile compounds by applying a vacuum (0.1 Pa) at moderate temperatures (60–80 °C) for typically 48 h. Then, both the water and chloride contents were analysed. Karl–Fischer titrations revealed very low levels of water (typically below 70 ppm) for all treated ionic liquids, as compared with values of 2500–5500 ppm of water for untreated samples. The Cl<sup>−</sup> specific electrode using the standard addition method has generally shown chloride contents in the range of 20–150 ppm. For the determination of the phase diagrams, fresh samples of the ionic liquids kept under vacuum were always used immediately prior to the measurements.  $\alpha$ -Methylstyrene (Aldrich, 99%, GC), and toluene (99.8%, HPLC) were purchased from Sigma-Aldrich while benzene (99.5% for analysis ACS-ISO) was purchased from Panreac. All solvents, except  $\alpha$ -methylstyrene, were further dried with 3 Å molecular sieves.

## 2.2. Apparatus and procedure

Some liquid–liquid equilibrium temperatures at 0.1 MPa nominal pressure were determined using a dynamic method with visual detection (naked eye determination of turbidity) of the phase transitions. The appropriate mixtures of the ionic liquid and solvent were heated very slowly (at less than 2 K h<sup>−1</sup> near the equilibrium temperature) with continuous stirring inside Pyrex glass capillaries, which were placed in a glass thermostat filled with water (from 293 K up to 343 K), or silicon oil (up to 500 K). The capillaries were sealed at both ends and the mixture occupied almost the entire internal volume ( $\pm 0.5$  cm<sup>3</sup>), leaving a small dead volume of gas phase. The mixtures were gravimetrically prepared and the error in the weight fraction composition was estimated to be within  $\pm 2 \times 10^{-5}$ . The temperature at which the last (first) signs of turbidity disappeared (appeared) was taken as the temperature of the liquid–liquid transition. Temperature was measured using a platinum resistance thermometer coupled to a Keithley 199 System DMM/Scanner. The thermometer was calibrated against high accuracy mercury thermometers ( $\pm 0.01$  K).

For [C<sub>10</sub>mim][NTf<sub>2</sub>] with benzene, toluene, or  $\alpha$ -methylstyrene, the pressure effects on the liquid–liquid equilibrium temperature were obtained by a He–Ne laser light scattering technique. The apparatus and the methodology used for the determination of phase transitions have already been described in detail.<sup>15</sup> Here, only a brief description is provided. The cell (with an internal volume of ca. 1.0 cm<sup>3</sup> and an optical length of ca. 2.6 mm) is a thick-walled Pyrex glass tube that is connected to a pressurisation line and separated from it by a mercury plug. The intensity of the scattered light is captured at a very low angle ( $2^\circ < 2\theta < 4^\circ$ ) in the outer portion of a bifurcated optical cable, whereas transmitted light is captured in the inner

portion of this cable. The intensity of scattered light ( $I_{sc}$ ) and transmitted light ( $I_{tr}$ ) are corrected for density fluctuations, reflections, and multiple scattering effects. The cloud-point is the point on the least-squares fits of  $(I_{sc,corr})^{-1}$  against pressure ( $p$ ) or temperature ( $T$ ) where the slope changes abruptly. Temperature accuracy is typically  $\pm 0.01$  K in the range  $240 < T/K < 380$ . As for pressure, accuracy is  $\pm 0.01$  MPa in the range  $0.1 < p/\text{MPa} < 5$ . The cell can be operated in the isobaric or isothermal mode.

In this work, this apparatus was mainly used for the determination of phase transitions at pressures different from atmospheric. Whenever possible, isothermal runs are preferred over isobaric ones. Pressure transmission (isothermal mode) is many orders of magnitude faster than thermal equilibration (isobaric mode). Also, the rate at which one is able to change pressure is much greater than that for temperature. Nonetheless, many runs had to be performed in the isobaric mode due to the common low  $T$ – $p$  slope presented by the binary mixtures being studied here.

Electro-spray mass spectra were measured on an ion trap instrument (Bruker, model Esquire 3000+, with upper mass to charge ( $m/z$ ) limit of 3000 Da) in the positive and negative modes for [C<sub>10</sub>mim][NTf<sub>2</sub>] using benzene as the solvent, flow rate of 100  $\mu\text{l h}^{-1}$ , and source temperature of 200 °C.

## 3. Results and discussion

The experimental LLE data measured at atmospheric pressure for [C<sub>*n*</sub>mim][NTf<sub>2</sub>] ( $n = 2, 4, 6, 8, 10$ ) with benzene, toluene, or  $\alpha$ -methylstyrene are reported in more detail in the ESI (Tables S1–S3)† and some phase diagrams are illustrated in Fig. 1 and 2. To the best of our knowledge, only solubilities of benzene in [C<sub>2</sub>mim][NTf<sub>2</sub>] and in [C<sub>4</sub>mim][NTf<sub>2</sub>] at 353.15 K are indirectly available<sup>13</sup> for comparison, and the agreement with our data is fairly good. Experimental cloud-points determined as a function of pressure ( $T$ – $p$  plots) for [C<sub>10</sub>mim][NTf<sub>2</sub>] with benzene, toluene, or  $\alpha$ -methylstyrene are summarised in the ESI (Table S4)† and presented in Fig. 3–5.

In all the cases studied, the miscibility of each bistriflamide with the aromatic solvents decreases in the order benzene > toluene >  $\alpha$ -methylstyrene. Holbrey *et al.*<sup>9</sup> observed a similar trend in their study of clathrate formation in mixtures of ionic liquids with arenes.

As for pressure effects, all three systems containing [C<sub>10</sub>mim][NTf<sub>2</sub>] show improved miscibility upon pressurisation (negative slopes—see Table 1—of the  $T$ – $p$  plots of the UCST branches of the phase diagrams). This type of behaviour at the UCST usually denotes that mixtures are formed upon contraction (excess volume,  $v^E < 0$ ), because under some common restrictive assumptions,<sup>16</sup> this constitutes a thermodynamic requirement. There are no density studies of these mixtures to test this prediction.

In respect of the influence of the cation alkyl chain length, C<sub>*n*</sub>, one observes that for  $n = 2$  liquid–liquid splitting is attained by temperature increase. This is a rarely found situation that, to the best of our knowledge, represents the second case known for ionic liquid solutions (the first<sup>3</sup> was observed for [C<sub>*n*</sub>mim][NTf<sub>2</sub>] with CHCl<sub>3</sub>). As the alkyl chain increases up to  $n = 6$ , the immiscible region of all systems is

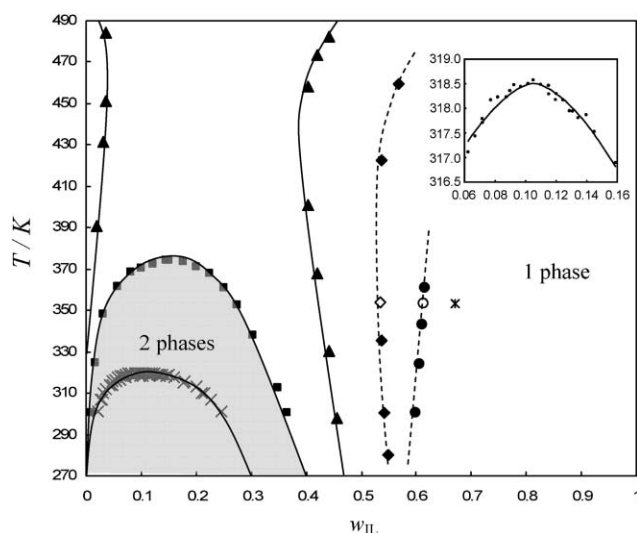


**Fig. 1** Liquid-liquid phase diagrams of  $[C_n\text{mim}][\text{NTf}_2]$  + benzene at a nominal pressure of 0.1 MPa;  $n$  is the number of carbon atoms in the alkyl chain of the cation, and  $w_{\text{IL}}$  is the weight fraction of ionic liquid; experimental data: \*,  $n = 1$  (datum calculated from VLE<sup>13</sup>); ●,  $n = 2$ ; ○,  $n = 2$  (datum calculated from VLE<sup>13</sup>); ◆,  $n = 4$ ; ◇,  $n = 4$  (datum calculated from VLE<sup>13</sup>); ▲,  $n = 6$ ; ■,  $n = 8$ ; ×,  $n = 10$ . For  $n = 8$  and  $n = 10$  the full lines represent the parameterised (see Table 2) scaling-type eqn (1). All other curves were drawn for visual aid. The shaded area depicts the demixing region for  $n = 8$ . The insert represents a detail of the liquid-liquid equilibrium of the system  $[C_{10}\text{mim}][\text{NTf}_2]$  + benzene for temperatures near the critical one; solid circles, experimental data; — values calculated using the scaling-type eqn (1).

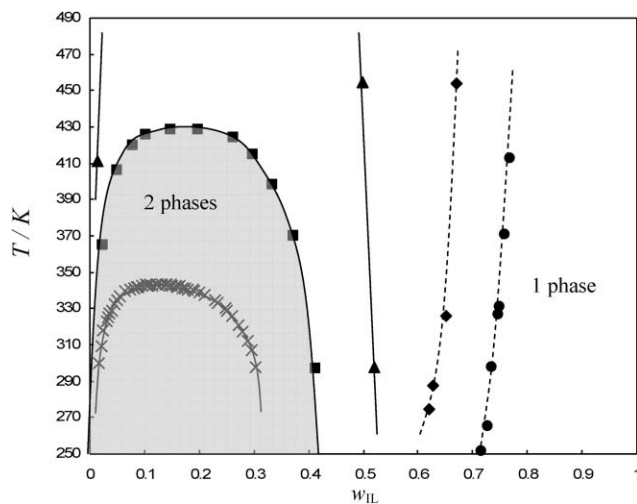


**Fig. 2** Liquid-liquid phase diagrams of  $[C_n\text{mim}][\text{NTf}_2]$  +  $\alpha$ -methylstyrene at a nominal pressure of 0.1 MPa;  $n$  is the number of carbon atoms in the alkyl chain of the cation, and  $w_{\text{IL}}$  is the weight fraction of ionic liquid; experimental data: ●,  $n = 2$ ; ◆,  $n = 4$ ; ▲,  $n = 6$ ; ■,  $n = 8$ ; ×,  $n = 10$ . For  $n = 8$  and  $n = 10$  the full lines represent the parameterised (see Table 2) scaling-type eqn (1). All other curves were drawn for visual aid. The shaded area depicts the demixing region for  $n = 8$ .

significantly reduced and changes the shape to the so-called “hourglass” type of phase diagram (merging of the LCST and UCST branches of the phase diagram). As the lengthening of

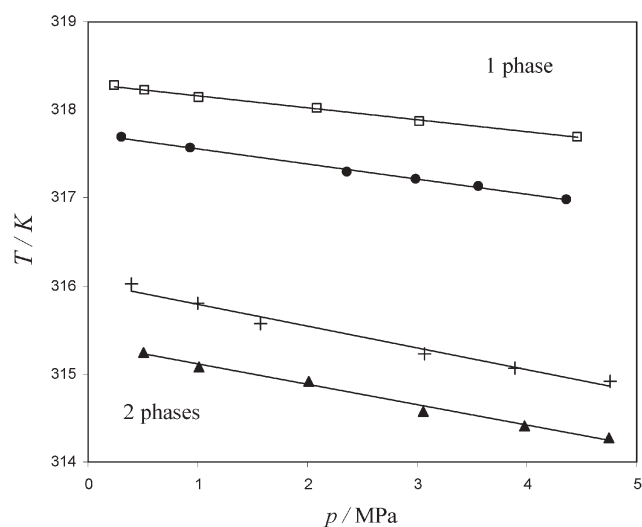


**Fig. 3** Liquid-liquid transition temperatures as a function of pressure for different concentrations of the ( $[C_{10}\text{mim}][\text{NTf}_2]$  + benzene) system;  $w_{\text{IL}}$  is the weight fraction of ionic liquid; experimental data: □,  $w_{\text{IL}} = 0.11510$ ; ●,  $w_{\text{IL}} = 0.07184$ ; +,  $w_{\text{IL}} = 0.05478$ ; ▲,  $w_{\text{IL}} = 0.17749$ .

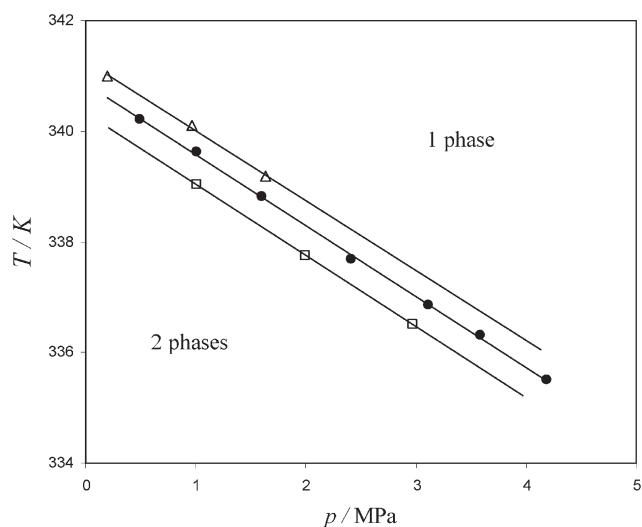


**Fig. 4** Liquid-liquid transition temperatures as a function of pressure for different concentrations of the ( $[C_{10}\text{mim}][\text{NTf}_2]$  + toluene) system;  $w_{\text{IL}}$  is the weight fraction of ionic liquid; experimental data: △,  $w_{\text{IL}} = 0.11736$ ; ●,  $w_{\text{IL}} = 0.16834$ ; □,  $w_{\text{IL}} = 0.09204$ .

the alkyl chain continues from hexyl, to octyl, to decyl, miscibility keeps improving and induces the appearance of only UCSTs, displacing the inherent LCSTs to high temperatures out of the working range ( $>500$  K). These changes can be appreciated in a single, schematic  $p$ - $T$  diagram—Fig. 6. Generally, the UCST decreases and the LCST increases as the number of carbons in the cationic alkyl chain of the bistriflamides increases. This complicated overall behaviour underlies very rich enthalpic phenomena upon mixing—the excess enthalpy,  $h^E$ , can change sign upon temperature variation and/or alkyl length change. The overall phase diagram of  $[C_n\text{mim}][\text{NTf}_2]$  and arene binary mixtures as  $n$  varies from 2 to 10 present both UCST and LCST branches. In



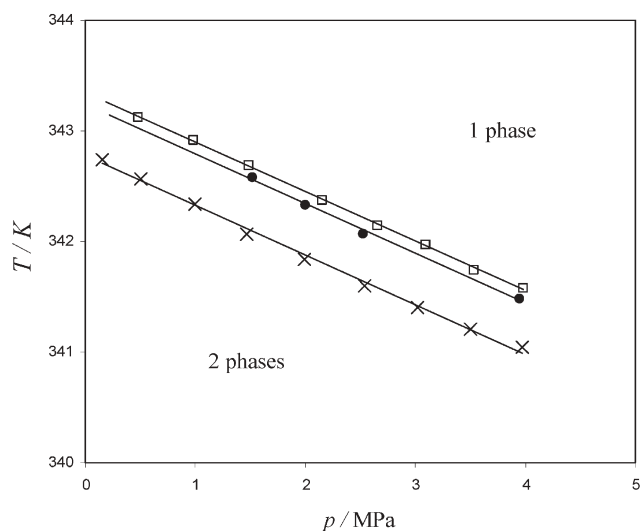


**Fig. 5** Liquid–liquid transition temperatures as a function of pressure for different concentrations of the ([C<sub>10</sub>mim][NTf<sub>2</sub>] +  $\alpha$ -methylstyrene) system;  $w_{\text{IL}}$  is the weight fraction of ionic liquid; experimental data:  $\times$ ,  $w_{\text{IL}} = 0.10647$ ;  $\bullet$ ,  $w_{\text{IL}} = 0.12255$ ;  $\square$ ,  $w_{\text{IL}} = 0.14193$ .

the neighbouring region of a UCST,  $h^E > 0$ , while  $h^E < 0$  should be found close to a LCST.<sup>16</sup> Kato *et al.*<sup>13</sup> determined the excess enthalpies of binary mixtures of [C<sub>2</sub>mim][NTf<sub>2</sub>] with benzene in the whole composition range of the homogeneous liquid and at 323.15 K, and, in fact, found  $h^E$  versus  $x_{\text{IL}}$  to be negative with an extremum at  $-730 \text{ J mol}^{-1}$  for  $x_{\text{IL}} = 0.3652$ . There are no comparative values for [C<sub>*n*</sub>mim][NTf<sub>2</sub>] ( $n > 2$ ) and/or substituted benzenes. Nonetheless, the temperature dependence of activity coefficients at infinite dilution [ $-\partial \ln \gamma^\infty / \partial T = h^{E,\infty} / RT^2$ ] also provide information about the enthalpic behaviour of the solutions. These studies exist<sup>13,17</sup> for benzene, toluene, and  $\alpha$ -methylstyrene in [C<sub>*n*</sub>mim][NTf<sub>2</sub>] up to  $n = 4$ . They all show that the infinite dilution activity coefficients increase as temperature rises up to about 330 K (thus,  $h^{E,\infty} < 0$ ) and that  $\gamma^\infty$  decreases in the order [C<sub>1</sub>mim][NTf<sub>2</sub>] > [C<sub>2</sub>mim][NTf<sub>2</sub>] > [C<sub>4</sub>mim][NTf<sub>2</sub>] at fixed arene species, as it does for  $\alpha$ -methylstyrene > toluene > benzene at fixed ionic liquid. These results are in perfect qualitative agreement with the degree of miscibility found in the current work. Conversely, we expect that for substituted imidazolium cations with longer alkyl chains, one will find  $h^E > 0$  and  $h^E < 0$  at low and high temperatures, respectively.

**Table 1**  $T$ - $p$  slopes of the UCST branch of the phase diagram of [C<sub>10</sub>mim][NTf<sub>2</sub>] + aromatics;  $x_{\text{IL}}$  and  $w_{\text{IL}}$ , and  $p$  and  $T$  are the mole and weight fraction of ionic liquid, and pressure and temperature of transition, respectively

$x_{\text{IL}}$	$w_{\text{IL}}$	$T/K$		$dT/dp$ K MPa <sup>-1</sup>	$x_{\text{IL}}$	$w_{\text{IL}}$	$T/K$		$dT/dp$ K MPa <sup>-1</sup>
		$(p = 0.1 \text{ MPa})$					$(p = 0.1 \text{ MPa})$		
[C <sub>10</sub> mim][NTf <sub>2</sub> ] + benzene									
0.00891	0.05478	316.02		-0.25	0.01978	0.11510	318.29		-0.14
0.01187	0.07184	317.71		-0.17	0.03239	0.17749	315.32		-0.23
[C <sub>10</sub> mim][NTf <sub>2</sub> ] + toluene									
0.01821	0.09204	340.18		-1.28	0.03572	0.16834	340.73		-1.28
0.02375	0.11736	341.15		-1.27					
[C <sub>10</sub> mim][NTf <sub>2</sub> ] + $\alpha$ -methylstyrene									
0.02721	0.10647	342.73		-0.45	0.03737	0.14193	343.30		-0.45
0.03174	0.12255	343.19		-0.45					

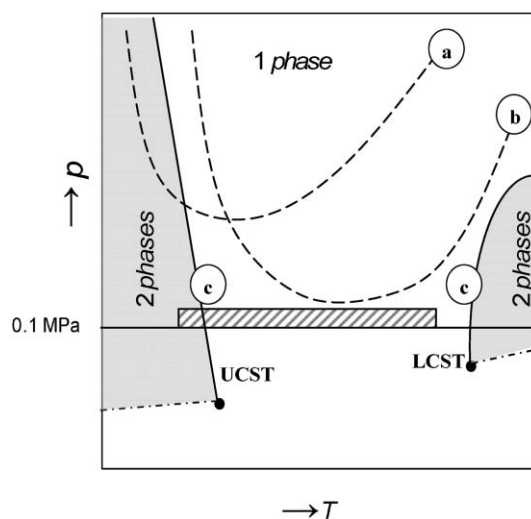


**Fig. 6** Schematic, simplified  $p$ - $T$  projection of the changes in the overall phase diagram of ([C<sub>*n*</sub>mim][NTf<sub>2</sub>] + aromatic) binary mixtures as  $n$  varies from 2 (case a), to 6 (case b), to 10 (case c). Full and dashed curves hold for L-L critical loci while dashed-dotted lines are for L-L-V equilibria. For the sake of clarity, vapour pressure lines of pure IL and solvent are omitted. The hatched rectangle illustrates the  $p$ - $T$  working conditions used in this work.

In order to attempt the determination of UCST critical parameters at a nominal pressure of 0.1 MPa, such as the critical temperature,  $T_c$ , and the critical mass fraction of the ionic liquid,  $w_c$ , scaling-type equations were applied to [C<sub>8</sub>mim][NTf<sub>2</sub>] and to [C<sub>10</sub>mim][NTf<sub>2</sub>] with benzene (shown as an example in the insert of Fig. 1), and with  $\alpha$ -methylstyrene:

$$|w - w_c| = A \left( \frac{T_c - T}{T_c} \right)^\beta \quad (1)$$

$T$  is the composition dependent temperature of the transition,  $w$  is the corresponding mass fraction of the ionic liquid, and the subscript c holds for critical conditions.  $A$  and  $\beta$  are the amplitude and exponent, respectively, and should be considered as mere fitting parameters in the neighbouring region of the critical point. The parameters of eqn (1) at atmospheric pressure are given in Table 2.

It is clear that the critical compositions correspond to relatively low concentrations of the ionic liquids in the solvent, much lower than those expected by direct consideration of an

**Table 2** Critical parameters of the scaling-type eqn (1) for a nominal pressure of 0.1 MPa.  $T_c$  is the critical temperature,  $w_c$  and  $x_c$  are the critical mass and mole fractions of IL, respectively. The parameters  $A$  and  $\beta$  are the fitted amplitude and exponent, respectively, with no meaning in terms of critical phenomena

Solvent	IL	$T_c/K$	$w_c$	$x_c$	$A$	$\beta$
Benzene	[C <sub>8</sub> mim][NTf <sub>2</sub> ]	374.36	0.15288	0.02879	0.843	0.602
	[C <sub>10</sub> mim][NTf <sub>2</sub> ]	318.51	0.10521	0.01791	1.341	0.614
$\alpha$ -Methylstyrene	[C <sub>8</sub> mim][NTf <sub>2</sub> ]	428.43	0.18154	0.05225	0.274	0.249
	[C <sub>10</sub> mim][NTf <sub>2</sub> ]	343.11	0.12532	0.03253	0.423	0.421

ion-pair type of structure in solution. In this work, values of  $x_{c,IL}$  can be directly obtained for [C<sub>8</sub>mim][NTf<sub>2</sub>] and [C<sub>10</sub>mim][NTf<sub>2</sub>] with arenes, and the critical molar fractions are found in the range  $0.01 < x_{c,IL} < 0.06$  (see Table 2). As explained below, this fact underlies the possibility that ionic liquids, even in dilute solutions, tend to form aggregates (typically three-dimensional clusters stabilised both by Coulombic forces, and specific, oriented interactions—probably hydrogen bonds). This is supported both by independent experimental evidence as well as theoretical deduction. For instance, it is relatively easy to demonstrate<sup>16</sup> that, within the frame of simple lattice-like models, binary mixtures composed of identically sized species present a critical mole fraction,  $x_c$ , equal to 0.5, and, that the critical value of the excess Gibbs energy that provokes phase separation is  $g^E/RTx(1-x) \geq g_c = 2$ . As one moves to systems composed of unlike molecules of different sizes (e.g., polymer + small molecules), the critical mole fraction of the largest component,  $x_c$ , decreases together with the critical value,  $g_c$ , necessary to induce phase separation,

$$x_c = \frac{1}{1+r^{3/2}}; \quad g_c = \frac{1}{2} \left( 1 + \frac{1}{r^{1/2}} \right)^2 \quad (2)$$

where  $r$  represents, at the first approximation, the ratio of the sizes of the two components. Assuming that the ionic liquids in solution would be formed by ion pairs, the relative sizes of the components in the binary mixtures could be calculated by using the ratio of molar volumes,  $r \sim V_{IL}/V_{solv}$ . On the other

hand, this ratio of sizes,  $r$ , calculated from the experimental critical concentration,  $x_c$ , and using eqn (2), is approximately two or three times the ratio of molar volumes of the larger component over that of the smaller one. Our interpretation is that, at this same low level of approximation, the bulk of the solution experiences, on average, “dimers” or “trimers” of cation–anion contact pairs of the ILs at concentrations near the critical one.

In a distinct but related perspective, note how the critical concentration significantly decreases (Table 2) as the alkyl chain of the imidazolium cation increases (“size” of the ionic liquid increases).

Our electro-spray mass spectrometric studies performed in the positive and negative modes for [C<sub>10</sub>mim][NTf<sub>2</sub>] using benzene as the solvent (dilution 1 : 1000) established the expected presence of the aggregates of IL in solution. The positive mode (Fig. 7a) shows major  $m/z$  peaks at 223 and 725. The first corresponds to the single cation [C<sub>10</sub>mim]<sup>+</sup> and the last one to the aggregate of two cations and one anion, [(C<sub>10</sub>mim)<sub>2</sub>(NTf<sub>2</sub>)]<sup>+</sup>. The negative mode (Fig. 7b) shows two peaks at 280 and 782 which correspond to the single anion [NTf<sub>2</sub>]<sup>−</sup> and the aggregate of two anions and one cation [(C<sub>10</sub>mim)(NTf<sub>2</sub>)<sub>2</sub>]<sup>−</sup>, respectively. As previously found in other ionic liquid/organic solvent systems, larger aggregates can be identified at higher concentrations of IL.

In some cases, a liquid clathrate phase formation in imidazolium-based ionic liquid–aromatic systems has been reported for the IL-rich phase.<sup>9,18</sup> Holbrey *et al.*<sup>9</sup> discussed the underlying specific interactions between the imidazolium cations and the aromatic hydrocarbon molecules. Judging from the observations made on the model system [C<sub>1</sub>mim][PF<sub>6</sub>] and benzene, the structure reveals that the imidazolium cations form a weak C–H⋯ $\pi$  hydrogen-bonded zigzag chain. In contrast, in crystal structures of [C<sub>1</sub>mim][PF<sub>6</sub>] $\cdot$ 0.5C<sub>6</sub>H<sub>6</sub>, a three-dimensional array of hydrogen-bonded cations and anions is formed. This three-dimensional network results in the formation of “channels” in which benzene molecules are included by a staggered  $\pi$ – $\pi$  “sandwich” between two imidazolium cations. Deetlefs *et al.*<sup>18</sup> also reported that the interactions between the ions and the benzene are dominated

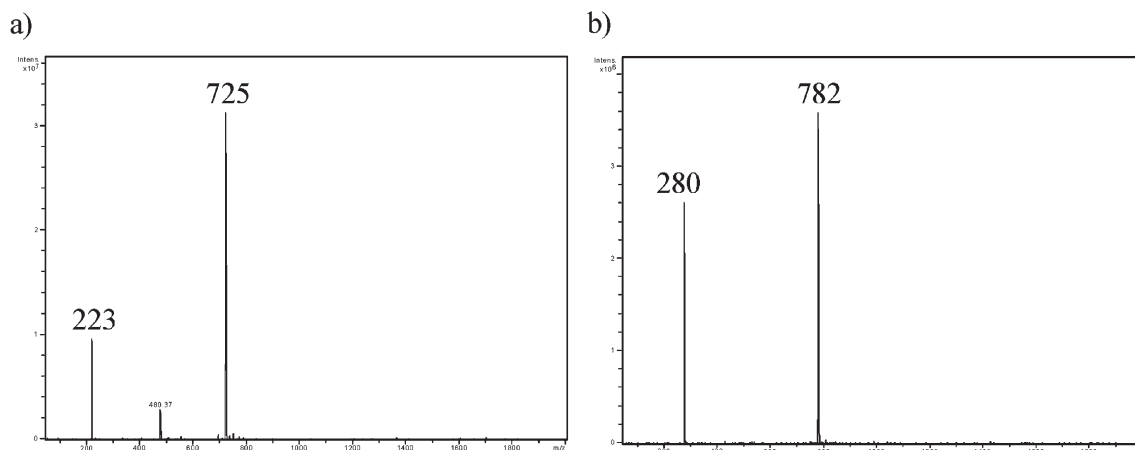


**Fig. 7** Electro-spray mass spectra in the positive (a) and negative (b) modes of [C<sub>10</sub>mim][NTf<sub>2</sub>] in benzene (dilution of 1 : 1000). Intensity versus ( $m/z$ ). Mass range 50–2000.

by the charge distribution around the benzene ring. On examination of the partial radial distribution functions for the H–H interactions between the cation and benzene, it is clear that short methyl hydrogen–benzene hydrogen interactions are present.

Ionic liquids containing dialkylimidazolium cations are thus able to form specific, oriented interactions with solvents such as arenes and chloroalkanes. These type of interactions, predominantly hydrogen bonds, are probably responsible for the richness of the ionic liquid binary phase diagrams with organic solvents.

## Acknowledgements

This work was funded by Fundação para a Ciência e Tecnologia, Portugal, under contract POCTI/EQU/35437/00 and post-doctoral grants for JL and JMSSE. We are also grateful to Elisabete Pires and Dr Ana Coelho for providing data from the Mass Spectrometry Service at the ITQB-UNL, Portugal.

## References

- 1 L. P. N. Rebelo, J. N. Canongia Lopes, J. M. S. S. Esperança and E. Filipe, *J. Phys. Chem. B*, 2005, **109**, 6040–6043.
- 2 M. J. Earle, J. M. S. S. Esperança, M. A. Gilea, J. N. Canongia Lopes, L. P. N. Rebelo, J. W. Magee, K. R. Seddon and J. A. Widegren, *Nature*, 2006, DOI: 10.1038/nature04451.
- 3 J. Łachwa, J. Szydłowski, V. Najdanovic-Visak, L. P. N. Rebelo, K. R. Seddon, M. Nunes da Ponte, J. M. S. S. Esperança and H. J. R. Guedes, *J. Am. Chem. Soc.*, 2005, **127**, 6542–6543.
- 4 K. E. Gutowski, G. A. Broker, H. D. Willauer, J. G. Huddleston, R. P. Swatloski, J. D. Holbrey and R. D. Rogers, *J. Am. Chem. Soc.*, 2003, **125**, 6632–6633.
- 5 V. Najdanovic-Visak, J. M. S. S. Esperança, L. P. N. Rebelo, M. Nunes da Ponte, H. J. R. Guedes, K. R. Seddon and J. Szydłowski, *Phys. Chem. Chem. Phys.*, 2002, **4**, 1701–1703.
- 6 V. Najdanovic-Visak, A. Serbanovic, J. M. S. S. Esperança, H. J. R. Guedes, L. P. N. Rebelo and M. Nunes da Ponte, *ChemPhysChem*, 2003, **4**, 520–522.
- 7 R. P. Swatloski, A. E. Visser, W. M. Reichert, G. A. Broker, L. M. Farina, J. D. Holbrey and R. D. Rogers, *Chem. Commun.*, 2001, 2070–2071.
- 8 A. M. Scurto, S. N. V. K. Aki and J. Brennecke, *J. Am. Chem. Soc.*, 2002, **124**, 10276–10277.
- 9 J. D. Holbrey, W. M. Reichert, M. Nieuwenhuyzen, O. Sheppard, C. Hardacre and R. D. Rogers, *Chem. Commun.*, 2003, 476–477.
- 10 P. Bonhôte, A.-P. Dias, M. Armand, N. Papageorgiou, K. Kalyanasundaram and M. Gratzel, *Inorg. Chem.*, 1996, **35**, 1168–1178.
- 11 J. G. Huddleston, A. E. Visser, W. M. Reichert, H. D. Willauer, G. A. Broker and R. D. Rogers, *Green Chem.*, 2001, **3**, 156–164.
- 12 (a) L. A. Blanchard and J. F. Brennecke, *Ind. Eng. Chem. Res.*, 2001, **40**, 287–292; (b) U. Domanska, *Pure Appl. Chem.*, 2005, **77**, 543–557; (c) U. Domanska and A. Marciniak, *J. Chem. Eng. Data*, 2003, **48**, 451–456; (d) T. M. Letcher and N. Deenadayalu, *J. Chem. Thermodyn.*, 2003, **35**, 67–76; (e) U. Domanska and L. Mazurowska, *Fluid Phase Equilib.*, 2004, **221**, 73–82.
- 13 R. Kato, M. Krummen and J. Gmehling, *Fluid Phase Equilib.*, 2004, **224**, 47–54.
- 14 (a) J. M. Crosthwaite, S. N. V. K. Aki, E. J. Maginn and J. F. Brennecke, *J. Phys. Chem. B*, 2004, **108**, 5113–5119; (b) V. Najdanovic-Visak, J. M. S. S. Esperança, L. P. N. Rebelo, M. Nunes da Ponte, H. J. R. Guedes, K. R. Seddon, H. C. de Sousa and J. Szydłowski, *J. Phys. Chem. B*, 2003, **107**, 12797–12807; (c) M. Wagner, O. Stanga and W. Schröer, *Phys. Chem. Chem. Phys.*, 2003, **5**, 3943–3950; (d) M. Wagner, O. Stanga and W. Schröer, *Phys. Chem. Chem. Phys.*, 2004, **6**, 4421–4431; (e) C.-T. Wu, K. N. Marsh, A. V. Deev and J. A. Boxall, *J. Chem. Eng. Data*, 2003, **48**, 486–491; (f) K. N. Marsh, A. V. Deev, A. C.-T. Wu, E. Tran and A. Klamt, *Korean J. Chem. Eng.*, 2002, **19**, 357–362; (g) A. Heintz, J. K. Lehmann and C. Wertz, *J. Chem. Eng. Data*, 2003, **48**, 472–474; (h) R. P. Swatloski, A. E. Visser, W. M. Reichert, G. A. Broker, L. M. Farina, J. D. Holbrey and R. D. Rogers, *Green Chem.*, 2002, **4**, 81–87; (i) M. Döker and J. Gmehling, *Fluid Phase Equilib.*, 2005, **227**, 255–266.
- 15 H. C. de Sousa and L. P. N. Rebelo, *J. Chem. Thermodyn.*, 2000, **32**, 355–387.
- 16 (a) I. Proginé and R. Defay, *Chemical Thermodynamics* (transl. D. H. Everett), Longmans Green, London, 1954, pp. 271–290; (b) G. Schneider, *Ber. Bunsen-Ges. Phys. Chem.*, 1966, **70**, 497–520; (c) L. P. N. Rebelo, *Phys. Chem. Chem. Phys.*, 1999, **1**, 4277–4286; (d) L. P. N. Rebelo, V. Najdanovic-Visak, Z. P. Visak, M. Nunes da Ponte, J. Troncoso, C. A. Cerdeiriña and L. Romani, *Phys. Chem. Chem. Phys.*, 2002, **4**, 2251–2259; (e) L. P. N. Rebelo, V. Najdanovic-Visak, Z. P. Visak, M. Nunes da Ponte, J. Szydłowski, C. A. Cerdeiriña, J. Troncoso, L. Romani, J. M. S. S. Esperança, H. J. R. Guedes and H. C. de Sousa, *Green Chem.*, 2004, **6**, 369–381.
- 17 (a) M. Krummen, P. Wasserscheid and J. Gmehling, *J. Chem. Eng. Data*, 2002, **47**, 1411–1417; (b) A. Heintz, D. Kulikov and S. P. Verevkin, *J. Chem. Eng. Data*, 2002, **47**, 894–899; (c) N. Deenadayalu, T. M. Letcher and P. Reddy, *J. Chem. Eng. Data*, 2005, **50**, 105–108.
- 18 M. Deetlefs, C. Hardacre, M. Nieuwenhuyzen, O. Sheppard and A. Soper, *J. Phys. Chem. B*, 2005, **109**, 1593–1598.

# Liquid–liquid equilibria in the binary systems (1,3-dimethylimidazolium, or 1-butyl-3-methylimidazolium methylsulfate + hydrocarbons)<sup>†‡</sup>

Urszula Domańska,<sup>\*a</sup> Aneta Pobudkowska<sup>a</sup> and Frank Eckert<sup>b</sup>

Received 12th October 2005, Accepted 8th December 2005

First published as an Advance Article on the web 6th January 2006

DOI: 10.1039/b514521j

Liquid–liquid equilibria in binary mixtures that contain a room-temperature ionic liquid and an organic solvent—namely, 1,3-dimethylimidazolium methylsulfate, [mmim][CH<sub>3</sub>SO<sub>4</sub>], or 1-butyl-3-methylimidazolium methylsulfate, [bmim][CH<sub>3</sub>SO<sub>4</sub>] with an aliphatic hydrocarbon (*n*-pentane, or *n*-hexane, or *n*-heptane, or *n*-octane, or *n*-decane), or a cyclohydrocarbon (cyclohexane, or cycloheptane), or an aromatic hydrocarbon (benzene, or toluene, or ethylbenzene, or propylbenzene, or *o*-xylene, or *m*-xylene, or *p*-xylene) have been measured at normal pressure by a dynamic method from 270 K to the boiling point of the solvent. Thermophysical basic characterization of pure ionic liquids are presented obtained *via* differential scanning calorimetry (TG/DSC), temperatures of decomposition and melting, enthalpies of fusion, and enthalpies of glass phase transition. The liquidus curves were predicted by the COSMO-RS method. For [bmim][CH<sub>3</sub>SO<sub>4</sub>] the COSMO-RS results correspond much better with experiment than those for [mmim][CH<sub>3</sub>SO<sub>4</sub>]. This can be explained partly by the stronger polarity of [mmim][CH<sub>3</sub>SO<sub>4</sub>]. The solubilities of [mmim][CH<sub>3</sub>SO<sub>4</sub>] and [bmim][CH<sub>3</sub>SO<sub>4</sub>] in alkanes, cycloalkanes and aromatic hydrocarbons decrease with an increase of the molecular weight of the solvent. The differences of the solubilities in *o*-, *m*-, and *p*-xylene are not significant. By increasing the alkyl chain length on the cation, the upper critical solution temperature, UCST decreased in all solvents except in *n*-alkanes.

## Introduction

Room temperature ionic liquids (ILs) have gained increasing attention over recent years due to their extraordinary properties as room temperature molten salts. The large number of combinations of organic cations and anions allows the modification of the thermodynamic properties of ILs over a wide range of miscibility with other solvents, solubility of gases, partition coefficients of solutes between ionic liquids and aqueous phases, their applicability in separation and extraction techniques and their use as thermal fluids.<sup>1</sup> Ionic liquids are emerging as novel replacements for volatile organic compounds, traditionally used as industrial solvents. They possess no significant vapour pressure and have the ability to dissolve a considerable variety of organic, inorganic and polymeric materials at very high concentrations (sometimes over the complete concentration range).<sup>2–4</sup> ILs have been studied in many chemical processes, for example, in bio processing operations, as electrolytes in electrochemistry, in gas separations such as the capturing of CO<sub>2</sub>, in liquid–liquid

extractions, and as heat-transfer fluids.<sup>5–12</sup> Many organic solvents evaporate into the atmosphere with detrimental effects on the environment and human health. However, room-temperature ionic liquids, with low viscosity and no measurable vapour pressure,<sup>13</sup> can be used as environmentally benign media for a range of industrially important chemical processes<sup>14–18</sup> despite uncertainties about thermal stability and sensitivity to oxygen and water. It is difficult to recover products, however, as extraction with water<sup>19</sup> works only for hydrophilic products, distillation is not suitable for poorly volatile or thermally labile products, and liquid–liquid extraction using organic solvents results in cross-contamination. It was found that non-volatile organic compounds can be extracted from ionic liquids using supercritical carbon dioxide, which is widely used to extract large organic compounds with minimal pollution.<sup>20–23</sup> Carbon dioxide dissolves in the liquid to facilitate extraction, but the ionic liquid does not dissolve in carbon dioxide, so a pure product can be recovered. Ionic liquids are good solvents for catalysis and synthesis.<sup>2,24,25</sup> To design any process involving ionic liquids on an industrial scale it is necessary not only to know a range of physical properties including viscosity, density but also heat capacity and other thermodynamic properties including phase equilibria such as vapor–liquid equilibria (VLE), liquid–liquid equilibria (LLE) and solid–liquid equilibria (SLE).<sup>26–40</sup>

The solubilities of 1-ethyl-3-methylimidazolium hexafluorophosphate, [emim][PF<sub>6</sub>] in aromatic hydrocarbons (benzene, or toluene, or ethylbenzene, or *o*-xylene, or *m*-xylene, or *p*-xylene) and of 1-butyl-3-methylimidazolium hexafluorophosphate, [bmim][PF<sub>6</sub>] in the same aromatic hydrocarbons, in *n*-alkanes (*n*-pentane, or *n*-hexane, or *n*-heptane, or *n*-octane) and in

<sup>a</sup>Physical Chemistry Division, Faculty of Chemistry, Warsaw University of Technology, Noakowskiego 3, 00-664 Warsaw, Poland.

E-mail: ula@ch.pw.edu.pl; Fax: +48-22-6282741; Tel: +48-22-6213115

<sup>b</sup>COSMOlogic GmbH&Co. KG, Burscheider Str. 515, D-51381

Leverkusen, Germany

<sup>†</sup>This work was presented at the 1st International Conference on Ionic Liquids (COIL), held in Salzburg, Austria, 19–22 June, 2005.

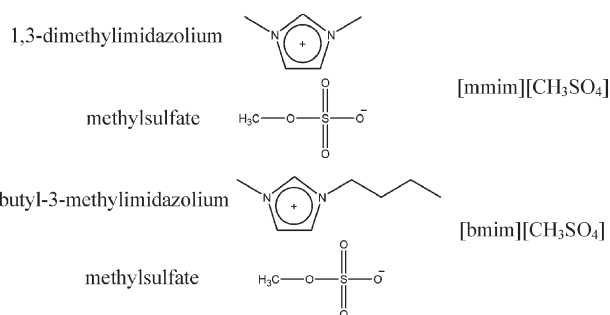
<sup>‡</sup>Electronic supplementary information (ESI) available: Tables describing the decomposition data and the COSMO-RS predicted temperatures of the LLE equilibrium. Figures showing the decomposition of the ILs and the various equilibria diagrams. See DOI: 10.1039/b514521j

cyclohydrocarbons (cyclopentane, or cyclohexane) have been measured in our laboratory.<sup>37</sup> The solubilities of [emim][PF<sub>6</sub>] and [bmim][PF<sub>6</sub>] in aromatic hydrocarbons decreased with an increase of the molecular weight of the solvent. The difference of the solubility in *o*-, or *m*-, or *p*-xylene is very small. The intermolecular solute–solvent interactions are not significant.

The LLE in ternary mixtures of (IL + aromatic hydrocarbon + *n*-alkane)<sup>36</sup> measurements have shown that the selectivity of the extraction of benzene from *n*-alkane increases with increasing carbon number of the *n*-alkane.

The current study focuses on solutions of 1,3-dimethylimidazolium methylsulfate, [mmim][CH<sub>3</sub>SO<sub>4</sub>] and 1-butyl-3-methylimidazolium methylsulfate, [bmim][CH<sub>3</sub>SO<sub>4</sub>] with *n*-alkanes (*n*-pentane, or *n*-hexane, or *n*-heptane, or *n*-octane, or *n*-decane), or cycloalkanes (cyclohexane or cycloheptane) and with aromatic hydrocarbons (benzene, or toluene, or ethylbenzene, or propylbenzene, or *o*-xylene, or *m*-xylene, or *p*-xylene). The data presented here will be useful from a technological perspective, because they show partial immiscibility at room temperature.

The formulas of the ionic liquids under study are as follows:



COSMO-RS is a thermodynamic prediction model, that was used for the prediction of the LLE in (IL + *n*-alcohol) binary mixtures.<sup>33</sup> Excellent agreement with the experimental points was obtained. This method has also shown the correct trends for both the variation of UCST and the alkyl chain length of the alcohol. In this paper the possible prediction of LLE of ILs in hydrocarbons is presented.

## Results and discussion

The thermophysical constants of pure ionic liquids are shown in Table 1. The salts investigated here show high decomposition temperatures. The temperature of decomposition is strongly dependent on the alkyl chain length on the imidazole ring. The TGA curves have a sigmoidal shape and can be split into three segments as is shown in Fig. 1S in the ESI.† The 5.0% mass loss was observed for both salts at the temperature

574 K (see Fig. 1S†). The first decomposition temperature is higher for the shorter alkyl chain (methyl) and is equal to 617 K with a mass loss of 10%. For the longer alkyl chain (butyl), the decomposition temperature decreases to 607 K with a mass loss of 10%. Compounds were decomposed in one step. The exact temperatures of the decomposition are shown in Fig. 2S in the ESI.† These temperatures are 649.45 K for [mmim][CH<sub>3</sub>SO<sub>4</sub>] and 633.25 K for [bmim][CH<sub>3</sub>SO<sub>4</sub>]. The mass loss percentage of ionic liquid at the final step of the decomposition increases as the alkyl chain length increases (see Table 1).

From differential scanning calorimetry (DSC) data, the half *C<sub>p</sub>* temperatures of the glass transition were measured for [mmim][CH<sub>3</sub>SO<sub>4</sub>] and [bmim][CH<sub>3</sub>SO<sub>4</sub>]. From the thermograph of the pure solute it was noted that [mmim][CH<sub>3</sub>SO<sub>4</sub>] exhibits the half *C<sub>p</sub>* extrapolated temperature of the glass transition at 185.85 K with  $\Delta C_p$  equal to 73.72 J K<sup>-1</sup> mol<sup>-1</sup> and [bmim][CH<sub>3</sub>SO<sub>4</sub>] exhibits the half *C<sub>p</sub>* extrapolated temperature of the glass transition at 193.78 K with  $\Delta C_p$  equal to 90.36 J K<sup>-1</sup> mol<sup>-1</sup>.

For this discussion, the liquid–liquid equilibria for new binary ionic liquid–organic solvent systems were determined. The experimental data of LLE in binary systems of [mmim][CH<sub>3</sub>SO<sub>4</sub>] and [bmim][CH<sub>3</sub>SO<sub>4</sub>] with aliphatic, cyclic and aromatic hydrocarbons are given in Tables 2 and 3 and are presented in Fig. 1–7 and in Fig. 3S–9S of the ESI.† The tables include the direct experimental results of the LLE temperatures, *T*/K versus *x*<sub>1</sub>, the mole fraction of the IL at the equilibrium temperatures for the investigated systems. The maximum of the curves was not observed because the boiling temperature of the solvent was lower.

The ability of an IL to form hydrogen bonds or other possible interactions with potential solvents is an important feature of its behaviour. Basic [mmim][CH<sub>3</sub>SO<sub>4</sub>] and [bmim][CH<sub>3</sub>SO<sub>4</sub>] ionic liquids can act both as hydrogen-bond acceptor ([CH<sub>3</sub>SO<sub>4</sub>]<sup>-</sup>) and donor ([m- or bmim]<sup>+</sup>) and would be expected to interact with solvents which have both accepting and donating sites. On the other hand, aromatic hydrocarbons are known to form *n*- $\pi$ , or  $\pi$ - $\pi$  interactions with many organic solvents.

Experimental phase diagrams of LLE investigated in this work are characterized mainly by the following: (1) the shape of the equilibrium curve is similar for both [mmim][CH<sub>3</sub>SO<sub>4</sub>] and [bmim][CH<sub>3</sub>SO<sub>4</sub>] with every *n*-alkane; the solubility decreases with an increase of the alkyl chain length of the *n*-alkane from C<sub>3</sub> to C<sub>10</sub> (see Fig. 1 and 3S in the ESI.†) (it might be a result of the packing effect); (2) an increase in the cycloalkanes ring resulted in an increase in the upper critical solution temperature (UCST), which is shown in Fig. 4S and 5S in the ESI.†; (3) the equilibrium curves for [bmim][CH<sub>3</sub>SO<sub>4</sub>]

**Table 1** Thermophysical constants of pure ionic liquids: melting temperature, *T*<sub>fus,1</sub>; enthalpy of fusion,  $\Delta_{\text{fus}}H_1$ ; temperature of glass transition, *T*<sub>g,1</sub>, as determined from differential scanning calorimetry (DSC) data

IL	<i>T</i> <sub>fus,1</sub> /K	$\Delta_{\text{fus}}H_1$ /kJ mol <sup>-1</sup>	<i>T</i> <sub>g,1</sub> /K	<i>T</i> <sub>decom</sub> /K	Mass loss (%)
[mmim][CH <sub>3</sub> SO <sub>4</sub> ]	308.90	16.58	185.85 <sup>a</sup>	649; 685 <sup>c</sup>	46; 77
[bmim][CH <sub>3</sub> SO <sub>4</sub> ]	—	—	193.78 <sup>b</sup>	633; 677 <sup>c</sup>	32; 84

<sup>a</sup>  $\Delta C_p$  at the glass transition is equal to 73.72 J mol<sup>-1</sup> K<sup>-1</sup>. <sup>b</sup>  $\Delta C_p$  at the glass transition is equal to 90.36 J mol<sup>-1</sup> K<sup>-1</sup>.<sup>41</sup> <sup>c</sup> The final decomposition step.

**Table 2** Liquid–liquid phase equilibria for  $\{x_1$  [mmim][CH<sub>3</sub>SO<sub>4</sub>] + (1 -  $x_1$ ) hydrocarbon mixtures}

$x_1$	$T/K$	$x_1$	$T/K$
<i>n</i> -Pentane			
0.7814	306.32	0.8210	298.08
0.7953	304.48	0.8398	293.63
0.8093	300.77	0.8619	288.21
<i>n</i> -Hexane			
0.6977	341.39	0.8742	321.78
0.7303	338.44	0.8866	319.43
0.7527	336.67	0.9185	313.36
0.7791	333.56	0.9322	308.98
0.8084	331.14	0.9582	301.52
0.8329	327.89	0.9731	295.87
0.8632	324.33		
<i>n</i> -Heptane			
0.7020	367.52	0.8340	346.12
0.7202	364.60	0.8753	337.86
0.7421	361.67	0.8982	331.79
0.7623	358.86	0.9293	322.66
0.7854	355.71	0.9666	313.07
0.8062	353.38	0.6812	371.00
0.8204	349.57		
<i>n</i> -Octane			
0.5462	396.20	0.8319	354.46
0.5942	388.79	0.8611	347.21
0.6273	384.29	0.8852	341.90
0.6829	376.82	0.9033	337.11
0.7016	374.04	0.9260	330.28
0.7239	370.81	0.9351	327.80
0.7612	366.39	0.9472	324.20
0.7988	360.03	0.9595	319.32
0.8086	357.85		
<i>n</i> -Decane			
0.5381	442.81	0.8257	377.83
0.5922	430.60	0.8763	363.72
0.6340	419.84	0.9176	354.00
0.6697	411.65	0.9344	350.23
0.6889	406.21	0.9585	328.50
0.7194	399.80	0.9681	322.66
0.7621	390.63	0.9809	318.18
0.8057	381.71	1.0000	308.30
Cyclohexane			
0.7404	348.12	0.9026	328.60
0.7857	343.98	0.9320	322.47
0.8503	337.39	0.9531	316.90
0.8787	333.17		
Cycloheptane			
0.6145	362.50	0.8223	349.98
0.6851	360.89	0.8613	343.30
0.7518	356.03	0.8820	337.21
0.7914	353.37	0.9571	313.98
Benzene			
0.5186	354.99	0.6284	318.48
0.5280	349.40	0.6422	312.60
0.5365	348.02	0.6481	313.61
0.5400	344.40	0.6687	309.79
0.5637	339.20	0.6707	308.57
0.5834	333.76	0.6875	305.98
0.5937	328.94	0.7043	303.99
0.5956	324.92	0.7074	302.51
0.6054	321.39	0.7192	301.53
0.6179	319.76	0.7354	300.29
0.6253	316.90	0.7437	301.92
Toluene			
0.6319	383.03	0.7718	318.92
0.6423	371.60	0.8042	313.26
0.6680	350.59	0.8547	310.03
0.6926	339.52	0.8931	309.59
0.7222	331.37	0.9224	308.12
0.7405	323.28	1.0000	305.65
Ethylbenzene			
0.8222	408.78	0.8653	362.02
0.8280	403.74	0.8723	353.22

**Table 2** Liquid–liquid phase equilibria for  $\{x_1$  [mmim][CH<sub>3</sub>SO<sub>4</sub>] + (1 -  $x_1$ ) hydrocarbon mixtures} (*Continued*)

$x_1$	$T/K$	$x_1$	$T/K$
0.8311	399.92	0.8862	341.50
0.8394	391.97	0.9029	326.99
0.8428	387.87	0.9207	301.88
0.8560	371.42		
Propylbenzene			
0.8570	428.26	0.9087	351.52
0.8610	416.84	0.9099	348.37
0.8875	388.86	0.9125	341.10
0.8963	368.48	0.9261	312.17
<i>o</i> -Xylene			
0.6231	410.68	0.7793	339.61
0.6516	393.06	0.8042	328.98
0.6896	374.67	0.8351	322.40
0.7204	362.93	0.8684	315.80
0.7394	355.96	0.9035	312.92
0.7538	352.72	0.9527	311.42
<i>m</i> -Xylene			
0.6238	415.97	0.7794	345.63
0.6416	402.19	0.8036	333.28
0.6579	394.46	0.8246	324.17
0.6900	380.92	0.8462	319.96
0.7134	370.98	0.8635	315.57
0.7383	362.93	0.8882	315.08
0.7733	348.56	0.9436	306.34
<i>p</i> -Xylene			
0.6297	411.50	0.7881	340.79
0.6432	404.18	0.8087	328.98
0.6743	388.35	0.8304	322.59
0.6926	378.37	0.8638	317.31
0.7088	372.96	0.8934	314.31
0.7311	365.87	0.9226	310.57
0.7507	355.93	0.9602	309.56
0.7673	349.17		

in aromatic hydrocarbons exhibit similar shapes; the mutual liquid–liquid solubility of [mmim][CH<sub>3</sub>SO<sub>4</sub>] and [bmim][CH<sub>3</sub>SO<sub>4</sub>] increases in the order benzene > toluene > ethylbenzene > propylbenzene (see Fig. 2 and 3); (4) the differences of the solubilities of [mmim][CH<sub>3</sub>SO<sub>4</sub>] and [bmim][CH<sub>3</sub>SO<sub>4</sub>] in *o*-, *m*-, and *p*-xylene are not remarkable (see Fig. 4 and 6S in the ESI†); slightly better solubility of [bmim][CH<sub>3</sub>SO<sub>4</sub>] was observed in the *p*-xylene at higher temperatures (see Fig. 4); (5) the effect of the cations, [m- or bmim]<sup>+</sup> on the solubility of these salts in the aliphatic and aromatic hydrocarbons are shown in Fig. 5 and 7S in the ESI† and in Fig. 6, 7 and 8S in the ESI,† respectively. For all linear *n*-alkanes from *n*-pentane to *n*-decane the miscibility gap is larger in the [bmim][CH<sub>3</sub>SO<sub>4</sub>] (see Fig. 5 and 7S in the ESI†). By contrast, the [bmim][CH<sub>3</sub>SO<sub>4</sub>] is more soluble than [mmim][CH<sub>3</sub>SO<sub>4</sub>] in cyclohydrocarbons (cyclohexane, cycloheptane) and in aromatic compounds (benzene, toluene, propylbenzene, xylene). These opposite effects were observed in aromatic hydrocarbons because the  $\pi$ - $\pi$  interaction may be expected between the imidazolium ring and benzene ring.

The stronger interaction on one side and the increased influence of the inductive effect of the longer alkyl chain on the imidazole ring on the other side can influence the solubility. Fig. 6, 7 and 8S, 9S in the ESI† show the liquid phase behaviour for these two ILs with benzene, ethylbenzene, propylbenzene and *p*-xylene, respectively. The UCST is significantly higher for the ionic liquid with the shorter alkyl

**Table 3** Liquid–liquid phase equilibria for  $\{x_1$  [bmim][CH<sub>3</sub>SO<sub>4</sub>] + (1 -  $x_1$ ) hydrocarbon} mixtures

$x_1$	$T/K$	$x_1$	$T/K$
<i>n</i> -Pentane			
0.8640	325.00	0.9411	298.47
0.8910	316.90	0.9456	294.88
0.9110	310.89	0.9499	289.96
0.9300	304.37	0.9522	288.48
<i>n</i> -Hexane			
0.8048	346.77	0.9450	312.54
0.8821	325.96	0.9770	302.52
<i>n</i> -Heptane			
0.4433	442.73	0.8855	343.24
0.4697	439.12	0.8936	341.88
0.4962	430.22	0.8963	340.42
0.5396	417.45	0.9010	338.59
0.6283	394.32	0.9101	336.96
0.6748	384.35	0.9230	334.69
0.7734	363.55	0.9291	332.08
0.7941	359.25	0.9343	330.24
0.8233	355.75	0.9443	328.17
0.8451	352.65	0.9487	326.69
0.8642	348.05	0.9883	299.85
0.8855	343.24		
<i>n</i> -Octane			
0.6109	401.69	0.7982	366.05
0.6286	397.66	0.8181	362.57
0.6494	394.65	0.8386	358.56
0.6682	389.67	0.8593	353.37
0.6941	385.66	0.8727	349.89
0.7160	382.65	0.8995	342.37
0.7338	378.18	0.9291	335.42
0.7535	374.88	0.9451	329.51
0.7773	370.04	0.9655	319.49
<i>n</i> -Decane			
0.5612	445.70	0.8442	380.92
0.6187	433.52	0.8622	375.53
0.6611	424.02	0.8970	365.75
0.7026	412.30	0.9114	358.06
0.7242	408.42	0.9333	349.67
0.7511	403.03	0.9548	342.22
0.7821	394.41	0.9625	332.69
0.8135	388.06	0.9726	325.77
0.8306	383.22	0.9912	320.76
Cyclohexane			
0.6627	353.35	0.8340	318.55
0.7132	344.55	0.8627	313.86
0.7421	340.75	0.8915	302.75
0.7706	333.11	0.9136	296.25
0.8076	325.62		
Cycloheptane			
0.7342	406.33	0.8958	350.42
0.7702	399.99	0.9090	342.01
0.8078	384.42	0.9257	328.59
0.8573	364.80	0.9416	318.11
0.8774	357.10		
Benzene			
0.2767	348.37	0.3558	315.75
0.2925	337.71	0.3708	313.58
0.3015	329.18	0.3857	311.96
0.3220	322.44	0.4258	308.57
0.3416	317.96	0.4533	303.12
Toluene			
0.4153	381.40	0.5577	320.66
0.4620	344.87	0.5919	313.37
0.5223	331.41	0.6044	311.33
0.5231	331.27	0.6440	302.77
0.5521	322.39	0.6740	295.76
Ethylbenzene			
0.5038	408.81	0.6222	350.88
0.5051	407.27	0.6326	348.07
0.5251	388.49	0.6422	343.18
0.5342	387.57	0.6542	337.53
0.5432	381.59	0.6664	333.76

**Table 3** Liquid–liquid phase equilibria for  $\{x_1$  [bmim][CH<sub>3</sub>SO<sub>4</sub>] + (1 -  $x_1$ ) hydrocarbon} mixtures (*Continued*)

$x_1$	$T/K$	$x_1$	$T/K$
0.5463	381.65	0.6664	335.48
0.5598	376.98	0.6856	330.56
0.5784	367.57	0.6952	328.86
0.5800	366.24	0.7228	320.96
0.5843	365.19	0.7415	317.19
0.6089	355.77		
Propylbenzene			
0.6457	430.20	0.8392	347.96
0.6720	414.83	0.8614	336.96
0.6931	405.76	0.8867	320.37
0.7074	397.96	0.9145	299.80
0.7495	384.57	0.9174	290.40
0.7824	371.44	0.9278	275.50
0.8159	356.29		
<i>o</i> -Xylene			
0.5870	412.47	0.7190	344.86
0.6044	406.56	0.7521	328.70
0.6454	384.88	0.7852	317.67
0.6856	365.96	0.8094	307.93
<i>m</i> -Xylene			
0.6075	410.08	0.7170	347.83
0.6246	399.82	0.7530	332.36
0.6355	391.75	0.7771	325.21
0.6497	385.67	0.8274	306.96
0.6554	382.09	0.8322	305.77
0.6635	377.18		
<i>p</i> -Xylene			
0.5750	411.18	0.7056	343.78
0.5882	405.75	0.7263	332.54
0.6020	400.82	0.7422	328.26
0.6116	396.56	0.7611	323.17
0.6212	385.79	0.7811	313.18
0.6383	376.27	0.7973	309.19
0.6465	373.49	0.8012	308.26
0.6782	354.97	0.8129	305.73
0.6980	345.45	0.8218	302.37

chain. The same influence of *n*-alkane chain of cation was observed previously for [emim][Tf<sub>2</sub>N] and [emim][Tf<sub>2</sub>N] in butanol, or for [bmim][BF<sub>4</sub>] and [hmim][BF<sub>4</sub>] in hexanol.<sup>32,33,42</sup> This effect was explained by the increasing van der Waals interactions between the alkyl chain of the cation and the alkyl chain of the alcohol.<sup>32</sup> The same effect of the cation was also observed in the solubilities of [e- or bmim][PF<sub>6</sub>] in hydrocarbons.<sup>43</sup> The solubility of [bmim][CH<sub>3</sub>SO<sub>4</sub>] was observed to be much higher than the solubility of [mmim][CH<sub>3</sub>SO<sub>4</sub>] in alcohols and in other polar solvents *e.g.* ethers or ketones.<sup>42,44</sup>

The influence of the length of the alkyl chain of the IL's cation on the solubility and the interaction with a solvent has been already discussed for different ionic liquids by the comparison of different thermodynamic properties.<sup>28,32,33,40,42,43</sup>

The decrease in the activity coefficients at infinite dilution of different solutes, dissolved in ILs, with increased alkyl chain length of the IL, was observed for *n*-alkanes and benzene in [mmim][Tf<sub>2</sub>N], [emim][Tf<sub>2</sub>N] and [bmim][Tf<sub>2</sub>N]. A much lower value of the activity coefficients at infinite dilution in benzene (higher interaction) were also observed.<sup>28</sup> The interaction of [mmim][CH<sub>3</sub>SO<sub>4</sub>] with different solvents was described recently *via* infinite dilution activity coefficients of various *n*-alkanes, cycloalkanes, aromatic hydrocarbons and alcohols.<sup>40</sup> The values of infinite dilution activity coefficient decrease in the order *n*-alkanes > cycloalkanes > aromatic

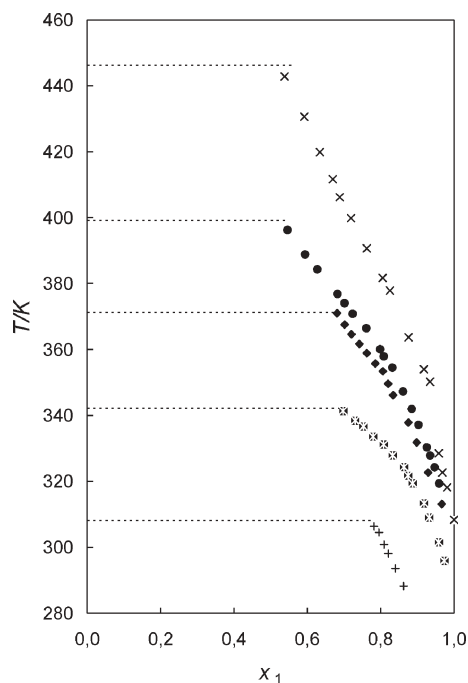


**Fig. 1** Liquid-liquid phase equilibria diagram of binary systems:  $\{x_1 [\text{mmim}][\text{CH}_3\text{SO}_4] + (1 - x_1) n\text{-alkane}\}$ : +, *n*-pentane; x, *n*-hexane; ◆, *n*-heptane; ●, *n*-octane; ×, *n*-decane; dotted line, boiling temperature of the solvent.

hydrocarbons > alcohols. The same trend as in our results was also observed for the increasing chain length of *n*-alkanes and *n*-alkane substituent at the benzene ring. The values of the

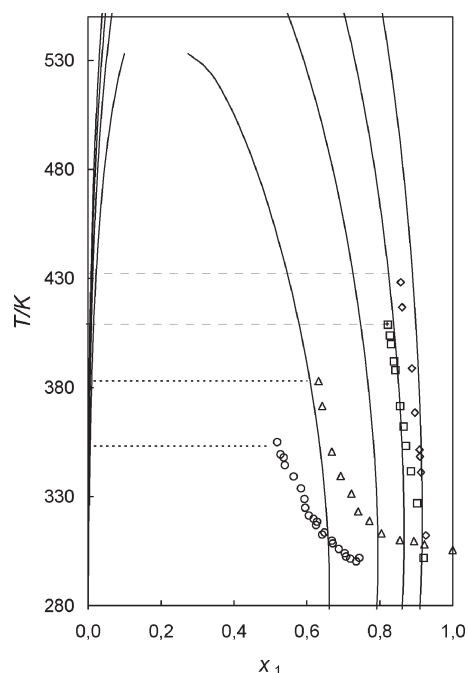


**Fig. 2** Liquid-liquid phase equilibria diagram of binary systems:  $\{x_1 [\text{mmim}][\text{CH}_3\text{SO}_4] + (1 - x_1) \text{aromatic hydrocarbon}\}$ : ○, benzene; △, toluene; □, ethylbenzene; ◇, propylbenzene; solid lines are calculated by the COSMO-RS method; dotted lines, boiling temperatures of the solvent.

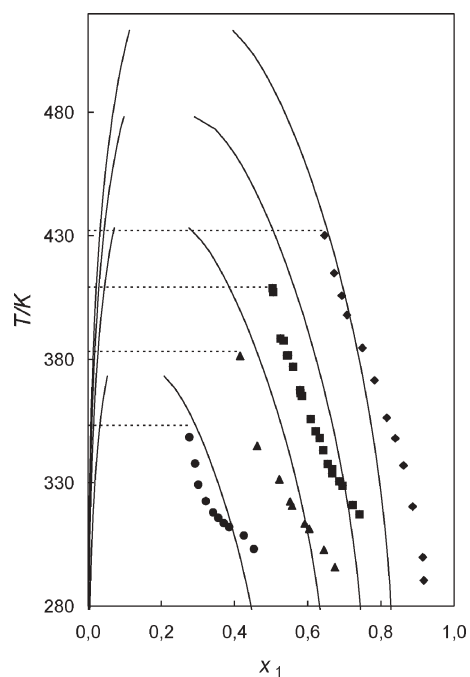


**Fig. 3** Liquid-liquid phase equilibria diagram of binary systems:  $\{x_1 [\text{bmim}][\text{CH}_3\text{SO}_4] + (1 - x_1) \text{aromatic hydrocarbon}\}$ : ●, benzene; ▲, toluene; ■, ethylbenzene; ◆, propylbenzene; solid lines are calculated by the COSMO-RS method; dotted lines, boiling temperatures of the solvent.

infinite dilution activity coefficients in  $[\text{mmim}][\text{CH}_3\text{SO}_4]$  were higher for the longer chain *n*-alkanes and were higher for ethylbenzene than in benzene.<sup>40</sup>

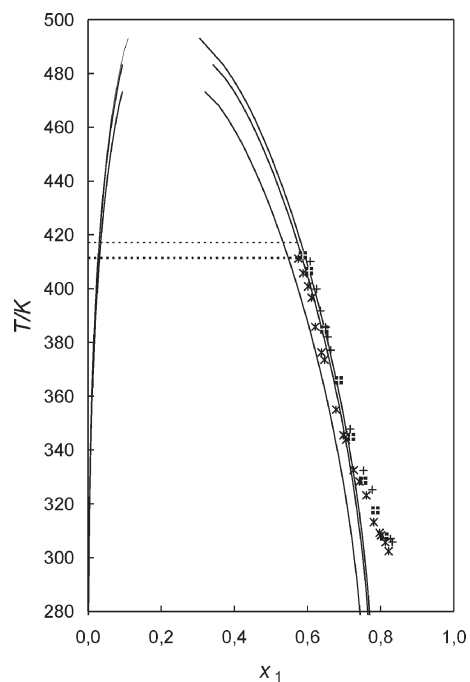


**Fig. 4** Liquid-liquid phase equilibria diagrams:  $\{x_1 [\text{bmim}][\text{CH}_3\text{SO}_4] + (1 - x_1) \text{xylene}\}$ : ■, *o*-xylene; +, *m*-xylene; \*, *p*-xylene; solid lines are calculated by the COSMO-RS method; dotted lines, boiling temperatures of the solvent.



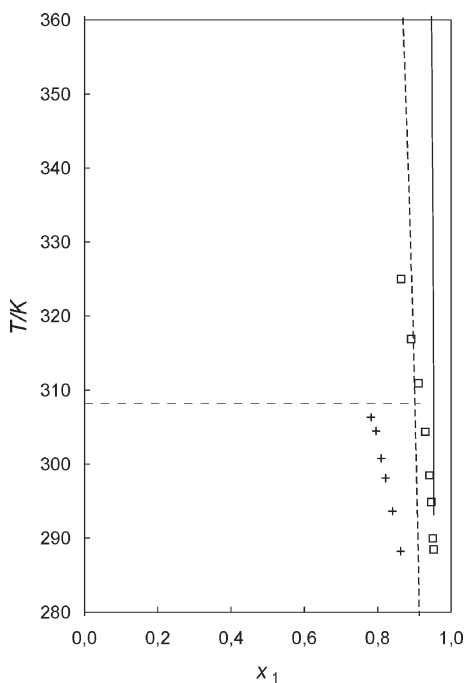


**Fig. 5** Solubility of +, [mmim][CH<sub>3</sub>SO<sub>4</sub>] (1) or □, [bmim][CH<sub>3</sub>SO<sub>4</sub>] (2) in *n*-pentane (2); lines are calculated by the COSMO-RS method: (—) [mmim][CH<sub>3</sub>SO<sub>4</sub>] and (- - -) [bmim][CH<sub>3</sub>SO<sub>4</sub>]; horizontal dashed line, boiling temperature of *n*-pentane.

For the investigated mixtures, it was impossible to detect by the visual method, the mutual solubility of ILs in the solvent-rich phase. These data can be approached by the COSMO-RS calculations.

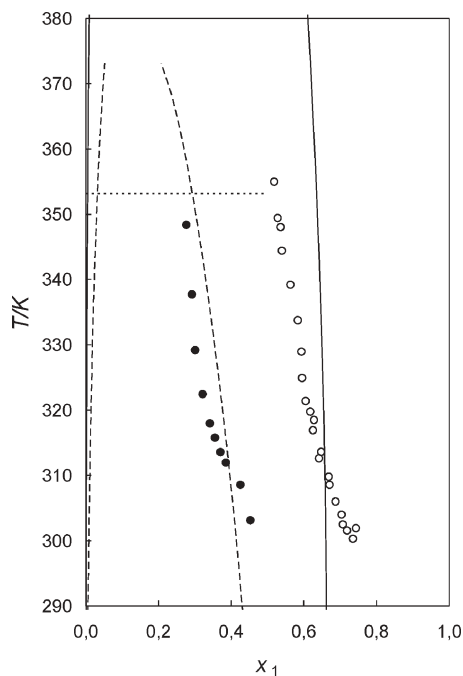


**Fig. 6** Solubility of ○, [mmim][CH<sub>3</sub>SO<sub>4</sub>] (1) or ●, [bmim][CH<sub>3</sub>SO<sub>4</sub>] (2) in benzene (2); lines are calculated by the COSMO-RS method: (—) [mmim][CH<sub>3</sub>SO<sub>4</sub>] and (- - -) [bmim][CH<sub>3</sub>SO<sub>4</sub>]; horizontal dotted line, boiling temperature of benzene.

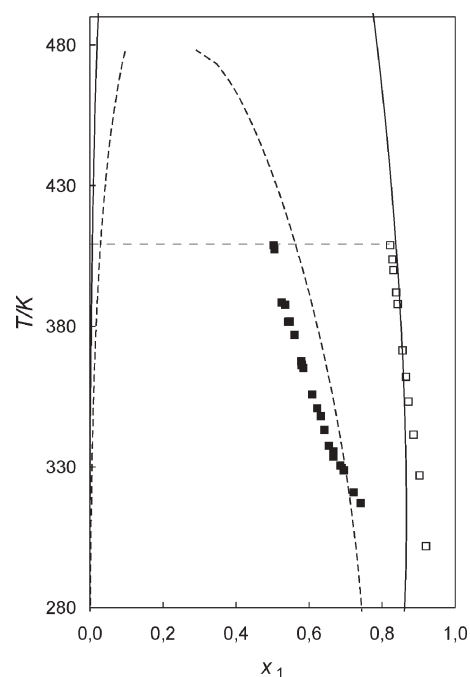


**Fig. 7** Solubility of □, [mmim][CH<sub>3</sub>SO<sub>4</sub>] (1) or ■ [bmim][CH<sub>3</sub>SO<sub>4</sub>] (2) in ethylbenzene (2); lines are calculated by the COSMO-RS method: (—) [mmim][CH<sub>3</sub>SO<sub>4</sub>] and (- - -) [bmim][CH<sub>3</sub>SO<sub>4</sub>]; horizontal dashed line, boiling temperature of ethylbenzene.

### Prediction of liquid–liquid phase equilibria

The conductor-like screening model for real solvents (COSMO-RS) is a unique method for predicting the thermodynamic properties of mixtures on the basis of unimolecular quantum chemical calculations for the individual molecules.<sup>45–48</sup> COSMO-RS combines the electrostatic advantages and the computational efficiency of the quantum chemical dielectric continuum solvation model COSMO<sup>49</sup> with a statistical thermodynamics method for local interaction of surfaces, which takes into account local deviations from dielectric behaviour as well as hydrogen bonding. In this approach all information about solutes and solvents is extracted from initial quantum chemical COSMO calculations, and only very few parameters have been adjusted to experimental values of partition coefficients and vapour pressures of a wide range of neutral organic compounds. COSMO-RS is capable of predicting activity coefficients, partition coefficients, vapour pressures and solvation free energies of neutral compounds with an error of 0.3 log-units (rms) and a lot of experience has been gathered during the past few years about its surprising ability to predict mixture thermodynamics.<sup>45–48</sup>

In addition, successful applications of COSMO-RS to the predictions of the thermodynamic properties of ions in solution and ionic liquids have been reported.<sup>33,50,51</sup> We applied the standard procedure for COSMO-RS calculations, which consists of two steps:

#### (1) Quantum chemical COSMO calculation for all molecular species involved

In these calculations, the solute molecules will be calculated in a virtual conductor environment. In such an environment, the

solute molecule induces a polarization charge density  $\sigma$  on the interface between the molecule and the conductor, that is, on the molecular surface. These charges act back on the solute and generate a more polarized electron density than in a vacuum. During the quantum chemical self-consistency algorithm SCF, the solute molecule is thus converged to its energetically optimal state in a conductor with respect to electron density. The quantum chemical calculation has to be performed once for each molecule of interest. The geometry of all compounds was fully relaxed at the density functional (DFT) level of theory.<sup>52</sup> This was done with the Turbomole program package<sup>52–54</sup> using the B-P density functional theory<sup>55,56</sup> with a TZVP quality basis set<sup>52,54</sup> and the RI approximation.<sup>57</sup> During these calculations the COSMO continuum solvation model was applied in the conductor limit ( $\epsilon = \infty$ ). Element-specific default radii from the COSMO-RS parameterizations have been used for the COSMO cavity construction.<sup>45,46</sup> Such calculations end up with the self-consistent state of the solute in the presence of a virtual conductor, that surrounds the solute outside the cavity.

## (2) COSMO-RS calculations

These were done using the COSMOtherm program.<sup>58</sup> In these calculations the deviations of a real solvent, in our case ionic liquids and organic solvents, compared to an ideal conductor are taken into account in a model of pair-wise interacting molecular surfaces. For this purpose, electrostatic energy differences and hydrogen bonding energies are quantified as functions of the local COSMO polarization charge densities  $\sigma$  and  $\sigma'$  of the two interacting surface pieces. The chemical potential differences arising from these interactions are evaluated using an exact statistical thermodynamics algorithm for independently pair-wise interacting surfaces, which is implemented in COSMOtherm. More detailed descriptions of the COSMO-RS method are given elsewhere.<sup>45–48</sup> The COSMO-RS method depends on a small number of adjustable parameters, some of which are predetermined from the known properties of the atoms. The others are determined from selected properties of mixtures, with none of the mixtures related to the mixtures under study here. The parameters are not specific to functional groups or molecule type. As the parameters are used as a basis for the calculations only, the resulting parametrization<sup>45</sup> is completely general. No special adjustments of radii or other parameters have been done for this application.

If more than one conformation was considered to be potentially relevant for a compound, several conformations have been calculated in step 1 and a thermodynamic Boltzmann average over the total Gibbs free energies of the conformers was consistently calculated by the COSMOtherm program in step 2. COSMO-RS' statistical thermodynamics procedure results in the chemical potential of all components of a given mixture. Thermodynamic properties of the mixture, such as activity coefficients and vapour–liquid equilibria can be derived from the chemical potentials. The liquid–liquid equilibrium properties have been calculated from the equity

$$x_i^I \gamma_i^I = x_i^{II} \gamma_i^{II} \quad (1)$$

where indices I and II denote the liquid phases,  $x_i$  are the mole fractions of the two solvents and  $\gamma_i$  are the activity coefficients of the solvents as computed by COSMO-RS.

The predictions for the LLE of mixtures of [mmim]-[CH<sub>3</sub>SO<sub>4</sub>] and [bmim][CH<sub>3</sub>SO<sub>4</sub>] with every investigated solvent are listed over a very wide temperature range as the ionic liquid mole fraction,  $x_1'$  in the ionic liquid rich phase and as the ionic liquid mole fraction,  $x_1''$  in the solvent rich phase in Tables 1S–2S in the ESI.†

In this work, the COSMO-RS calculations correspond much better with the experiment for [bmim][CH<sub>3</sub>SO<sub>4</sub>] than for [mmim][CH<sub>3</sub>SO<sub>4</sub>]. This can be explained partly by the stronger polarity of [mmim][CH<sub>3</sub>SO<sub>4</sub>], because for molecules that are extremely polar, such as [mmim]<sup>+</sup>, larger errors in the COSMO-RS predictions have to be expected than for less polar compounds.<sup>45</sup> This conclusion can be drawn from the polarity of the molecular surface as computed by quantum chemistry. The quantum chemical COSMO calculation provides the charge distribution on the molecular surface. This charge distribution (sigma) can be visualized in a histogram function (sigma-profile). The sigma profile shows the amount of polar surface charge on the molecular surface. Generally, the correspondence of the COSMO-RS prediction with measurements is better for the [bmim][CH<sub>3</sub>SO<sub>4</sub>] mixtures. COSMO-RS overestimates the polarity difference of the compounds and thus the predicted miscibility gap is too wide and the UCST is too high, especially for the non-polar solutes such as the *n*-alkanes. As one would expect from the above consideration, this overestimation is stronger for the [mmim][CH<sub>3</sub>SO<sub>4</sub>] mixtures. If only the curves below the boiling point of the solvent are compared it looks very optimistic, even for the *n*-alkanes. At room temperature the predictions are quite close to the experimental results for all the solvents and ILs considered here (see Fig. 2–7).

Comparing [mmim][CH<sub>3</sub>SO<sub>4</sub>] LLE experimental results with those for [bmim][CH<sub>3</sub>SO<sub>4</sub>] LLE, the same trends are observed. For all linear alkanes from *n*-pentane to *n*-decane experiment shows that the miscibility gap is larger in the [bmim][CH<sub>3</sub>SO<sub>4</sub>] LLE than in the [mmim][CH<sub>3</sub>SO<sub>4</sub>]. COSMO-RS prediction shows for all compounds from *n*-pentane to *n*-decane that the miscibility gap is larger for the [mmim][CH<sub>3</sub>SO<sub>4</sub>] than for the [bmim][CH<sub>3</sub>SO<sub>4</sub>]. This is the only major difference. However, this may be very well explained from electrostatics, because [mmim][CH<sub>3</sub>SO<sub>4</sub>] is more polar than [bmim][CH<sub>3</sub>SO<sub>4</sub>]. Thus from electrostatics we would expect the miscibility gap of [mmim][CH<sub>3</sub>SO<sub>4</sub>] with a non-polar compound (such as a linear *n*-alkane) to be larger than for the less polar [bmim][CH<sub>3</sub>SO<sub>4</sub>], which then is more like the non-polar *n*-alkane and thus more likely to mix with it. It can be noticed as well, that the longer the *n*-alkane chain the worse the COSMO-RS prediction (see Fig. 7S in the ESI.†).

Measurements of the xylene systems both for [bmim]-[CH<sub>3</sub>SO<sub>4</sub>] and [mmim][CH<sub>3</sub>SO<sub>4</sub>] show that the xylenes all behave in a similar way with the exception of [bmim][CH<sub>3</sub>SO<sub>4</sub>] with *p*-xylene at high temperatures. However, COSMO-RS predicts that the *o*-xylene should behave somewhat different from *m*- and *p*-xylene, which simply reflects the steric and electronic “*ortho*-effect” of multisubstituted aromatic compounds.

## Experimental

### Materials

The origins of the chemicals (in parentheses Chemical Abstract registry numbers, the manufacturers, and mass percent purities) were as follows: [mmim][CH<sub>3</sub>SO<sub>4</sub>] (CAS No. 97345-90-9, Solvent Innovation GmbH, >98%); [bmim][CH<sub>3</sub>SO<sub>4</sub>] (CAS No. 401788-98-5, Solvent Innovation GmbH, >98%); *n*-pentane (CAS No. 110-66-0, Fluka, purum); *n*-hexane (CAS No. 110-54-3, Merck, 99%); *n*-heptane (CAS No. 142-82-5, Sigma-Aldrich, 99%); *n*-octane (CAS No. 111-65-9, Sigma-Aldrich, 99%); *n*-decane (CAS No. 124-18-5, Sigma-Aldrich, 99+); cyclohexane (CAS No. 110-82-7, Intern. Enz. Lim., for spectroscopy), cycloheptane (CAS No. 291-64-5, Sigma-Aldrich, 98+), benzene (CAS No. 71-43-2, Sigma-Aldrich, 99.97+); toluene (CAS No. 108-88-3, Fluka, >99.7%); ethylbenzene (CAS No. 100-41-4, Sigma-Aldrich, 99%); propylbenzene (CAS No. 103-65-1, Merck, 98%); *o*-xylene (CAS No. 95-47-6, Fluka, >99%); *m*-xylene (CAS No. 108-38-3, Fluka, >99%); *p*-xylene (CAS No. 106-42-3, Sigma-Aldrich, 99%).

### Decomposition of compounds

Simultaneous thermogravimetry/differential thermal analysis (TG/DTA) experiments were performed using a MOM Derivatograph-PC (Hungary). Generally, runs were performed using matched labyrinth platonic crucibles with Al<sub>2</sub>O<sub>3</sub> in the reference pan. The crucible design hampered the migration of volatile decomposition products, reducing the rate of gas evolution and, in turn, increasing contact time of the reactants. The TG/DTA curves were obtained at a heating rate of 5 K min<sup>-1</sup> with a dynamic nitrogen atmosphere (flow rate of 20 dm<sup>3</sup> h<sup>-1</sup>). The main two decomposition temperatures and mass-loss percentages are presented in Table 1 and in Fig. 1S and 2S in the ESI.‡

### Differential scanning microcalorimetry (DSC)

The melting temperature, the enthalpy of fusion and the glass transition temperatures were measured by a Perkin-Elmer Pyris 1 differential scanning calorimetry (DSC) apparatus. Measurements were carried out at a scan rate of 10 K min<sup>-1</sup>, with a power sensitivity of 16 mJ s<sup>-1</sup> and with the recorder sensitivity of 5 mV. Each time the instrument was used, it was calibrated with the 99.9999 mol% purity indium sample. The calorimetric accuracy was ±1%, and the calorimetric precision was ±0.5%. The thermophysical properties are shown in Table 1.

### Liquid–liquid phase equilibria apparatus and measurements

Liquid–liquid phase equilibria (LLE) temperatures have been determined using a dynamic method that has previously been described in detail.<sup>37</sup> Appropriate mixtures of IL and solvent placed under the nitrogen in a drybox into a Pyrex glass cell were heated very slowly (less than 2 K h<sup>-1</sup> near the equilibrium temperature) with continuous stirring inside the cell. The sample was placed in a glass thermostat filled with silicone oil, or water. The temperature of the liquid bath was varied slowly

until the one phase was obtained. The two phase disappearance temperatures in the liquid phase were detected visually during an increasing temperature regime. The observation of the “cloud point” with decreasing temperature was very difficult in these mixtures. ILs under study often remain in a metastable state and it is hard to detect the real phase separation. The observation of the “cloud point” with decreasing temperature was not repeatable during the experiment. The effect of precooling and kinetics of the phenomenon of binary-phase creation were the reasons that the temperature of “cloud point” was not repeatable. The differences in observed results were as high as  $\Delta T = 5$  K. The temperature was measured with an electronic thermometer P 550 (DOSTMANN electronic GmbH) with the probe totally immersed in the thermostating liquid. The thermometer was calibrated on the basis of ITS-90. The accuracy of the temperature measurements was judged to be ±0.01 K. Mixtures were prepared by mass, and the errors did not exceed  $\delta x_1 = 0.0002$  and  $\delta T_1/K = 0.1$  in the mole fraction and temperature, respectively. The LLE measurements were limited at the upper temperature by the boiling point of the solvent. However, in two systems: [bmim][CH<sub>3</sub>SO<sub>4</sub>] with *n*-pentane and *n*-heptane, the data were measured using a special cell at temperatures higher than the boiling temperature of *n*-alkanes.

## Conclusion

Knowledge of the impact of different factors on the liquid phase behaviour of ILs with other liquids is useful for developing ILs as designer solvents. The area of two liquid phases decreases with an increase in the chain length of the alkyl substituent at the imidazole ring. The observations of upper critical solution temperatures (UCSTs) were limited by the boiling temperature of the solvent. The observation of the liquid–liquid demixing at the solvent rich phase was inhibited by the permanently foggy solution.

The noticeable differences in the solubilities of [mmim]-[CH<sub>3</sub>SO<sub>4</sub>] or [bmim][CH<sub>3</sub>SO<sub>4</sub>] in the *n*-alkanes and in benzene, or ethylbenzene, suggest that ILs can be considered as possible alternative solvents for the aliphatic/aromatic extraction. Unfortunately, the results obtained for xylenes are not so optimistic.

The existence of the liquid–liquid equilibria in these mixtures is evidence that the interaction between the IL and the solvent is not insignificant. The molecules in the liquid phase very often occur as complex structures, such as ILs formed with the aid of hydrogen bonds. Dissolution of such an associated liquid in a nonpolar solvent may involve the transfer of lattice-borne multimers into the solution. Thus, the structure of ILs is very important and is responsible for the different phase diagrams obtained with different hydrocarbons, where insignificant A–B interaction exists. The solubility of [bmim][CH<sub>3</sub>SO<sub>4</sub>] is higher than the solubility of [mmim][CH<sub>3</sub>SO<sub>4</sub>] in all solvents except in *n*-alkanes. The interaction with solvents increases as the alkyl chain of the cation increases. The structure of [bmim][CH<sub>3</sub>SO<sub>4</sub>] is less H-bonded than in [mmim][CH<sub>3</sub>SO<sub>4</sub>] in the pure state. This is probably due to the fact that the molecule is more flat and that

is why this salt is also a liquid at room temperature (compared with [mmim][CH<sub>3</sub>SO<sub>4</sub>]) and its decomposition temperature is much lower. This makes it easier for the solvent molecule to be closer to the [bmim][CH<sub>3</sub>SO<sub>4</sub>] molecule.

The COSMO-RS prediction for ILs in aromatic hydrocarbons is reasonably satisfactory. It is easy to observe that the UCST for [bmim][CH<sub>3</sub>SO<sub>4</sub>] in benzene is lower than 380 K at  $x_1 = 0.12$  (see Fig. 3); for toluene it is lower than 440 K at  $x_1 = 0.15$  (see Fig. 3) and for [bmim][CH<sub>3</sub>SO<sub>4</sub>] in ethylbenzene it is lower than 482 K at  $x_1 = 0.20$  (see Fig. 7). Recently, Kato and Gmehling<sup>59</sup> have used the modified version of COSMO-RS (model 01) for the prediction of activity coefficients and their temperature dependence ( $H^E$ ) of water, alkanes, alkenes, cycloalkenes and alcohols in different ionic liquids.

Due to the differences in solubilities, ILs used in this work have attracted significant attention as potential solvents for industrial reactions.

## Acknowledgements

Funding for this research was provided by the Warsaw University of Technology. The authors would like to thank Mrs A. Wiśniewska for some of the solubility measurements.

## References

- R. D. Rogers and K. R. Seddon, *Ionic Liquids. Industrial Applications to Green Chemistry*, ACS Symposium Series, 2002, p. 818.
- J. Dupont, R. F. De Souza and P. A. Z. Suarez, *Chem. Rev.*, 2002, **102**, 3667.
- Ch. J. Adams, M. J. Earle and K. R. Seddon, *Green Chem.*, 2000, **2**, 21.
- J. L. Scott, D. R. MacFarlane, C. L. Raston and Ch. M. Teoh, *Green Chem.*, 2000, **2**, 123.
- P. A. Z. Suarez, J. E. L. Dullius, S. Einloft, R. F. De Souza and J. Dupont, *Polyhedron*, 1996, **15**, 1217.
- J. Dupont, P. A. Z. Suarez, R. F. De Souza, R. A. Burrow and J.-P. Kintzinger, *Chem.-Eur. J.*, 2000, **6**, 2377.
- P. Wasserscheid and W. Keim, *Angew. Chem., Int. Ed.*, 2000, **39**, 3773.
- R. S. Varma and V. V. Namboodiri, *Chem. Commun.*, 2001, 643.
- F. Zulfqar and T. Kitazume, *Green Chem.*, 2000, **2**, 137.
- F. Zulfqar and T. Kitazume, *Green Chem.*, 2000, **2**, 296.
- C. W. Lee, *Tetrahedron Lett.*, 1999, **40**, 2461.
- C. Cadena, J. L. Anthony, J. K. Shah, T. I. Morrow, J. F. Brennecke and E. J. Maginn, *J. Am. Chem. Soc.*, 2004, **126**, 5300.
- K. R. Seddon, *J. Chem. Technol. Biotechnol.*, 1997, **68**, 351.
- Y. Chauvin and H. Olivier-Bourbigou, *CHEMTECH*, 1995, **25**, 26.
- C. J. Adams, M. J. Earle, G. Roberts and K. R. Seddon, *Chem. Commun.*, 1998, 2097.
- M. J. Earle, P. B. McCormac and K. R. Seddon, *Chem. Commun.*, 1998, 2245.
- M. J. Earle, P. B. McCormac and K. R. Seddon, *Green Chem.*, 1999, **1**, 23.
- B. Ellis, W. Keim and P. Wasserscheid, *Chem. Commun.*, 1999, 337.
- J. G. Huddleston, H. D. Willauer, R. P. Swatloski, A. E. Visser and R. D. Rogers, *Chem. Commun.*, 1998, 1765.
- J. F. Brennecke, *Chem. Ind.*, 1996, **16**, 831.
- N. M. B. Flichy, S. G. Kazarin, C. J. Lawrence and B. J. Briscoe, *J. Phys. Chem. B*, 2002, **106**, 754.
- L. A. Blanchard, Z. Gu and J. F. Brennecke, *J. Phys. Chem. B*, 2001, **105**, 2437.
- A. M. Scurto, S. N. V. K. Akai and J. F. Brennecke, *J. Am. Chem. Soc.*, 2002, **124**, 10276.
- J. D. Holbrey and K. R. Seddon, *Clean Prod. Process.*, 1999, **1**, 223.
- Ch. Wheeler, K. N. West, Ch. L. Liotta and Ch. A. Eckert, *Chem. Commun.*, 2001, 887.
- V. N. Najdanovic-Visac, J. M. S. S. Esperanca, L. P. N. Rebelo, M. Nunes da Ponte, H. J. R. Guedes, K. R. Seddon and J. Szydłowski, *Phys. Chem. Chem. Phys.*, 2002, **4**, 1701.
- V. N. Najdanovic-Visac, J. M. S. S. Esperanca, L. P. N. Rebelo, M. Nunes da Ponte, H. J. R. Guedes, K. R. Seddon and J. Szydłowski, *J. Phys. Chem. B*, 2003, **107**, 12797.
- M. Krummen and J. Gmehling, Presented at the 17th IUPAC Conference on Chemical Thermodynamics, Rostock, Germany 2002, July 28–August 2.
- C. Jork, M. Seiler and W. Arlt, Presented at Thermodynamics 2003, Cambridge, UK, 2003, April 9–11.
- R. Kato, M. Krummen and J. Gmehling, *Fluid Phase Equilib.*, 2004, **224**, 47.
- L. S. Belveze, J. F. Brennecke and M. A. Stadtherr, *Ind. Eng. Chem. Res.*, 2004, **43**, 815.
- J. M. Crosthwaite, S. N. V. K. Aki, E. J. Maginn and J. F. Brennecke, *J. Phys. Chem. B*, 2004, **108**, 5113.
- C. T. Wu, K. N. Marsh, A. V. Deev and J. A. Boxall, *J. Chem. Eng. Data*, 2003, **48**, 486.
- J. M. Crosthwaite, S. N. V. K. Aki, E. J. Maginn and J. F. Brennecke, *Fluid Phase Equilib.*, 2005, **228–229**, 303.
- K. N. Marsh, A. Deev, A. C.-T. Wu, E. Tran and A. Klamt, *Kor. J. Chem. Eng.*, 2002, **19**, 357.
- T. M. Letcher and N. Deenadayalu, *J. Chem. Thermodyn.*, 2003, **35**, 67.
- U. Domańska and A. Marciniak, *J. Chem. Eng. Data*, 2003, **48**, 451.
- A. Heintz, D. V. Kulikov and S. P. J. Verevkin, *J. Chem. Eng. Data*, 2002, **47**, 894.
- A. Heintz, D. V. Kulikov and S. P. J. Verevkin, *J. Chem. Eng. Data*, 2001, **46**, 1526.
- R. Kato and J. Gmehling, *Fluid Phase Equilib.*, 2004, **226**, 37.
- U. Domańska and L. Mazurowska, *Fluid Phase Equilib.*, 2004, **221**, 73.
- U. Domańska, *Pure Appl. Chem.*, 2005, **77**, 543.
- U. Domańska and A. Marciniak, *J. Phys. Chem. B*, 2004, **108**, 2376.
- U. Domańska, A. Pobudkowska and F. Eckert, *J. Chem. Thermodyn.*, 2006, DOI: 10.1016/j.jct.2005.07.024.
- E. Eckert and A. Klamt, *AIChE J.*, 2002, **48**, 369.
- A. Klamt and F. Eckert, *Fluid Phase Equilib.*, 2000, **172**, 43.
- A. Klamt, V. Jonas, T. Bürger and J. C. W. Lohrenz, *J. Phys. Chem.*, 1998, **102**, 5074.
- A. Klamt, *J. Phys. Chem.*, 1995, **99**, 2224.
- A. Klamt and G. Schürmann, *J. Chem. Soc., Perkin Trans. 2*, 1993, 799.
- M. Diedenhofen, F. Eckert and A. Klamt, *J. Chem. Eng. Data*, 2003, **48**, 475.
- W. Arlt, O. Spuhl and A. Klamt, *Chem. Eng. Proc.*, 2004, **43**, 221.
- A. Schäfer, A. Klamt, D. Sattel, J. C. W. Lohrenz and F. Eckert, *Phys. Chem. Chem. Phys.*, 2000, **2**, 2187.
- R. Ahlrichs, M. Bär, H.-P. Baron, R. Bauernschmitt, S. Böcker, M. Ehrig, K. Eichkorn, S. Elliott, F. Furche, F. Haase, M. Häser, H. Horn, C. Hattig, C. Huber, U. Huniar, M. Kattannek, M. Köhn, C. Kölmel, M. Kollwitz, K. May, C. Ochsenfeld, H. Öhm, A. Schäfer, U. Schneider, O. Treutler, M. von Arnim, F. Weigend, P. Weis and H. Weiss, Turbomole Version 5.6, 2002.
- R. Ahlrichs, M. Bär, M. Häser, H. Horn and C. Kölmel, *Chem. Phys. Lett.*, 1989, **162**, 165.
- A. D. Becke, *Phys. Rev. A*, 1988, **38**, 3098.
- J. P. Perdew, *Phys. Rev. B*, 1986, **33**, 8822.
- K. Eichkorn, O. Treutler, H. Öhm, M. Häser and R. Ahlrichs, *Chem. Phys. Lett.*, 1995, **242**, 652.
- F. Eckert and A. Klamt, COSMOtherm, Version C2.1-Revision 01.04; COSMOlogic GmbH&CoKG, Leverkusen, Germany, 2004.
- R. Kato and J. Gmehling, *J. Chem. Thermodyn.*, 2005, **37**, 603.

# Selective *N*-alkylation of anilines in ionic liquids†

Cinzia Chiappe,\* Paolo Piccioli and Daniela Pieraccini

Received 11th June 2005, Accepted 9th September 2005

First published as an Advance Article on the web 28th September 2005

DOI: 10.1039/b509851c

A simple and efficient method for the preparation of *N*-monoalkyl-substituted anilines employing ionic liquids (ILs) as the solvent is presented. The reactions have been performed in several ionic liquids using differently substituted anilines as substrates and alkyl, allyl and benzyl halides as alkylating agents in order to establish the factors that affect the reactivity and the chemoselectivity of the *N*-alkylation process.

## Introduction

*N*-Alkyl-substituted anilines are valuable industrial intermediates in the manufacture of dyes, plastics, pharmaceuticals and agrochemicals. Traditionally, these compounds are prepared in liquid phase using mineral acids as catalysts and alkyl halides or dimethyl sulfate as alkylating agents.<sup>1</sup> Though new various heterogeneous catalysts and non-toxic alkylating agents, such as methanol<sup>2</sup> and dimethyl carbonate,<sup>3</sup> have been introduced, yields or products selectivity are, with few exceptions, low and depend on the nature of the catalysts and on the reaction conditions. The major synthetic problem is competing over-alkylation, which leads to mixtures of secondary and tertiary amines and quaternary ammonium salts. The difficulty in preventing over-alkylation is especially true when highly reactive electrophilic compounds (methyl, ethyl, benzyl and allyl alkylating agents) are used. Besides the *N*-alkylation,<sup>4</sup> other general methods for the synthesis of secondary amines are amide reduction<sup>5</sup> and reductive amination.<sup>6</sup> Although these methods are quite reliable, also in this case the possibility to control the concomitant overalkylations, when the amine is employed as the limiting substrate, often reduces the application of these methods.

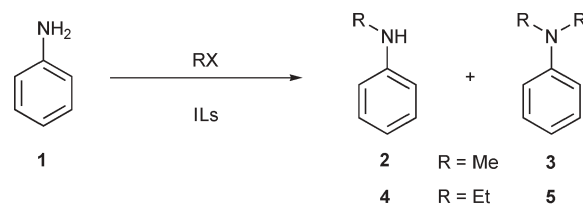
Room temperature ionic liquids are emerging as potential green alternatives to volatile organic solvents and recently they have been used as environmentally benign media for several important reactions, due to their unique physical and chemical properties.<sup>7</sup> In particular, it has been shown that the use of ILs as reaction media for the alkylation of *N*-alkylamines minimised over-alkylation.<sup>8</sup> Moreover, the mild reaction conditions generally employed to perform these reactions enabled the application of this protocol to substrates with labile substituents. In this respect, and considering our interest to explore new application of ILs in organic synthesis, we have investigated the direct monoalkylation of aromatic amines. Secondary amines have been prepared with excellent yields and high selectivity by reacting anilines with alkyl halides and tosylates. 1-Butyl-3-methylimidazolium hexafluorophosphate [bmim][PF<sub>6</sub>], 1-butyl-3-methylimidazolium

bis(trifluoromethylsulfonyl)imide [bmim][Tf<sub>2</sub>N], 1-ethyl-3-methylimidazolium bis(trifluoromethylsulfonyl)imide [emim][Tf<sub>2</sub>N], 1-butyl-3-methylimidazolium triflate [bmim][OTf], 1-ethyl-3-methylimidazolium tosylate [emim][OTs] and 1-ethyl-3-methylimidazolium ethylsulfate [emim][EtSO<sub>4</sub>] have been used as solvents.

## Results and discussion

As a preliminary screening aimed at evaluating if ILs were effectively able to promote *N*-alkylation, ethylation and methylation of aniline were performed in different ILs at different temperatures.

Reactions were typically carried out by addition of methyl or ethyl iodide (5.5 mmol), under stirring, to the ionic liquids (2 ml) containing an equimolar amount of aniline. Generally, after few minutes (the time interval ranged from 10 to 60 min) the formation of a white solid indicated the end of the reaction. This solid has been identified by NMR analysis (see below) as the ammonium salt (*N*-alkylaniline hydroiodide) arising from aniline monoalkylation. Product distribution analysis of the reaction mixtures at prolonged times after the precipitation of the salt showed no appreciable variation in the product composition. To isolate the formed *N*-alkylanilines an aqueous solution of NaHCO<sub>3</sub> was added to the reaction mixtures, and the products were extracted with *n*-hexane (extraction yield always >90–95%). The reaction mixtures were analyzed by NMR and the products were identified on the basis of their <sup>1</sup>H and <sup>13</sup>C NMR spectra (product purity >95%). Generally, the residue ILs were washed with water, dried and reused at least three times for other alkylation reactions without any significant modification in yields and selectivity (Scheme 1).



RX: MeI, EtI  
 ILs: [bmim][NTf<sub>2</sub>], [emim][NTf<sub>2</sub>], [bmim][PF<sub>6</sub>]

**Scheme 1** Aniline alkylation.

Dipartimento di Chimica Bioorganica e Biofarmacia, via Bonanno 33, Pisa, Italy. E-mail: cinziac@farm.unipi.it; Fax: +39 050 2219660; Tel: +39 050 2219669

† This work was presented at the 1st International Congress on Ionic Liquids (COIL), held in Salzburg, Austria, 19–22 June 2005.

**Table 1** *N*-Methylation and *N*-ethylation of aniline in ionic liquids (ILs)

Entry	RX	ILs	Temp/°C	Time/min	Conversion <sup>a</sup> (%)	2 : 3 <sup>b</sup>	
1	MeI	[bmim][Tf <sub>2</sub> N]	25	10	90	60	40
2	MeI	[bmim][Tf <sub>2</sub> N]	0	30	76	90	10
3	MeI	[emim][Tf <sub>2</sub> N]	25	10	90	65	35
4	MeI	[emim][Tf <sub>2</sub> N]	0	30	68	70	30
5	MeI	[bmim][PF <sub>6</sub> ]	25	10	75	55	45
6	MeI	[bmim][PF <sub>6</sub> ]	0	30	50	80	20
7	MeI	[bmim][OTf]	25	10	65	30	70
8	MeI	[bmim][OTf]	0	30	73	50	50
9	MeI	[emim][OTs]	25	10	80	35	65
10	MeI	[emim][OTs]	0	30	71	45	55
11	MeI	[emim][EtSO <sub>4</sub> ]	25	10	73	35	65
12	MeI	[emim][EtSO <sub>4</sub> ]	0	30	76	50	50
13	MeI	DMSO	25	10	50 <sup>c</sup>	0	>95
14	MeI	CH <sub>3</sub> CN	25	10	50 <sup>c</sup>	66	33
15	MeI	CH <sub>2</sub> Cl <sub>2</sub>	25	10	10 <sup>c</sup>	>95	Nd

Entry	RX	ILs	Temp/°C	Time/min	Conversion <sup>a</sup> (%)	4 : 5	
16	EtI	[bmim][Tf <sub>2</sub> N]	25	60	70	90	10
17	EtI	[bmim][Tf <sub>2</sub> N]	0	No react	—	—	—
18	EtI	[emim][Tf <sub>2</sub> N]	25	60	75	85	15
19	EtI	[emim][Tf <sub>2</sub> N]	0	No react	—	—	—
20	EtI	[bmim][PF <sub>6</sub> ]	25	60	75	85	15
21	EtI	[bmim][PF <sub>6</sub> ]	0	No react	—	—	—

<sup>a</sup> The extraction yields were always >90–95%. The remaining product was identified as the unreacted aniline. <sup>b</sup> Determined by <sup>1</sup>H NMR. <sup>c</sup> The extraction yields were always around 30%.

As a comparison, methylation of aniline has been performed also in three molecular solvents (DMSO, acetonitrile and dichloromethane) under the same conditions used for the reactions in ILs. The data collected so far, are reported in Table 1.

As shown by the data reported in Table 1, temperature and nature of the solvent affect both conversion and selectivity. With respect to the methylation, the use of ILs as reaction medium generally is accompanied by improved product recovery, increased conversions and selectivities. In molecular solvents, a high selectivity was observed only in dichloromethane, where however the reaction was characterized by an extremely low conversion (around 10%). In DMSO, only the dialkylation product was isolated whereas in acetonitrile a 2 : 1 mixture of *N*-methyl and *N,N*-dimethylaniline was obtained. Moreover, in all three molecular solvents the extraction yields were very low, around 30%.

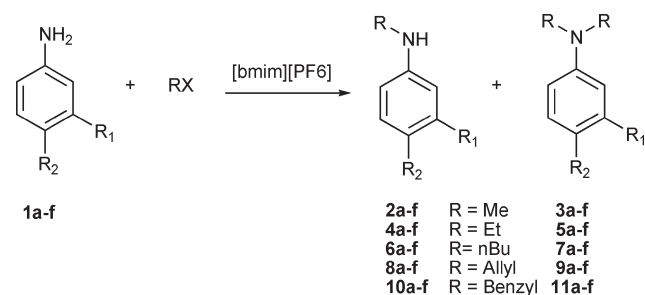
In ILs the selective production of *N*-methylaniline significantly improved on decreasing the reaction temperature from 25 to 0 °C, although as expected at the lower temperature the increased selectivity was generally associated with lower conversions. A different behavior is observed when ethyl iodide was used as alkylating agent; practically no alkylation product was observed at 0 °C. The formation of ethylaniline proceeded however with a good selectivity even at 25 °C, in particular when [bmim][Tf<sub>2</sub>N] was used as solvent. [bmim][Tf<sub>2</sub>N], [emim][Tf<sub>2</sub>N] and [bmim][PF<sub>6</sub>] were also the best reaction media to obtain high conversions and higher selectivity in *N*-methylaniline synthesis. At variance, no selectivity and lower conversions characterized the reactions performed in [bmim][OTf], [emim][OTs] and [emim][EtSO<sub>4</sub>] at 0 °C. On the other hand, these solvents at higher temperatures favor the formation of *N,N*-dimethylaniline.

It is noteworthy that with respect to the methylation of aniline, a fairly good correlation may be envisaged between

selectivity and H-bond acceptor ability of the anion: the best selectivity is achieved in the solvent with the poorest H-bond acceptor anion, whilst the least selectivity occurs when the anion is a good H-bond acceptor. Anion basicity may affect the deprotonation–alkylation process discussed below.

Considering the promising results obtained in methylation and ethylation of aniline at least in some of the used ILs, the subsequent step was to investigate how the presence of substituents on the phenyl ring and/or the nature of the alkylating agent may affect the reaction selectivity. The alkylation of differently substituted anilines with several alkylating agents have been therefore carried out in [bmim][PF<sub>6</sub>] (Scheme 2). The product distribution data are reported in Table 2. Although on the basis of the data reported in Table 1 the best IL seems to be [bmim][Tf<sub>2</sub>N] in this screening it has been replaced with the [bmim][PF<sub>6</sub>], since the products are more readily recovered in this latter solvent.

As we might expect, the presence of electron-withdrawing groups on the aniline ring extended reaction times (from few minutes to several hours), so that lower conversions were found for the reactions of **1b**, **1c**, **1d** and **1f**. In particular, more

**Scheme 2** Aniline alkylation.

**Table 2** *N*-Alkylation of anilines in ionic liquids (ILs)<sup>a</sup>

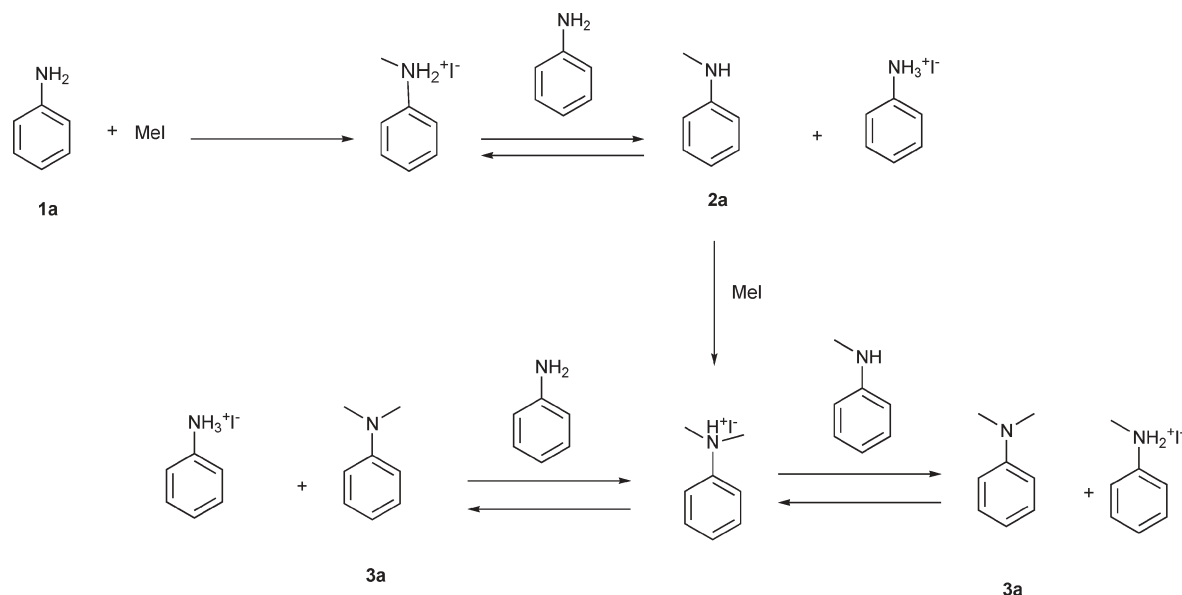
Entry	Substrate	R <sub>1</sub>	R <sub>2</sub>	RX	Temp/ <sup>o</sup> C	Time/min	Conversion <sup>b</sup> /%	<i>N</i> -Monosub <sup>c</sup>	<i>N,N</i> -Disub <sup>c</sup>
1	<b>1a</b>	H	H	MeI	0	30	50	80	20
2	<b>1a</b>	H	H	MeI	25	10	67	60	40
3	<b>1a</b>	H	H	OMe <sup>d</sup>	0	0.5	50	75	25
4	<b>1a</b>	H	H	OMe <sup>d</sup>	25	1	70	50	50
5	<b>1a</b>	H	H	EtI	0	60	—	—	—
6	<b>1a</b>	H	H	EtI	25	60	75	85	15
7	<b>1a</b>	H	H	EtI	60	30	60	85	15
8	<b>1a</b>	H	H	BuCl	25	60	—	—	—
9	<b>1a</b>	H	H	BuCl	60	60	—	—	—
10	<b>1a</b>	H	H	BuBr	25	60	50	85	15
11	<b>1a</b>	H	H	BuBr	60	60	70	80	20
12	<b>1a</b>	H	H	CH <sub>2</sub> =CH-CH <sub>2</sub> Br	25	0.5	70	40	60
13	<b>1a</b>	H	H	CH <sub>2</sub> =CH-CH <sub>2</sub> Br	60	0.5	70	40	60
14	<b>1a</b>	H	H	BnBr	25	0.5	47	55	45
15	<b>1a</b>	H	H	BnBr	60	0.5	60	30	70
16	<b>1b</b>	Br	H	MeI	25	20	50	63	37
17	<b>1b</b>	Br	H	MeI	60	10	70	45	55
18	<b>1b</b>	Br	H	OMe <sup>d</sup>	25	20	50	45	55
19	<b>1b</b>	Br	H	OMe <sup>d</sup>	60	10	70	40	60
20	<b>1b</b>	Br	H	EtI	25	30	30	90	10
21	<b>1b</b>	Br	H	EtI	60	30	50	90	10
22	<b>1b</b>	Br	H	BuCl	25	60	—	—	—
23	<b>1b</b>	Br	H	BuCl	60	60	—	—	—
24	<b>1b</b>	Br	H	BuBr	25	60	5	100	0
25	<b>1b</b>	Br	H	BuBr	60	60	20	100	0
26	<b>1b</b>	Br	H	CH <sub>2</sub> =CH-CH <sub>2</sub> Br	25	10	90	80	20
27	<b>1b</b>	Br	H	CH <sub>2</sub> =CH-CH <sub>2</sub> Br	60	10	70	60	40
28	<b>1b</b>	Br	H	BnBr	25	10	45	45	55
29	<b>1b</b>	Br	H	BnBr	80	10	60	35	65
30	<b>1c</b>	H	NO <sub>2</sub>	MeI	90	360	30	95	5
31	<b>1c</b>	H	NO <sub>2</sub>	OMe <sup>d</sup>	90	360	20	90	10
32	<b>1c</b>	H	NO <sub>2</sub>	EtI	90	360	10	100	0
33	<b>1c</b>	H	NO <sub>2</sub>	BuCl	90	360	—	—	—
34	<b>1c</b>	H	NO <sub>2</sub>	BuBr	90	360	10	100	0
35	<b>1c</b>	H	NO <sub>2</sub>	CH <sub>2</sub> =CH-CH <sub>2</sub> Br	90	360	85	84	16
36	<b>1c</b>	H	NO <sub>2</sub>	BnBr	90	360	36	74	26
37	<b>1d</b>	Cl	Cl	MeI	90	180	80	70	30
38	<b>1d</b>	Cl	Cl	OMe <sup>d</sup>	90	180	50	33	67
39	<b>1d</b>	Cl	Cl	EtI	90	180	90	86	14
40	<b>1d</b>	Cl	Cl	BuCl	90	180	—	—	—
41	<b>1d</b>	Cl	Cl	BuBr	90	180	30	<95	<5
42	<b>1d</b>	Cl	Cl	CH <sub>2</sub> =CH-CH <sub>2</sub> Br	90	180	74	48	52
43	<b>1d</b>	Cl	Cl	BnBr	90	180	50	46	54
44	<b>1e</b>	H	Me	MeI	25	10	74	48	52
45	<b>1e</b>	H	Me	OMe <sup>d</sup>	25	1	65	40	60
46	<b>1e</b>	H	Me	EtI	25	30	67	80	20
47	<b>1e</b>	H	Me	BuCl	25	60	—	—	—
48	<b>1e</b>	H	Me	BuBr	25	60	85	95	5
49	<b>1e</b>	H	Me	CH <sub>2</sub> =CH-CH <sub>2</sub> Br	25	0.5	70	30	70
50	<b>1e</b>	H	Me	BnBr	25	0.5	30	20	80
51	<b>1f</b>	H	Br	MeI	90	180	85	70	30
52	<b>1f</b>	H	Br	OMe <sup>d</sup>	90	180	85	55	45
53	<b>1f</b>	H	Br	EtI	90	180	70	88	12
54	<b>1f</b>	H	Br	BuCl	90	180	—	—	—
55	<b>1f</b>	H	Br	BuBr	90	180	40	92	8
56	<b>1f</b>	H	Br	CH <sub>2</sub> =CH-CH <sub>2</sub> Br	90	180	65	60	40
57	<b>1f</b>	H	Br	BnBr	90	180	60	60	40

<sup>a</sup> Products were extracted immediately after the formation of a white solid (the time interval ranged from few seconds to six-seven hours) or at prefixed times, as reported. <sup>b</sup> The extraction yield was always >90–95%. The remaining products were identified as the unreacted aniline.

<sup>c</sup> Determined by <sup>1</sup>H NMR. <sup>d</sup> OMe: methoxy *p*-methylbenzenesulfonate.

drastic conditions (temperature around 90 °C) were necessary to obtain the alkylation of *p*-NO<sub>2</sub> aniline, 3,4-dichloroaniline and *p*-bromoaniline.

Generally, the reactivity of these substrates depended on the nature of the alkylating agent: butyl chloride, practically does not react with any substrate even at higher temperature



Scheme 3 Multiequilibria in ionic liquids.

(90 °C). At variance, butyl bromide reacted with all substrates, although with deactivated anilines even at 90 °C for six seven hours quite low conversions were obtained. Gradually, lower temperatures were needed for alkylation with EtI, MeI and methoxy *p*-methylsulfonate whereas activated halides, such as allyl bromide and benzyl bromide, reacted quantitatively in relatively short times with all the examined substrates.

Also the chemoselectivity of the alkylation of substituted anilines in [bmim][PF<sub>6</sub>] depended on the reagents: when activated alkyl halides reacted with activated anilines (**1a**, **1e**), tertiary amines were the main products; on the other hand, deactivated anilines (**1b-d** and **1f**) gave always predominantly or exclusively secondary amines. Finally, it is noteworthy that the employment of methoxy *p*-methylbenzenesulfonate for the methylation of the investigated substrates generally does not improve the conversions, which are always comparable to that obtained with methyl iodide. On the other hand, the chemoselectivity is normally lower than that characterizing the reaction with MeI and this may be attributed to an increased alkylating capability of methoxy *p*-methylbenzenesulfonate with respect to methyl iodide.

Methylation and ethylation of aniline was followed also by <sup>1</sup>H NMR. The reactions were carried in the low viscous [emim][Tf<sub>2</sub>N], at 25 °C, in a coaxial tube using CD<sub>3</sub>COOD as external lock. To an exactly measured amount of aniline (0.7 M) an equimolar amount of MeI or EtI was added and the spectra were registered at regular intervals of times. It is noteworthy that, after ten minutes in the case of methylation, and sixty minutes for the ethylation reaction (around 25–30% of conversion), we observed a relevant broadening of the signals, due to the precipitation of a white solid identified, after filtration and dissolution in CD<sub>3</sub>CN or DMSO-*d*<sub>6</sub>, as a mixture of mono- and dialkylanilinium salts. It is noteworthy that in the mixture arising from the methylation reaction the

monoalkylation product was preponderant while in the ethylation it was practically the sole reaction product.

On the basis of this latter result, we therefore hypothesize that the chemoselectivity observed in ILs is mainly due to the precipitation of the mono-*N*-alkylanilinium salt (Ph-NHMe·HI). Considering the simultaneous equilibria involved in the formation of mono- and polyalkylated amines, reported in Scheme 3, the precipitation of **2a**·HI may be attributed not only to a decreased solubility in these ionic media but also to a different basicity of the reacting species in the ILs (Scheme 3).

## Conclusions

In conclusion, this paper shows the possibility to obtain secondary aromatic amines with high conversions and chemoselectivities using simply alkyl halides in ionic liquids. In many cases, the ionic liquid not only promotes the *N*-alkylation but also reduces or eliminates the formation of overalkylation products.

## Experimental

<sup>1</sup>H and <sup>13</sup>C NMR were recorded with a Bruker AC 200 instrument. Methyl iodide (Aldrich, ≥98%), ethyl iodide (Aldrich, ≥98%), methoxy *p*-methylsulfonate (Aldrich, ≥98%), butyl chloride (Aldrich, ≥98%), butyl bromide (Aldrich, ≥98%), benzyl bromide (Aldrich, ≥98%), allyl bromide (Aldrich, ≥98%), aniline (Aldrich, ≥98%), *m*-bromoaniline (Aldrich, ≥98%), *p*-bromoaniline (Aldrich, ≥98%), *p*-nitroaniline (Aldrich, ≥98%), 3,4-dichloroaniline (Aldrich, ≥98%), were used as supplied. [emim][OTf] and [emim][EtSO<sub>4</sub>] (ECOENG 212) were purchased from Solvent Innovation. [bmim][OTf] was purchased from Merck. [bmim][Tf<sub>2</sub>N], [emim][Tf<sub>2</sub>N] and [bmim][PF<sub>6</sub>] were prepared following the reported procedures;<sup>9</sup> attention was paid to the elimination of Cl<sup>-</sup> present in the solvent as impurities.



## General procedures for *N*-alkylation of aromatic amines in ionic liquids

To a solution of aromatic amine (5.5 mmol) in the ionic liquid or molecular solvent (2 ml), the required alkyl halide (5.5 mmol) was added and the mixture was stirred at the temperatures reported in Table 1 and 2 until the formation of a white solid indicated the end of the reaction. The reaction mixture was washed with aqueous NaHCO<sub>3</sub> (1 ml), extracted with *n*-hexane (6 × 2 ml) and the combined organic layers were dried over anhydrous Na<sub>2</sub>SO<sub>4</sub>. After removing the solvent under reduced pressure, the crude product mixture was analyzed by NMR. The products were identified on the basis of <sup>1</sup>H and <sup>13</sup>C NMR spectra, by comparison with the data reported in literature or with those of authentic samples.<sup>10</sup>

## Acknowledgements

Financial support for this research was provided by MIUR (PRIN 2003035403\_002) and the University of Pisa.

## References

- (a) C. Brielles, J. J. Harnett and E. Doris, *Tetrahedron Lett.*, 2001, **42**, 8301; (b) D. H. R. Barton and E. Doris, *Tetrahedron Lett.*, 1996, **37**, 3295; (c) S. Yuvaraj, V. V. Balasubramanian and M. Palanichamy, *Appl. Catal., A*, 1999, **176**, 111; (d) Y. Yoshida and Y. Tanabe, *Synthesis*, 1999, **10**, 1739; (e) S. Narayanan and K. Deshpande, *Appl. Catal., A*, 1996, **135**, 125; (f) P. S. Singh, R. Bandyopadhyay and B. S. Rao, *Appl. Catal., A*, 1996, **136**, 177; (g) M. A. Aramendia, V. Borau, C. Jimenez, J. M. Marinas and F. J. Romero, *Appl. Catal., A*, 1999, **183**, 73; (h) B. L. Su and D. Barthomeuf, *Appl. Catal., A*, 1995, **124**, 73; (i) I. I. Ivanova, E. B. Pomakhina, A. I. Rebrov, M. Hunger, Y. G. Kolyagin and J. Weitkamp, *J. Catal.*, 2001, **203**, 375; (j) K. Nishamol, K. S. Rahna and S. Sugunan, *J. Mol. Catal. A*, 2004, **209**, 89; (k) K. Okano, H. Tokuyama and T. Fukuyama, *Org. Lett.*, 2003, **5**, 4987.
- A-N. Ko, C.-L. Yang, W. Zhu and H. Lin, *Appl. Catal., A*, 1996, **134**, 53.
- M. Selva, P. Tundo and A. Perosa, *J. Org. Chem.*, 2001, **66**, 677.
- (a) R. N. Salvatore, A. S. Nagle and K. W. Jung, *J. Org. Chem.*, 2002, **67**, 674; (b) J. A. O'Meara, N. Gardee, M. Jung, R. N. Ben and T. Durst, *J. Org. Chem.*, 1998, **63**, 3177; (c) F. Valot, R. Jacquot, M. Sagnol and T. Lemaire, *Tetrahedron Lett.*, 1999, **40**, 3689.
- S. Salomaa, in *The Chemistry of Carbonyl Group*, ed. S. Patai, Wiley, New York, 1996, vol. 1, pp. 177–210.
- (a) A. K. Szardening, T. S. Burkoth, G. C. Look and D. A. Campbell, *J. Org. Chem.*, 1996, **61**, 6720; (b) T. Rische, B. Kitsos-Rzychon and P. Eibracht, *Tetrahedron Lett.*, 1998, **54**, 2723.
- Ionic Liquids in Synthesis*, ed. P. Wasserscheid and T. Welton, Wiley-VCH, New York, 2003.
- (a) C. Chiappe and D. Pieraccini, *Green Chem.*, 2003, **5**, 193; (b) L. Crowhurst, N. L. Lancaster, J. M. Pérez Aralandis and T. Welton, *J. Am. Chem. Soc.*, 2004, **126**, 11549.
- J. Fuller, R. T. Carlin, H. C. De Long and D. Haworth, *J. Chem. Soc., Chem. Commun.*, 1994, 299.
- 2a** 100-61-8; **2b** 66584-32-5; **2c** 100-15-2; **2d** 40750-59-2; **2e** 623-08-5; **2f** 6911-87-1; **3a** 121-69-7; **3b** 16518-62-0; **3c** 100-23-2; **3d** 5866-66-8; **3e** 99-97-8; **3f** 586-77-6; **4a** 103-69-5; **4b** 398151-69-4; **4c** 3665-80-3; **4d** 17847-40-4; **4e** 622-57-1; **4f** 68254-64-8; **5a** 91-66-7; **5b** 53142-19-1; **5c** 2216-15-1; **5d** 55039-58-2; **5e** 613-48-9; **5f** 2052-06-4; **6a** 1126-78-9; **6b** 581789-36-9; **6c** 58259-34-0; **6d** 28592-34-9; **6e** 10387-24-3; **6f** 81100-29-0; **7a** 613-29-6; **7e** 31144-33-9; **7f** 53358-54-6; **8a** 114320-54-6; **8c** 4138-40-3; **8d** 54405-33-3; **8e** 15258-46-5; **8f** 2274-76-1; **9a** 6247-00-3; **9b** 188745-07-5; **9c** 101130-93-2; **9d** 51937-30-5; **9e** 3480-96-4; **9f** 30438-95-0; **10a** 518329-18-5; **10b** 213814-61-0; **10c** 14309-92-3; **10d** 51597-75-2; **10e** 5405-17-4; **10f** 65145-14-4; **11a** 253684-09-2; **10b** 148491-07-0; **10c** 65052-89-3; **10d** 80576-51-8; **10e** 5459-79-0; **10f** 2879-83-6.

# Structure and activity of *Candida antarctica* lipase B in ionic liquids†

Fred van Rantwijk,<sup>a</sup> Francesco Secundo<sup>b</sup> and Roger A. Sheldon<sup>\*a</sup>

Received 14th September 2005, Accepted 8th November 2005

First published as an Advance Article on the web 1st December 2005

DOI: 10.1039/b513062j

The effects of ionic liquid media on the activity of *Candida antarctica* lipase B in a simple transesterification reaction were studied. In ionic liquids containing dicyanamide, alkylsulfate, nitrate and lactate anions, which dissolved CaLB, the reaction was at least ten times slower than in [BMIm][BF<sub>4</sub>]. Only [Et<sub>3</sub>MeN][MeSO<sub>4</sub>] was an exception, as dissolved CaLB maintained its activity in this solvent. A cross-linked enzyme aggregate of CaLB was twice as active in [BMIm][dca] as in *tert*-butyl alcohol, whereas the free enzyme was irreversibly deactivated in this latter ionic liquid.

## Introduction

The seminal work by Klibanov in the early 1980s has made it clear that many enzymes maintain their activity in hydrophobic organic solvents.<sup>1</sup> It has subsequently been found that many lipases, as well as some proteases, are so stable that they remain active even in anhydrous organic solvents. A major reason for applying lipases under such conditions is to avoid hydrolysis when performing non-hydrolytic transformations, such as the (enantioselective) acylation of alcohols and amines, which are now major industrial applications.<sup>2</sup> The minimum water requirement is enzyme-dependent and ranges from a few tightly bound water molecules per molecule of enzyme<sup>3</sup> to a nearly intact hydration shell.

The commonly used organic media—heptane, toluene, ethers, *tert*-butyl alcohol—do not seem to interact very much with enzymes; consequently, enzyme dissolution is never observed. Nonaqueous solvents that do interact with proteins strongly enough to break the intermolecular protein bonds and cause dissolution, such as, for example, DMSO and DMF, also interfere with the intramolecular bonds, resulting in unfolding and deactivation. In consequence, anhydrous biocatalysis is mainly limited to “freely” dispersed enzyme powders or carrier-supported preparations.<sup>4</sup>

The enzyme that we are particularly interested in, *Candida antarctica* lipase B (CaLB), is very stable, even compared with other lipases. CaLB is routinely used in anhydrous organic media in the presence of activated zeolite ( $a_w \sim 0.004$ ),<sup>5</sup> after preconditioning over phosphorus pentoxide.<sup>6</sup> Evidently, CaLB does not require a hydration shell to be active. This latter characteristic, as well as its quite relaxed reactant specificity and its operational stability, make CaLB a valuable synthetic tool.<sup>7</sup>

Enzymes maintain, sometimes precariously, an active conformation when dissolved in water.<sup>8</sup> A large number of

hydrogen bonds maintain this active conformation, supplemented by water networks and hydrophobic interaction. This latter effect actually results from the surface tension of water, which reduces the surface area of hydrophobic regions to a minimum.

Dehydrating enzymes causes conformational changes, as has been confirmed spectroscopically.<sup>9</sup> These can be ascribed to Coulombic interactions between charged groups, which are up to 80 times stronger in a low dielectric constant medium than in water, as well as to the loss of water networks. The combined effects usually are a general tightening of the structure. A detailed FT-IR study of CaLB showed that  $\beta$ -sheets increased at the expense of  $\alpha$ -helical contents.<sup>10,11</sup>

Lipases, as well as other enzymes, generally are much less active in organic media than in water, which is mainly, but not exclusively, due to reactant stabilisation.<sup>12</sup> This latter effect—which is equivalent with increased solubility—is translated kinetically into an increase in  $K_m$  and can be remedied by performing reactions at increased concentrations.<sup>4</sup> The remaining rate loss, one to two orders of magnitude, is ascribed to the combined effects of destabilisation of the transition state,<sup>13</sup> conformational changes and loss of flexibility.<sup>4,13</sup> Transition state destabilisation is caused by the low dielectric constant of common organic media, which increases the energy of the highly polarised transition state in comparison with water.<sup>13</sup> One reason to investigate the use of CaLB in ionic liquids is the expectation that these can be designed, on the basis of their highly polar nature, to remedy the transition state destabilisation, the conformational change caused by dehydration and the loss of flexibility.

## CaLB in ionic liquids

Many modes of biocatalysis in ionic liquids have been reported, mixed aqueous, aqueous biphasic *etc.*,<sup>14,15</sup> but here the discussion will be restricted to pure, anhydrous ionic liquids. Relevant issues when investigating the use of lipases in such media are:

- (i) To introduce novel, efficient reaction technologies, based on the unconventional properties of ionic liquids;
- (ii) Improving the—already impressive—operational stability of lipases;

<sup>a</sup>Laboratory of Biocatalysis and Organic Chemistry, Delft University of Technology, Julianalaan 136, 2628 BL, The Netherlands.

E-mail: r.a.sheldon@ttnw.tudelft.nl

<sup>b</sup>Istituto di Chimica del Riconoscimento Molecolare, CNR, Via Mario Bianco 9, Milano, Italy. E-mail: francesco.secundo@icrm.cnr.it

† This work was presented at the 1st International Conference on Ionic Liquids (COIL), held in Salzburg, Austria, 19–22 June, 2005.

(iii) Improving the biocatalyst activity by transition state stabilisation and by inducing a more active conformation.

**Dispersions in weakly coordinating ionic liquids.** Early ionic liquid-related biocatalysis research mainly involved ionic liquids composed of weakly coordinating ions, such as [BMIm][BF<sub>4</sub>] (for a list of ionic liquids see Table 3 in the Experimental section) which is water-miscible, and [BMIm][PF<sub>6</sub>] and [BMIm][NTf<sub>2</sub>], which are not. It was generally found that CaLB, as well as many other enzymes, maintained their activity when dispersed in such ionic liquids;<sup>14</sup> dissolution was generally not observed (but see later). CaLB catalysed a number of non-natural reactions in anhydrous ionic liquids of these latter types, such as transesterification, ammoniolytic, perhydrolysis, acylation of carbohydrates and enantioselective acylation of chiral alcohols.<sup>14</sup> The reaction rates were comparable with, or slightly better than those observed in conventional solvents, such as *tert*-butyl alcohol or diisopropyl ether, although the enantioselectivity of chiral alcohols improved in a number of cases.<sup>16</sup>

Evidence that CaLB, as well as some other hydrolases, are more thermally and operationally stable in some ionic liquids than in common solvents had been accumulating for some years<sup>14,17</sup> and recently has been supported by fluorescence and CD spectroscopy.<sup>18</sup>

Ionic liquids do not mix with supercritical CO<sub>2</sub>, in contrast with conventional organic solvents. On this basis, reaction methodologies have been developed that encompass an ionic liquid working phase, which contains a lipase dispersion, and a supercritical CO<sub>2</sub> extractive phase.<sup>19,20</sup> Methodologies like these, that do not involve volatile organic solvents at all, are a portent of the revolution in reaction technology that ionic liquids may bring about.

### Dissolution of CaLB

So far, we have discussed ionic liquid dispersions of CaLB but such weakly-interacting media cannot be expected to repair the defects of conventional organic media. This latter objective requires ionic liquids that interact with proteins in a water-like way and, hence, dissolve them, which mainly depends on the H-bond accepting properties of the anion.<sup>21</sup>

CaLB indeed dissolved in [BMIm] acetate, lactate and nitrate, which are better H-bond acceptors and are also environmentally more acceptable than the fluorinated anions, but the resulting solutions were only minutely active in a simple transesterification test reaction (see Fig. 1 and Table 1).<sup>11</sup> The activity loss was partially reversible as 33–73% of the original hydrolytic activity was recovered from the supernatant upon rehydration. Experiments with the remarkable ionic liquid [BMIM][dca],<sup>22,23</sup> which dissolves carbohydrates in hundreds of g L<sup>-1</sup> quantities<sup>24</sup> fell into a

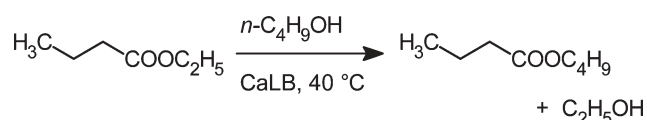


**Fig. 1** Transesterification of ethyl butanoate with 1-butanol.

**Table 1** *C. antarctica* lipase B in ionic liquids: activity in the transesterification of ethyl butanoate, solubility and activity recovery upon rehydration<sup>a</sup>

Medium	Conversion (%; 24 h)	Dissolution	Recovery from the supernatant <sup>b</sup> (%)
<i>tert</i> -Butyl alcohol	74	no	0
[BMIm][BF <sub>4</sub> ]	78	no	0
[BMIm][PF <sub>6</sub> ]	71	no	0
[BMIm][lactate]	5	yes	42
[BMIm][NO <sub>3</sub> ]	3	yes	73
[Et <sub>3</sub> MeN][MeSO <sub>4</sub> ]	26	see text	n.d.

<sup>a</sup> Reaction conditions: ethyl butanoate (60 mM), 1-butanol (120 mM), Novozym 435 (15 mg) in solvent (0.5 mL) at 40 °C for 24 h. <sup>b</sup> Hydrolytic activity (triacetin) recovered from the supernatant after 24 h incubation at 40 °C, followed by rehydration; original activity = 100%.

similar pattern as CaLB dissolved with irreversible loss of activity. Remarkably, some transesterification activity was maintained when CaLB was added to a saturated solution of sucrose in [BMIm][dca].<sup>25</sup> The obvious conclusion so far is that enzyme activity and solubility in ionic liquids are anion dependent<sup>26</sup> and mutually exclusive.

The behaviour of CaLB in [Et<sub>3</sub>MeN][MeSO<sub>4</sub>] did not correspond with the simple pattern set out above, as a modest transesterification activity was maintained, even with small amounts of enzyme which were observed to dissolve (see Table 2). To confirm this latter observation, a reaction was performed with a presaturated solution of CaLB in [Et<sub>3</sub>MeN][MeSO<sub>4</sub>]. On the basis of the conversion (Table 2), it would seem that [Et<sub>3</sub>MeN][MeSO<sub>4</sub>] dissolves approx. 3 mg mL<sup>-1</sup> of CaLB.

This latter result with [Et<sub>3</sub>MeN][MeSO<sub>4</sub>] strongly indicates that the case solubility vs. activity is by no means closed. We note, in support, that the redox enzyme morphine dehydrogenase stays active upon dissolution in the hydroxylated ionic liquid 1-(3-hydroxypropyl)-3-methylimidazolium glycolate.<sup>27</sup>

**FT-IR spectroscopy.** To support the notion that hydrophilic ionic liquids induce conformational changes that result in the deactivation of CaLB, we measured the FT-IR spectra in the amide I region (see Fig. 2). Here, it can be observed that the protein shows a similar patterns of bands in [Et<sub>3</sub>MeN][MeSO<sub>4</sub>] and in aqueous solution. In particular it is important to note the presence in both media of the bands at around 1649 and 1656 cm<sup>-1</sup>, typically assigned to  $\alpha$ -helix structural elements, and at 1660 and 1667 cm<sup>-1</sup>, which might be assigned to  $\beta$ -turns.<sup>11</sup> This similarity strongly suggests that CaLB

**Table 2** Transesterification of ethyl butanoate with CaLB in [Et<sub>3</sub>MeN][MeSO<sub>4</sub>]<sup>a</sup>

Solvent	SP525/mg mL <sup>-1</sup> , conversion in %				
	1.2	3	6	20	Supernatant <sup>b</sup>
[Et <sub>3</sub> MeN][MeSO <sub>4</sub> ]	14 <sup>c</sup>	19	46	54	25
<i>tert</i> -Butyl alcohol	18	46	63	68	0

<sup>a</sup> Reaction conditions: see Table 1. <sup>b</sup> SP525 (20 mg mL<sup>-1</sup>) was incubated in ionic liquid for 24 h at 40 °C and centrifuged; the transesterification was carried out in the supernatant. <sup>c</sup> All enzyme dissolved.

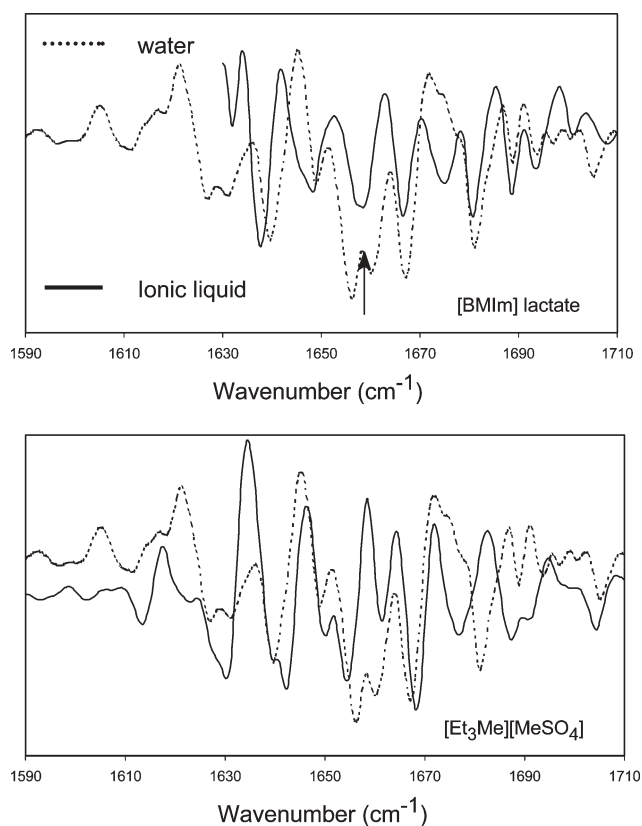


**Fig. 2** Second-derivative FT-IR spectra of CaLB dissolved in [BMIM][lactate] and [Et<sub>3</sub>MeN][MeSO<sub>4</sub>].<sup>11</sup>

preserves the native secondary structure in the ionic liquid. On the contrary, the spectrum in [BMIM][lactate] shows, in comparison with the spectrum in water, a merging of the peaks at 1656 and 1660 cm<sup>-1</sup> into one peak at 1658 cm<sup>-1</sup>, which indicates a loss of  $\alpha$ -helix and  $\beta$ -turn contents.

#### Cross-linked enzyme aggregates in a denaturing ionic liquid.

Stabilisation of CaLB as a cross-linked enzyme aggregate (CLEA) makes it possible to reap the potential benefits of denaturing ionic liquids while avoiding activity loss. CLEAs are easily prepared by treatment of an aqueous enzyme solution with a suitable precipitant—an organic solvent or a salt—followed by crosslinking of the precipitated enzyme aggregates.<sup>28</sup> We explored the use of various types of CaLB CLEAs in the ionic liquid [BMIM][dca], again using the transesterification test reaction. The outcome depended on the nature of the CLEA and one CLEA was twice as active in [BMIM][dca] as in *tert*-butyl alcohol (Fig. 3).<sup>29</sup>

We reasoned that a small amount of water could possibly influence the bulk properties of the ionic liquid in a beneficial way while being chemically inactive because ionic liquids often bind some water, equivalent with a hemihydrate,<sup>30</sup> quite tightly. We accordingly performed a transesterification experiment in [BMIM][dca] hemihydrate; extensive hydrolysis took place, however, without any gain in transesterification rate. Hence, the rule that non-hydrolytic reactions in the presence of lipase require an anhydrous environment also holds for hydrophilic ionic liquids.

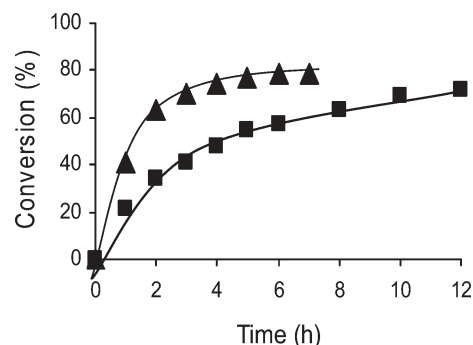


**Fig. 3** Transesterification of ethyl butyrate with butanol in the presence of a CaLB CLEA in [BMIM][dca] (▲) and *tert*-butyl alcohol (■). Reaction conditions: ethyl butanoate (40 mM), 1-butanol (200 mM), CaLB CLEA (1 mg) in solvent (1.0 mL) at 40 °C.

**Ionic liquids, hydrogen bonds and activity.** Hydrogen bonds, such as shown in Fig. 4a, cement the structure of hydrated as well as dehydrated enzymes. Any structural change requires a considerable number of hydrogen bonds to dissociate at the same time, which may contribute significantly to enzyme stability and could also explain hydration-memory and hysteresis effects.<sup>4</sup>

Hydrogen bonding could also be the key to understanding the interactions of proteins and ionic liquids. Ionic liquids, in particular anions, that form strong hydrogen bonds may dissociate the hydrogen bonds that maintain the structural integrity of the  $\alpha$ -helices and  $\beta$ -sheets, causing the protein to unfold wholly or partially. The lactate ion, for example, could easily form stable hydrogen bonds with the polypeptide backbone (see Fig. 4b). Ion size could matter, because sterically demanding ions would require many hydrogen bonds to be broken to create a few new ones, which could contribute to maintaining stability.

We have already noted that deactivation of CaLB by [BMIM] nitrate and lactate, as well some other ionic liquids, is partially reversible.<sup>11</sup> This finding is in agreement with the generally adopted kinetic model of enzyme deactivation, which involves a reversible first step and an irreversible second one. Deactivation by [BMIM][dca], in contrast, was irreversible and a small angle neutron scattering experiment indicated the formation of aggregates,<sup>31</sup> as is often observed upon unfolding. Presumably, hydrogen bonds also maintain the conformation of reversibly deactivated enzymes. Reconstitution requires these hydrogen bonds to be dissociated and remade into the native ones. Dilute denaturants

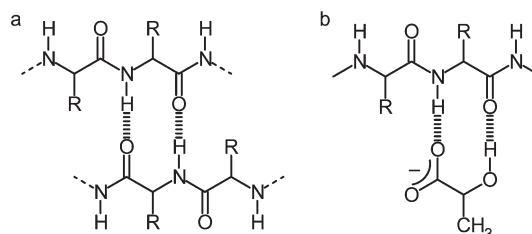


**Fig. 4** a: Schematic representation of hydrogen bonding in a  $\beta$ -sheet; b: putative hydrogen bonds between a peptide chain and a lactate ion.

often facilitate reconstitution, which includes the ionic liquid  $[\text{EtNH}_3][\text{NO}_3]$ .<sup>32,33</sup> Presumably, such strongly hydrogen-bonding compounds facilitate the reconstitution by forming transient hydrogen bonds.

## Conclusion

A solution of CaLB in the ionic liquid  $[\text{Et}_3\text{MeN}][\text{MeSO}_4]$  is catalytically competent, in contrast with solutions in similar ionic liquids.

CLEAs of CaLB stay active in ionic liquids that denature the native enzyme. Hence, there are prospects for combining the potential benefits of strongly interacting ionic liquids with the stability of CLEAs.

## Experimental

### Materials

Novozym 435 (immobilised *Candida antarctica* lipase B), SP525 (free *Candida antarctica* lipase B) and purified CaLB lyophilisate were kindly donated by Novozymes (Bagsvaerd, Denmark). Cross-linked enzyme aggregates of *Candida antarctica* lipase B were received from CLEA Technologies (Delft, The Netherlands) as a gift. The ionic liquid  $[\text{BMIm}][\text{lactate}]$  was kindly donated by Prof. K. R. Seddon (Queen's University of Belfast).  $[\text{BMIm}][\text{BF}_4]$  and  $[\text{BMIm}][\text{PF}_6]$ ,<sup>34</sup>  $[\text{BMIm}][\text{NO}_3]$ ,<sup>35</sup>  $[\text{Et}_3\text{NMe}][\text{MeSO}_4]$ <sup>36</sup> were synthesised according to published procedures<sup>11</sup> and checked for the absence of chloride and acid.<sup>37</sup> Structural details of the ionic liquids used are listed in Table 3. All other compounds were purchased from ACROS.

### Analytical methods

FT-IR measurements were carried out as described.<sup>11</sup>

The transesterification of ethyl butyrate was monitored by HPLC on a Waters custom-packed  $8 \times 100$  mm  $5 \mu\text{m}$  Symmetry  $\text{C}_{18}$  column; eluent 65 : 35 (v/v) MeOH-aqueous 0.05 M acetate buffer pH 4.5 at  $1.0 \text{ mL min}^{-1}$  with refractive index detection (Shodex SE-51 RI).

### Transesterification of ethyl butyrate with butanol

The transesterification of ethyl butyrate (0.06 M) with *n*-butanol (0.12 M) was carried out in 0.5 mL of ionic liquid

**Table 3** Structures of ionic liquids

Abbreviation	Type R	X <sup>-</sup>
$[\text{BMIm}][\text{BF}_4]$	<b>1</b> <i>n</i> -C <sub>4</sub> H <sub>9</sub>	BF <sub>4</sub> <sup>-</sup>
$[\text{BMIm}][\text{PF}_6]$	<b>1</b> <i>n</i> -C <sub>4</sub> H <sub>9</sub>	PF <sub>6</sub> <sup>-</sup>
$[\text{BMIm}][\text{NO}_3]$	<b>1</b> <i>n</i> -C <sub>4</sub> H <sub>9</sub>	NO <sub>3</sub> <sup>-</sup>
$[\text{BMIm}][\text{lactate}]$	<b>1</b> <i>n</i> -C <sub>4</sub> H <sub>9</sub>	CH <sub>3</sub> CH(OH)COO <sup>-</sup>
$[\text{Et}_3\text{MeN}][\text{MeSO}_4]$	<b>2</b> CH <sub>3</sub> C <sub>2</sub> H <sub>5</sub> C <sub>2</sub> H <sub>5</sub> C <sub>2</sub> H <sub>5</sub>	CH <sub>3</sub> OSO <sub>3</sub> <sup>-</sup>

as the solvent. Novozym 435 (15 mg) and 1,3-dimethoxybenzene (internal standard, 0.06 M) were added and the reaction was carried out at 40 °C. The reactions were monitored for 24 h by taking 50  $\mu\text{L}$  samples that were diluted with 100  $\mu\text{L}$  of HPLC eluent.

**Solubility of CaLB.** SP525 (15 mg) was added to 500  $\mu\text{L}$  of ionic liquid and was incubated for 24 h at 40 °C. The supernatant was separated from the solid enzyme by filtration followed by centrifugation. The lipase activity in the supernatant was measured in the hydrolysis of triacetin.

### Activity test of CaLB

A 0.2 mL sample of ionic liquid supernatant was diluted with 10 mL of 0.1 M sodium phosphate buffer pH 7.5. Triacetin (0.1 M) was added and the reaction was monitored by titration with 0.12 M KOH.

## Acknowledgements

Gifts of ionic liquids by Prof. K. R. Seddon are gratefully acknowledged. The authors wish to thank Novozymes for gifts of Novozym 435 and SP525, as well as a purified sample of *C. antarctica* lipase B. Thanks are due to CLEA Technologies for kind donations of CaLB CLEAs.

## References

- A. Zaks and A. M. Klivanov, *Proc. Natl. Acad. Sci. U. S. A.*, 1983, **82**, 3196–3392; A. M. Klivanov, *CHEMTECH*, 1986, **16**, 354–359.
- A. Schmidt, J. S. Dordick, B. Hauer, A. Kiener, M. Wubbolts and B. Witholt, *Nature*, 2001, **409**, 258–268.
- M. Dolman, P. J. Halling, B. D. Moore and S. Waldron, *Biopolymers*, 1996, **41**, 313–321.
- P. J. Halling, *Philos. Trans. R. Soc. London, Ser. B*, 2004, **359**, 1287–1297.
- For a description of the use of water activity see: P. J. Halling, *Enzyme Microb. Technol.*, 1994, **16**, 178–206.
- A. T. J. W. de Goede, W. Benckhuijsen, F. van Rantwijk, L. Maat and H. van Bekkum, *Recl. Trav. Chim. Pays-Bas*, 1993, **112**, 567–572.
- E. M. Anderson, M. Karin and O. Kirk, *Biocatal. Biotransform.*, 1998, **16**, 181–204.
- The free energy of stabilisation is on average only  $45 \pm 15 \text{ kJ mol}^{-1}$ , see: R. Jaenicke, *Naturwissenschaften*, 1996, **83**, 544–554.
- U. R. Desai and A. M. Klivanov, *J. Am. Chem. Soc.*, 1995, **117**, 3940–3945.
- G. Vecchio, F. Zambianchi, P. Zacchetti, F. Secundo and G. Carrea, *Biotechnol. Bioeng.*, 1999, **64**, 545–551.
- R. Madeira Lau, M. J. Sorgedragar, G. Carrea, F. van Rantwijk, F. Secundo and R. A. Sheldon, *Green Chem.*, 2004, **6**, 483–487.
- A. M. Klivanov, *Trends Biotechnol.*, 1997, **15**, 97–101.
- D. S. Clark, *Philos. Trans. R. Soc. London, Ser. B*, 2004, **359**, 1299–1307.
- F. van Rantwijk, R. Madeira Lau and R. A. Sheldon, *Trends Biotechnol.*, 2003, **21**, 131–138.
- Z. Yang and W. Pan, *Enzyme Microb. Technol.*, 2005, **37**, 19–28.
- K.-W. Kim, B. Song, M.-Y. Choi and M.-J. Kim, *Org. Lett.*, 2001, **3**, 1507–1509.
- P. Lozano, T. de Diego, S. Gmouh, M. Vaultier and J. L. Iborra, *Biotechnol. Prog.*, 2004, **20**, 661–669.
- T. de Diego, P. Lozano, S. Gmouh, M. Vaultier and J. L. Iborra, *Biomacromolecules*, 2005, **6**, 1457–1464.
- P. Lozano, T. de Diego, D. Carrié, M. Vaultier and J. L. Iborra, *Chem. Commun.*, 2002, 692–693.
- M. T. Reetz, W. Wiesenhöfer, G. Franciò and W. Leitner, *Adv. Synth. Catal.*, 2003, **345**, 1221–1228.

- 21 J. L. Anderson, J. Ding, T. Welton and D. W. Armstrong, *J. Am. Chem. Soc.*, 2002, **124**, 14247–14254.
- 22 D. R. MacFarlane, J. Golding, S. Forsyth, M. Forsyth and G. B. Deacon, *Chem. Commun.*, 2001, 1430–1431.
- 23 Q. Liu, M. H. A. Janssen, F. van Rantwijk and R. A. Sheldon, *Green Chem.*, 2005, **7**, 39–42.
- 24 S. A. Forsyth and D. R. MacFarlane, *J. Mater. Chem.*, 2003, **13**, 2451–2456.
- 25 M. H. A. Janssen, F. van Rantwijk and R. A. Sheldon, paper in preparation.
- 26 J. L. Kaar, A. M. Jesionowski, J. A. Berberich, R. Moulton and A. J. Russell, *J. Am. Chem. Soc.*, 2003, **125**, 4125–4131.
- 27 A. J. Walker and N. C. Bruce, *Tetrahedron*, 2004, **60**, 561–568.
- 28 L. Cao, F. van Rantwijk and R. A. Sheldon, *Org. Lett.*, 2000, **2**, 1361–1364; P. López-Serrano, L. Cao, F. van Rantwijk and R. A. Sheldon, *Biotechnol. Lett.*, 2002, **24**, 1379–1383; R. Schoevaart, M. W. Wolbers, M. Golubovic, M. Ottens, A. P. G. Kieboom, F. van Rantwijk, L. A. M. van der Wielen and R. A. Sheldon, *Biotechnol. Bioeng.*, 2004, **87**, 754–762.
- 29 A. Ruiz Toral, F. van Rantwijk and R. A. Sheldon, paper in preparation.
- 30 L. Cammarata, S. G. Kazarian, P. A. Salter and T. Welton, *Phys. Chem. Chem. Phys.*, 2001, **3**, 5192–5200.
- 31 D. Sate, M. H. A. Janssen, R. A. Sheldon and J. Lu, paper in preparation.
- 32 D. K. Magnuson, J. W. Bodley and D. Fennell Evans, *J. Solution Chem.*, 1984, **13**, 583–587.
- 33 C. A. Summers and R. A. Flowers II, *Protein Sci.*, 2000, **9**, 1992–2008.
- 34 S. G. Cull, J. D. Holbrey, V. Vargas-Mora, K. R. Seddon and G. J. Lye, *Biotechnol. Bioeng.*, 2000, **69**, 227–233.
- 35 J. S. Wilkes and M. J. Zaworotko, *J. Chem. Soc., Chem. Commun.*, 1992, 965–967.
- 36 J. D. Holbrey, W. M. Reichert, R. P. Swatloski, G. A. Broker, W. R. Pitner, K. R. Seddon and R. D. Rogers, *Green Chem.*, 2002, **4**, 407–413.
- 37 K. R. Seddon, A. Stark and M.-J. Torres, *Pure Appl. Chem.*, 2000, **72**, 2275–2287.

# Chemical Science

An exciting news supplement providing a snapshot of the latest developments across the chemical sciences



Free online and in print issues of selected RSC journals!\*

**Research Highlights** – newsworthy articles and significant scientific advances

**Essential Elements** – latest developments from RSC publications

**Free access** to the original research paper from every online article

\*A separately issued print subscription is also available

RSC Publishing

[www.rsc.org/chemicalscience](http://www.rsc.org/chemicalscience)

# Solubility of carbon dioxide in systems with [bmim][BF<sub>4</sub>] and some selected organic compounds of interest for the pharmaceutical industry†

Eliane Kühne,<sup>a</sup> Cor J. Peters,<sup>\*a</sup> Jaap van Spronsen<sup>b</sup> and Geert-Jan Witkamp<sup>b</sup>

Received 15th September 2005, Accepted 6th December 2005

First published as an Advance Article on the web 20th January 2006

DOI: 10.1039/b513132d

This work presents phase equilibrium data of the ternary system CO<sub>2</sub> + [bmim][BF<sub>4</sub>] + solute. Three different organic compounds were studied as the solute in the ternary system: 1-methyl-3-phenylpiperazine (MPhPz), 2-chloro-nicotinonitrile (NtN) and 2-(4-methyl-2-phenyl-1-piperazinyl)-3-pyridinecarbonitrile (PCN). Experiments were carried out in a pressure and temperature range of 1–14 MPa and 343.15–443.15 K, respectively. Samples were prepared with CO<sub>2</sub> molar fractions of 0.10 until 0.40 for the system with NtN as the solute, and 0.20 for the other two systems for comparison. The data collected show how the various solutes affect the phase behavior of the binary system CO<sub>2</sub> + [bmim][BF<sub>4</sub>], and at which conditions homogeneous phase can be obtained.

## Introduction

Pharmaceutical companies are facing nowadays a hard challenge: how to achieve more environmentally benign and sustainable technology. Since the reduction of volatile organic solvents (VOS's) used in their processes is one of the most important issues, ionic liquids are a very interesting, promising and effective way in achieving this goal.

This fact can be proven by the increasing attention that the use of ionic liquids as a reaction medium, sometimes even acting simultaneously as solvent and catalyst, has received in the last couple of years.<sup>1–6</sup> Their insignificant vapor pressure and the fact that they can be designed according to a specific use make ionic liquids great candidates for green chemistry.<sup>1</sup> When associated with supercritical fluids in reaction–extraction processes, the new clean processes can ensure similar or higher efficiencies than the currently used ones, with the advantage of less hazardous substances involved as well as less loss of solvents and catalyst leaching.

The use of ionic liquids in combination with supercritical fluids has unlimited advantages. For instance, ionic liquids themselves can be used in membranes for separation of gases, as it was successfully demonstrated by Scovazzo *et al.*<sup>7</sup> Therefore, solubility of different gasses in ionic liquids is also an important issue. Recently published articles reflect this need for having knowledge on the solubility of various gases in ionic liquids, either by experiments or by prediction from models.<sup>8–12</sup> When working with reactions involving gasses as reactants, a higher solubility of the gas in the reaction medium promotes higher yields. However, gasses do not play a key role in syntheses only as reactants, but they can also be used to

manipulate the phase behavior of the system, improving reaction rates.

It is already known that supercritical (sc) carbon dioxide can be applied for phase separation of organic solvents or water from the ionic liquid, as well as extraction of organic compounds from the liquid phase.<sup>13–15</sup> It is also proved that carbon dioxide is highly soluble in ionic liquids, and that no significant traces of ionic liquids can be found in CO<sub>2</sub>.<sup>14</sup> It means that, when scCO<sub>2</sub> is used to extract products from an ionic liquid medium, the desired product will be free from solvent contamination. The product can be recovered from the supercritical phase by simply decreasing the pressure, and depending on the solubility of reactants and catalysts in scCO<sub>2</sub>, no further purification is necessary. The ionic liquid, together with the catalyst, can be then recycled and reused for another few batches.<sup>6</sup>

The feasibility of such a process was already studied, for instance, in extraction of organic products from [bmim][PF<sub>6</sub>].<sup>13</sup> One must be aware, however, that the main advantage of using ionic liquids in combination with scCO<sub>2</sub> for extractions (it means, negligible solubility of ionic liquids in the supercritical phase) can be influenced by dissolved polar compounds which may act as cosolvents, increasing the solubility of the ionic liquid in the supercritical phase.<sup>16,17</sup> Thus, previous studies about solubility of the components involved and ionic liquid in scCO<sub>2</sub> are always necessary for extraction processes, including the effects of the interaction of those components in the system.

The number of publications on phase behavior in systems containing ionic liquid, organic compounds and/or scCO<sub>2</sub> indicates the importance of this study.<sup>18–23</sup> For instance, our group has been measuring the phase behavior at high pressures of systems composed of imidazolium-based ionic liquids (mainly with [BF<sub>4</sub>]<sup>−</sup> and [PF<sub>6</sub>]<sup>−</sup> anions) and supercritical carbon dioxide.<sup>18–20</sup>

Recently, the existence of homogeneous one-phase regions in the multiple fluid phase behavior of mixtures of ionic liquids and organic solvents has been identified.<sup>22</sup> This is a proof of the miscibility switch phenomena, in which phase behavior of

<sup>a</sup>Laboratory of Physical Chemistry and Molecular Thermodynamics, Faculty of Applied Sciences, Delft University of Technology, Julianalaan 136, 2628 BL, Delft, The Netherlands. E-mail: cor.peters@tnw.tudelft.nl

<sup>b</sup>Laboratory for Process Equipment, Faculty of Mechanical, Maritime and Materials Engineering, Delft University of Technology, Leeghwaterstraat 44, 2628 CA, Delft, The Netherlands

† This work was presented at the 1st International Conference on Ionic Liquids (COIL), held in Salzburg, Austria, 19–22 June, 2005.

the system is advantageously used to split phases and separate components in a mixture.<sup>14–15,24–25</sup>

Therefore, the phase behavior of the system is of great importance. Understanding when homogeneous conditions are achieved, as well as how each one of the compounds involved affect the phase equilibrium, will maximize the efficiency of the reaction and provide a cleaner, environmentally friendly and economically attractive production process. At the same time, splitting phases is a powerful tool to improve extraction of compounds from ionic liquids.

This study aims at understanding how the addition of a solute in the system [bmim][BF<sub>4</sub>]-CO<sub>2</sub> will affect its phase behavior. Three organic compounds, represented in Fig. 1, were used as solute: 2-chloro-nicotinonitrile (NtN), 1-methyl-3-phenylpiperazine (MPhPz) and 2-(4-methyl-2-phenyl-1-piperazinyl)-3-pyridinecarbonitrile (PCN). The measured bubble points determine the solubility of CO<sub>2</sub> in the ternary system. Measurements were performed at temperatures ranging from 343.15 to 443.15 K. In order to compare the phase behavior for systems with and without solute, data obtained previously by Shariati *et al.* are also used.<sup>20</sup>

## Experimental

**Ionic liquid.** [bmim][BF<sub>4</sub>] used in this study was synthesized using our facilities.<sup>26</sup> After keeping the ionic liquid in a drying oven at 80 °C under vacuum for 5 days, water content was measured by Karl-Fischer analysis as 150 ppm. The ionic liquid was stored under vacuum conditions, ensuring the content of water did not increase.

**Carbon dioxide.** Carbon dioxide was supplied by HoekLoos B.V., with 99.995% purity.

**Solutes.** The three solutes used in this work were provided by Organon Nederland bv.

## Methodology

Bubble point measurements were carried out in a Cailletet apparatus. In this apparatus, the temperature is kept constant, and by varying the pressure applied on the sample, the disappearance of the last tiny bubble present is observed visually. The maximum pressure and temperature that can be reached in this apparatus is 14.0 MPa and 573.15 K, respectively. Dow Corning 550 Silicon Oil was used as heating medium for the sample.

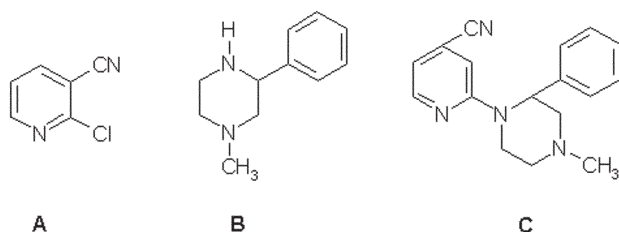


**Fig. 1** The three compounds studied in this work. A = NtN; B = MPhPz; C = PCN.

In this apparatus, the sample with known composition is confined in a thick-walled Pyrex glass tube, which is placed inside a glass jacket. The tube is closed at one end, and mercury is used as a sealing and pressure transmitting liquid between the sample and the oil in the high-pressure equipment. The pressure is measured with a dead-weight gauge with an accuracy of 0.05 bar (0.005 MPa).

A scheme of the Cailletet apparatus is presented in Fig. 2. More detailed information can be found elsewhere.<sup>27,28</sup>

The samples were prepared by inserting with a micro-syringe a known, weighted amount of the ionic liquid into the Cailletet tube. The [bmim][BF<sub>4</sub>] was kept in a desiccator under vacuum conditions, ensuring that a minimum amount of water would be present. The solute was then added to the tube in a fixed amount of 17.6 mg of solute per ml of [bmim][BF<sub>4</sub>], in the form of pellets which were weighted until the desired amount was obtained.

The sample with both components was then degassed, and carbon dioxide was added volumetrically according to the desired molar fraction. The ternary system was then ready to be inserted into the Cailletet apparatus, and data were collected.

## Results and discussions

For the measurements of CO<sub>2</sub> solubility in a range of concentrations, NtN (see Fig. 1) was chosen as solute in the ternary system [bmim][BF<sub>4</sub>] + CO<sub>2</sub> + solute. This choice was based on the fact that MPhPz has an amine group, and it is known that primary and secondary amines can interact with carbon dioxide forming carbamates.<sup>29–33</sup> This reaction, although reversible, could cause some inaccuracy in our data.

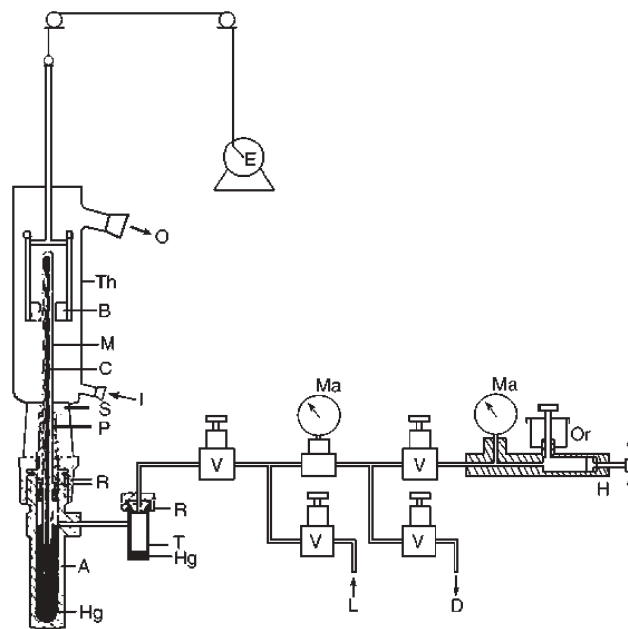


**Fig. 2** The Cailletet apparatus; A, autoclave; B, magnets; C, capillary glass tube; D, drain; E, motor; H, rotating hand pump; Hg, mercury; I, thermostat liquid in; L, line to dead weight pressure gauge; M, mixture being investigated; Ma, manometers; O, thermostat liquid out; Or, hydraulic oil reservoir; P, closing plug; R, Viton-O-rings; S, silicone rubber stopper; T, mercury trap; Th, glass thermostat; V, valve.



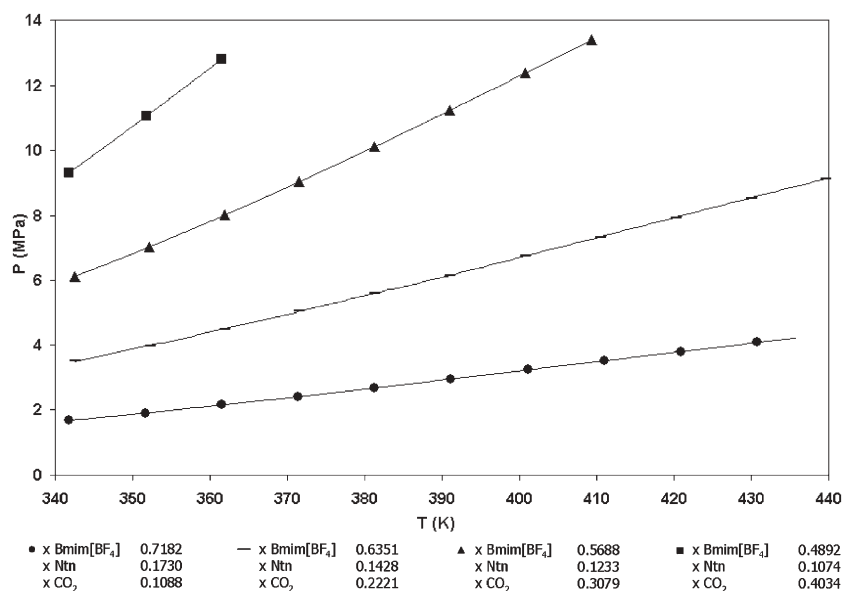


Fig. 3 Pressure *versus* temperature diagram for NtN, representing the bubble points for different compositions of CO<sub>2</sub>. Legend: molar fractions of each component in the ternary system.

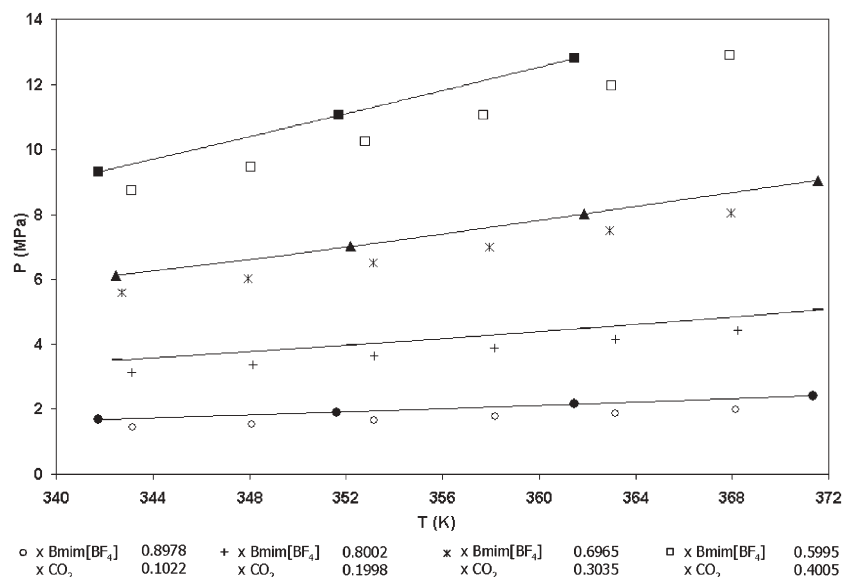


Fig. 4 Effect of the addition of NtN to the system [bmim][BF<sub>4</sub>] + CO<sub>2</sub>, for different compositions of the gas. Legend: molar fractions of each component in the binary system. For the ternary system, please refer to Fig. 3.

Therefore, four samples were prepared with CO<sub>2</sub> molar fractions of 10, 20, 30 and 40%, and the concentration of NtN in [bmim][BF<sub>4</sub>] was kept at a constant value of 17.65 mg ml<sup>-1</sup>. The results are shown in Fig. 3.

Although NtN is not completely soluble in [bmim][BF<sub>4</sub>] at the concentration we intended to work with, carbon dioxide acted as a co-solvent for this compound. Initially our system was biphasic, with a liquid phase rich in ionic liquid and the solute, and one vapor phase rich in CO<sub>2</sub>. At constant temperature, an increase in pressure resulted in an increase of CO<sub>2</sub> solubility in the liquid phase. This process was continued until the last bubble disappeared (the so-called bubble point). In this case, an homogeneous liquid phase was obtained. For each

composition of carbon dioxide, the homogeneous phase is located in the *P versus T* diagram as the region above the corresponding equilibrium curve in Fig. 3.

In order to establish the effect of the solute on the solubility of CO<sub>2</sub>, a comparison chart between our data and data for the binary system *bmim*[BF<sub>4</sub>] + CO<sub>2</sub> measured by Shariati *et al.*<sup>20</sup> is presented in Fig. 4.‡

‡ Although a comparison is made with data measured for binary systems with [bmim][BF<sub>4</sub>], it is worth mentioning that the water content was different for both samples (300 ppm for Shariati *et al.* and 150 ppm in our ionic liquid). Impurities were, most probably, also distinct. Therefore, deviation between both series of measurements could be expected.

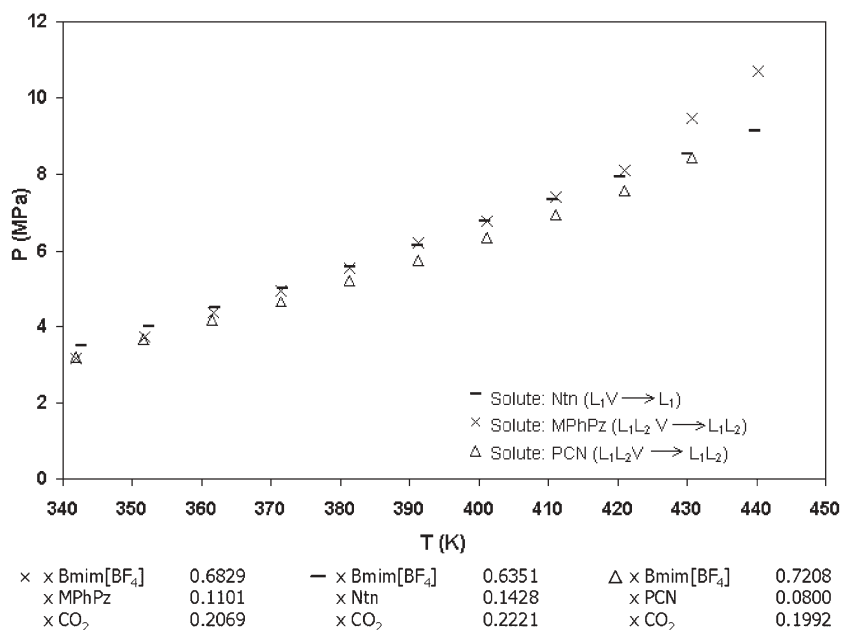


**Fig. 5** Comparison of the effect on the phase behavior for the three different organic compounds on the system  $\text{bmim}[\text{BF}_4] + \text{CO}_2$  (approximately 20 mol%  $\text{CO}_2$ ). Compositions of samples in the legend are in molar fraction.

From Fig. 4 one can see that addition of NtN to the binary system  $[\text{bmim}][\text{BF}_4] + \text{CO}_2$  causes an increase of pressure needed for complete solubility of the gas in the ionic liquid. This observation is an important feature that must be taken into account when working with reactions in an homogeneous phase, for instance. Additionally, for the same amount of solute, this effect is less pronounced for lower  $\text{CO}_2$  compositions in the ternary system.

The next step was to study how each one of the molecules may influence the phase behavior. Fig. 5 shows a comparison of the pressure needed to dissolve 20 mol%  $\text{CO}_2$  in the ternary system for the three different solutes studied.

As can be seen in Fig. 5, the most significant influence of the solutes on the original binary mixture is the nature of the phase transitions that occur. Only the solute NtN gives a phase transition  $\text{LV} \rightarrow \text{L}$ , whereas both MPhPz and PCN give a phase transition  $\text{L}_1\text{L}_2\text{V} \rightarrow \text{L}_1\text{L}_2$  at pressures below 10 MPa, *i.e.* both solutes show liquid–liquid immiscibility in the investigated experimental region, which is not the case for solute NtN.

An interesting feature is that the pressure needed for complete disappearance of the vapor phase remains practically the same in all three cases. The influence of the different molecules studied in this work on the solubility of carbon dioxide in the system is not very pronounced for lower temperatures, although for temperatures above 420 K this effect becomes more apparent. In this case, MPhPz has a large deviation from the pressures measured for PCN and NtN as solute.

## Conclusions

In this work we demonstrated that the addition of an organic compound to the binary system  $[\text{bmim}][\text{BF}_4] + \text{scCO}_2$  can cause significant changes in its phase behavior. At the same temperature, pressure and composition, the ternary system with NtN shows a normal vapor–liquid transition  $\text{LV} \rightarrow \text{L}$ ,

whereas both solutes MPhPz and PCN show liquid–liquid immiscibility leading to the presence of the phase transformation  $\text{L}_1\text{L}_2\text{V} \rightarrow \text{L}_1\text{L}_2$ . Obviously, this is an important issue for reactions and separations, since for the reaction step an inhomogeneous two-phase system is undesirable, while for separations this may be advantageous to perform the extraction of a specific compound.

## Acknowledgements

We would like to thank Organon Nederland B.V. for supplying the three organic chemicals used in this work.

## References

- P. Wasserscheid and W. Keim, *Angew. Chem., Int. Ed.*, 2000, **39**, 21, 3772–3789.
- H. Olivier-Bourbigou and L. Magna, *J. Mol. Catal. A: Chem.*, 2002, **182–183**, 419–437.
- R. Sheldon, *Chem. Commun.*, 2001, 2399–2407.
- E. Mizushima, T. Hayashi and M. Tanaka, *Green Chem.*, 2001, **3**, 2, 76–79.
- H.-P. Nguyen, H. Matondo and M. Baboulène, *Green Chem.*, 2003, **5**, 3, 303–305.
- J. Peng and Y. Deng, *New J. Chem.*, 2001, **25**, 4, 639–641.
- P. Scovazzo, J. Kieft, D. A. Finan, C. Koval, D. DuBois and R. Noble, *J. Membr. Sci.*, 2004, **238**, 57–63.
- P. Scovazzo, D. Camper, J. Kieft, J. Poshusta, C. Koval and R. Noble, *Ind. Eng. Chem. Res.*, 2004, **43**, 21, 6855–6860.
- Y. S. Kim, W. Y. Choi, J. H. Jang, K.-P. Yoo and C. S. Lee, *Fluid Phase Equilib.*, 2005, **228–229**, 439–445.
- J. Kumelan, A. Perez-Salado Kamps, D. Tuma and G. Maurer, *Fluid Phase Equilib.*, 2005, **228–229**, 207–211.
- C. Cadena, J. L. Anthony, J. K. Shah, T. I. Morrow, J. F. Brennecke and E. J. Maginn, *J. Am. Chem. Soc.*, 2004, **126**, 16, 5300–5308.
- I. Urukova, J. Vorholz and G. Maurer, *J. Phys. Chem. B*, 2005, **109**, 12154–12159.
- L. A. Blanchard and J. F. Brennecke, *Ind. Eng. Chem. Res.*, 2001, **40**, 1, 287–292.

- 14 A. M. Scurto, S. N. V. K. Aki and J. F. Brennecke, *J. Am. Chem. Soc.*, 2002, **124**, 35, 10276–10277.
- 15 A. M. Scurto, S. N. V. K. Aki and J. F. Brennecke, *Chem. Commun.*, 2003, 572–573.
- 16 W. Wu, J. Zhang, B. Han, J. Chen, Z. Liu, T. Jiang, J. He and W. Li, *Chem. Commun.*, 2003, 1412–1413.
- 17 W. Wu, W. Li, B. Han, T. Jiang, D. Shen, Z. Zhang, D. Sun and B. Wang, *J. Chem. Eng. Data*, 2004, **49**, 6, 1597–1601.
- 18 A. Shariati and C. J. Peters, *J. Supercrit. Fluids*, 2004, **30**, 2, 139–144.
- 19 A. Shariati and C. J. Peters, *J. Supercrit. Fluids*, 2003, **25**, 2, 109–111.
- 20 M. C. Kroon, A. Shariati, M. Costantini, J. van Spronsen, G.-J. Witkamp, R. A. Sheldon and C. J. Peters, *J. Chem. Eng. Data*, 2005, **50**, 1, 173–176.
- 21 J. M. Crosthwaite, S. N. V. K. Aki, E. J. Maginn and J. F. Brennecke, *Fluid Phase Equilib.*, 2005, **228–229**, 303–309.
- 22 J. Lachwa, J. Szydowski, V. Najdanovic-Visak, L. P. N. Rebelo, K. R. Seddon, M. Nunes da Ponte, J. M. S. S. Esperanca and H. J. R. Guedes, *J. Am. Chem. Soc.*, 2005, **127**, 18, 6542–6543.
- 23 L. A. Blanchard, Z. Gu and J. F. Brennecke, *J. Phys. Chem. B*, 2001, **105**, 12, 2437–2444.
- 24 F. Liu, M. B. Abrams, R. T. Baker and W. Tumas, *Chem. Commun.*, 2001, 433.
- 25 S. V. Dzyuba and R. A. Bartsch, *Angew. Chem., Int. Ed.*, 2003, **42**, 2, 148.
- 26 244.70 g of 1-methylimidazole was reacted with 327.50 g of 1-chlorobutane at 80 °C under nitrogen for 5 days. The excess of 1-chlorobutane was removed by rotary evaporation yielding a slightly yellow viscous oil ([bmim][Cl], 521.40 g). 309.60 g of [bmim][Cl] prepared previously was dissolved in 1000 ml of dichloromethane, and 203.10 g of sodium tetrafluoroborate was added. The mixture was stirred at room temperature for 20 h and filtered. The filtrate was concentrated by rotary evaporation yielding a slightly yellow, viscous liquid (392.30 g). The ionic liquid was then purified by column chromatography over silica-gel (Merck type 9385, 230–400 mesh, 60A), with a recovery of 80% of colourless [bmim][BF<sub>4</sub>]. <sup>1</sup>H-NMR (300.2 MHz, CDCl<sub>3</sub>, TMS): δ 0.88 (t, 3H), 1.31 (m, 2H), 1.82 (m, 2H), 3.90 (s, 3H), 4.16 (t, 2H), 7.42 (s, 2H), 8.66 (s, 1H). <sup>13</sup>C-NMR (CDCl<sub>3</sub>, TMS) δ 13.33, 19.32, 31.92, 36.10, 49.67, 122.56, 123.85, 136.06.
- 27 Th.W. de Loos, H. J. van der Kooij, W. Poot and P. L. Ott, *Delft Prog. Rep.*, 1983, **8**, 200.
- 28 C. J. Peters, J. L. de Roo and J. de Swaan Arons, *Fluid Phase Equilib.*, 1993, **85**, 301–312.
- 29 M. Abla, J.-C. Choi and T. Sakakura, *Chem. Commun.*, 2001, 2238–2239.
- 30 M. Caplow, *J. Am. Chem. Soc.*, 1968, **90**, 24, 6795–6803.
- 31 M. Aresta, A. Dibenedetto, E. Quaranta, M. Boscolo and R. Larsson, *J. Mol. Catal. A: Chem.*, 2001, **174**, 7–13.
- 32 V. Ermatchkov, Á. Pérez-Salado Kamps and G. Maurer, *J. Chem. Thermodyn.*, 2003, **35**, 1277–1289.
- 33 E. M. Hampe and D. M. Rudkevich, *Tetrahedron*, 2003, **59**, 9619–9625.

# A new method for dialkyl peroxides synthesis in ionic liquids as solvents†‡

Stefan Baj,\* Anna Chrobok and Sebastian Derfla

Received 29th September 2005, Accepted 6th October 2005

First published as an Advance Article on the web 27th October 2005

DOI: 10.1039/b513863a

Organic hydroperoxides undergo smooth nucleophilic displacement reactions with alkyl bromides in the presence of 30% water solution of NaOH in several ionic liquids (ILs) at room temperature to afford the corresponding dialkyl peroxides in excellent yields under extremely mild conditions. Additionally, symmetrical dialkyl peroxides were obtained in ionic liquids as solvent with good yields.

## Introduction

Organic peroxides have found wide application in industrial organic synthesis, for example as initiators of free radical reactions, cross-linking agents, bleaching or oxidising agents and pharmaceutical additives. Synthesis of dialkyl peroxides should be conducted at relatively low temperatures because of the low thermal stability of peroxy compounds. Additionally, in the presence of strong bases and acids, decomposition of peroxy compounds can be observed and is accelerated with increasing temperature.<sup>1</sup> That is why mild methods for synthesis of dialkyl peroxides are researched. One of them, nucleophilic substitution between sodium alkyl peroxides (which could be generated *in situ*) and alkyl halides using phase-transfer catalysis (PTC), has become a very useful synthetic route for unsymmetrical dialkyl peroxides.<sup>2</sup> It is worth noting that the same reaction carried out without a PT catalyst practically does not proceed. A general synthetic procedure for symmetrical dialkyl peroxides is the reaction of an alkyl sulfonate with 0.5 molar equiv. of hydrogen peroxide. Primary dialkyl peroxides can be obtained in about 50% yield while secondary dialkyl peroxides are difficult to obtain in good yields using the appropriate alkyl methanesulfonate.<sup>3</sup>

Recently, there has been a significant interest in the use of ionic liquids as environmentally benign solvents for stoichiometric and catalytic reactions. Characteristics such as: high thermal stability, low viscosity, wide liquid range, low vapour pressure and an excellent ability to dissolve organic compounds, salts and metals, make ILs extremely useful reaction media, which are becoming increasingly important technologically.<sup>4</sup> Ionic liquids are composed entirely of ions and seem well suited for the types of reactions for which PTC is effective, particularly because of bulky organic cations. There is a growing literature of the effects of ILs on nucleophilic substitutions.<sup>5</sup> Authors state that in some reactions ionic liquids can act as both solvent and catalyst to activate the anion for

reaction. It should be noted that typical organic solvents, which are used in conventional PTC are very often environmentally undesirable because of their toxicity, flammability and volatility. Catalyst separation and recovery are also common problems in phase-transfer catalysis.

We present a new approach to dialkyl peroxides synthesis involving application of ionic liquids that affect the efficiency of the reaction.

## Results and discussion

We selected the following room temperature ionic liquids as solvent: 1-butyl-3-methylimidazoliumhexafluorophosphate ([bmim]PF<sub>6</sub>); 1-butyl-3-methylimidazoliumtetrafluoroborate ([bmim]BF<sub>4</sub>); 1-butyl-3-methylimidazoliumtrifluoromethanesulfonate ([bmim]CF<sub>3</sub>SO<sub>3</sub>), 1-butyl-3-methylimidazoliummethylsulfate ([bmim]MeSO<sub>4</sub>), 1-butyl-3-methylimidazoliumethylsulfate ([bmim]EtSO<sub>4</sub>), and 1-butyl-3-methylimidazoliumoctylsulfate ([bmim]OcSO<sub>4</sub>). All these ILs are water and air stable, commonly available and widely used.

As a model reactant we chose 1-methyl-1-phenylethyl hydroperoxide (cumyl hydroperoxide, CHP), *tert*-butyl hydroperoxide, hydrogen peroxide, alkyl (C2–C7) bromides, *n*-butyl and *sec*-butyl methanesulfonate.

It is known that dialkyl peroxides and hydroperoxides can easily decompose in the presence of various factors. That is why it was important to test stability of these substances in the reaction conditions by stirring them in IL overnight. We observed no decomposition products on HPLC chromatograms.

Syntheses of unsymmetrical dialkyl peroxides were carried out at room temperature in a 10 ml two necked round bottom flask stirring with a magnetic stirrer for 15 min to 4 h at room temperature. The concentration of CHP in ionic liquid was 1.2 mol dm<sup>-3</sup>. An equimolar amount of alkyl bromide and two times stoichiometric amount of NaOH (30% water solution) were used. Products were extracted with diethyl ether. Although the solvent extraction process may be controversial (using an ionic liquid to avoid atmospheric emissions and substituting using a volatile organic solvent to extract the product) it could have an environmental benefit.<sup>6</sup> The organic extractant does not also have to be a good solvent for peroxide synthesis, so ether or hexane can be used instead of aromatics like chlorobenzene.<sup>2</sup>

Department of Chemical Organic Technology and Petrochemistry, Silesian University of Technology, Gliwice, Poland.

E-mail: baj@polsl.gliwice.pl; Fax: +48 32237 32 10; Tel: +48 32237 29 17

† This work was presented at the 1st International Conference on Ionic Liquids (COIL), held in Salzburg, Austria, 19–22 June, 2005.

‡ Electronic supplementary information (ESI) available: Characterisation of the peroxides. See DOI: 10.1039/b513863a

As a result we obtained dialkyl peroxides (**1–9**) with high yields (Table 1). The reactions proceeded efficiently and very fast at room temperature in ILs; conventional methods require higher temperatures (higher than 60 °C) and longer reaction times (2–5 h).<sup>2</sup>

In the case of cumyl alkyl (C6–C7) and cumyl isopropyl peroxides, we observed somewhat lower yields resulting from lower reactivity of bromides with longer or branched alkyl chains.

[bmim]BF<sub>4</sub> is the best solvent we used for synthesis. In the case of ethyl cumyl peroxide the reaction was completed after 15 min of stirring at room temperature. We have observed similar activity for ionic liquids using 1-butyl-3-methylimidazoliumalkylsulfates (Table 2). These substances

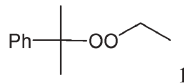
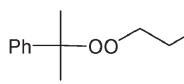
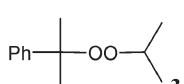
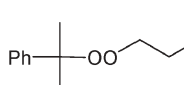
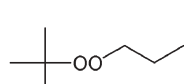


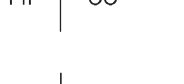
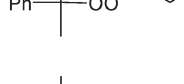
are all halogen-free, based on alkylsulfate anions, relatively new and ecological ionic liquids.

We observed low activity of [bmim]PF<sub>6</sub>. It is known that this kind of ionic liquid (based on the PF<sub>6</sub><sup>-</sup> anion) easily hydrolyses. This is probably a competitive process which consumes the hydroxide anion required for the reaction. It may explain the poor performance of hexafluorophosphate.

We have also shown that alkyl methanesulfonates can be employed successfully in the alkylation process of hydrogen peroxides in ionic liquids to give primary and secondary symmetrical dialkyl peroxides with good yields. Examples of the synthesis of *n*-butyl and *sec*-butyl peroxides in the presence of 1-butyl-3-methylimidazoliumtetrafluoroborate are

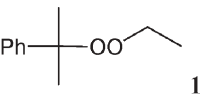
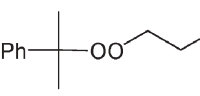
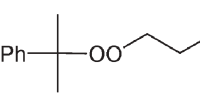
**Table 1** Alkylation of CHP in ionic liquids

$$\text{R}^1-\text{C}(\text{Ph})_2-\text{OOH} + \text{R}^2\text{Br} \xrightarrow[\text{room temp., 30\% NaOH}]{\text{ionic liquid}} \text{R}^1-\text{C}(\text{Ph})_2-\text{OO}-\text{R}^2$$

Dialkyl peroxides	[bmim]BF <sub>4</sub>			[bmim]PF <sub>6</sub>		[bmim]CF <sub>3</sub> SO <sub>3</sub>		[bmim]MeSO <sub>4</sub>	
	Yield <sup>a</sup> (%)	Yield <sup>b</sup> (%)	Reaction time/min	Yield <sup>a</sup> (%)	Reaction time/min	Yield <sup>a</sup> (%)	Reaction time/min	Yield <sup>a</sup> (%)	Reaction time/min
 <b>1</b>	98	90	10	75	30	77	30	97	30
 <b>2</b>	86	81	30	45	60	76	60	77	60
 <b>3</b>	44	38	180	10	240	—	—	—	—
 <b>4</b>	75	69	45	44	180	66	180	79	120
 <b>5</b>	—	60	60	—	—	—	—	—	—
 <b>6</b>	40	36	180	10	240	—	—	—	—
 <b>7</b>	71	65	60	—	240	66	240	66	240
 <b>8</b>	61	55	120	—	240	60	240	66	240
 <b>9</b>	62	50	180	—	240	60	240	65	240

<sup>a</sup> yields determined by HPLC; <sup>b</sup> isolated yields.

**Table 2** Alkylation of CHP in 1-butyl-3-methylimidazoliumalkylsulfate

Dialkyl peroxide	[bmim]MeSO <sub>4</sub>			[bmim]EtSO <sub>4</sub>		[bmim]OcSO <sub>4</sub>	
	Yield <sup>a</sup> (%)	Yield <sup>b</sup> (%)	Reaction time/min	Yield <sup>a</sup> (%)	Reaction time/min	Yield <sup>a</sup> (%)	Reaction time/min
 <b>1</b>	97	90	30	93	30	87	30
 <b>2</b>	77	70	60	71	60	73	60
 <b>4</b>	79	69	120	65	240	62	120

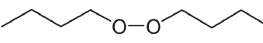
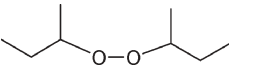
<sup>a</sup> Yield determined by HPLC. <sup>b</sup> Isolated yields.

demonstrated in Table 3. Yields are similar to yields obtained from syntheses in methanol as a reaction media.<sup>3</sup>

The ionic liquids used in these reactions can be recycled and reused for subsequent reactions. However, at first it is necessary to remove NaBr which is a by-product. In the case of hydrophobic ILs it is possible to wash IL with water and dry by evaporation. Miscible with water, ILs were filtered to remove NaBr and dried from traces of water. We showed that ILs after purification can be reused four times without any loss of activity. Examples of the reaction carried out in the recycled [bmim]BF<sub>4</sub> is presented in Table 4. The yields of cumyl ethyl peroxide were basically similar to those observed using fresh non-recycled ionic liquid.

In summary, we report an efficient and mild method for dialkyl peroxide syntheses using ionic liquids as novel media. While there is still a need to use organic solvents for the product extraction, the process provides opportunities to reduce solvent consumption and the selection of less hazardous

**Table 3** Synthesis of symmetrical dialkyl peroxides in 1-butyl-3-methylimidazoliumtetrafluoroborate

Dialkyl peroxide	Yield <sup>a</sup> (%)
	48
	18

<sup>a</sup> Isolated yields.

**Table 4** Yields of cumyl ethyl peroxide in recycled [bmim]BF<sub>4</sub>

Recycle	Yield <sup>a</sup> (%)	Yield <sup>b</sup> (%)
Fresh, non-recycled IL	98	90
First	98	89
Second	98	90
Third	98	88
Fourth	98	88

<sup>a</sup> Yields determined by HPLC. <sup>b</sup> Isolated yields.

solvents compared to previous techniques (PTC). Simplicity of the methodology, ease of the product isolation, lack of by-products, mild conditions, possibility of IL recycling and higher safety at work could make this process available in the future on the industrial scale.

## Experimental

### Materials

Alkyl bromides (Merck) and ionic liquids (Solvent Innovation) were commercial materials; 1-methyl-1-phenylethyl (cumyl) and *tert*-butyl hydroperoxides<sup>7</sup> and alkyl methanesulfonates<sup>8</sup> were prepared according to the known procedures.

**Asymmetrical dialkyl peroxides syntheses.** In a typical experiment, into a 10 ml two necked round bottom flask alkyl hydroperoxide (1.16 mmol) and ionic liquid (1 ml) were added and stirred with a magnetic stir bar. Then 30% water solution of NaOH (2.32 mmol) and alkyl bromide (1.16 mmol) were added. Afterwards, a content of the flask was stirring at room temperature for 15 min to 4 h (depending of the reaction rate). The reaction progress was followed by HPLC. The product was extracted with diethyl ether (6 × 5 ml); organic phase was dried and concentrated yielding dialkyl peroxide. For reusing, hydrophobic ILs were washed with water to remove NaBr and were dried by evaporation (3 mbar, 70 °C, 3 h). In the case of water soluble IL filtration (if too viscous for filtration, the IL can be dissolved a little in methylene chloride) and drying from traces of water were done before recycling.

**Symmetrical dialkyl peroxides syntheses.** A mixture of 16 mmol of appropriate alkyl methanesulfonate, 8 mmol of 30% aqueous hydrogen peroxide and 2.5 ml of 1-butyl-3-methylimidazolium tetrafluoroborate were cooled to 5 °C. 8 mmole of 50% aqueous potassium hydroxide was slowly added with stirring. The reaction mixture was allowed to come to room temperature. After 5 h of stirring, another portion (4 mmol) of 30% hydrogen peroxide was added. After another 5 h of stirring the reaction was worked up by adding water in

an amount to dissolve the potassium methanesulfonate. The ionic liquid–aqueous solution was extracted with several 5 ml portions of hexane. The hexane layer was washed with 3 ml of 5% potassium hydroxide solution to remove any hydroperoxide, the hexane layer washed with distilled water until the washings were neutral and dried over anhydrous sodium sulfate. The solvent was then removed under vacuum yielding dibutyl peroxides.

**Analysis.**  $^1\text{H}$  NMR and  $^{13}\text{C}$  NMR spectra were recorded at 300 MHz in  $\text{CDCl}_3$  (Varian Unity Inova plus, internal TMS). Elemental analyses were obtained on a Perkin-Elmer analyser. HPLC was performed using a liquid chromatograph (Alliance, Waters 2690 system) with a Waters photodiode array detector and  $3.9 \times 150$  mm cartridge column (Nova-Pak C18, 60 Å, 4  $\mu\text{m}$ ); the solvent system included methanol/water (70/30 v/v, flow rate 1 ml  $\text{min}^{-1}$ ). The active oxygen was determined by iodometric titration.

### Acknowledgements

This work was financially supported by the Polish State Committee for Scientific Research (Grant no 3 T09B 002 26).

### References

- 1 S. Matsugo and I. Saito, *Organic peroxides*, ed. W. Ando, Wiley-Interscience, New York, 1992, p. 157.
- 2 N. Hideo and S. Vashiko, *Jpn. Pat.*, 1975, 51-110-504; N. Hideo and S. Vashiko, *Chem. Abstr.*, 1975, **86**, 72197; M. Bourgeois, E. Montaudon and B. Maillard, *Tetrahedron*, 1993, **49**, 2477; S. Baj, *J. Mol. Catal.*, 1996, **106**, 11.
- 3 W. A. Pryor, D. M. Huston, T. R. Fiske, T.L. Pickering and E. Ciuffrin, *J. Am. Chem. Soc.*, 1964, **80**, 4238.
- 4 T. Welton, *Chem. Rev.*, 1999, **99**, 2071; P. Wasserscheid and K. Wilhelm, *Angew. Chem., Int. Ed.*, 2000, **39**, 3772; H. Olivier-Bourbigou and L. Magna, *J. Mol. Catal. A: Chem.*, 2002, **182**, 419; J. Dupont, R. F. de Souza and P. A. Z. Suarez, *Chem. Rev.*, 2002, **102**, 3667; M. Earle, A. Forestier, H. Olivier-Bourbigou and P. Wasserscheid, *Ionic Liquids in Synthesis*, ed. P. Wasserscheid, T. Welton, Wiley-VCH, Weinheim, 2003, p. 174.
- 5 Z. M. Yudeh, Hao-Yu Shen, B. Ching Chi, Li-Chun Feng and S. Selvasothi, *Tetrahedron Lett.*, 2002, **43**, 9381; C. Wheeler, K. N. West, C. L. Liotta and C. A. Eckert, *Chem. Commun.*, 2001, 887; N. L. Lancaster, T. Welton and G. B. Young, *J. Chem. Soc., Perkin Trans. 2*, 2001, 2267; D. W. Kim, C. E. Song and D. Y. Chi, *J. Org. Chem.*, 2003, **68**, 4281; C. Chiappe, D. Pieraccini and P. Saullo, *J. Org. Chem.*, 2003, **68**, 6710.
- 6 R. Sheldon, *Chem. Commun.*, 2001, 2399.
- 7 E. Milchert, *Pol. J. Appl. Chem.*, 1988, **32**, 171; Houben-Weyl, *Methoden der organischen Chemie*, Stuttgart, 1952, vol. 8, p. 36.
- 8 H. R. Williams and H. S. Mosher, *J. Am. Chem. Soc.*, 1954, **76**, 2984.

# Clean Beckmann rearrangement of cyclohexanone oxime in caprolactam-based Brønsted acidic ionic liquids†‡

Shu Guo, Zhengyin Du, Shiguo Zhang, Dongmei Li, Zuopeng Li and Youquan Deng\*

Received 15th September 2005, Accepted 6th December 2005

First published as an Advance Article on the web 21st December 2005

DOI: 10.1039/b513139a

The Beckmann rearrangement of cyclohexanone oxime to afford caprolactam in a novel caprolactam-based Brønsted acidic ionic liquid as catalyst and reaction medium proceeded with high conversion and selectivity at 100 °C. The occurrence of the Beckmann rearrangement of cyclohexanone oxime in such a Brønsted acidic IL was also confirmed with *in situ* FT-Raman observation. The key point is that the caprolactam product was one component of the ionic liquid, and a dynamic exchange between the resulting caprolactam product and the caprolactam from the ionic liquid is expected. Therefore, the strong chemical combination between the caprolactam product and the acidic ionic liquid was greatly decreased and the desired product in the solid was recovered through extraction with organic solvent after the reaction.

## Introduction

Caprolactam has been an important intermediate for the production of nylon synthetic fibers and resins. The commercial production of  $\epsilon$ -caprolactam has been realized through the rearrangement of cyclohexanone oxime known as the Beckmann rearrangement, in which a large amount of oleum was employed as catalyst and reaction medium and a large amount of ammonium sulfate as by-product was produced because ammonium hydroxide was used to neutralize the sulfuric acid to release the desired product. As particular attention has been paid to the environmental impact of chemical industry processes, a clean Beckmann rearrangement process has long been expected, and great efforts have been put into the development of ammonium sulfate free processes.<sup>1</sup> For example, vapor-phase Beckmann rearrangements catalyzed by solid acid such as modified molecular sieves were reported.<sup>2</sup> A higher reaction temperature (*ca.* 300 °C) was necessary for such processes and rapid deactivation of catalyst was unavoidable due to coke formation.<sup>3</sup> Recently, it was reported that the Beckmann rearrangement has also been carried out in supercritical water with a short reaction time and excellent selectivity.<sup>4</sup> However, it is too rigorous to be used in an industrial application. More recently, Al-containing MCM-41 materials were reported to be more effective catalysts for both liquid and vapour-phase Beckmann rearrangement of cyclohexanone oxime in comparison to zeolites and other mesoporous catalysts.<sup>5</sup> However, the conversions and selectivities could not simultaneously reach more than 80% and some

ring-opening byproducts and tars were also formed. Very recently, a one-step catalytic Beckmann rearrangement from cyclohexanone to caprolactam using an AlPO catalyst doped with manganese and magnesium with 68% of conversion and 78% of selectivity was reported<sup>6</sup> and reviewed.<sup>7</sup> The reaction conditions were very mild (80 °C), but the conversion and selectivity need to be further improved before practical application. Therefore, to develop a liquid-phase catalytic Beckmann rearrangement without formation of ammonium sulfate as by-product is highly desirable.

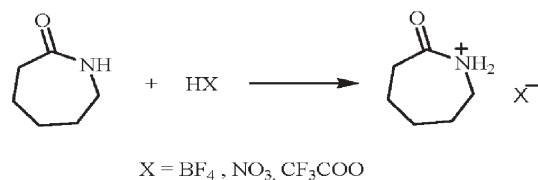
Room temperature ionic liquids (RTILs) as new reaction media and catalysts have been widely recognized and accepted.<sup>8</sup> Previously reported work<sup>9</sup> suggested that, for a Beckmann rearrangement catalyzed with a strong Brønsted acid, the first step was protonization of ketoxime to form a positively charged intermediate. A strong electrostatic field possessed with RTILs may stabilize such a charged intermediate, thus making RTILs a favorable reaction media for Beckmann rearrangement. Efforts to use RTILs as reaction media for Beckmann rearrangement of cyclohexanone oxime have been made in our group and by other colleagues.<sup>10</sup> Although good results have been obtained, phosphorous compounds like P<sub>2</sub>O<sub>5</sub> and PCl<sub>5</sub> catalysts are environmentally unfriendly and are difficult to reuse. Brønsted acidic RTILs consisting of sulfonyl chloride as reaction media and catalysts were also tested for Beckmann rearrangement of cyclohexanone oxime without any additional co-catalyst and solvent,<sup>11</sup> but the synthetic procedure for such RTILs was so complicated that they would be too expensive to be used for Beckmann rearrangement in practice. Another problem was that the resulting caprolactam would chemically combine with the RTILs due to the basicity of caprolactam and the acidity of the RTILs, which made it almost impossible to separate the desired product from the RTILs after reaction. Therefore, the key for designing RTIL as catalyst and reaction medium for liquid-phase Beckmann rearrangement is that the desired  $\epsilon$ -caprolactam product could be easily separated from the reaction system.

Centre for Green Chemistry and Catalysis, Lanzhou Institute of Chemical Physics, Chinese Academy of Sciences, Lanzhou 730000, P. R. China. E-mail: ydeng@lzb.ac.cn; Fax: (+86)-931-4968116

† This work was presented at the 1st International Conference on Ionic Liquids (COIL), held in Salzburg, Austria, 19–22 June, 2005.

‡ Electronic supplementary information (ESI) available: Differential scanning calorimetry (DSC) (Fig. S1); thermogravimetric (TG) (Fig. S2); cyclic voltammograms (Fig. S3); NMR spectral data (Fig. S4–S7); ESI-MS (Fig. S8). See DOI: 10.1039/b513139a





**Scheme 1** Preparation of caprolactam cation-based ILs.

Recently, we had successfully developed a new family of lactam cation-based Brønsted acidic ILs through a simple and atom-economic neutralization between lactam, such as caprolactam and butyrolactam, and a Brønsted acid and their physicochemical properties were preliminarily characterized and investigated (Scheme 1).<sup>12</sup>

In this work, we wish to report our new finding that the above-mentioned caprolactam cation (abbreviated as [NHC])-based Brønsted acidic ILs could be effective catalysts and reaction media for Beckmann rearrangement of cyclohexanone oxime to caprolactam. In comparison with dialkyl imidazolium, caprolactam is cheaper, more environmentally benign, and available on an industrial scale, which would be attractive in industry if incorporated into RTILs as catalyst and medium for Beckmann rearrangement. From another aspect, the separation of the desired product from acidic ionic liquids as catalyst and reaction medium is a great challenge in the Beckmann rearrangement reaction of cyclohexanone oxime to caprolactam. Because the rearrangement reaction product is one component of ILs used in this work, it can be conjectured that there would be a dynamic exchange between caprolactam ILs and the produced caprolactam during the rearrangement reaction (Scheme 2), and the strong chemical combination between caprolactam and acidic catalyst would be largely avoided. That is to say that the product separation from the acidic ILs system through organic solvent extraction and the recycling of ILs would be easily facilitated.

## Experimental

### Measurement and analysis

The <sup>1</sup>H- and <sup>13</sup>C-NMR spectra were recorded on a Bruker AMX FT 400 MHz NMR spectrometer. Chemical shifts were reported in parts per million (ppm,  $\delta$ ). Electrospray ionization mass spectra were recorded on a Bruker Daltonics APEX II 47e FTMS. The Hammett Brønsted acid scales ( $H_0$ ) of ILs were determined by using Agilent 8453 UV-vis spectrophotometer with a modified method.<sup>12,13</sup> The thermal properties were examined by DSC-Q100 (TA Instruments Inc.) differential scanning calorimeter and Pyrid Diamond TG thermo gravimetric analyzer (Perkin Elmer Co.) with a scan rate of 20 °C min<sup>-1</sup>. Electrochemical stability was

analyzed by cyclic voltammetry using a CHI660A Instruments Electrochemical Work Station at room temperature. The ionic conductivity was determined with a conductivity meter (DDS-11A) produced by Shanghai YULONG Scientific Instrument Co. Ltd. *In situ* FT-Raman studies were conducted during the Beckmann rearrangement with a Thermo Nicolet 5700 FT-Raman spectrometer with AsGaIn detector and Nd:YAG laser (1064 nm). The IL and cyclohexanone oxime with a 1 : 1 molar ratio was charged into a transparent glass capillary tube specified for FT-Raman measurement and sealed. The tube containing the reaction mixture was then fixed into the sample chamber and was heated to 100 °C with a self-made electric heating device, and in the meantime, the spectra were continuously recorded during the reaction.

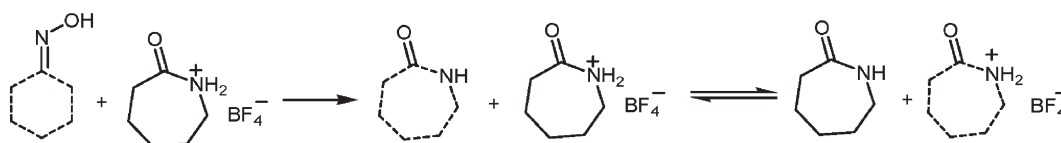
### Preparation of ILs

[NHC][BF<sub>4</sub>] was prepared as follows: 11.3 g (0.1 mol) caprolactam was dissolved in 22 g (0.1 mol) 40% fluoroboric acid water solution, and was stirred for 30 min at room temperature, and then water was evaporated with a spin-evaporator. The residual trace water was removed under vacuum (5–10 mmHg) for 4 h at 90 °C and a light yellow clear liquid was obtained with a yield of 20.0 g (99%). <sup>1</sup>H-NMR (400 MHz, *d*<sub>6</sub>-DMSO):  $\delta$  1.45–1.66 (m, 6H), 2.38 (t, 2H), 3.10 (t, 2H), 8.26 (s, 1H), 11.98 (s, 1H). <sup>13</sup>C-NMR (100 MHz, *d*<sub>6</sub>-DMSO):  $\delta$  22.86, 29.15, 30.08, 35.42, 42.18, 179.25. ESI-MS for cation: *m/z* 114.0912 versus calculated 114.0913.

[NHC][NO<sub>3</sub>] and [NHC][CF<sub>3</sub>COO] were also prepared with the same procedure as for [NHC][BF<sub>4</sub>]. For the purpose of comparison, methylimidazolium tetrafluoroborate, [HmIm][BF<sub>4</sub>], was prepared according to the previously reported literature.<sup>14</sup> Their spectra data are listed here. [NHC][NO<sub>3</sub>]: mp 45 °C. <sup>1</sup>H-NMR (400 MHz, CDCl<sub>3</sub>) 1.65–1.82 (m, 6H), 2.57 (t, 2H), 3.35 (d, 2H), 8.38(s, 1H); <sup>13</sup>C-NMR (100 MHz, CDCl<sub>3</sub>) 22.61, 29.04, 30.16, 35.69, 42.91, 179.27; ESI-MS for cation: *m/z* 114.0912 versus calculated 114.0913. [NHC][CF<sub>3</sub>COO]: <sup>1</sup>H-NMR (400 MHz, CDCl<sub>3</sub>): 1.65–1.82 (m, 6H), 2.51 (q, 2H), 3.27 (q, 2H), 8.06(s, 1H), 15.89 (s, 1H); <sup>13</sup>C-NMR (100 MHz, CDCl<sub>3</sub>) 22.74, 28.86, 30.25, 35.76, 42.83, 115.23 (q, CF<sub>3</sub>), 160.99, 181.02; ESI-MS for cation: *m/z* 114.0910 versus calculated 114.0913. [HmIm][BF<sub>4</sub>]: mp 49 °C. <sup>1</sup>H-NMR (400 MHz, *d*<sub>6</sub>-DMSO) 4.07 (s, 3H), 7.65 (t, 1H), 7.66 (t, 1H), 8.84 (s, 1H), 12.65 (s, 1H).

### General procedure for the Beckmann rearrangement reaction

The Beckmann rearrangement of cyclohexanone oxime was processed as follows: 0.565 g (5 mmol) cyclohexanone oxime and the corresponding amount of ionic liquid (molar ratio of IL/substrate = 2/1–4/1) were charged into a 10 ml round-bottomed flask equipped with a magnetic stirrer. Then the



**Scheme 2** Possible dynamic exchange between caprolactam and [NHC][BF<sub>4</sub>].

**Table 1** Some physicochemical properties of caprolactam-based ILs

ILs	$T_g/^\circ\text{C}$	$T_d/^\circ\text{C}$	$H_0$	Conductivity/ $\text{S cm}^{-1}$	Viscosity/cP	$E/V$
[NHC][BF <sub>4</sub> ]	-74.0	239	-0.22	$7.31 \times 10^{-4}$	503	2.0
[NHC][CF <sub>3</sub> COO]	-73.0	135	3.35	$3.83 \times 10^{-4}$	28	2.1
[NHC][NO <sub>3</sub> ]	— <sup>a</sup>	188	2.08	$8.40 \times 10^{-4}$	— <sup>b</sup>	2.2

<sup>a</sup> No glass temperature was observed. <sup>b</sup> It is solid at 25 °C.

reaction was continued for 3–5 h at the desired temperature (80–100 °C). After the reaction the resulting mixture was dissolved with 5 ml acetone for GC-MS and GC analyses. Qualitative analyses were conducted with a HP 6890/5973 GC-MS with chemstation containing a NIST Mass Spectral Database. Quantitative analyses were conducted with an Agilent 6820 GC equipped with a FID using an external standard method.

After the reaction, the product separation was conducted as follows: the resulting liquid mixture was extracted with organic solvents such as ether or CCl<sub>4</sub> three times, the organic phase containing desired product was evaporated at an elevated temperature to remove organic solvent, and solid caprolactam was obtained.

Since the rearrangement reaction product is one component of ILs, a parallel experiment for recovery of the caprolactam was also conducted so as to obtain a precise yield resulting from the rearrangement of cyclohexanone oxime, *i.e.* the resulting liquid mixture after reaction was neutralized with 30% ammonium hydroxide solution until pH = 7.0, then separated by a silica gel column chromatograph with 1 : 1 CH<sub>2</sub>Cl<sub>2</sub>/hexane as eluents to obtain total and pure caprolactam which resulted from the rearrangement of cyclohexanone oxime and from the caprolactam-based IL. The isolated and real yield was obtained according to the following calculation: yield% = [isolated caprolactam by column chromatograph – caprolactam released from [NHC][BF<sub>4</sub>]/cyclohexanone oxime added.

## Results and discussion

### Physicochemical properties of caprolactam cation-based ILs

Some physicochemical properties of caprolactam cation-based ILs used in this work are summarized in Table 1. At room temperature (*ca.* 20 °C), [NHC][BF<sub>4</sub>] and [NHC][CF<sub>3</sub>COO] are liquid and have no distinct freezing points and melting points but possess lower glass transition temperatures (-74 °C and -73 °C, respectively). The thermal decomposition temperatures ( $T_d$ , with mass loss of 10%) of [NHC][BF<sub>4</sub>], [NHC][CF<sub>3</sub>COO] and [NHC][NO<sub>3</sub>] ILs are 239, 135 and 188 °C, respectively, suggesting that the thermal stability of caprolactam-based ILs are not higher in comparison with that of [BMIm][BF<sub>4</sub>] but high enough for a general chemical process (at or below 100 °C). The resulting Hammett Brønsted acid scales ( $H_0$ ) using UV-vis spectroscopy were -0.22, 3.35, and 2.08 for [NHC][BF<sub>4</sub>], [NHC][CF<sub>3</sub>COO], and [NHC][NO<sub>3</sub>], respectively, suggesting that Brønsted acidity of [NHC][BF<sub>4</sub>] was relatively strong. The ionic conductivities of caprolactam-based ILs are slightly smaller than that of [BMIm][PF<sub>6</sub>] ( $1.4 \times 10^{-3} \text{ S cm}^{-1}$ ). Relatively narrow electrochemical

windows, *i.e.* *ca.* 2.0–2.2 V were observed due to the presence of active H in these ILs.

### Beckmann rearrangement of cyclohexanone oxime over caprolactam-based ILs

The results of Beckmann rearrangement of cyclohexanone oxime to caprolactam over caprolactam-based ILs and [HMIM][BF<sub>4</sub>] (just for the purpose of comparison) as catalyst and reaction medium are summarized in Table 2. Firstly, the effect of molar ratio of [NHC][BF<sub>4</sub>]/oxime on rearrangement reaction was examined at 80 °C. The conversion and the selectivity increased greatly with the increase of molar ratio of [NHC][BF<sub>4</sub>]/oxime from 2/1 to 4/1 (entries 1–3). Since higher viscosity of reaction mixture resulted if the oxime was added into [NHC][BF<sub>4</sub>] with a higher molar ratio, which may prevent the reaction proceeding to a certain extent, additional reactions under different agitation rates were further conducted. The conversion, however, only increased *ca.* 1% when the agitation rate was changed from 200 rpm to 1000 rpm (entries 4 and 5). This indicated that the agitation rate, or expressed more precisely, the viscosity of the reaction mixture, has little effect on the conversion of the BR reaction, and the amount of the IL used as reaction medium and catalyst has a strong impact on the conversion. Another important point derived from the above experiment is that the Beckmann rearrangement of cyclohexanone oxime does occur in such a Brønsted acidic IL as catalyst and reaction medium although its Brønsted acidity is much lower than that of oleum, in other words, it may not be necessary to use a strong Brønsted acid as catalyst and reaction medium for a Beckmann rearrangement.

**Table 2** Results of Beckmann rearrangement of cyclohexanone oxime to caprolactam

Entry	ILs	ILs/oxime	$T/^\circ\text{C}$	$t/\text{h}$	Conv. (%)	Sel. (%)
1	[NHC][BF <sub>4</sub> ]	2 : 1	80	3	12.3	64.5
2	[NHC][BF <sub>4</sub> ]	3 : 1	80	3	47.8	90.1
3	[NHC][BF <sub>4</sub> ]	4 : 1	80	3	61.8	91.2
4 <sup>a</sup>	[NHC][BF <sub>4</sub> ]	3 : 1	80	3	47.5	90.3
5 <sup>a</sup>	[NHC][BF <sub>4</sub> ]	3 : 1	80	3	48.4	89.7
6	[NHC][BF <sub>4</sub> ]	3 : 1	100	3	77.5	90.2
7	[NHC][BF <sub>4</sub> ]	3 : 1	100	4	93.4	87.2
8	[NHC][BF <sub>4</sub> ]	3 : 1	100	5	95.1	85.1
9	[NHC][BF <sub>4</sub> ]	4 : 1	100	4	92.6	88.9
10	[NHC][CF <sub>3</sub> COO]	3 : 1	100	4	92.3	52.1
11	[NHC][NO <sub>3</sub> ]	3 : 1	100	4	71.4	58.3
12	[HMIm][BF <sub>4</sub> ]	3 : 1	100	4	43.8	33.1
13	[NHC][BF <sub>4</sub> ]	3 : 1	100	4	Isolated yield = 79.6% <sup>b</sup>	
14	[NHC][BF <sub>4</sub> ]	3 : 1	100	4	Isolated yield = 42% <sup>c</sup>	

<sup>a</sup> The agitation rates for entries 4 and 5 were 200 rpm and 1000 rpm, respectively. <sup>b</sup> The yield by column chromatography after neutralization with ammonium hydroxide. <sup>c</sup> The yield by ether extraction of the resulting mixture.

In order to confirm the occurrence of a Beckmann rearrangement of cyclohexanone oxime in such a Brønsted acidic IL, *in situ* FT-Raman was conducted (Fig. 1). For the pure cyclohexanone oxime (a), there is a strong peak at  $1660\text{ cm}^{-1}$  ( $\nu(\text{C}=\text{N})$ ), which is assigned to the characteristic band of cyclohexanone oxime. For the pure  $[\text{NHC}][\text{BF}_4]$  (b), there is a peak at  $1690\text{ cm}^{-1}$  ( $\nu(\text{C}=\text{O})$ ), which was shifted from the original  $1636\text{ cm}^{-1}$  ( $\nu(\text{C}=\text{O})$ ) which is assigned to the characteristic band of pure caprolactam (g).<sup>16</sup> Such a shift from  $1636$  to  $1690\text{ cm}^{-1}$  may be attributed to the protonation of N after combination between caprolactam and  $\text{HBF}_4$ , which could be assigned to the characteristic band of caprolactam in  $[\text{NHC}][\text{BF}_4]$ . As for the mixture of cyclohexanone oxime and  $[\text{NHC}][\text{BF}_4]$  before reaction (c), a new peak at  $1673\text{ cm}^{-1}$  appeared, which is assigned to  $\nu(\text{C}=\text{N})$  in cyclohexanone oxime in which N was protonized due to the presence of  $[\text{NHC}][\text{BF}_4]$ . At  $100\text{ }^\circ\text{C}$  and as the reaction proceeded, the peak strength at  $1673\text{ cm}^{-1}$  was gradually reduced, indicating that cyclohexanone oxime was transformed. At the same time, the peak strength at  $1636\text{ cm}^{-1}$ , which could be assigned to the characteristic band of caprolactam, became stronger. This means that the Beckmann rearrangement of cyclohexanone oxime to caprolactam did occur.

Based on the experimental results obtained, the Beckmann rearrangement of cyclohexanone oxime in different Brønsted acidic ILs and for different reaction time at constant temperature ( $100\text{ }^\circ\text{C}$ ) was further tested. With a 3/1

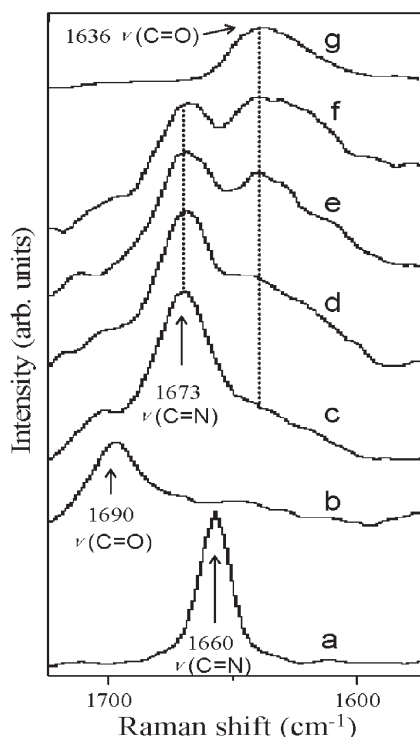


**Fig. 1** *In situ* Raman spectra of Beckmann rearrangement of cyclohexanone oxime in  $[\text{NHC}][\text{BF}_4]$  with a molar ratio of 1 : 1 at  $100\text{ }^\circ\text{C}$ . (a) Pure cyclohexanone oxime; (b) pure  $[\text{NHC}][\text{BF}_4]$ ; (c) 0 min (reaction mixture); (d) 20 min; (e) 60 min; (f) 100 min; (g) pure caprolactam.

$[\text{NHC}][\text{BF}_4]$ /oxime molar ratio, the conversion increased to 77.5% and further reached 95.1% when the reaction time was increased from 3 to 5 h although the corresponding selectivity for the desired product decreased slightly (entries 6–8). At this temperature, the conversion and selectivity approached a constant even if the  $[\text{NHC}][\text{BF}_4]$ /oxime molar ratio increased to 4/1 (entry 9). It is worth noting that, although the selectivity for the desired product was not very high, the byproduct was only cyclohexanone, implying that such a byproduct could be recovered, reused and was less detrimental to the purity of the caprolactam product. When  $[\text{NHC}][\text{BF}_4]$  was replaced by  $[\text{NHC}][\text{CF}_3\text{COO}]$  and  $[\text{NHC}][\text{NO}_3]$ , poor conversions and selectivities were obtained (entries 10 and 11). For the purpose of comparison,  $[\text{HMIm}][\text{BF}_4]$  ( $H_0 = 1.605$ ) as catalyst and reaction medium under the above-mentioned optimum conditions was also tested (entry 12). Lower conversions and selectivities were also obtained. These experimental results suggested that the acidity of ILs was important but not the unique factor for the rearrangement reaction, and both cation and anion RTIL have a strong impact on the rearrangement reaction although a detailed reaction mechanism is still not clear at this stage. In order to precisely determine the amount of caprolactam transformed from cyclohexanone oxime during the rearrangement reaction, the resulting liquid mixture of entry 5 was also neutralized with 30% ammonium hydroxide until  $\text{pH} = 7.0$  to dissociate all the caprolactam molecule, including those from  $[\text{NHC}][\text{BF}_4]$ . Then the resulting solution was separated by a silica gel column using 1 : 1  $\text{CH}_2\text{Cl}_2$ /hexane as eluent. After evaporation of the eluent, total caprolactam (2.14 g) was obtained as a light yellow solid. When subtracting caprolactam from the IL (1.69 g), 0.45 g caprolactam product which was derived from rearrangement of the cyclohexanone oxime, could be obtained, corresponding to 79.6% of isolated yield (containing *ca.* 2% of cyclohexanone oxime) (entry 13). This result is just slightly lower than the GC yield of entry 5 (81.4%).

The product separation from the reaction system is a key step for a clean Beckmann rearrangement. The extraction with organic solvents was preliminarily adopted in this work, and ether as extracting solvent to recover the caprolactam from the resulting liquid mixture after reaction was employed due to its immiscibility with the IL and good solubility for caprolactam. When the resulting liquid mixture after reaction of entry 7 was extracted with ether three times ( $15\text{ ml} \times 3$ ) and then the upper ether phase containing caprolactam was evaporated at  $40\text{ }^\circ\text{C}$  to remove ether, a white solid (containing *ca.* 2% of cyclohexanone) could be recovered in *ca.* 42% of isolated yield (entry 14). This means that, on the one hand, a dynamic exchange between the caprolactam IL and the produced caprolactam does exist, and a strong chemical combination between caprolactam and acidic catalyst would be greatly avoided in the reaction system used in this work. On the other hand, there is still some chemical interaction between caprolactam product and acidic IL since not all caprolactam product could be recovered through the extraction. It can be conjectured that such an interaction may be derived from the hydrogen bond between caprolactam and acidic IL, and such an interaction could be further reduced through adjusting the extraction conditions.

## Conclusions

In conclusion, the Beckmann rearrangement of cyclohexanone oxime to afford caprolactam over a novel caprolactam tetrafluoroborate Brønsted acidic IL as catalyst and reaction medium was successfully followed with high conversion and selectivity under mild reaction conditions. The strong chemical combination between caprolactam product and acidic [NHC][BF<sub>4</sub>] was largely avoided. Preliminary results of direct product extraction using ether from the IL system suggested that product recovery without neutralization is possible. The catalyst system, reaction conditions and separation method could be further optimized. A possible reaction mechanism and separation mechanism using *in situ* FT-IR and FT-Raman is now underway.

## Acknowledgements

Financial support from the National Natural Science Foundation of China (No. 20233040, 20225309 and 20533080) is acknowledged.

## References

- H. Ichihashi and H. Soto, *Appl. Catal., A: Gen.*, 2001, **221**, 359.
- (a) Y. Ko, M. H. Kim, S. J. Kim, G. Seo, M. Y. Kim and Y. S. Uh, *Chem. Commun.*, 2000, 829; (b) R. Maheswari, K. Shanthi, T. Sivakumar and S. Narayanan, *Appl. Catal., A: Gen.*, 2003, **248**, 291; (c) P. Albers, K. Seibold, T. Haas, G. Prescher and W. F. Hölderich, *J. Catal.*, 1998, **176**, 561; (d) G. P. Heitmann, G. Dahlhoff and W. F. Hölderich, *J. Catal.*, 1999, **186**, 12; (e) G. P. Heitmann, G. Dahlhoff, J. P. M. Niederer and W. F. Hölderich, *J. Catal.*, 2000, **194**, 122.
- (a) R. Maheswari, K. Shanthi, T. Sivakumar and S. Narayanan, *Appl. Catal., A: Gen.*, 2003, **248**, 291; (b) M. Ishida, T. Suzuki, H. Ichihashi and A. Shig, *Catal. Today*, 2003, **87**, 187 and references cited therein.
- (a) Y. Ikushima, O. Sato, M. Sato, K. Hatakeda and M. Arai, *Chem. Eng. Sci.*, 2003, **58**, 935; (b) Y. Ikushima, K. Hatakeda, O. Sato, T. Yokoyama and M. Arai, *J. Am. Chem. Soc.*, 2000, **122**, 1908; (c) M. Boero, T. Ikeshoji, C. C. Liew, K. Terakura and M. Parrinello, *J. Am. Chem. Soc.*, 2004, **126**, 6280; (d) O. Sato, Y. Ikushima and T. Yokoyama, *J. Org. Chem.*, 1998, **63**, 9100.
- (a) C. Ngamcharussrivichai, P. Wu and T. Tatsumi, *J. Catal.*, 2004, **227**, 448; (b) L. Forni, C. Tosi, G. Fornasari, F. Trifirò, A. Vaccari and J. B. Nagy, *J. Mol. Catal. A: Chem.*, 2004, **221**, 97.
- J. M. Thomas and R. Raja, *Proc. Natl. Acad. Sci. USA*, 2005, **102**, 13732.
- R. Mokaya and M. Poliakoff, *Nature*, 2005, **437**, 1243.
- For recent reviews on ionic liquids, see (a) J. H. Davis, Jr. and P. A. Fox, *Chem. Commun.*, 2003, 1209; (b) J. Dupont, R. F. de Souza and P. A. Z. Suarez, *Chem. Rev.*, 2002, **102**, 3667; (c) R. Sheldon, *Chem. Commun.*, 2001, 2399; (d) P. Wasserscheid and W. Keim, *Angew. Chem., Int. Ed.*, 2000, **39**, 3772; (e) T. Welton, *Chem. Rev.*, 1999, **99**, 2071.
- (a) Y. Izumi, S. Sato and K. Urabe, *Chem. Lett.*, 1983, 1649; (b) M. T. Nguyen, G. Raspoet and L. G. Vanquickenborne, *J. Am. Chem. Soc.*, 1997, **119**, 2552.
- (a) J. Peng and Y. Deng, *Tetrahedron Lett.*, 2001, **42**, 403; (b) R. X. Ren, L. Zueva and W. Ou, *Tetrahedron Lett.*, 2001, **42**, 8441.
- Z. Du, Z. Li, Y. Gu, J. Zhang and Y. Deng, *J. Mol. Catal. A: Chem.*, 2005, **237**, 80.
- (a) Y. Deng, Z. Du, S. Guo, Z. Li and L. Zhu, *Chin. Pat.*, 2004 CN 04555657.4; (b) Z. Du, Z. Li, S. Guo, J. Zhang, L. Zhu and Y. Deng, *J. Phys. Chem. B*, 2005, **109**, 19542.
- (a) C. Thomazeau, H. Olivier-Bourbigou, L. Magna, S. Luts and B. Gilbert, *J. Am. Chem. Soc.*, 2003, **125**, 5264; (b) Y. Gu, J. Zhang, Z. Duan and Y. Deng, *Adv. Synth. Catal.*, 2005, **347**, 512.
- J. D. Holbrey and K. R. Seddon, *J. Chem. Soc., Dalton Trans.*, 1999, 2133.
- S. U. Lee, J. Jung and Y.-K. Han, *Chem. Phys. Lett.*, 2005, **406**, 332.
- J. Trace and G. S. Thomas, *J. Raman Spectrosc.*, 1995, **26**, 867.

# Acylation and carbanilation of cellulose in ionic liquids†‡

Susann Barthel and Thomas Heinze\*

Received 16th September 2005, Accepted 6th December 2005

First published as an Advance Article on the web 22nd December 2005

DOI: 10.1039/b513157j

Ionic liquids (ILs) namely 1-*N*-butyl-3-methylimidazolium chloride ( $[\text{C}_4\text{mim}]^+\text{Cl}^-$ ), 1-*N*-ethyl-3-methylimidazolium chloride ( $[\text{C}_2\text{mim}]^+\text{Cl}^-$ ), 1-*N*-butyldimethylimidazolium chloride ( $[\text{C}_4\text{dmim}]^+\text{Cl}^-$ ) and 1-*N*-allyl-2,3-dimethylimidazolium bromide ( $[\text{Admim}]^+\text{Br}^-$ ) were investigated as solvent for the homogeneous acylation and carbanilation of the biopolymer cellulose. Cellulose acetates with a degree of substitution (DS) in the range from 2.5 to 3.0 are accessible within 2 h at 80 °C in a complete homogeneous procedure. The acylation of cellulose with the fatty acid chloride lauroyl chloride leads to cellulose laurates with DS from 0.34 to 1.54. The reaction starts homogeneously and continues heterogeneously. The synthesis of cellulose carbanilates succeeds in the ionic liquid  $[\text{C}_4\text{mim}]^+\text{Cl}^-$  without any catalyst. The new homogeneous path gives pure cellulose carbanilates. All reactions are carried out under mild conditions, low excess of reagent and a short reaction time. The reaction media applied can be easily recycled and reused.

## Introduction

The renewable biopolymer cellulose has to be considered as raw material for the future. Cellulose is not only the most abundant organic polymer but also a very uniform macromolecule consisting of  $\beta$ -(1 $\rightarrow$ 4)-linked anhydroglucose repeating units. Cellulose is stereoregular, chiral, biocompatible and reactive. From the chemist's point of view a broad variety of chemical modification reactions both at the OH groups and the C atoms are possible. However, up to now product and hence property design by chemical modification is limited on some ethers and esters, which are produced commercially applying exclusively heterogeneous reaction conditions at least at the beginning of the conversion. Homogeneous paths of cellulose chemistry may open new avenues for the design of products with unconventional functional groups and with a controlled functionalization pattern.<sup>1,2</sup> Moreover, homogeneous synthesis paths provide opportunities to control the degree of substitution (DS) and they create more options to introduce novel functional groups including bulky and really exotic functions.<sup>3</sup> Although cellulose solvents like *N,N*-dimethylacetamide/LiCl<sup>4</sup> and dimethyl sulfoxide (DMSO)/tetrabutylammonium fluoride<sup>5,6</sup> have proved to be appropriate for the preparation of unconventional cellulose derivatives in lab scale procedure, various shortcomings contradict the commercial application as, *e. g.*, difficult and expensive

recycling, combustibility and reactivity like Swern oxidation in case of DMSO leading to undesired structures. Therefore, there is an increasing interest in new cellulose solvent that are efficient and recyclable. In this context, molten salt hydrates like  $\text{LiX}\cdot n\text{H}_2\text{O}$  ( $\text{X} = \text{I}^-, \text{NO}_3^-, \text{CH}_3\text{COO}^-, \text{ClO}_4^-$ ) were studied as solvent for cellulose.<sup>7</sup> Both the high dissolution temperature and the high amount of water results in problems during homogeneous functionalization of cellulose. In these solvents a rather high excess of reagent is needed in order to obtain a sufficient DS. Moreover, various side reactions appeared.<sup>8</sup>

Recently, ionic liquids (ILs) are in the focus of interest in various fields of research and development.<sup>9</sup> It was found by Swatowski *et al.*<sup>10,11</sup> that ILs, in particular 1-*N*-butyl-3-methylimidazolium ( $[\text{C}_4\text{mim}]^+$ ), combined with different anions dissolve cellulose. In particular  $[\text{C}_4\text{mim}]^+\text{Cl}^-$  seems to be the most efficient solvent. It was demonstrated that the homogeneous acetylation of cellulose in 1-allyl-3-methylimidazolium chloride yields cellulose acetates of high DS.<sup>12</sup> Furthermore,  $[\text{C}_4\text{mim}]^+\text{Cl}^-$  dissolves cellulose with a high degree of polymerization (DP) up to 1200 without degradation and acetylation reactions of the biopolymer can successfully be carried out.<sup>13</sup>

In this context we studied homogeneous phase chemistry of polysaccharides, especially the application of IL as reaction medium for cellulose functionalization. The combination of the renewable raw material cellulose with the recyclable IL was investigated to yield a contribution to environment protection. This paper deals with results for the acylation and carbanilation of the biopolymer cellulose.

## Experimental

### Materials

The cellulose samples used (Avicel, spruce sulfite pulp, cotton linters) were purchased from Fluka. After drying in vacuum at

*Institute of Organic Chemistry and Macromolecular Chemistry, Center of Excellence for Polysaccharide Research, Friedrich Schiller University of Jena, Humboldtstrasse 10, D-07743, Jena, Germany.*

*E-mail: Thomas.Heinze@uni-jena.de; Fax: +49 (0) 3641-948272;*

*Tel: +49 (0) 3641-948270*

† This work was presented at the 1st International Conference on Ionic Liquids (COIL), held in Salzburg, Austria, 19–22 June, 2005.

‡ Electronic supplementary information (ESI) available: <sup>1</sup>H and <sup>13</sup>C NMR spectra of the recycled IL and the starting material; and IR spectrum of the completely functionalized cellulose carbanilate; and <sup>13</sup>C NMR spectrum of a mixture of  $[\text{C}_4\text{mim}]^+\text{Cl}^-$  and phenyl isocyanate stirred for 2 h at 80 °C. See DOI: 10.1039/b513139a

100 °C for 12 h, the cellulose was used without any further purification. The IL 1-*N*-butyl-3-methylimidazolium chloride ([C<sub>4</sub>mim]<sup>+</sup>Cl<sup>-</sup>), mp 73 °C was employed as received from Solvent Innovation, Köln, Germany. 1-*N*-Ethyl-3-methylimidazolium chloride ([C<sub>2</sub>mim]<sup>+</sup>Cl<sup>-</sup>), mp 80 °C was obtained from the BASF AG, Ludwigshafen, Germany and used as purchased. The other ILs 1-*N*-butyl-2,3-dimethylimidazolium chloride ([C<sub>4</sub>dmim]<sup>+</sup>Cl<sup>-</sup>) and 1-*N*-allyl-2,3-dimethylimidazolium bromide ([Admim]<sup>+</sup>Br<sup>-</sup>) were synthesized by Dr A. Stark, Institute for Technical Chemistry and Environmental Chemistry, Friedrich Schiller University of Jena, Germany and used after freeze drying for 24 h. [C<sub>4</sub>dmim]<sup>+</sup>Cl<sup>-</sup> was prepared according to published procedures.<sup>14</sup> Acetyl chloride, acetic anhydride and lauroyl chloride (Merck) were used as obtained. All other chemicals were reagent grade and used without purification.

### Preparation of 1-*N*-allyl-2,3-dimethylimidazolium bromide

1,2-Dimethylimidazole (48.1 g; 0.5 mol) were carefully added to allyl bromide (72.9 g; 0.6 mol; 1.2 equivalents) dissolved in 100 ml of toluene under stirring. As the reaction may proceed strongly exothermic, an ice-bath must be used. After the addition, the temperature raises to 70 °C and a dark-red, second phase is formed. 20 ml acetonitrile were added and after stirring for 10 h at room temperature, the phases were separated and any volatiles were removed in vacuum from the lower phase. 50 ml of water were added and the aqueous solution was extracted with diethyl ether (5 × 20 ml). Water was removed and the product was dried in vacuum at 80 °C and 15 mbar for 12 h.

Yield: 108 g (91%); water content: 3.2 wt% (Karl-Fischer); organic impurities: >3 wt% (NMR spectroscopy); <sup>1</sup>H NMR (200 MHz, CDCl<sub>3</sub>, ppm vs. TMS): δ = 2.82 (s, 3H); 4.04 (s, 3H); 5.03 (d, 2H, J<sub>1</sub> = 5.86, J<sub>2</sub> = 1.46); 5.34 (m, 2H); 6.00 (m, 1H); 7.76 (dd, 2H, J<sub>1</sub> = 26.71, J<sub>2</sub> = 2.20); <sup>13</sup>C NMR (200 MHz, CDCl<sub>3</sub>, ppm vs. TMS): δ = 10.21; 35.40; 50.13; 119.77; 120.63; 122.22; 129.35; 143.35.

### Measurements

<sup>1</sup>H and <sup>13</sup>C NMR spectra were measured with a Bruker AC-250 and a Bruker AC-400 spectrometer by using a standard 5 mm probe at room temperature. The acylated cellulose samples (DS < 3.0) were measured after perpropionylation in chloroform-d<sub>1</sub> to determine the DS.

The intrinsic viscosities of the cellulose samples (starting material and regenerated sample) were measured by capillary viscosimetry according to DIN 54270 applying copper(II)-ethylenediamine (Cuen) as solvent. From the intrinsic viscosities the DP can be calculated according to the eqns (1)–(3).

$$[\eta] = \frac{(\eta_{\text{rel}} - 1)/c}{1 + K_n(\eta_{\text{rel}} - 1)} \quad (1)$$

$$M_w = ([\eta]/006)^{1/0.83} \quad (2)$$

$$\text{DP} = M_w/162 \quad (3)$$

where  $[\eta]$  is the intrinsic viscosity (ml g<sup>-1</sup>);  $[\eta_{\text{rel}}] = t/t_0$  is the relative viscosity;  $t$  is the flow rate of the solution (s);  $t_0$  is the

flow rate of the solvent (s);  $c$  is the concentration of the solution (g ml<sup>-1</sup>); and  $K_n$  is the instrument constant, where  $K_n = 0.29$ .

### Dissolution of the cellulose

For dissolution of the cellulose, the biopolymer was mixed with the molten IL and the temperature was increased to about 10 °C above the melting point of the IL applied. The mixture of cellulose/IL was stirred at this temperature up to 12 h to guarantee the complete dissolution.

### Acetylation of cellulose in [C<sub>4</sub>mim]<sup>+</sup>Cl<sup>-</sup>

1.09 ml acetyl chloride (5 mol mol<sup>-1</sup> anhydroglucose unit) were carefully added to a solution of 0.5 g (3.09 mmol) cellulose in 4.5 g [C<sub>4</sub>mim]<sup>+</sup>Cl<sup>-</sup> kept at 80 °C. The temperature was kept at 80 °C for 2 h. Isolation was carried out by precipitation of the product into 200 ml methanol (MeOH), washing with MeOH and finally drying under vacuum at 60 °C (sample A10).

Yield: 0.75 g (86%); DS<sub>Acetate</sub> = 3.0 (determined by means of <sup>1</sup>H NMR spectroscopy); IR (KBr): 2890 ν(CH), 1750 ν(C=O<sub>Ester</sub>) cm<sup>-1</sup>; <sup>13</sup>C NMR (DMSO-d<sub>6</sub>): δ = 168.9–170.2 (C=O), 62.1, 71.3, 75.9 and 99.2 ppm (cellulose backbone).

If pyridine was added, it was added before the addition of the acetylating agent.

### Acylation of cellulose with lauroyl chloride in [C<sub>4</sub>mim]<sup>+</sup>Cl<sup>-</sup>

Lauroyl chloride (2.14 ml, 9.27 mmol) was added to a solution of 0.5 g (3.09 mmol) cellulose in 4.5 g [C<sub>4</sub>mim]<sup>+</sup>Cl<sup>-</sup>. The reaction mixture was stirred for 2 h at 80 °C. The polymer was separated from the heterogeneous mixture formed by precipitation into 200 ml methanol. The polymer was collected by filtration. After washing three times with methanol, the polymer was dried in vacuum at 60 °C (A15).

Yield: 0.35 g (62.5%); DS<sub>Laur</sub> = 1.54 (determined by means of <sup>1</sup>H NMR spectroscopy after perpropionylation); IR (KBr): 3481 ν(OH), 2924, 2853 ν(CH), 1237 ν(COC<sub>Ester</sub>), 1748 ν(C=O<sub>Ester</sub>) cm<sup>-1</sup>; <sup>13</sup>C NMR (CDCl<sub>3</sub>): δ = 173. (CO), 100.4 (C-1), 101.6 (C-1'), 72.1 (C-2), 73.3 (C-3), 77.5 (C-4), 76.4 (C-5), 22.6–33.8 (C<sub>Methylene</sub>), 14.1 (C<sub>Methyl</sub>) ppm.

### Carbanilation of cellulose with phenyl isocyanate in [C<sub>4</sub>mim]<sup>+</sup>Cl<sup>-</sup>

A solution of 0.5 g (3.09 mmol) cellulose (Avicel) in 4.5 g [C<sub>4</sub>mim]<sup>+</sup>Cl<sup>-</sup> was kept at 80 °C and 3.57 g phenyl isocyanate (10 mol mol<sup>-1</sup> anhydroglucose unit) were carefully added. The temperature was kept at 80 °C for 2 h. After cooling, dry methanol (MeOH, 2 ml) was added to eliminate excess phenyl isocyanate and the mixture was precipitated into MeOH. After washing with MeOH, the cellulose carbanilate was dried under vacuum at 60 °C (sample A23).

Yield: 1.54 g (98.9%); DS<sub>N</sub> = 3.0 (determined by elemental analysis); IR (KBr): 3300 ν(NH), 2890 ν(CH), 1750 ν(C=O<sub>Ester</sub>), 1602 ν(C=C<sub>Phenyl</sub>) cm<sup>-1</sup>; <sup>13</sup>C NMR (DMSO-d<sub>6</sub>): δ = 152.2 (C=O), 11.5–138.5 (phenyl), 62.1–99.2 (cellulose backbone) ppm.

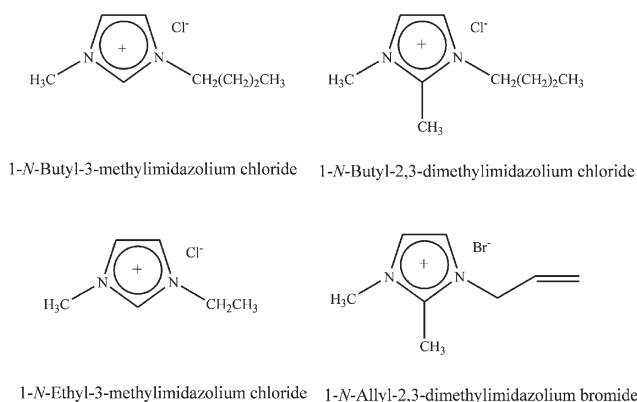


Fig. 1 The structure of the ILs used in these studies.

## Results and discussion

ILs dissolve cellulose.<sup>10,11</sup> Recently it was shown that a homogeneous acetylation of the biopolymer can be carried out.<sup>12,13</sup> It was found that not only does 1-*N*-butyl-3-methylimidazolium chloride ( $[\text{C}_4\text{mim}]^+\text{Cl}^-$ ) dissolve the biopolymer cellulose to a high concentration compared to other solvents (Fig. 1, Table 1) but also 1-*N*-ethyl-3-methylimidazolium chloride ( $[\text{C}_2\text{mim}]^+\text{Cl}^-$ ), 1-*N*-butyl-2,3-dimethylimidazolium chloride ( $[\text{C}_4\text{dmim}]^+\text{Cl}^-$ ) and 1-*N*-allyl-2,3-dimethylimidazolium bromide ( $[\text{Admim}]^+\text{Br}^-$ ) are appropriate solvents for the biopolymer. A solution of

cellulose in different ILs can be obtained at 80 °C under permanent stirring. It was observed that the amount of dissolved polymer decreases with increasing DP, 290 to 1200.

Moreover, the amount of cellulose in the solution depends on the type of IL (Table 1).  $[\text{C}_4\text{mim}]^+\text{Cl}^-$  is the most efficient solvent for the biopolymer, *i.e.* a solution of the highest concentration can be obtained.  $[\text{C}_2\text{mim}]^+\text{Cl}^-$  and  $[\text{Admim}]^+\text{Br}^-$  dissolve less polymer compared to  $[\text{C}_4\text{mim}]^+\text{Cl}^-$ . With regard to applications like fiber production, it is worth mentioning that  $[\text{C}_4\text{dmim}]^+\text{Cl}^-$  and  $[\text{Admim}]^+\text{Br}^-$  could easily be separated from the regenerated cellulose.

The DP values both of the starting cellulose and the regenerated samples were determined by capillary viscometry in Cuen. No degradation during the dissolution process appears independent of the cellulose type applied.

The ILs can be easily recycled as a hygroscopic liquid. In order to receive a sample that dissolves cellulose it is necessary to dry the IL. Freeze drying leads to water free solids. The removal of water is an essential prerequisite to avoid side reactions. The recycled IL had the same efficiency to dissolve cellulose compared to the starting IL.

To investigate the reactivity of the cellulose dissolved in IL, the acylation with acetyl and lauroyl chloride and with acetic anhydride was studied. Highly substituted cellulose acetates were obtained (Table 2) by applying acetyl chloride and acetic anhydride as reagent. DS values in the range from 2.5 to 3.0 can be achieved independent of the type of cellulose. It is even

Table 1 Solubility and DP of the cellulose samples in ILs:  $[\text{C}_4\text{mim}]^+\text{Cl}^-$ ,  $[\text{C}_2\text{mim}]^+\text{Cl}^-$ ,  $[\text{C}_4\text{dmim}]^+\text{Cl}^-$  and  $[\text{Admim}]^+\text{Br}^-$

Cellulose type	DP	Solubility in							
		$[\text{C}_4\text{mim}]^+\text{Cl}^-$		$[\text{C}_2\text{mim}]^+\text{Cl}^-$		$[\text{C}_4\text{dmim}]^+\text{Cl}^-$		$[\text{Admim}]^+\text{Br}^-$	
		%	DP <sup>a</sup>	%	DP <sup>a</sup>	%	DP <sup>a</sup>	%	DP <sup>a</sup>
Avicel	286	18	307	12	329	9	377	12	320
Spruce sulfite pulp	593	13	544	6	580	6	622	4	599
Cotton linters	1198	10	812	4	1181	4	1102	4	1203

<sup>a</sup> After regeneration.

Table 2 DS and solubility of the cellulose acetates homogeneously prepared in different ionic liquids (reaction temperature 80 °C)

No.	Cellulose type	Reaction medium	Acetylation reagent		Time min	DS <sup>b</sup>	Solubility <sup>c</sup>	
			Type	Mol per mol AGU			(CH <sub>3</sub> ) <sub>2</sub> SO	CHCl <sub>3</sub>
A1	Avicel	$[\text{C}_4\text{mim}]^+\text{Cl}^-$	Acetic anhydride	3.0	120	1.87	+	–
A2	Avicel	$[\text{C}_4\text{mim}]^+\text{Cl}^-$	Acetic anhydride	5.0	120	2.72	+	–
A3	Avicel	$[\text{C}_4\text{mim}]^+\text{Cl}^-$	Acetic anhydride	3.0 <sup>a</sup>	120	2.56	+	–
A4	Avicel	$[\text{C}_4\text{mim}]^+\text{Cl}^-$	Acetic anhydride	5.0 <sup>a</sup>	120	2.94	+	+
A5	Avicel	$[\text{C}_4\text{mim}]^+\text{Cl}^-$	Acetic anhydride	10.0 <sup>a</sup>	120	3.0	+	+
A6	Avicel	$[\text{C}_4\text{mim}]^+\text{Cl}^-$	Acetyl chloride	5.0 <sup>a</sup>	120	2.93	+	–
A7	Avicel	$[\text{C}_4\text{mim}]^+\text{Cl}^-$	Acetyl chloride	3.0	120	2.81	+	–
A8	Avicel	$[\text{C}_4\text{mim}]^+\text{Cl}^-$	Acetyl chloride	5.0	15	2.93	+	+
A9	Avicel	$[\text{C}_4\text{mim}]^+\text{Cl}^-$	Acetyl chloride	5.0	30	3.0	+	+
A10	Avicel	$[\text{C}_4\text{mim}]^+\text{Cl}^-$	Acetyl chloride	5.0	120	3.0	+	+
A11	Avicel	$[\text{C}_2\text{mim}]^+\text{Cl}^-$	Acetic anhydride	3.0	120	3.0	+	–
A12	Avicel	$[\text{C}_4\text{dmim}]^+\text{Cl}^-$	Acetic anhydride	3.0	120	2.92	+	–
A13	Avicel	$[\text{Admim}]^+\text{Br}^-$	Acetic anhydride	3.0	120	2.67	–	–
B1	Spruce sulfite pulp	$[\text{C}_4\text{mim}]^+\text{Cl}^-$	Acetyl chloride	3.0	120	3.0	+	+
B2	Spruce sulfite pulp	$[\text{C}_4\text{mim}]^+\text{Cl}^-$	Acetyl chloride	5.0	120	3.0	+	+
C1	Cotton linters	$[\text{C}_4\text{mim}]^+\text{Cl}^-$	Acetyl chloride	3.0	120	2.85	+	+
C2	Cotton linters	$[\text{C}_4\text{mim}]^+\text{Cl}^-$	Acetyl chloride	5.0	120	3.0	+	+

<sup>a</sup> Additionally, 2.5 mol pyridine per mol AGU. <sup>b</sup> DS of the ester obtained determined *via* <sup>1</sup>H NMR spectroscopy. <sup>c</sup> + Soluble; – insoluble.

possible to synthesize cellulose acetate samples directly in  $[\text{C}_4\text{mim}]^+\text{Cl}^-$  without any additional base. At a molar ratio of 5.0 mol acetyl chloride per mol anhydroglucose unit (AGU), the reaction leads to completely functionalized cellulose acetate within 2 h at 80 °C (Table 2, **A10**, **B2**, **C2**). The cellulose acetate samples synthesized are soluble in DMSO. Starting from  $\text{DS} > 2.85$  they dissolve in chloroform. However, the cellulose acetates are not soluble in acetone, which is an important solvent from a technical point of view, especially for fiber spinning.

Comparing the acetylating reagents, it was found that acetyl chloride is more effective than acetic anhydride at a comparable molar ratio. With acetic anhydride, a cellulose acetate with a DS of 2.72 (**A2**) was obtained while acetyl chloride leads to complete acetylation ( $\text{DS} = 3$ , samples **A9–A11**, Table 2) even with a short reaction time of 30 min. The DS values of the cellulose acetate samples are slightly higher (compare **A3** and **A4** with **A1** and **A2**) if the base pyridine is used additionally. An amazing result was that a different solubility was found at similar DS value (**A6**, **A10**). The reaction in the presence of pyridine yields the acidic pyridinium hydrochloride, which may lead to a partial deacetylation of the samples and hence to a alternative distribution of functional groups resulting in different solubility. The acetylation of cellulose dissolved in  $[\text{C}_2\text{mim}]^+\text{Cl}^-$ ,  $[\text{C}_4\text{dmim}]^+\text{Cl}^-$  or  $[\text{Admim}]^+\text{Br}^-$  was also successful, however, different DS values under comparable conditions were reached indicating an influence of the IL on the reactivity of the polymer (Table 2). The reactivity of cellulose increases in the order  $[\text{C}_4\text{mim}]^+\text{Cl}^- < [\text{Admim}]^+\text{Br}^- < [\text{C}_4\text{dmim}]^+\text{Cl}^- < [\text{C}_2\text{mim}]^+\text{Cl}^-$  at a molar ratio of 3.0 mol acetic anhydride per mol AGU (see samples **A1**, **A11**, **A12**, **A13**). The IL can be easily recycled and the by-products were completely separated by washing with methanol.  $^1\text{H}$  and  $^{13}\text{C}$  NMR studies of the IL after recycling show no differences with the starting solvent.

The cellulose acetates synthesized by Wu *et al.*<sup>12</sup> with acetic anhydride in 1-*N*-allyl-3-methylimidazolium chloride ( $[\text{Amim}]^+\text{Cl}^-$ ) possess lower DS values than the cellulose derivatives prepared in  $[\text{C}_4\text{mim}]^+\text{Cl}^-$ ,  $[\text{C}_2\text{mim}]^+\text{Cl}^-$ ,  $[\text{C}_4\text{dmim}]^+\text{Cl}^-$  or  $[\text{Admim}]^+\text{Br}^-$  even by using lower molar ratio. An acetylation in  $[\text{Amim}]^+\text{Cl}^-$  leads to DS values of 1.61 (after 1 h), 1.86 (after 2 h) and reaches 2.49 after 8 h of reaction time.<sup>12</sup> Thus the ILs applied in our studies are more efficient for homogeneous acetylation of cellulose. Higher substituted cellulose acetates (Table 2) are obtained applying a lower molar ratio and shorter reaction time (2 h). Moreover, the acetylation of cellulose dissolved in DMA/LiCl<sup>15</sup> indicates that cellulose acetates with a DS from 1.0 to 2.94 can be synthesized within 2 h at 80 °C. Comparison of DMA/LiCl and IL as solvent for homogeneous acetylation confirms the high efficiency of the IL.

In a next set of experiments, acylation of cellulose with long-chain aliphatic acids was investigated. The acylation of cellulose dissolved in IL applying lauroyl chloride for 2 h at 80 °C starts homogeneously, however, the cellulose laurate precipitates during the reaction. Cellulose laurates with DS values in the range from 0.34 to 1.54 were obtained using  $[\text{C}_4\text{mim}]^+\text{Cl}^-$  as medium and 1–5 mol acid chloride per mol AGU (**A14**, **A15**, **A16**, Table 3). The cellulose laurates are

**Table 3** DS of the cellulose laurates prepared in different ionic liquids with lauroyl chloride for 2 h at 80 °C (cellulose Avicel)

No.	Solvent	Molar ratio <sup>a</sup>	DS <sup>b</sup>
<b>A14</b>	$[\text{C}_4\text{mim}]^+\text{Cl}^-$	1.0/1.0	0.34
<b>A15</b>	$[\text{C}_4\text{mim}]^+\text{Cl}^-$	1.0/3.0	1.54
<b>A16</b>	$[\text{C}_4\text{mim}]^+\text{Cl}^-$	1.0/5.0	1.44
<b>A17</b>	$[\text{C}_2\text{mim}]^+\text{Cl}^-$	1.0/3.0	0.77
<b>A18</b>	$[\text{C}_4\text{dmim}]^+\text{Cl}^-$	1.0/3.0	0.36
<b>A19</b>	$[\text{Admim}]^+\text{Br}^-$	1.0/3.0	0.12

<sup>a</sup> Mol anhydroglucose unit per mol lauroyl chloride. <sup>b</sup> DS of the cellulose laurate determined by  $^1\text{H}$  NMR spectroscopy after perpropionylation.

soluble in chloroform but do not dissolve in DMSO and acetone. A cellulose laurate with DS of 3.0 was not accessible under the conditions used, which may be due to the formation of a heterogeneous system. The differences in reactivity found for the ILs applied as reaction medium may also result from the partially heterogeneous path (Table 3). Additional studies are necessary to explore the carboxylic acids that can be reacted with cellulose under totally homogeneous conditions.

Summarizing the results, it becomes obvious that the reactivity of cellulose dissolved in the ILs,  $[\text{C}_4\text{mim}]^+\text{Cl}^-$ ,  $[\text{C}_2\text{mim}]^+\text{Cl}^-$ ,  $[\text{C}_4\text{dmim}]^+\text{Cl}^-$  and  $[\text{Admim}]^+\text{Br}^-$  depends on the IL in question, the acylation agent (acetic anhydride *versus* acetyl chloride) and on the state of dissolution/dispersion as found with lauroyl chloride (Fig. 2). ILs are interesting and efficient reaction media yielding products of high DS values using acetic anhydride (**A1**, **A11**, **A12**, **A13**). Acetyl chloride as acetylating reagent and  $[\text{C}_4\text{mim}]^+\text{Cl}^-$  as reaction medium lead to cellulose acetate with a DS = 2.81 (**A7**). In contrast, the application of acetyl chloride in  $[\text{C}_2\text{mim}]^+\text{Cl}^-$ ,  $[\text{C}_4\text{dmim}]^+\text{Cl}^-$  and  $[\text{Admim}]^+\text{Br}^-$  yields both degradation of the IL and the polymer.

Cellulose can be smoothly reacted with phenyl isocyanate in a dipolar aprotic medium in the presence of pyridine forming the cellulose tricarbonyl. Although the conversion needs a large excess of phenyl isocyanate only negligible chain degradation occurs and almost no by-product is formed. The excess of phenyl isocyanate can be decomposed by addition of dry methanol. Terbojevich *et al.* studied the carbanilation of cellulose homogeneously using DMA/LiCl as solvent and

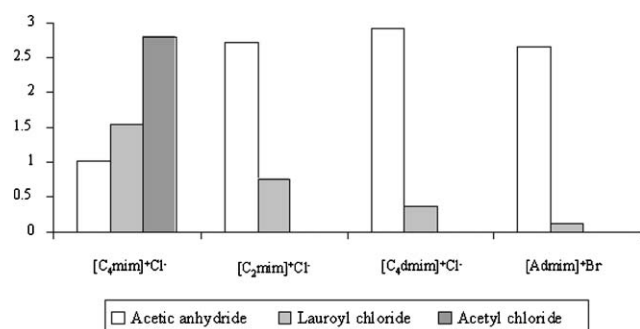


**Fig. 2** Representation of the DS values of the acylated cellulose samples, comparison of the acylating reagents (acetic anhydride, lauroyl chloride, acetyl chloride), synthesized at 80 °C within 2 h in different ILs with a molar ratio 1.0/3.0 (mol anhydroglucose unit per mol acylating reagent).



found that a number of advantages like large reaction rate and good yield under relatively mild conditions appeared.<sup>16</sup> The soluble cellulose derivative is well suited for the determination of the molar mass distribution applying size exclusion chromatography (SEC).<sup>17</sup> Moreover, cellulose carbanilates were included in studies about the state of dissolution.<sup>18</sup> Cellulose tricarbaniates with various functional groups in the aromatic moiety form lyotropic liquid crystalline mesophases<sup>19,20</sup> and they may separate enantiomers.<sup>21,22</sup>

In the frame of our studies applying ILs as reaction medium, carbanilation of cellulose dissolved in  $[\text{C}_4\text{mim}]^+\text{Cl}^-$  with phenyl isocyanate was investigated. The results show that cellulose carbanilates can be synthesized directly in  $[\text{C}_4\text{mim}]^+\text{Cl}^-$  without an additional catalyst. DS values in the range from 0.26 to 3.0 were reached depending on the molar ratio and the reaction time (Table 4). A DS of about 0.5–0.6 resulted applying a molar ratio of 1.0 mol phenyl isocyanate to 1.0 mol AGU after conversion for 120 min at 80 °C. Only spruce sulfite pulp shows a significantly lower reactivity (compare samples **A1**, **B1**, **C1**, Table 4). The different reactivity in  $[\text{C}_4\text{mim}]^+\text{Cl}^-$  of both Avicel and cotton linters, on one hand, and of spruce sulfite pulp, on the other, may be caused by the hemicellulose present in the pulp. Further studies are in progress to get a satisfactory explanation of this effect. Cellulose carbanilates with higher DS up to a complete functionalization are accessible by increasing molar ratio and reaction time. In contrast to low DS values, the complete functionalization occurs with all cellulose types studied. The IR spectrum of the completely functionalized sample (**A24**) shows the typical signals for the carbanilated cellulose at 3391  $\nu(\text{NH})$ , 3317  $\nu(\text{CH})$ , 1735  $\nu(\text{C}=\text{O}_{\text{Ester}})$  and 1601  $\nu(\text{C}=\text{C}_{\text{Phenyl}})$   $\text{cm}^{-1}$ . The solubility of the cellulose derivatives depends on the DS (Table 4).

**Table 4** DS, determined *via* elemental analysis and solubility (+ soluble; – insoluble) of cellulose carbanilate samples homogeneously prepared with phenyl isocyanate in 1-*N*-butyl-3-methylimidazolium chloride (reaction temperature 80 °C)

No. <sup>a</sup>	Molar ratio <sup>b</sup>	Time/min	DS	Solubility <sup>c</sup>		
				DMSO	THF	DMF
<b>A20</b>	1.0	120	0.60	+	–	–
<b>A21</b>	3.0	120	2.74	+	+	+
<b>A22</b>	5.0	120	2.97	+	+	+
<b>A23</b>	10.0	120	3.0	+	+	+
<b>A24</b>	10.0	240	3.0	+	+	+
<b>A24</b>	5.0	15	0.82	–	–	–
<b>A26</b>	5.0	30	1.24	–	–	–
<b>A27</b>	5.0	45	1.69	+	–	–
<b>A28</b>	5.0	60	2.30	+	+	–
<b>B3</b>	1.0	120	0.26	–	–	–
<b>B4</b>	3.0	120	1.46	+	–	+
<b>B5</b>	5.0	120	2.39	+	+	+
<b>B6</b>	10.0	120	2.55	+	+	+
<b>B7</b>	10.0	240	3.0	+	+	+
<b>C3</b>	1.0	120	0.50	+	–	–
<b>C4</b>	3.0	120	2.08	+	+	+
<b>C5</b>	5.0	120	2.48	+	+	+
<b>C6</b>	10.0	120	2.75	+	+	+
<b>C7</b>	10.0	240	3.0	+	+	+

<sup>a</sup> Cellulose type: **A**: Avicel, **B**: spruce sulfite pulp, **C**: cotton linters.

<sup>b</sup> Mol phenyl isocyanate per mol anhydroglucose unit. <sup>c</sup> Dimethyl sulfoxide, tetrahydrofuran, *N,N*-dimethyl formamide.

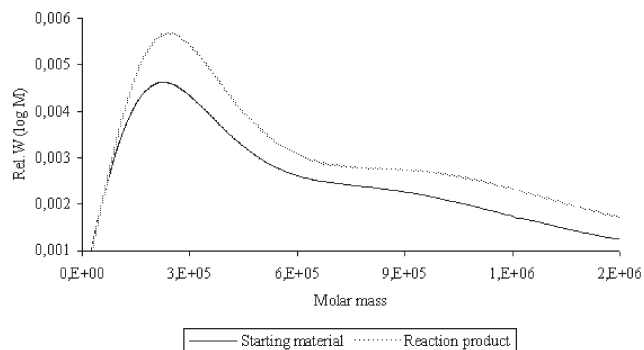


**Fig. 3** Comparison of the size exclusion chromatographic curves of the starting material (spruce sulfite pulp) heterogeneously carbanilated in pyridine and the cellulose carbanilate obtained in  $[\text{C}_4\text{mim}]^+\text{Cl}^-$  (**B7**).

Cellulose carbanilates with DS > 2.4 are completely soluble in DMSO, DMF, and THF.

The reaction of cellulose in ILs with phenyl isocyanate may be connected with the liberation of  $\text{CO}_2$  and the formation of aniline which is generated by the reaction of phenyl isocyanate with water present in the IL. The aniline formed was verified by  $^{13}\text{C}$  NMR spectroscopy showing the typical peaks at 117, 129, 134 and 149 ppm (phenyl). The aniline can be simply removed from the cellulose carbanilate and from the IL by washing with a mixture of MeOH/ $\text{H}_2\text{O}$  (90/10). The recycled  $[\text{C}_4\text{mim}]^+\text{Cl}^-$  dissolves the cellulose and can be used for the conversion again. A freeze drying is necessary to reduce the water content to obtain an IL that dissolves cellulose.

The cellulose tricarbaniates obtained were studied regarding their molecular mass by the means of SEC (Fig. 3). For the cellulose tricarbaniate **B7** synthesized in ILs a molecular mass and a molecular mass distribution were found that are comparable with the values of the starting material measured after heterogeneous carbanilation in pyridine.

## Conclusion

The ionic liquids  $[\text{C}_4\text{mim}]^+\text{Cl}^-$ ,  $[\text{C}_2\text{mim}]^+\text{Cl}^-$ ,  $[\text{C}_4\text{dmim}]^+\text{Cl}^-$  and  $[\text{Admim}]^+\text{Br}^-$  dissolve cellulose with a DP of up to 1200. The dissolution process occurs without a significant degradation of the polymer chain. Thus, ionic liquids are interesting cellulose solvents both for shaping and as reaction medium for homogeneous functionalization of the polysaccharide. It was shown that cellulose acetates with different DS can be obtained by varying the molar ratio and the reaction time in a completely homogeneous synthesis. In the case of preparation of cellulose laurates, the reaction starts homogeneously leading to a heterogeneous system during the acylation. Furthermore, the IL  $[\text{C}_4\text{mim}]^+\text{Cl}^-$  can be used as medium for the homogeneous carbanilation of cellulose. Preparation of further cellulose derivatives including cellulose esters of different aliphatic and aromatic acids and detailed studies about the interaction cellulose/solvent are under investigation.

## Acknowledgements

S. Barthel would like to thank the “Deutsche Bundesstiftung Umwelt” Osnabrück, Germany for a scholarship. The authors

thank Dr Annegret Stark, Institute for Technical Chemistry and Environmental Chemistry, Friedrich Schiller University of Jena, Germany for preparing the ionic liquids  $[\text{C}_4\text{dmim}]^+\text{Cl}^-$  and  $[\text{Admim}]^+\text{Br}^-$ . The general support of the ‘‘Forschungsvereinigung Werkstoffe aus nachwachsenden Rohstoffen e.V. Rudolstadt’’, Rudolstadt, Germany is gratefully acknowledged.

## References

- 1 D. Klemm, B. Philipp, T. Heinze, U. Heinze and W. Wagenknecht, *Comprehensive Cellulose Chemistry*, Wiley-VCH, 2001.
- 2 T. Heinze, *Chemical Functionalization of Cellulose*, in *Poly-saccharide: Structural Diversity and Functional Versatility*, ed. S. Dumitriu, Marcel Dekker, New York, Basel, Hong Kong, 2nd edn, 2004, p. 551.
- 3 T. Heinze and T. Liebert, *Prog. Polym. Sci.*, 2001, **26**, 1689.
- 4 S. L. Williamson and C. L. McCormick, *J. Macromol. Sci., Pure Appl. Chem.*, 1998, **A35**, 1915.
- 5 T. Heinze, R. Dicke, A. Koschella, A. H. Kuhl, E. A. Klohr and W. Koch, *Macromol. Chem. Phys.*, 2000, **201**, 627.
- 6 M. A. Hussain, T. Liebert and T. Heinze, *Macromol. Rapid Commun.*, 2004, **25**, 916.
- 7 S. Fischer, W. Voigt and K. Fischer, *Cellulose*, 1999, **6**, 213.
- 8 S. Fischer, *Habilitation Thesis*, University of Freiberg, Germany, 2003.
- 9 T. Welton, *Chem. Rev.*, 1999, **99**, 2071; H. Zhao and S. V. Malhorta, *Aldrichimica Acta*, 2002, **35**, 75; P. Wasserscheid and T. Welton, *Ionic Liquids in Synthesis*, Wiley-VCH, Weinheim, 2003.
- 10 WO 03/029329, The University of Alabama, invs: R. P. Swatloski, S. K. Spear and J. D. Holbrey, *Chem. Abstr.*, 2003, **138**, 289216.
- 11 R. P. Swatloski, S. K. Spear, J. D. Holbrey and R. D. Rogers, *J. Am. Chem. Soc.*, 2002, **124**, 4974.
- 12 J. Wu, J. Zhang, H. Zhang, J. He, Q. Ren and M. Guo, *Biomacromolecules*, 2004, **5**, 266.
- 13 T. Heinze, K. Schwikal and S. Barthel, *Macromol. Biosci.*, 2005, **5**, 520.
- 14 P. B. Webb, M. F. Sellin, T. E. Kunen, S. Williamson, A. M. Z. Slawin and D. J. Cole-Hamilton, *J. Am. Chem. Soc.*, 2003, **125**, 15577.
- 15 T. Heinze, T. Liebert, K. Pfeiffer and M. A. Hussain, *Cellulose*, 2003, **10**, 283.
- 16 M. Terbojevich, A. Cosani, M. Camilot and B. Focher, *J. Appl. Polym. Sci.*, 1995, **55**, 1663.
- 17 B. Saake, R. Patt, J. Puls and B. Philipp, *Papier (Darmstadt)*, 1991, **45**, 727.
- 18 W. Burchard and L. Schulz, *Papier (Darmstadt)*, 1989, **43**, 665.
- 19 P. Zugenmaier, K. Schmidt and F. I. Hildebrandt, *ACS Symp. Ser.*, 1999, **737**, 127.
- 20 W. Mormann and C. Kuckertz, *Macromol. Symp.*, 2002, **181**, 113.
- 21 X. Chen, L. Yang, H. Zou, Q. Zhang and J. Ni, *Fenxi Huaxue*, 2000, **28**, 1074.
- 22 E. Yashima, J. Naguchi and Y. Okamoto, *Macromolecules*, 1995, **28**, 8368.

# HMImPF<sub>6</sub> ionic liquid that separates the azeotropic mixture ethanol + heptane†

A. B. Pereiro,<sup>a</sup> E. Tojo,<sup>b</sup> A. Rodríguez,\*<sup>a</sup> J. Canosa<sup>a</sup> and J. Tojo‡<sup>a</sup>

Received 14th September 2005, Accepted 6th February 2006

First published as an Advance Article on the web 21st February 2006

DOI: 10.1039/b513079d

1-Hexyl-3-methylimidazolium hexafluorophosphate (HMImPF<sub>6</sub>) is suitable for use as the solvent in the petrochemical extraction process for the removal of heptane from its azeotropic mixture with ethanol. The experimental determination of the liquid–liquid equilibrium (LLE) for the ternary system heptane + ethanol + HMImPF<sub>6</sub> at 298.15 K was carried out. The solute distribution ratio and the selectivity of the HMImPF<sub>6</sub> have been determined from the tie-line data. A comparative study has been made in terms of selectivity and solute distribution data with other ionic liquids. The NRTL equation was verified to accurately correlate the experimental data.

## Introduction

Nowadays, ionic liquids (ILs) are gaining wide recognition as potential environmental solvents due to their unique properties. ILs defined as organic salts containing an organic cation are liquids over a wide temperature range and present excellent solvation properties. A major reason for the interest in ILs is their negligible vapor pressure, which decreases the risk of worker exposure and the loss of solvent to the atmosphere.

Several separation and product recovery techniques employing ILs are currently under investigation. In the case of azeotropic systems a separation by ordinary distillation becomes impossible. Extractive distillation is the separation process most widely used to remove one of the components in the azeotropic system. The addition of a new solvent (entrainer) is used to interact with the components of the original mixture altering their relative volatilities. Thus, the mixture containing an azeotrope is separated into the desired pure components.

In general, distillation processes need energy to create a fluid phase system (liquid, vapor). However, the liquid–liquid separation based on the immiscibility between two liquid phases that exhibits preferential affinity or selectivity towards one or more of the components in the feed, emerges as a beneficial separation process reducing the energy consumption and the environmental impact with regard to the use of volatile organic solvents as entrainer to break the binary azeotrope avoiding the possible solvent loss to the atmosphere.

In this paper, liquid extraction has been proposed as a promising recovery technique for the separation of heptane from the azeotropic mixture with ethanol and as an alternative to the conventional extractive distillation taking into account the experimental LLE diagram at 298.15 K. The mass transfer

operation consists of the removal of heptane from the azeotropic system with ethanol by contact with HMImPF<sub>6</sub> forming two immiscibility phases, one of them rich in one of the desired products (heptane), the extract and the raffinate, the residual feed containing the HMImPF<sub>6</sub> and ethanol. The IL is a good candidate for separating azeotropic mixtures because it is mostly soluble in ethanol and it is practically immiscible in heptane. By distillation under low pressure the IL was removed from ethanol and re-used as solvent in the extractive process, reducing the volatile organic solvent consumption.

## Results and discussion

### Liquid–liquid equilibrium

LLE was studied for the ternary mixture (heptane + ethanol + HMImPF<sub>6</sub>) at 298.15 K. The experimental tie-lines were determined in a jacketed glass vessel containing a magnetic stirrer connected to a temperature controlled circulating bath (controlled to 0.01 K). The vessel was closed to moisture and could be flushed with dry nitrogen. Temperature in the cell was measured with a F200 ASL digital thermometer with an uncertainty of 0.01 K. The measurements were started with the addition of 100 ml of immiscible ternary mixture with known composition to the vessel, the temperature was adjusted and the mixture was stirred vigorously during 1 h and left to settle for 4 h. Samples were taken by a syringe from the upper and lower phases. A series of LLE measurements were made over the entire composition range.

Tie-line compositions were determined by measuring the density and applying the corresponding fitting polynomials. Experimental densities were used to determine the phase composition at 298.15 K using an Anton Paar DMA 46 digital vibrating tube density meter. The precision of the technique for the determination of the tie-line composition was  $\pm 0.001$  mole fraction.

The LLE was determined by two techniques: the experimental determination of the tie-lines that shows us the composition of each layer and the determination of the

<sup>a</sup>Chemical Engineering, Vigo University, P. O. Box 36310, Vigo, Spain. E-mail: aroque@uvigo.es; Tel: +34 986 81 23 12

<sup>b</sup>Organic Chemistry Department, Vigo University, P. O. Box 36310, Vigo, Spain

† This work was presented at the 1st International Conference on Ionic Liquids (COIL), held in Salzburg, Austria, 19–22 June, 2005.

‡ This paper is dedicated to the memory of Prof. José Tojo who recently passed away.

**Table 1** Composition of the experimental tie-lines, solute distribution ratio ( $\beta$ ) and selectivity ( $S$ ) for the system heptane (1) + ethanol (2) + HMImPF<sub>6</sub> (3) at 298.15 K

$x_1^I$	$x_2^I$	$x_1^{II}$	$x_2^{II}$	$\beta$	$S$
0.992	0.008	0.000	0.207	25.6	25 349
0.974	0.026	0.000	0.315	12.0	11 666
0.862	0.138	0.000	0.459	3.3	2831
0.857	0.143	0.000	0.473	3.3	2568
0.843	0.157	0.000	0.478	3.0	1062
0.662	0.338	0.000	0.543	1.6	493.4
0.492	0.508	0.000	0.570	1.1	310.6
0.463	0.537	0.000	0.573	1.1	551.2
0.428	0.572	0.000	0.580	1.0	433.7
0.381	0.619	0.000	0.586	0.9	360.5
0.343	0.657	0.000	0.594	0.9	231.5
0.279	0.721	0.000	0.599	0.8	196.8
0.244	0.756	0.000	0.610	0.8	171.9
0.216	0.783	0.000	0.622	0.8	84.71
0.117	0.883	0.000	0.638	0.7	43.42
0.062	0.938	0.000	0.685	0.7	8.47
0.045	0.950	0.000	0.710	0.7	4.33

binodal curve that shows the immiscible region of the ternary system.

The binodal curve was determined by adding known quantities of the three components corresponding to the immiscible region into the equilibrium cell. Then, we added slowly known quantities of ethanol maintaining the stirring until the “cloud point”.

The tie-lines of the ternary LLE were determined at 298.15 K. The measured composition of the experimental tie-line ends for the ternary system are reported in Table 1. A triangular diagram containing the experimental tie-lines is presented for the ternary system in Fig. 1.

An examination of Fig. 1 indicates a wide immiscibility region as well as a reverse slope of the tie-lines that is just typical in the solutropic<sup>1</sup> mixtures. The IL as solvent would be favourable for the azeotropic mixture separation close to the heptane vertex.

### Selectivity and solute distribution ratio

The selectivity ( $S$ ) and solute distribution ratio ( $\beta$ ) were determined from the tie-lines data at 298.15 K.  $S$  indicates the HMImPF<sub>6</sub> capability to remove heptane from the azeotropic mixture.  $\beta$  compares the feasible of HMImPF<sub>6</sub> and heptane to solvate ethanol. These parameters are defined by the following expressions,

$$S = \frac{x_1^I x_2^{II}}{x_1^{II} x_2^I} \quad (1)$$

$$\beta = \frac{x_2^{II}}{x_2^I} \quad (2)$$

where  $x$  is the mole fraction, 1 and 2 refer to heptane and ethanol composition, respectively and superscripts I and II indicate the poor and rich phases in the IL, respectively.  $S$  and  $\beta$  values are shown in Table 1.

Fig. 2a and 2b show the selectivity and solute distribution ratio plotted against ethanol mole fraction in the IL rich phase as well as the data taken from the literature<sup>2</sup> for the azeotropic system involving 1-methyl-3-octylimidazolium chloride (MeOctImCl) as solvent, respectively. In this case, higher values of selectivity are reached with HMImPF<sub>6</sub>. A reason for it may be the excellent capability of HMImPF<sub>6</sub> to solvate alcohols.

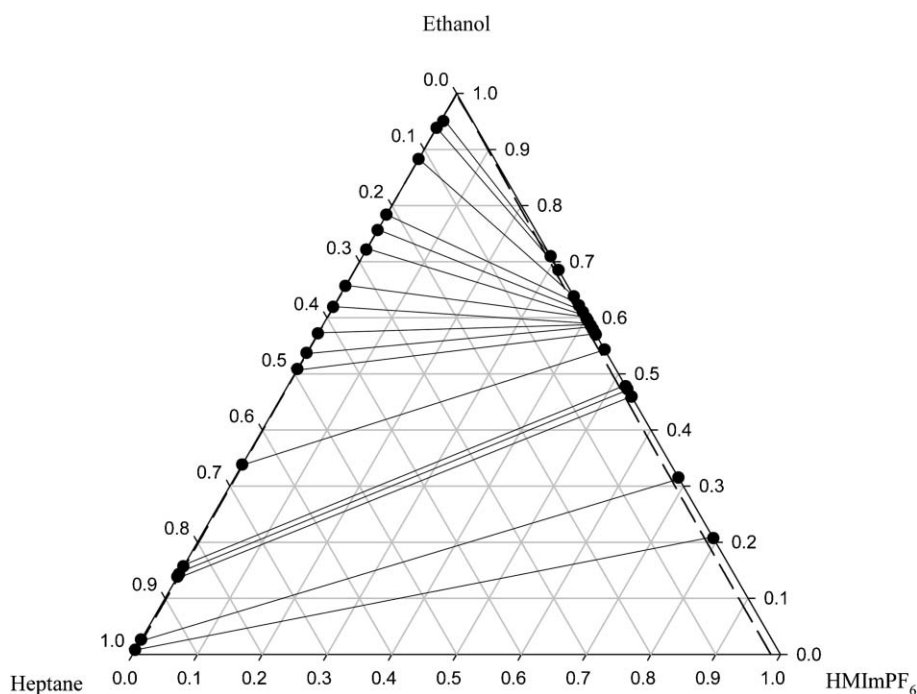


**Fig. 1** Experimental tie-lines (●, solid line) for LLE of the ternary system heptane + ethanol + HMImPF<sub>6</sub> at 298.15 K. The corresponding binodal curve is correlated by means of the NRTL equation (dashed line).

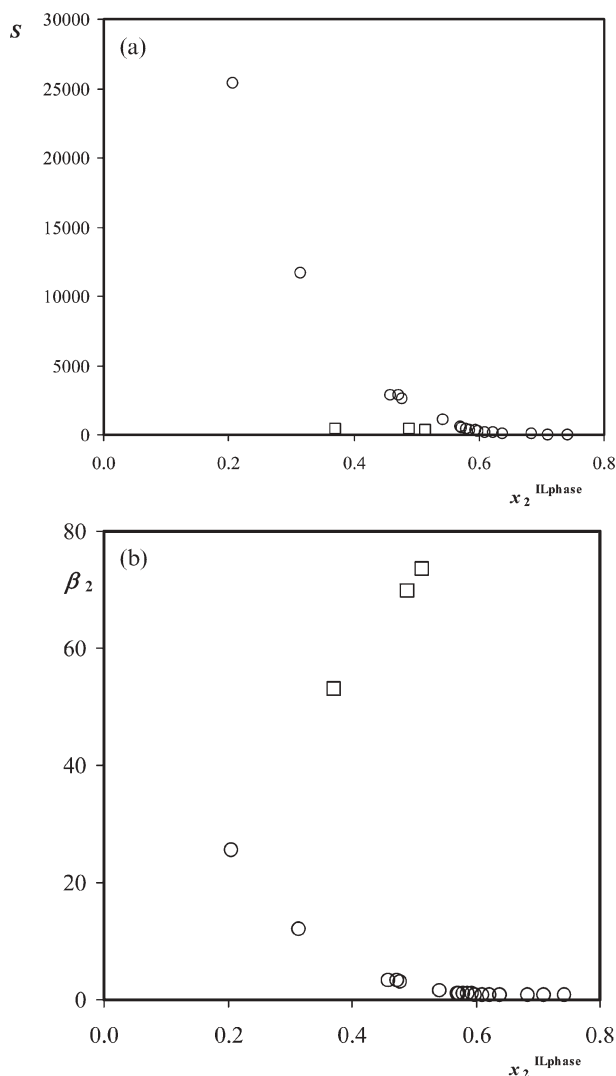


**Fig. 2** (a) Selectivity for the systems: heptane + ethanol + HMImPF<sub>6</sub> (○) and heptane + ethanol + MeOctImCl<sup>2</sup> (□) versus ethanol mole fraction in the IL-rich phase at 298.15 K. (b) Solute distribution ratio for the systems: heptane + ethanol + HMImPF<sub>6</sub> (○) and heptane + ethanol + MeOctImCl<sup>2</sup> (□) versus ethanol mole fraction in the IL-rich phase at 298.15 K.

### LLE data correlation

The experimental data were correlated by means of the NRTL equation<sup>3</sup> despite being a model initially developed for non-electrolyte solutions. However, literature results confirm that the equation can satisfactorily correlate LLE data involving electrolytes as ionic liquids.<sup>2,4,5</sup>

The activity coefficients were calculated by the equation:

$$\ln\gamma_i = \frac{\sum_{j=1}^m \tau_{ji} G_{ji} x_j}{\sum_{l=1}^m G_{li} x_l} + \sum_{j=1}^m \frac{x_j G_{ij}}{\sum_{l=1}^m G_{lj} x_l} \left( \tau_{ij} - \frac{\sum_{r=1}^m x_r \tau_{rj} G_{rj}}{\sum_{l=1}^m G_{lj} x_l} \right) \quad (3)$$

where:

$$\tau_{ji} = \frac{g_{ji} - g_{ii}}{RT} \quad (4)$$

$$G_{ji} = \exp(-\alpha_{ji} \tau_{ji}), \quad (5)$$

where  $g_{ji} - g_{ii}$  are the fitting parameters. The nonrandomness parameter  $\alpha$  was previously set to 0.3 and the correlation was performed. The DISTILL<sup>6</sup> 3.0 spreadsheet was employed to minimize the difference between the experimental and calculated mole fraction defined as:

$$OF = \sum_{i=1}^n \left[ (x_{1i}^I - x_{1i}^I(\text{calc}))^2 + (x_{2i}^I - x_{2i}^I(\text{calc}))^2 + (x_{1i}^{II} - x_{1i}^{II}(\text{calc}))^2 + (x_{2i}^{II} - x_{2i}^{II}(\text{calc}))^2 \right] \quad (6)$$

where  $x_{1i}^I$ ,  $x_{2i}^I$ ,  $x_{1i}^{II}$  and  $x_{2i}^{II}$  are the experimental mole fraction,  $x_{1i}^I(\text{calc})$ ,  $x_{2i}^I(\text{calc})$ ,  $x_{1i}^{II}(\text{calc})$  and  $x_{2i}^{II}(\text{calc})$  are the calculated mole fraction and superscripts I and II indicate the poor and rich phases in the IL, respectively.

Table 2 summarizes the NRTL fitting parameters and the root-mean-square deviations. These deviations were calculated by applying the following expression:

$$\sigma = \left( \sum_i (x_{ilm}^{\text{exp}} - x_{ilm}^{\text{calc}})^2 / 6k \right)^{1/2} \quad (7)$$

where  $x$  is the mole fraction and the subscripts  $i$ ,  $l$  and  $m$  provide a designation for the component, the phase and the tie-line, respectively. The value  $k$  designates the number of interaction components. The value of  $\sigma$  provides a measure of the accuracy of the correlation, in this case 0.01.

A comparison between the experimental data and the ones obtained from their correlation using the NRTL equation are shown in Fig. 1. In this figure, the NRTL equation gives successfully correlating data corresponding to the ternary system.

### Conclusions

In this work, the experimental determination of LLE for the ternary system (heptane + ethanol + HMImPF<sub>6</sub>) at 298.15 K was carried out. The NRTL model correlates accurately the experimental data. Selectivities for this system confirm a successful extraction of heptane from the azeotropic mixture with ethanol by means of a liquid–liquid operation with the ionic liquid HMImPF<sub>6</sub>.

The separation sequence for the azeotropic mixture (ethanol + heptane) is shown in Fig. 3. The ionic liquid is fed as the extractor of the mixture. The feasible separation sequence takes heptane to the top of the extractive column, leaving ethanol and HMImPF<sub>6</sub> together in the bottom. These components are separated in the vacuum distillation column. This column yields pure ethanol as distillate and pure IL at the bottom. The IL will be recycled to the extractive column.

**Table 2** Fitting parameters for the correlation with the NRTL equation for the ternary system at 298.15 K

Components	Parameters ( $\alpha = 0.3$ )	
$i, j$	$g_{ij} - g_{ij}/\text{cal mol}^{-1}$	$g_{ji} - g_{ii}/\text{cal mol}^{-1}$
1, 2	87009	87895
1, 3	2053	3389
2, 3	-482.5	8408

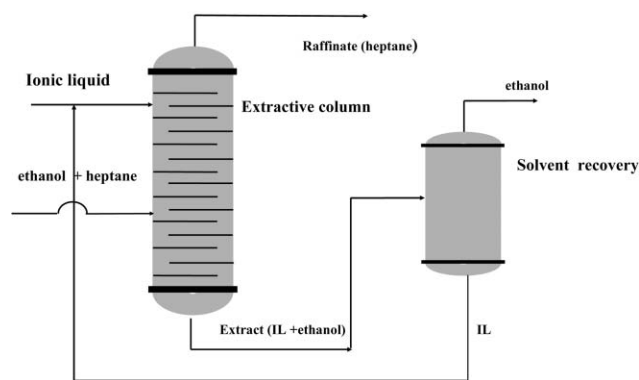


Fig. 3 Liquid-liquid extraction scheme.

This process leads to an environmentally friendly extraction process for the separation of azeotropic mixtures as an alternative to azeotropic distillation,<sup>7</sup> pervaporation<sup>8</sup> and reverse osmosis<sup>9</sup> where volatile organic compounds, high pressures and energy to evaporate the mixture are used to separate it into the desired pure components. Moreover there are no losses of ionic liquid to the atmosphere and operation costs are reduced with the extractive column, thus not contributing to the air pollution and then minimizing the environmental impact, the safety of workers and the solvent investment with respect to conventional solvents.

## Experimental

Heptane ( $\geq 99$  mass%, Aldrich), and ethanol ( $\geq 99.7$  mass%, Merck) were degassed ultrasonically and stored over molecular sieves type 0.4 nm (supplied by Aldrich) for several weeks. A Karl Fisher 756 coulometer was used to determine the water content since these quantities are negligible. Chromatographic tests of the solvents showed purities which complied with purchaser specifications.

NMR spectra were measured on a Bruker ARX 600 with chemical shifts given in parts per million and coupling constants ( $J$ ) in hertz. Positive FAB mass spectra were recorded on a FISON VG Autospec spectrometer using 3-nitrobenzyl alcohol as matrix.

HMImpF<sub>6</sub> was synthesized according to slightly modified literature procedures.<sup>10</sup> Equimolar amounts of 1-methylimidazole and chlorohexane were added to a two-necked, round-bottomed flask equipped with a reflux condenser, magnetic stirrer and a gas inlet. The reaction mixture was heated under N<sub>2</sub> at 343.15–353.15 K stirring for 48 to 72 h depending on the amount of starting materials (the progress of the reaction was

monitored by thin layer chromatography using silica gel 60 GF-254 aluminium sheets and chloroform + 10% methanol as eluent). The resulting viscous liquid was cooled to room temperature and ethyl acetate (70 ml per 0.4 mol of starting chlorohexane) was added with thorough mixing. Ethyl acetate was decanted and the procedure repeated three times using fresh ethyl acetate. After the final washing the remaining ethyl acetate was removed by heating at 343.15 K under vacuum. The resulting liquid, HMImpCl, was transferred to a 2 l plastic container (lined with a perfluorinated material) followed by addition of deionized water (500 ml per mol HMImpCl). An aqueous solution of 60% HPF<sub>6</sub> in a 1.1 : 1 molar ratio was added (this addition must be made slowly to minimize the amount of heat generated). After stirring for 12 to 16 h two phases were formed. The upper phase, acidic aqueous layer, was decanted and the lower ionic liquid portion was washed with deionized water (10 × 500 ml per mol HMImpCl) until the washings were no longer acidic. The ionic liquid obtained was dried under high vacuum ( $2 \times 10^{-1}$  Pa), stirring for 18 h. Yield: 75%. <sup>1</sup>H NMR (600 MHz, CDCl<sub>3</sub>, Me<sub>4</sub>Si):  $\delta$  8.51 [s, 1 H, H(2)], 7.28 [s, 1 H, H(4)], 7.24 [s, 1 H, H(5)], 4.13 [t,  $J = 7.5$  Hz, 2 H, NCH<sub>2</sub>], 3.91 [s, 3 H, NCH<sub>3</sub>], 1.86 [m, 2 H, NCH<sub>2</sub>CH<sub>2</sub>], 1.30 [m, 6 H, NCH<sub>2</sub>CH<sub>2</sub>(CH<sub>2</sub>)<sub>3</sub>], 0.87 [t,  $J = 7.0$  Hz, 3 H, N(CH<sub>2</sub>)<sub>5</sub>CH<sub>3</sub>]. <sup>13</sup>C NMR (100 MHz, acetone-d<sub>6</sub>):  $\delta$  138.08 [C(1)], 125.43 and 124.10 [C(4) and C(5)], 51.29 [NCH<sub>3</sub>], 37.33 [NCH<sub>2</sub>], 32.62 [NCH<sub>2</sub>CH<sub>2</sub>], 31.46 [NCH<sub>2</sub>CH<sub>2</sub>CH<sub>2</sub>], 27.20 [N(CH<sub>2</sub>)<sub>3</sub>CH<sub>2</sub>], 23.85 [N(CH<sub>2</sub>)<sub>4</sub>CH<sub>2</sub>], 15.10 [N(CH<sub>2</sub>)<sub>5</sub>CH<sub>3</sub>]. <sup>19</sup>F NMR (376 MHz, acetone-d<sub>6</sub>, CCl<sub>3</sub>F): two peaks at  $\delta$  -70.93 and -72.82. Positive FABMS (3-nitrobenzyl alcohol as matrix):  $m/z$  167 [HMImp]<sup>+</sup> (100%), 168 [HMImp + 1]<sup>+</sup> (12%).

## References

- 1 J. M. Soerensen, T. Magnussen, P. Rasmussen and A. Fredenslund, *Fluid Phase Equilib.*, 1979, **2**, 297–309.
- 2 T. M. Letcher, N. Deenadayalu, B. Soko, D. Ramjugernath and P. K. Naicker, *J. Chem. Eng. Data*, 2003, **48**, 904–907.
- 3 H. Renon and J. M. Prausnitz, *AIChE J.*, 1968, **14**, 135–144.
- 4 T. M. Letcher and N. Deenadayalu, *J. Chem. Thermodyn.*, 2003, **35**, 67–76.
- 5 A. Arce, O. Rodríguez and A. Soto, *Ind. Eng. Chem. Res.*, 2004, **43**, 8323–8327.
- 6 DISTILL 3.0 Manual, Hyprotech Ltd., 1998.
- 7 L. Laroche, N. Bekiaris, H. W. Andersen and M. Morari, *Can. J. Chem. Eng.*, 1991, **69**, 1302–1319.
- 8 T. Okada and T. Matsuura, *Proc. Int. Conf. Pervaporation Processes Chem. Ind.*, 3rd, 1988, 224–230.
- 9 M. Laatikainen and M. Lindstrom, *Acta Polytech. Scand., Chem. Technol. Metall. Ser.*, 1986, **175**, 61.
- 10 J. G. Huddleston, A. E. Visser, W. M. Reichert, H. D. Willauer, G. A. Broker and R. D. Rogers, *Green Chem.*, 2001, **3**, 156–164.

The  
first



More databases at  
[www.rsc.org/databases](http://www.rsc.org/databases)

for analytical  
scientists...

28110549

# Analytical Abstracts

For up-to-the-minute abstracts on all areas of analytical science including the latest applications and cutting edge techniques.

## Features include:

- **Online** access
- Unique search parameters including **chemical name**
- **Weekly** online updates
- **Comprehensive archive** spanning 25 years
- Coverage of over **100 international journals**
- Now incorporating **bio-analytical science**



RSC Publishing

[www.rsc.org/AA](http://www.rsc.org/AA)



# JEM

## Journal of Environmental Monitoring

Comprehensive, high quality coverage of multidisciplinary, international research relating to the measurement, pathways, impact and management of contaminants in all environments.

- Dedicated to the analytical measurement of environmental pollution
- Assessing exposure and associated health risks
- Fast times to publication
- Impact factor: 1.366
- High visibility - cited in MEDLINE



RSC Publishing

[www.rsc.org/jem](http://www.rsc.org/jem)